# Modeling and Computational Strategies for Optimal Oilfield Development Planning under Fiscal Rules and Endogenous Uncertainties

Submitted in partial fulfillment of the requirements for

the degree of

Doctor of Philosophy

in

Chemical Engineering

Vijay Gupta

B. Tech., Chemical Engineering, IIT Roorkee

Carnegie Mellon University
Pittsburgh, PA

May, 2013

*To my parents and siblings*

# Acknowledgments

First and foremost, I would like to express my gratitude to my advisor, Prof. Ignacio E. Grossmann, for providing me tremendous knowledge in the area of process systems engineering and optimization, motivation and encouragement for an innovative thinking, and being patient. It was a wonderful experience for me to work with him during the last five years. I would like to thank members of my thesis committee, Professors Nikolaos Sahinidis, Erik Ydstie, Andrew Schaefer and François Margot for their invaluable time and inputs. I would also like to thank my mentor Bora Tarhan for all of his suggestions during the several project meetings.

I would like to acknowledge financial support from ExxonMobil Upstream Research Company. I would also like to express my sincere gratitude towards the Process Control and Logistics group at Air Liquide Delaware Research and Technology Center, and Computational Methods group at ExxonMobil Upstream Research Company for two amazing summer internship experiences. In particular, I would like to thank Jeffrey Arbogast, Jean André, Sujata Pathak, Jeffrey Grenda, Rick Mifflin and Vikas Goel for being great mentors and friends during these internships.

I am grateful to the students at CMU and visitors to the group for their friendship and helpful discussions. Special thanks go to: Anshul Agarwal, Fengqi You, Juan Du, Sylvain Mouret, Sebastián Terrazas, Juan Pablo Ruiz, Bruno Calfa, Pablo Garcia Herreros, Sumit Mitra, Francisco Trespalacios, Yisu Nie, Satyajith Amaran, Yan Zhang, Bharat Mhatre, Ricardo Lima, Pablo Marchetti, Fabricio Oliveira, Brage Knudsen and Mariano Martin.

Finally, I would like to thank my parents, Mr. Kailash Chandra Gupta and Mrs. Geeta Devi Gupta, and my brothers, Vishnu and Ajay, and sister, Pinky, for all their support and love they have given me throughout my life and the motivation to accomplish what I could not have imagine. My gratitude to them is beyond what words can express and I would like to dedicate the thesis to them.

# Abstract

This dissertation proposes new mixed-integer optimization models and computational strategies for optimal offshore oil and gas field infrastructure planning under fiscal rules of the agreements with the host government, accounting for endogenous uncertainties in the field parameters using a stochastic programming framework. First, a multiperiod mixed-integer nonlinear programming (MINLP) model is proposed in Chapter 2 that incorporates field level investment and operating decisions, and maximizes the net present value (NPV). Two theoretical properties are proposed to remove the bilinear terms from the model, and further converting it to an MILP approximation to solve the problem to global optimality. Chapter 3 extends the basic deterministic model in Chapter 2 to include complex fiscal rules maximizing total contractor's (oil company) share after paying royalties, profit share, etc. to the host government. The resulting model yields improved decisions and higher profit than the previous one. Due to the computational issues associated with the progressive (sliding scale) fiscal terms, a tighter formulation, a relaxation scheme, and an approximation technique are proposed. Chapter 4 presents a general multistage stochastic MILP model for endogenous uncertainty problems where decisions determine the timings of uncertainty realizations. To address the issue of exponential growth of non-anticipativity (NA) constraints in the model, a new theoretical property is identified. Moreover, three solution strategies, i.e. a *k*-stage constraint strategy; a NAC relaxation strategy; and a Lagrangean decomposition algorithm, are also proposed to solve the realistic instances and applied to process network examples. In Chapter 5, the deterministic formulations in Chapter 2 and 3 for oilfield development are extended to a multistage stochastic programming formulation to account for the endogenous uncertainties in field sizes, oil deliverabilities, water-oil-ratios and gas-oil-ratios. The Lagrangean decomposition approach from Chapter 4 is used to solve the problem, with parallel solutions of the scenarios. To improve the quality of the dual bound during this decomposition

approach, a novel partial decomposition is proposed in Chapter 6. Chapter 7 presents a method to update the multipliers during the solution of a general two-stage stochastic MILP model, combining the idea of dual decomposition and integer programming sensitivity analysis, and comparing it with the subgradient method. Finally, Chapter 8 summarizes the major findings of the dissertation and suggests future work on the subject.

# Contents

# List of Tables

# List of Figures

# Chapter 1

# Introduction

The development planning of offshore oil and gas field infrastructures has received significant attention in recent years given the new discoveries of large oil and gas reserves in the last decade around the world. These have been facilitated by the new technologies available for exploration and production of oilfields in remote locations that are often hundreds of miles offshore. Surprisingly, there has been a net increase in the total oil reserves in the last decade because of these discoveries despite increase in the total demand (BP, Statistical review Report 2011). Therefore, there is currently a strong focus on exploration and development activities for new oil fields all around the world, specifically at offshore locations. However, installation and operating decisions in these projects involve very large investments that potentially can lead to large profits, but also to losses if these decisions are not made carefully. Therefore, the goal of this thesis is to develop efficient mixed-integer optimization models and computational strategies for optimal development planning of offshore oil and gas field infrastructure considering multi-field site, nonlinear reservoir profiles, complex fiscal rules, and endogenous uncertainties in the field parameters using a stochastic programming framework.

This chapter begins with an overview of the offshore oil and gas field infrastructure planning problem. Then, the various approaches used in the literature to model and solve this problem ranging from a basic deterministic model to incorporate fiscal and uncertainty considerations. A brief review of stochastic programming is presented with a particular focus on the endogenous (decision-dependent) uncertainty problems. Finally, we outline the specific research objectives of the work, and conclude it with a unified modeling framework used in the thesis for this oil and gas field development problem and a brief overview of the corresponding chapters.

## 1.1 Development planning of offshore oil and gas fields

The development planning of offshore oil and gas field infrastructures represents a very critical problem since it involves multi-billion dollar investments (Babusiaux et al., 2007). An offshore oilfield infrastructure (Figure 1.1) is usually very complex and comprises various production facilities such as Floating Production, Storage and Offloading (FPSO), Figure 1.2, Tension Leg platform (TLP), Figure 1.3, and connecting pipelines to produce oil and gas from the reserves. Each oilfield consists of a number of potential wells to be drilled using drilling rigs, which are then connected to the facilities through pipelines to produce oil. The produced oil is transported to the shore either though pipelines or using large tankers.

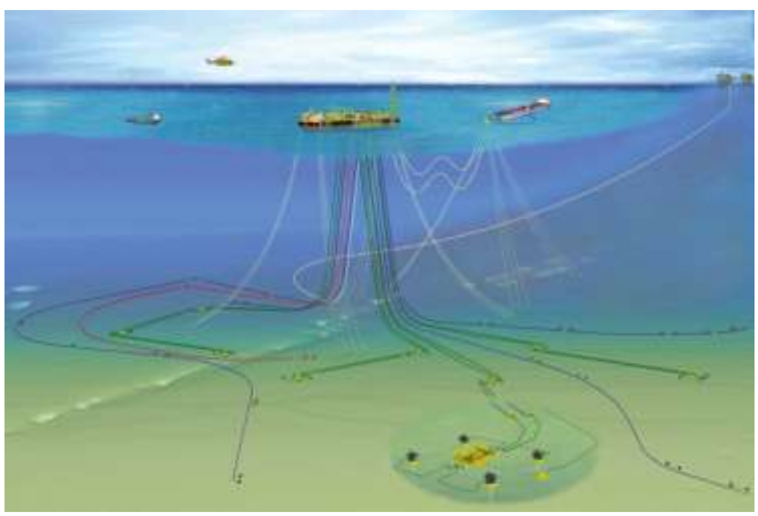

Figure 1.1: Offshore oilfield infrastructure

Figure 1.2: FPSO facility

Figure 1.3: TLP facility

The life cycle of a typical offshore oilfield project consists of the following five steps:

**(1) Exploration:** This activity involves geological and seismic surveys followed by exploration wells to determine the presence of oil or gas.

**(2) Appraisal:** It involves drilling of delineation wells to establish the size and quality of the potential field. Preliminary development planning and feasibility studies are also performed.

**(3) Development:** Following a positive appraisal phase, this phase aims at selecting the most appropriate development plan among many alternatives. This step involves capital-intensive investment and operating decisions that include facility installations, drilling, sub-sea structures, etc.

**(4) Production:** After the facilities are built and wells are drilled, production starts where gas or water is usually injected in the field at a later time to enhance productivity.

**(5) Abandonment:** This is the last phase of an oilfield development project and involves the decommissioning of facility installations and subsea structures associated with the field.

Given that most of the critical investments are usually associated with the development planning phase of the project, this thesis focuses on the key strategic/tactical decisions during this phase of the project. The major decisions involved in the oilfield development planning phase are the following:

(i) Selecting platforms to install and their sizes

(ii) Deciding which fields to develop and what should be the order to develop them
(iii) Deciding which wells and how many are to be drilled in the fields and in what sequence
(iv) Deciding which fields are to be connected to which facility
(v) Determining how much oil and gas to produce from each field

Therefore, there are a very large number of alternatives that are available to develop a particular field or group of fields. However, these decisions should account for the physical and practical considerations, such as the following: a field can only be developed if a corresponding facility is present; nonlinear profiles of the reservoir that are obtained from reservoir simulators (e.g. ECLIPSE) to predict the actual flowrates of oil, water and gas from each field; limitation on the number of wells that can be drilled each year due to availability of the drilling rigs; and long-term planning horizon that is the characteristic of these projects. Therefore, optimal investment and operating decisions are essential for this problem to ensure the highest return on the investments over the time horizon considered. By including all the considerations described here in an optimization model, this leads to a large-scale multiperiod mixed-integer nonlinear programming (MINLP) problem that is difficult to solve to global optimality. The extension of this model to the cases where we explicitly consider the fiscal rules with the host government and the uncertainties can further lead to a very complex problem to model and solve.

In the next sub-sections we briefly review the various approaches used in the literature to address this problem either using a deterministic formulation or a stochastic one.

### 1.1.1 Deterministic approaches for oil and gas field development planning

The oilfield development planning has traditionally been modeled as LP (Lee and Aranofsky, 1958; and Aronofsky and Williams, 1962) or MILP (Frair, 1973) models under certain assumptions to make them computationally tractable. Simultaneous optimization of the investment and operating decisions has been addressed in Bohannon (1970), Sullivan (1982) and Haugland et al. (1988) using

MILP formulations with different levels of details. Behrenbruch (1993) emphasized the need to consider a correct geological model and to incorporate flexibility into the decision process for an oilfield development project.

Iyer et al. (1998) proposed a multiperiod MILP model for optimal planning and scheduling of offshore oilfield infrastructure investment and operations. The model considers the facility allocation, production planning, and scheduling within a single model and incorporates the reservoir performance, surface pressure constraints, and oil rig resource constraints. To solve the resulting large-scale problem, the nonlinear reservoir performance equations are approximated through piecewise linear approximations. As the model considers the performance of each individual well, it becomes expensive to solve for realistic multi-field sites. Moreover, the flow rate of water was not considered explicitly for facility capacity calculations.

Van den Heever and Grossmann (2000) extended the work of Iyer et al. (1998) and proposed a multiperiod generalized disjunctive programming model for oil field infrastructure planning for which they developed a bilevel decomposition method. As opposed to Iyer and Grossmann (1998), they explicitly incorporated a nonlinear reservoir model into the formulation but did not consider the drill-rig limitations.

Grothey and McKinnon (2000) addressed an operational planning problem using an MINLP formulation where gas has to be injected into a network of low pressure oil wells to induce flow from these wells. Lagrangean decomposition and Benders decomposition algorithms were proposed for the efficient solution of the model. Kosmidis et al. (2002) considered a production system for oil and gas consisting of a reservoir with several wells, headers and separators. The authors presented a mixed integer dynamic optimization model and an efficient approximation solution strategy for this system.

Barnes et al. (2002) optimized the production capacity of a platform and the drilling decisions for wells associated with this platform. The authors addressed the problem by solving a sequence of MILPs. Ortiz-Gomez et al. (2002) presented three mixed-integer multiperiod optimization models of varying complexity for the oil production planning. The problem considers fixed topology and is concerned with the decisions involving the oil production profiles and operation/shut in times of the wells in each time period assuming nonlinear reservoir behavior.

Lin and Floudas (2003) considered the long-term investment and operations planning of the integrated gas field site. A continuous-time modeling and optimization approach was proposed introducing the concept of event points and allowing the well platforms to come online at potentially any time within the planning horizon. A two-level solution framework was proposed to solve the resulting MINLP problems which showed that the continuous time approach can reduce the computational efforts substantially and solve problems that were intractable for the discrete-time model.

Kosmidis et al. (2005) presented a mixed integer nonlinear (MINLP) model for the daily well scheduling in petroleum fields, where the nonlinear reservoir behavior, the multiphase flow in wells and constraints from the surface facilities were simultaneously considered. The authors also proposed a solution strategy involving logic constraints, piecewise linear approximations of each well model and an outer approximation based algorithm. Results showed an increase in oil production of up to 10% compared to typical heuristic rules widely applied in practice.

Carvalho and Pinto (2006a) considered an MILP formulation for oilfield planning based on the model developed by Tsarbopoulou (2000), and proposed a bilevel decomposition algorithm for solving large-scale problems where the master problem determines the assignment of platforms to wells and a planning subproblem calculates the timing for the fixed assignments. The work was further extended by Carvalho and Pinto (2006b) to consider multiple reservoirs within the model.

Barnes et al. (2007) addressed the optimal design and operational management of offshore oil fields where at the design stage optimal production capacity of a main field was determined with an adjacent satellite field and a well drilling schedule. The problem was formulated as an MILP model. Continuous variables involved individual well, jacket and topsides costs, whereas binary variables were used to select individual wells within a defined field grid. An MINLP model was proposed for the operational management to model the pressure drops in pipes and wells for multiphase flow. Non-linear cost equations were derived for the production costs of each well accounting for the length, the production rate and their maintenance. Operational decisions included the oil flowrates, the operation/shut-in for each well and the pressures for each point in the piping network.

Gunnerud and Foss (2010) considered the real-time optimization of oil production systems with a decentralized structure and modeled nonlinearities with piecewise linear approximations, resulting in an MILP model. The Lagrange relaxation and Dantzig–Wolfe decomposition methods were studied on a semi-realistic model of the Troll west oil rim in Norway, which showed that both approaches offers an interesting option to solve the complex oil production systems as compared to the fullspace method.

### 1.1.2 Incorporating complex fiscal rules

The major limitation with the above approaches in the oilfield development planning is that they do not consider the fiscal rules explicitly in the optimization model that are associated to these fields, and mostly rely on the simple net present value (NPV) as an objective function. Therefore, the models with these objectives may yield the solutions that are very optimistic, which can in fact be suboptimal after considering the impact of fiscal terms. Bagajewicz (2008) discussed the merits and limitations of using NPV in the investment planning problems and pointed out that additional consideration and procedures are needed for these problems, e.g. return on investments, to make the better decisions. Laínez et al. (2009) emphasizes that enterprise-wide decision problems must be formulated with realistic detail, not just in the technical aspects, but also in the financial components in order to generate solutions that are of value to an enterprise. This requires systematically incorporating supplier/buyer options contracts within the framework of supply-chain problems.

In the context of oilfield planning, fiscal rules of the agreements between the oil company (contractor) and the host government, e.g. production sharing contracts, usually determine the share of each of these entities in the total oil production or gross revenues and the timing of these payments. Hence, including fiscal considerations as part of the oilfield development problem can significantly impact the optimal decisions and revenue flows over the planning horizon, as a large fraction of the total oil produced is paid as royalties, profit share, etc. The models and solutions approaches in the literature that consider the fiscal rules within oilfield infrastructure planning are either very specific or simplified. Van den Heever et al. (2000) and Van den Heever and Grossmann (2001) considered optimizing the complex economic objectives including royalties, tariffs, and taxes for the multiple gas field site where the schedule for the drilling of wells was predetermined as a function of the timing of the installation of the well platform. Moreover, the fiscal rules presented were specific to the gas field site considered, but not in general form. Based on a continuous time formulation for gas field development with complex economics of similar nature as Van den Heever and Grossmann (2001), Lin and Floudas (2003) proposed an MINLP model and solved it with a two-stage algorithm. Approaches based on simulation (Blake and Roberts, 2006) and meta-modeling (Kaiser and Pulsipher, 2004) have also been considered for the analysis of the different fiscal terms. However, the papers that address the mathematical programming models and solution approaches for the oilfield investments and operations with fiscal considerations are still very limited.

### 1.1.3 Incorporating uncertainties in the development planning

In the literature work described above, one of the major assumptions is that there is no uncertainty in the model parameters, which in practice is generally not true. Although limited, there has been some work that accounts for uncertainty in the problem of optimal development of oil and/or gas fields. Haugen (1996) proposed a single parameter representation for uncertainty in the size of reserves and incorporates it into a stochastic dynamic programming model for scheduling of oil fields. However, only decisions related to the scheduling of fields were considered. Meister et al. (1996) presented a model to derive exploration and production strategies for one field under uncertainty in reserves and future oil prices. The model was analyzed using stochastic control techniques.

Jonsbraten (1998a) addressed the oilfield development planning problem under oil price uncertainty using an MILP formulation that was solved with a progressive hedging algorithm. Aseeri et al. (2004) introduced uncertainty in the oil prices and well productivity indexes, financial risk management, and budgeting constraints into the model proposed by Iyer and Grossmann (1998), and solved the resulting stochastic model using a sampling average approximation algorithm.

Jonsbraten (1998b) presented an implicit enumeration algorithm for the sequencing of oil wells under uncertainty in the size and quality of oil reserves. The author uses a Bayesian approach to represent the resolution of uncertainty with investments. The paper considers investment and operation decisions only for one field. Lund (2000) addressed a stochastic dynamic programming model for evaluating the value of flexibility in offshore development projects under uncertainty in future oil prices and in the reserves of one field using simplified descriptions of the main variables.

Cullick et al. (2003) proposed a model based on the integration of a global optimization search algorithm, a finite-difference reservoir simulation, and economics. In the solution algorithm, new decision variables were generated using meta-heuristics, and uncertainties were handled through simulations for fixed design variables. They presented examples having multiple oil fields with uncertainties in the reservoir volume, fluid quality, deliverability, and costs. Few other papers, (Begg et al., 2001; Zabalza-Mezghani et al., 2004; Bailey et al., 2005; and Cullick et al., 2007), have also used a combination of reservoir modeling, economics and decision making under uncertainty through simulation-optimization frameworks.

Ulstein et al. (2007) addressed the tactical planning of petroleum production that involves regulation of production levels from wells, splitting of production flows into oil and gas products, further processing of gas and transportation in a pipeline network. The model was solved for different cases with demand variations, quality constraints, and system breakdowns.

Elgsæter et al. (2010) proposed a structured approach to optimize offshore oil and gas production with uncertain models that iteratively updates setpoints, while documenting the benefits of each proposed setpoint change through excitation planning and result analysis. The approach is able to realize a significant portion of the available profit potential, while ensuring feasibility despite large initial model uncertainty.

However, most of these works either consider the very limited flexibility in the investment and operating decisions, or handle the uncertainty in an ad-hoc manner. Stochastic programming provides a systematic framework to model problems that require decision-making in the presence of uncertainty by taking uncertainty into account of one or more parameters in terms of probability distribution functions, (Birge and Louveaux, 1997). The concept of recourse action in the future, and availability of probability distribution in the context of oilfield development planning problems, makes it one of the most suitable candidates to address uncertainty. Moreover, extremely conservative decisions are usually ignored in the solution utilizing the probability information given the potential of high expected profits in the case of favorable outcomes.

In the context of stochastic programming, Goel and Grossmann (2004) considered a gas field development problem under uncertainty in the size and quality of reserves where decisions on the timing of field drilling were assumed to yield an immediate resolution of the uncertainty, i.e. the problem involves decision-dependent uncertainty as discussed in Jonsbraten et al. (1998); Goel and Grossmann (2006); and Gupta and Grossmann (2011a). Linear reservoir models, which can provide a reasonable approximation for gas fields, were used. In their solution strategy, the authors used a relaxation problem to predict upper bounds, and solved multistage stochastic programs for a fixed scenario tree for finding lower bounds. Goel et al. (2006) later proposed the theoretical conditions to reduce the number of non-anticipativity constraints in the model. The authors also developed a branch and bound algorithm for solving the corresponding disjunctive/mixed-integer programming model where lower bounds were generated by Lagrangean duality. The proposed decomposition strategy relies on relaxing the disjunctions and logic constraints for the conditional non-anticipativity constraints while dualizing the initial ones at the root node. Ettehad et al. (2011) presented a case study for the development planning of an offshore gas field under uncertainty optimizing facility size, well counts, compression power and production policy. A two-stage stochastic programming model was developed to investigate the impact of uncertainties in original gas in place and inter-compartment transmissibility. Results of two solution methods, optimization with Monte Carlo sampling and stochastic programming, were compared which showed that the stochastic programming approach is more efficient. The models were also used in a value of information (VOI) analysis.

Moreover, the gradual uncertainty reduction has also been addressed for problems in this class. Stensland and Tjøstheim (1991) have worked on a discrete time problem for finding optimal decisions with uncertainty reduction over time and applied their approach to oil production. These authors expressed the uncertainty in terms of a number of production scenarios. Their main contribution was combining production scenarios and uncertainty reduction effectively for making optimal decisions. Dias (2002) presented four propositions to characterize technical uncertainty and the concept of revelation towards the true value of the variable. These four propositions, based on the theory of conditional expectations, are employed to model technical uncertainty.

Tarhan et al. (2009) addressed the planning of offshore oil field infrastructure involving endogenous uncertainty in the initial maximum oil flowrate, recoverable oil volume, and water breakthrough time of the reservoir, where decisions affect the resolution of these uncertainties. The authors extend the work of Goel and Grossmann (2004) and Goel et al. (2006) but with three major differences: (a) The model focuses on a single field consisting of several reservoirs rather than multiple fields but more detailed decisions are considered. (b) Nonlinear, rather than linear, reservoir models are considered. (c) The resolution of uncertainty is gradual over time instead of being resolved immediately. The authors also developed a multistage stochastic programming framework that was modeled as a disjunctive/mixed-integer nonlinear programming model consisting of individual non-convex MINLP subproblems connected to each other through initial and conditional non-anticipativity constraints. A duality-based branch and bound algorithm was proposed taking advantage of the problem structure and globally optimizing each scenario problem independently. An improved solution approach was also proposed that combines global optimization and outer-approximation to optimize the investment and operations decisions (Tarhan et al., 2011). However, it considers either gas/water or oil/water components for single field and single reservoir at a detailed level. Hence, realistic multi-field site instances can be expensive to solve with this model.

In the next section we briefly outline the basic elements of the stochastic programming that will be used as a modeling framework in this thesis.

## 1.2 Stochastic Programming

A stochastic program is a mathematical program in which some of the parameters defining a problem instance are random (e.g. uncertain reservoir size, product demand, yields, prices). In general, multiperiod industrial planning, scheduling, supply-chain etc. problems under uncertainty are formulated as stochastic programs since it allows to incorporate probability distribution of the uncertain parameters explicitly into the model while making investment and operating decisions, and provides an opportunity to take corrective actions in the future (recourse) based on the actual outcomes (see Ierapetritou and Pistikopoulos, 1994; Clay and Grossmann, 1997; Iyer and Grossmann, 1998; Schultz, 2003; Ahmed and Garcia, 2003; Sahinidis, 2004; Ahmed et al. 2004; Li and Ierapetritou, 2012). This area is receiving increasing attention given the limitations of deterministic models.

Discrete probability distributions of the uncertain parameters are widely considered to represent uncertainty in terms of the scenarios where a scenario is given by the combination of the realization of the uncertain parameters.

Depending on the number of decision stages involved in the model, the stochastic program corresponds to either a two-stage or a multistage problem. The main idea behind two-stage stochastic programming is that we make some decisions (stage 1) here and now based on not knowing the future outcomes of the uncertain parameters, while the rest of the decisions are stage-2 (recourse actions) decisions that are made after uncertainty in those parameters is revealed. In this work, we focus on more general multistage stochastic programming models where the uncertain parameters are revealed sequentially, i.e. in multiple stages (time periods), and the decision-maker can take corrective actions over a sequence of the stages. In the two-stage and multistage case the cost of the decisions and the expected cost of the recourse actions are optimized.

Based on the type of uncertain parameters involved in the problem, stochastic programming models can be classified into two broad categories (Jonsbraten, 1998b): exogenous uncertainty where stochastic processes are independent of decisions that are taken (e.g. demands, prices), and endogenous uncertainty where stochastic processes are affected by these decisions (e.g. reservoir size and its quality). In the process systems area, Ierapetritou and Pistikopoulos (1994), Clay and Grossmann (1997) and Iyer and Grossmann (1998) solved various production planning problems that considered exogenous uncertainty and formulated as the two-stage stochastic programs. Furthermore, detailed reviews of previous work on problems with exogenous uncertainty can be found in Schultz (2003) and Sahinidis (2004). However, a number of planning problems involving very large investments at an early stage of the project have endogenous (technical) uncertainty that is at-least comparable if not greater than the exogenous (market) uncertainty. In such cases, it is essential to incorporate endogenous uncertain parameters while making the investment decisions since it can have a large impact on the overall project profitability.

In the context of endogenous uncertainty, our decisions can affect the stochastic processes in two different ways (Goel and Grossmann, 2006): either they can alter the probability distributions (type 1) (see Viswanath et al., 2004; and Held and Woodruff, 2005), or they can determine the timing when uncertainties in the parameters are resolved (type 2) (see Goel et al., 2006; Tarhan et al., 2009). Surprisingly, these problems have received relatively little attention in the literature despite their practical importance. Pflug (1990) addressed endogenous uncertainty problems in the context of discrete event dynamic systems where the underlying stochastic process depends on the optimization decisions. Jonsbraten et al. (1998) proposed an implicit enumeration algorithm for the problems in this class where decisions that affect the uncertain parameter values are made at the first stage. Ahmed (2000) presented several examples having decision dependent uncertainties that were formulated as MILP problems and solved by LP-based branch and bound algorithms. Moreover, Viswanath et al. (2004) and Held and Woodruff (2005) addressed the endogenous uncertainty problems where decisions can alter the probability distributions.

There are multiple sources of uncertainty in the oil and gas field development problem as can be seen from the literature work afore-mentioned. The market price of oil/gas, quantity and quality of reserves at a field are the most important sources of the uncertainty in this context. The uncertainty in oil prices is influenced by the political, economic or other market factors and it belongs to the exogenous uncertainty problems. The uncertainty in the reserves on the other hand, is linked to the accuracy of the reservoir data (technical uncertainty). While the existence of oil and gas at a field is indicated by seismic surveys and preliminary exploratory tests, the actual amount of oil in a field, and the efficiency of extracting the oil will only be known after capital investment has been made at the field (Goel and Grossmann, 2004), i.e. endogenous uncertainty. Both, the price of oil and the quality of reserves directly affect the overall profitability of a project, and hence it is important to consider the impact of these uncertainties when formulating the decision policy. However, due to the significant computational challenge in this thesis we only address the uncertainty in the field parameters where timing of uncertainty realizations is decision-dependent. In particular, we focus on the type 2 of endogenous uncertainty where the decisions are used to gain more information, and resolve uncertainty either immediately or in a gradual manner. Therefore, the resulting scenario tree is decision-dependent that requires modeling a superstructure of all possible scenario trees that can occur based on the timing of the decisions (see Goel et al., 2006; Tarhan et al., 2009).

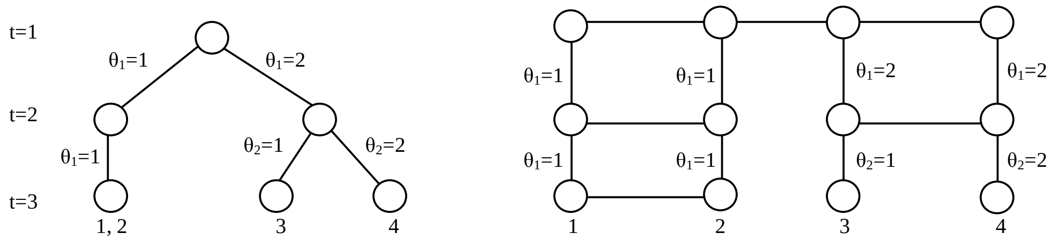

(a) Standard Scenario Tree with uncertain parameters $\theta_1$ and $\theta_2$ (b) Alternative Scenario Tree

Figure 1.4: Tree representations for discrete uncertainties over 3 stages

Specifically, to address the stochastic programming problem under consideration, we assume in this thesis that the uncertain parameters follow discrete probability distributions and that the planning horizon consists of a fixed number of time periods that correspond to decision points. Using these two assumptions, the stochastic process can be represented with scenario trees. In a scenario tree (Figure 1.4-a) each node represents a possible state of the system at a given time period. Each arc represents the possible transition from one state in time period $t$ to another state in time period $t$+1, where each state is associated with the probabilistic outcome of a given uncertain parameter. A path from the root node to a leaf node represents a scenario.

An alternative representation of the scenario tree was proposed by Ruszczynski (1997) where each scenario is represented by a set of unique nodes (Figure 1.4-b). The horizontal lines connecting nodes in time period $t$ mean that nodes are identical as they have the same information and those scenarios are said to be indistinguishable in that time period. These horizontal lines correspond to the non-anticipativity (NA) constraints in the model that link different scenarios and prevent the problem from being amenable to decomposition. In this work, since we focus on multistage stochastic programming (MSSP) problems with endogenous uncertainty where the structure of scenario tree is decision-dependent, we use the above alternative scenario tree representation to model these problems effectively.

In addition to the oil and gas field development problems under endogenous uncertainties (type 2) as described in the previous section (Goel and Grossmann, 2004; Goel et al., 2006; and Tarhan et al., 2009), there are few other practical applications that have been addressed. In particular, Tarhan and Grossmann (2008) applied endogenous uncertainty in the synthesis of process networks with uncertain yields, and used gradual uncertainty resolution in the model. Solak (2007) considered the project portfolio optimization problem that deals with the selection of research and development projects and determination of optimal resource allocations under decision dependent uncertainty where uncertainty is resolved gradually. The author used the sample average approximation method for solving the problem, where the sample problems were solved through Lagrangean relaxation and heuristics. Boland et al. (2008) addressed the open pit mine production scheduling problem considering endogenous uncertainty in the total amount of rock and metal contained in it, where the excavation decisions resolve this uncertainty. These authors also compared the fullspace results for this mine-scheduling problem with the one where non-anticipativity constraints were included as the 'lazy constraints' during the solution. Colvin and Maravelias (2008, 2010) presented several theoretical properties, specifically for the problem of scheduling of clinical trials having uncertain outcomes in the pharmaceutical R&D pipeline, and developed a branch-and-cut framework to solve these MSSP problems with endogenous uncertainty under the assumption that only few non-anticipativity constraints be active at the optimal solution.

## 1.3 Research Objectives

Following are the major objectives of this thesis:

1. Develop an efficient deterministic model for offshore oil and gas field development planning considering multiple fields, facility expansions in the future, lead times for facility installation and expansions, individual

oil, water and gas flowrates, drilling rig limitations, with the objective to maximize the net present value for the given planning horizon

2. Extend the simple NPV based deterministic oilfield planning model to include general complex fiscal rules such as the ones in production sharing agreements
3. Develop reformulation, approximation and decomposition based approaches to improve the computational efficiency of the oilfield model with fiscal rules
4. Apply these deterministic models with/without fiscal contracts and computational strategies to realistic oilfield development planning examples
5. Formulate a general multistage stochastic mixed-integer linear programming model for addressing endogenous uncertainties where the optimization decisions affect the timing when uncertainties in the parameters are resolved
6. Develop model reduction approaches and solution strategies to overcome the computational expense of the above multistage stochastic model
7. Apply these multistage stochastic model and solution strategies to the process network planning problem under uncertain yields, and to the oilfield development planning under uncertain field parameters with/without fiscal contracts
8. Develop and implement a new Lagrangean decomposition algorithm based on grouping of the scenarios for efficiently solving general multistage stochastic programs under endogenous uncertainties, and apply it to process network and oilfield planning examples to compare it with the standard approaches
9. Develop a method for improving the dual bound generated during the solution of a stochastic mixed-integer linear programming model using the dual decomposition and integer programming sensitivity analysis, and benchmark the results against the standard subgradient method

## 1.4 Overview of thesis

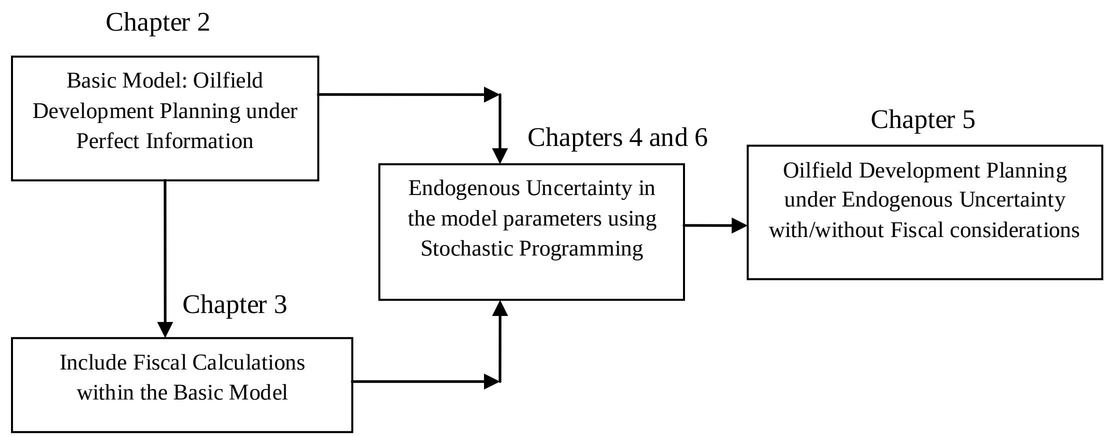


Figure 1.5: A unified framework for oilfield development planning under complex fiscal rules and endogenous uncertainties

In this thesis we consider a unified modeling framework (Figure 1.5) to address the offshore oil and gas field development planning problem under complex fiscal rules and endogenous uncertainties. We start by developing a basic deterministic model in Chapter 2 that includes sufficient level of detail to be realistic as well as computationally efficient. Then, we discuss the extension of the model to incorporate fiscal rules defined by the terms of the contract between oil companies and governments in Chapter 3. In addition, several computational strategies are proposed to solve the realistic instances of the fiscal model.

To address the issue of endogenous uncertainties in the field parameters where timing of uncertainty realization depends on investment decisions, we first consider a general multistage stochastic programming model in Chapter 4 and propose solution strategies to handle the large instances. The stochastic programming framework and solution approach presented in Chapter 4 is used for the oilfield problem in Chapter 5 considering the deterministic models from Chapter 2 and 3 as basis. An improved decomposition approach to solve the general multistage stochastic formulation under endogenous uncertainties is also proposed in Chapter 6. In Chapter 7 we present a new method to update the Lagrangean multipliers during dual decomposition for two-stage stochastic mixed-integer linear programs under exogenous uncertainties. A more detailed overview of the chapters in the thesis is presented below:

### 1.4.1 Chapter 2

Chapter 2 presents an efficient basic deterministic model for offshore oil and gas field development problem. In particular, we develop a multiperiod non-convex MINLP model for multi-field site that includes three components (oil, water and gas) explicitly in the formulation using higher order polynomials avoiding bilinear and other nonlinear terms. With the objective of maximizing total NPV for long-term planning horizon, the model involves decisions related to FPSO (floating production, storage and offloading) installation and expansions, field-FPSO connections, well drilling and production rates in each time period. Furthermore, it is reformulated into an MILP after piecewise linearization and exact linearization techniques that can be solved to global optimality in an efficient way. Solutions of realistic instances involving 10 fields, 3 FPSOs, 84 wells and 20 years planning horizon are reported, as well as comparisons between the computational performance of the proposed MINLP and MILP formulations.

### 1.4.2 Chapter 3

In Chapter 3, we extend the simple NPV (net present value) based optimal oilfield development planning model developed in Chapter 2 to include general complex fiscal rules having progressive fiscal terms and ringfencing provisions. The progressive fiscal terms penalize higher production rates based on the certain profitability measures such as cumulative oil produced, daily production, rate of return defined in the contract. On the other hand, ringfencing provisions divide the fields in certain groups such that only fields in a given ringfence can share the cost and revenues for fiscal calculations, but not with the fields from other ringfences. Therefore, these provisions further increase the complexity of the model. We explain the reduction of the proposed fiscal model to a variety of contracts. The impact of the explicit consideration of the fiscal terms during oilfield development planning on the investment and operating decisions is analyzed. Since, the fiscal model can become computationally very expensive to solve, we propose logic constraints and valid inequalities to reformulate the model that can be solved more efficiently. A relaxation scheme and an approximation technique are also provided that work as good heuristics for the large-scale problems. The proposed model and computational strategies are applied to several instances of the oilfield development problems with fiscal contracts. Preliminary results on a bi-level decomposition approach are provided that can predict the rigorous bounds for the large instances involving ringfencing provisions.

### 1.4.3 Chapter 4

Chapter 4 considers a general multistage stochastic mixed-integer linear programming (MSSP) model with endogenous uncertainty in some of the parameters, where the optimization decisions affect the times when the uncertainties in those parameters are resolved. To address the issue that the number of non-anticipativity (NA) constraints increases exponentially with the number of uncertain parameters and/or its realizations, we present a new theoretical property that significantly reduces the problem size and complements two previous properties proposed by Goel and Grossmann (2006). Since one might generate reduced models that are still too large to be solved directly, we also propose three solution strategies: a *k*-stage constraint strategy where we only include the NA constraints up to a specified number of stages, an iterative NAC relaxation strategy, and a Lagrangean decomposition algorithm that decomposes the problem into scenarios. Numerical results for two process network examples are presented to illustrate the performance of the proposed solution strategies.

### 1.4.4 Chapter 5

Chapter 5 presents a multistage stochastic programming model for investment and operations planning of offshore oil and gas field infrastructure. In particular, we consider the deterministic models proposed in Chapters 2 and 3 as basis, and utilize the stochastic programming framework presented in Chapter 4 to formulate the model with/without fiscal contracts. We also consider correlations among the endogenous uncertain parameters for a field such as field size, oil deliverability, water-oil ratio and gas-oil ratio, which reduce the total number of scenarios in the resulting multistage stochastic formulation. To solve the large instances of the problem, the Lagrangean decomposition approach proposed in Chapter 4 allowing parallel solution of the scenario subproblems is implemented in the GAMS grid computing environment. Computational results on a variety of oilfield development planning examples are presented to illustrate the efficiency of the model and the decomposition approach.

### 1.4.5 Chapter 6

In Chapter 6, we propose a new decomposition algorithm for solving general large-scale multistage stochastic programs (MSSP) with endogenous uncertainties. Instead of dualizing all the initial non-anticipativity constraints (NACs) and removing all the conditional non-anticipativity constraints to decompose the problem into scenario subproblems as in Chapters 4 and 5, the basic idea relies on a partial decomposition scheme. It is proved that the algorithm provides a dual bound that is at least as tight as the standard approach. The algorithm has been applied to process network examples and oilfield development planning problem to compare the quality of the bounds obtained at the root node and impact on the computational effort.

### 1.4.6 Chapter 7

Chapter 7 presents a method for improving the dual bound of decomposable MILP models using integer programming sensitivity analysis based on the previous work by Tarhan (2009). In particular, it proposes a new linear program that involves constraints from the primal and dual sensitivity analysis (Dawande and Hooker, 2000) using the information from branch and bound tree of each subproblem solution during Lagrangean decomposition, and yields improved multipliers which results in faster convergence of the algorithm. The method has been applied to several example problems to compare its performance against standard subgradient method.

### 1.4.7 Chapter 8

Chapter 8 provides a summary of the major contributions of the thesis and suggestions for future work.

This thesis has led to the following papers:

- Gupta, V., Grossmann, I. E., 2011a. Solution Strategies for Multistage Stochastic Programming with Endogenous Uncertainties. Computers and Chemical Engineering 35, 2235–2247.

- Gupta, V., Grossmann, I. E., 2011b. Offshore Oilfield Development Planning under Uncertainty and Fiscal Considerations. Optimization and Analytics in the Oil and Gas Industry, Part I; Springer Edition, submitted for publication.

- Gupta, V., Grossmann, I. E., 2012a. An Efficient Multiperiod MINLP Model for Optimal planning of Offshore Oil and Gas Field Infrastructure. Industrial and Engineering Chemistry Research 51 (19), 6823–6840.

- Gupta, V., Grossmann, I. E., 2012b. Modeling and Computational Strategies for Offshore Oilfield Development Planning under Complex Fiscal Rules. Industrial and Engineering Chemistry Research 51, 14438−14460.

- Gupta, V., Grossmann, I. E., 2013a. Multistage Stochastic Programming Approach for Offshore Oilfield Infrastructure Planning under Production Sharing Agreements and Endogenous Uncertainties, manuscript in preparation.

- Gupta, V., Grossmann, I. E., 2013b. A new Decomposition Algorithm for Multistage Stochastic Programs with Endogenous Uncertainties, submitted for publication.

- Tarhan, B., Gupta V., Grossmann, I. E., 2013. Improving Dual Bound for Stochastic MILP Models using Sensitivity Analysis, to be submitted.

# Chapter 2

# An efficient multiperiod MINLP model for optimal planning of offshore oil and gas field infrastructure

## 2.1 Introduction

In this chapter, we focus on developing a basic deterministic model for the strategic/tactical planning of offshore oil and gas fields, which includes sufficient level of details to be useful for realistic oilfield development projects, as well as it can be extended to include fiscal and uncertainty considerations as in the subsequent chapters. In particular, there are following major extensions and differences that are addressed in the proposed deterministic model as compared to the previous work:

(1) We consider three components (oil, water and gas) explicitly in the formulation for a multi-field site, which allows considering realistic problems for facility installation and capacity decisions.

(2) Nonlinear reservoir behavior in the model is approximated by $3^{rd}$ and higher order polynomials to ensure sufficient accuracy for the predicted reservoir profiles.

(3) The number of wells is used as a variable for each field to capture the realistic drill rig limitations and the resulting trade-offs among various fields.

(4) We include the possibility of expanding the facility capacities in the future, and including the lead times for construction and expansions for each facility to ensure realistic investments.

A typical offshore oilfield infrastructure (Figure 2.1) consists of various production facilities such as Floating Production, Storage and Offloading (FPSO), fields, wells and connecting pipelines to produce oil and gas from the reserves. Each oilfield consists of a number of potential wells to be drilled using drilling rigs, which are then connected to the facilities through pipelines to produce oil. There is a multi-phase flow in these pipelines due to the presence of gas and liquid that comprises oil and water. Therefore, there are three main components present, and their relative amounts depend on certain parameters like cumulative oil produced. The field to facility connection involves trade-offs associated to the flowrates of oil and gas for a particular field-facility connection, connection costs, and possibility of other fields to connect to that same facility, while the number of wells that can be drilled in a field depends on the availability of the drilling rig that can drill a certain number of wells each year.

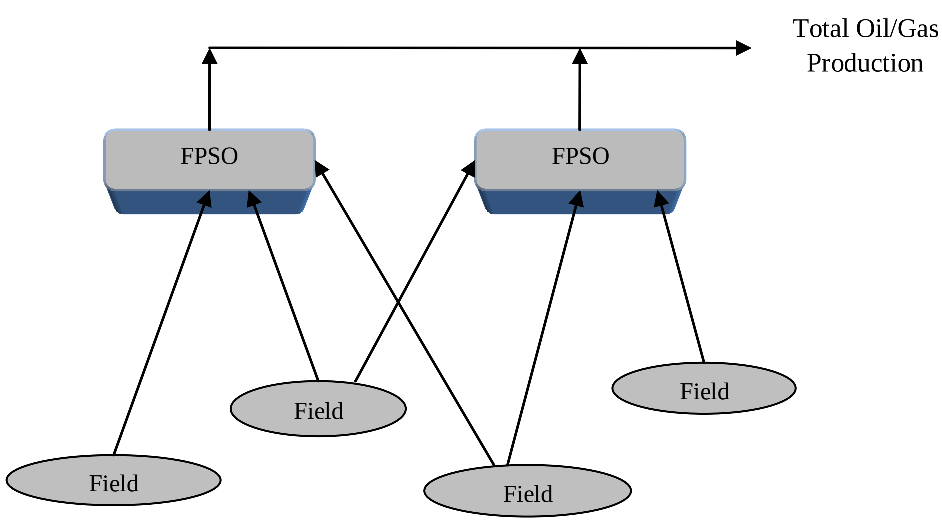


Figure 2.1: Typical Offshore Oilfield Infrastructure Representation

We assume in this work that the type of offshore facilities connected to fields to produce oil and gas are FPSOs with continuous capacities and ability to expand them in the future. These FPSO facilities costs multi-billion dollars each depending on their sizes and have the capability of operating in remote locations for very deep offshore oilfields (200m-2000m) where seabed pipelines are not cost effective. FPSOs are large ships that can process the produced oil and store until it is shipped to the onshore site or sales terminal. Processing includes the separation of oil, water and gas into individual streams using separators located at these facilities. Each FPSO facility has a lead time between the construction or expansion decision, and the actual availability. The wells are subsea wells in each field that are drilled using drilling ships. Therefore, there is no need to have a facility present to drill a subsea well. The only requirement to recover oil from it is that the well must be connected to a FPSO facility.

The facilities and connection involved in the offshore planning are often in operation over many years, and it is therefore important to take future conditions into consideration when designing an initial infrastructure or any expansions. This can be incorporated by dividing the planning horizon, for example, 20 years, into a number of time periods with a length of 1 year, and allowing investment and operating decisions in each period, which leads to a multi-period planning problem.

When oil is extracted from a reservoir oil deliverability, water-to-oil ratio (WOR) and gas-to-oil ratio (GOR) change nonlinearly as a function of the cumulative oil recovered from the reservoir. The initial oil and gas reserves in the reservoirs, as well as the relationships for WOR and GOR in terms of fractional oil recovery ($f_c$), are estimated from geologic studies. Figures 2.2 (a)–(c) represent the oil deliverability from a field per well, WOR and GOR versus fractional oil recovered from that field. We can see from these figures that there are different nonlinear field profiles for different field-FPSO connections to account for the variations in the flows for each of these possible connections.

The maximum oil flowrate (field deliverability) per well can be represented as a 3rd order polynomial equation (2.1) in terms of the fractional oil recovery. Furthermore, the actual oil flowrate ($x_f$ ) from each of the wells is restricted by both the field deliverability $Q_f^d$ , eq. (2.2), and facility capacity. We assume that there is no need for enhanced recovery, i.e., no need for injection of gas or water into the reservoir. The oil produced from the wells ($x_f$ ) contains water and gas and their relative rates depend on water-to-oil ratio ($wor_f$) and gas-to-oil ratio ($gor_f$) that are approximated using 3rd order polynomial functions in terms of fractional oil recovered (eqs. (2.3)-(2.4)). The water and gas flow rates can be calculated by multiplying the oil flowrate ($x_f$) with water-to-oil ratio and gas-to-oil ratio as in eqs. (2.5) and (2.6), respectively. Note that the reason for considering fractional oil recovery compared to cumulative amount of oil was to avoid numerical difficulties that could arise due to very small magnitude of the polynomial coefficients in that case.

$$Q_f^d = a_{1,f}(fc_{f,t})^3 + b_{1,f}(fc_f)^2 + c_{1,f}\, fc_f + d_1 \qquad \forall f \tag{2.1}$$

$$x_f \le Q_f^d \qquad \forall f \tag{2.2}$$

$$wor_f = a_{2,f}(fc_f)^3 + b_{2,f}(fc_f)^2 + c_{2,f}\, fc_f + d_{2,f} \qquad \forall f \tag{2.3}$$

$$gor_f = a_{3,f}(fc_f)^3 + b_{3,f}(fc_f)^2 + c_{3,f}\, fc_f + d_{3,f} \qquad \forall f \tag{2.4}$$

$$w_f = wor_f\, x_f \qquad \forall f \tag{2.5}$$

$$g_f = gor_f\, x_f \qquad \forall f \tag{2.6}$$

In Appendix A we derive the polynomial equations for the cumulative water and cumulative gas produced as a function of fractional oil recovery using equations (2.3) and (2.4), respectively, in order to avoid the bilinear terms (2.5)-(2.6) that are required in the model based on the above reservoir equations. Notice that in this chapter we focus on a multi-field site and include sufficient details in the model to account for the various trade-offs involved without going into much detail for each of these fields. However, the proposed model can easily be extended to include various facility types and other details in the oilfield development planning problem.

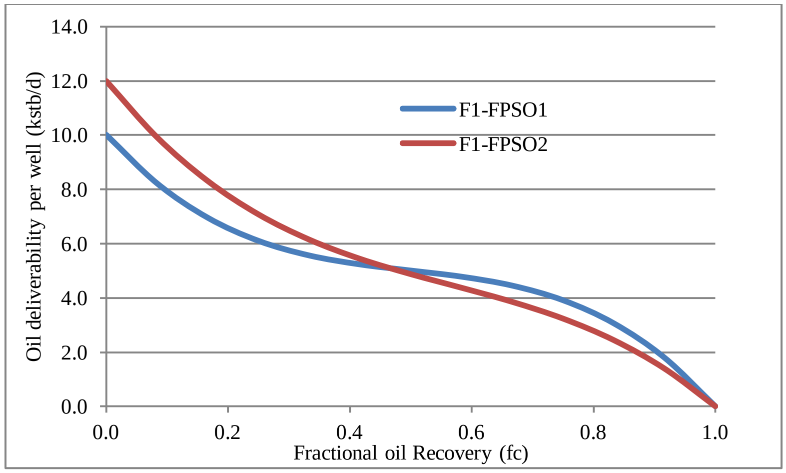


(a) Oil Deliverability per well for field (F1)

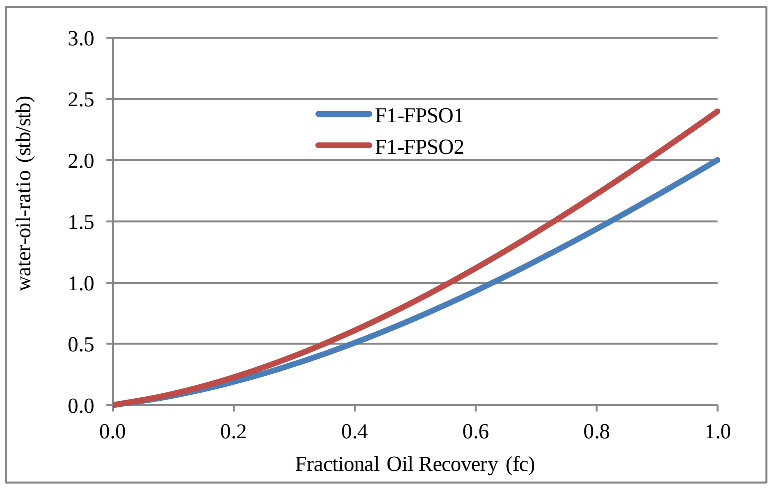


(b) Water to oil ratio for field (F1)

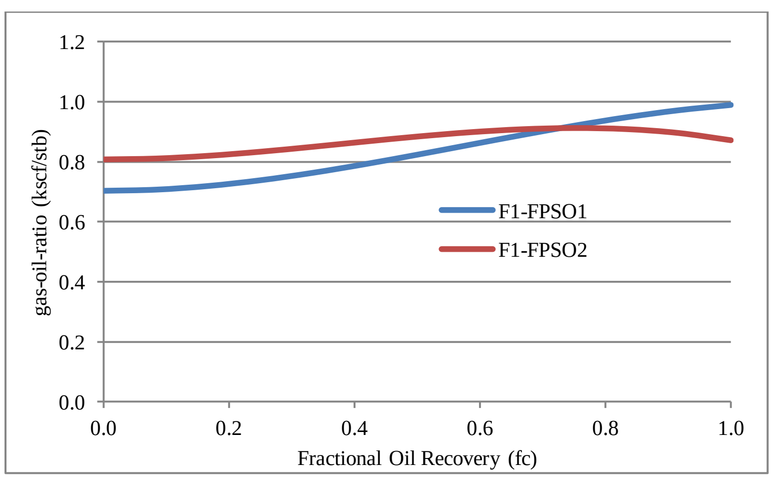


(c) Gas to oil ratio for field (F1)

Figure 2.2: Nonlinear Reservoir Characteristics for field (F1) for 2 FPSOs (FPSO 1 and 2)

The outline of this chapter is as follows. In section 2.2, we provide a formal description of the oilfield development problem considered that is formulated as an MINLP problem in section 2.3. The MINLP model is then reformulated as an MILP problem in section 2.4. Furthermore, section 2.5 introduces a procedure to reformulate both the models with reduced number of binary variables. Section 2.6 presents numerical results on the three realistic oilfield development cases involving up to 10 oilfields, 20 years of planning horizon and 84 wells, and compares the performance of the proposed models.

## 2.2 Problem Statement

Given is a typical offshore oilfield infrastructure consisting of a set of oil fields $F = \{1,2,\ldots\}$ available for producing oil using a set of FPSO (Floating, Production, Storage and Offloading) facilities, $FPSO = \{1,2,\ldots\}$, (see Figure 2.1). To produce oil from a field, it must be connected to a FPSO facility that can process the produced oil, store and offload it to the other tankers.

We assume that the location of each FPSO facility and its possible connections to the given fields are known (Figure 2.1). Notice that each FPSO facility can be connected to more than one field to produce oil while a field can only be connected to a single FPSO facility. In addition, the potential number of wells in each field is also given. There can be a significant amount of water and gas that comes out with the oil during the production process that needs to be considered while planning for FPSO capacity installations and expansions. The water is usually re-injected after separation from the oil while the gas can be sold in the market. In this case for simplicity we do not consider water or gas re-injection i.e. natural depletion of the reserves.

To develop and operate such a complex and capital intensive offshore oilfield infrastructure, we have to make the optimum investment and operation decisions to maximize the net present value considering a long-term planning horizon. The planning horizon is discretized into a number of time periods $t$, typically each with 1 year of duration. Investment decisions in each time period $t$ include which FPSO facilities should be installed or expanded, and their respective installation or expansion capacities for oil, liquid and gas, which fields should be connected to which FPSO facility, and the number of wells that should be drilled in a particular field *f* given the restrictions on the total number of wells that can be drilled in each time period *t* over all the given fields. Operating decisions include the oil/gas production rates from each field *f* in each time period *t*. It is assumed that all the installation and expansion decisions occur at the beginning of each time period *t*, while operation takes place throughout the time period. There is a lead time of $l_1$ years for each FPSO facility initial installation and a lead time of $l_2$ years for the expansion of an earlier installed FPSO facility. Once installed, we assume that the oil, liquid (oil and water) and gas capacities of a FPSO facility can be expanded only once.

Field deliverability, i.e. maximum oil flowrate from a field, WOR and GOR are approximated by a cubic equations, while cumulative water produced and cumulative gas produced from a field are represented by fourth order polynomials in terms of the fractional oil recovered from that field. Notice that these $4^{th}$ order polynomials correspond to the integration of the cubic equations for WOR and GOR as explained in Appendix A. The motivation for using polynomials for cumulative water produced and cumulative gas produced as compared to WOR and GOR is to avoid bilinear terms in the formulation and to allow converting the resulting model into an MILP formulation. Furthermore, all the wells in a particular field *f* are assumed to be identical for the sake of simplicity leading to the same reservoir profiles, eqs. (2.1)-(2.6), for each of these wells. However, the model can easily be extended to include different reservoir profiles for each of these wells for a specific field-FPSO connection, which may result in a significant increase in the computational effort due to the additional nonlinearities and constraints in the model.

## 2.3 MINLP Model

We present in this section a multiperiod MINLP model for the offshore oil and gas field infrastructure optimization problem. Reader should refer to the nomenclature section at the end of this chapter for the definitions of the various parameters and variables used in the model. The objective function (2.7) is to maximize the total net present value (NPV) of the project. Constraint (2.8) represents the overall NPV as a function of the difference between total revenue and total cost in each time period t taking the discount factors $d_t$ into account.

$$Max \quad NPV \tag{2.7}$$

$$NPV = \sum_t d_t (REV_t - COST_t) \tag{2.8}$$

The total revenues (2.9) in each time period t are computed based on the total amount of oil and gas produced in that time period and respective selling prices where total oil, water and gas flowrates in each time period t, ( $x_t^{tot}, w_t^{tot}, g_t^{tot}$ ) are calculated as the sum of the production rate of these components over all the FPSO facilities in equations (2.10)-(2.12), respectively.

$$REV_t = \delta_t (\alpha_t x_t^{tot} + \beta_t g_t^{tot}) \qquad \forall t \tag{2.9}$$

$$x_t^{tot} = \sum_{fpso} x_{fpso,t} \qquad \forall t \tag{2.10}$$

$$w_t^{tot} = \sum_{fpso} w_{fpso,t} \qquad \forall t \tag{2.11}$$

$$g_t^{tot} = \sum_{fpso} g_{fpso,t} \qquad \forall t \tag{2.12}$$

The total cost incurred in (2.13) is the sum of capital and operating expenses in each time period t. The overall capital expenses (2.14) consist of the fixed installation costs for FPSO facilities, variable installation and expansion costs corresponding to the FPSOs liquid and gas capacities, connection costs between a field and a FPSO facility and cost of drilling the wells for each field in each time period t. The total operating expenses (2.15) are the operation cost occurred corresponding to the total amount of liquid and gas produced in each time period t.

$$COST_t = CAP_t + OPER_t \qquad \forall t \tag{2.13}$$

$$CAP_t = \sum_{fpso}\Big[FC_{fpso,t} b_{fpso,t} + VC^{liq}_{fpso,t}(QI^{liq}_{fpso,t} + QE^{liq}_{fpso,t}) + VC^{gas}_{fpso,t}(QI^{gas}_{fpso,t} + QE^{gas}_{fpso,t})\Big]$$
$$+ \sum_{f}\sum_{fpso} FC^{C}_{f,fpso,t} b^{c}_{f,fpso,t} + \sum_{f} FC^{well}_{f,t} I^{well}_{f,t}$$
$$\forall t \qquad (2.14)$$

$$OPER_t = \delta_t\Big[OC^{liq}_t (x^{tot}_t + w^{tot}_t) + OC^{gas}_t g^{tot}_t\Big] \qquad \forall t \qquad (2.15)$$

Constraints (2.16)-(2.19) predict the reservoir behavior for each field $f$ in each time period t. In particular, constraint (2.16) restricts the oil flow rate from each well for a particular FPSO-field connection in time period t to be less than the deliverability (maximum oil flow rate) of that field per well where equation (2.17) represents the field deliverability per well at the beginning of time period t+1 for a particular FPSO-field connection as the cubic equation in terms of the fractional oil recovered by the end of time period t from that field. Constraint (2.17a) corresponds to the oil deliverability in time period 1 while (2.17b) represents for the rest of time periods in the planning horizon. Constraints (2.18) and (2.19) represent the value of water-to-oil and gas-to-oil ratios in time period t for a specific field-FPSO connection as cubic equations in terms of the fractional oil recovery by the end of previous time period, respectively.

$$x^{well}_{f,fpso,t} \le Q^{d,well}_{f,fpso,t} \qquad \forall f, fpso, t \qquad (2.16)$$

$$Q^{d,well}_{f,fpso,1} = d_{1,f,fpso} \qquad \forall f, fpso \qquad (2.17a)$$

$$Q^{d,well}_{f,fpso,t+1} = a_{1,f,fpso}(fc_{f,t})^3 + b_{1,f,fpso}(fc_{f,t})^2 + c_{1,f,fpso}\, fc_{f,t} + d_{1,f,fpso}$$
$$\forall f, fpso, t < |T| \qquad (2.17b)$$

$$wor_{f,fpso,t} = a_{2,f,fpso}(fc_{f,t-1})^3 + b_{2,f,fpso}(fc_{f,t-1})^2 + c_{2,f,fpso}\, fc_{f,t-1} + d_{2,f,fpso}$$
$$\forall f, fpso, t \qquad (2.18)$$

$$gor_{f,fpso,t} = a_{3,f,fpso}(fc_{f,t-1})^3 + b_{3,f,fpso}(fc_{f,t-1})^2 + c_{3,f,fpso} fc_{f,t-1} + d_{3,f,fpso} \qquad \forall f, fpso, t \qquad (2.19)$$

The predicted WOR and GOR values in equations (2.18) and (2.19) are further used in equations (2.20) and (2.21) to calculate the respective water and gas flowrates from field to FPSO in time period t by multiplying it with the corresponding oil flow rate. Notice that these equations give rise to the bilinear terms in the model.

$$w_{f,fpso,t} = wor_{f,fpso,t} x_{f,fpso,t} \qquad \forall f, fpso, t \qquad (2.20)$$

$$g_{f,fpso,t} = gor_{f,fpso,t} x_{f,fpso,t} \qquad \forall f, fpso, t \qquad (2.21)$$

The total oil flow rate in (2.22) from each field *f* in time period t is the sum of the oil flow rates that are directed to FPSO facilities in that time period t, whereas oil that is directed to a particular FPSO facility from a field *f* is calculated as the multiplication of the oil flow rate per well and number of wells available for production in that field, eq. (2.23).

$$x_{f,t} = \sum_{fpso} x_{f,fpso,t} \qquad \forall f, t \qquad (2.22)$$

$$x_{f,fpso,t} = N^{well}_{f,t} \cdot x^{well}_{f,fpso,t} \qquad \forall f, fpso, t \qquad (2.23)$$

Eq. (2.24) computes the cumulative amount of oil produced from field $f$ by the end of time period *t*, while (2.25) represents the fractional oil recovery by the end of time period *t*. The cumulative oil produced is also restricted in (2.26) by the recoverable amount of oil from the field.

$$xc_{f,t} = \sum_{\tau=1}^{t} (x_{f,\tau}\delta_\tau) \qquad \forall f, t \qquad (2.24)$$

$$fc_{f,t} = \frac{xc_{f,t}}{REC_f} \qquad \forall f, t \qquad (2.25)$$

$$xc_{f,t} \le REC_f \qquad \forall f, t \qquad (2.26)$$

Eqs. (2.27)-(2.29) compute total oil, water and gas flow rates into each FPSO facility, respectively, in time period t from all the given fields.

$$x_{fpso,t} = \sum_{f} x_{f,fpso,t} \qquad \forall fpso, t \qquad (2.27)$$

$$w_{fpso,t} = \sum_{f} w_{f,fpso,t} \qquad \forall fpso, t \qquad (2.28)$$

$$g_{fpso,t} = \sum_{f} g_{f,fpso,t} \qquad \forall fpso, t \qquad (2.29)$$

There are three types of capacities i.e. oil, liquid (oil and water) and gas that are used for modeling the capacity constraints for FPSO facilities. Specifically, constraints (2.30)-(2.32) restrict the total oil, liquid and gas flow rates into each FPSO facility to be less than its corresponding capacity in each time period t respectively. These three different kinds of capacities of a FPSO facility in time period *t* are computed by equalities (2.33)-(2.35) as the sum of the corresponding capacity at the end of previous time period t-1, installation capacity at the beginning of time period $t$-$l_1$ and expansion capacity at the beginning of time period $t$-$l_2$. Specifically, the term $QI^{oil}_{fpso,t-l_1}$ in equation (2.33) represents the oil capacity of a FPSO facility that started to install $l_1$ years earlier and is expected to be ready for production in time period *t*, to account for the lead time of $l_1$ years for a FPSO facility installation. The term $QE^{oil}_{fpso,t-l_1}$ represents the expansion decision in the oil capacity of an already installed FPSO facility that is taken $l_2$ years before time period t, to consider the lead time of $l_2$ years for capacity expansion. Similarly, the corresponding terms in equations (2.34) and (2.35) represent the lead times for liquid and gas capacity installation or expansion, respectively. Notice that due to one installation and expansion of a FPSO facility, $QI^{oil}_{fpso,t-l_1}$ and $QE^{oil}_{fpso,t-l_1}$ can have non-zero values only once in the planning horizon while $Q^{oil}_{fpso,t-1}$ can be non-zero in the multiple time periods.

$$x_{fpso,t} \leq Q^{oil}_{fpso,t} \qquad \forall fpso,t \qquad (2.30)$$

$$x_{fpso,t} + w_{fpso,t} \leq Q^{liq}_{fpso,t} \qquad \forall fpso,t \qquad (2.31)$$

$$g_{fpso,t} \leq Q^{gas}_{fpso,t} \qquad \forall fpso,t \qquad (2.32)$$

$$Q^{oil}_{fpso,t} = Q^{oil}_{fpso,t-1} + QI^{oil}_{fpso,t-l_1} + QE^{oil}_{fpso,t-l_2} \qquad \forall fpso,t \qquad (2.33)$$

$$Q^{liq}_{fpso,t} = Q^{liq}_{fpso,t-1} + QI^{liq}_{fpso,t-l_1} + QE^{liq}_{fpso,t-l_2} \qquad \forall fpso,t \qquad (2.34)$$

$$Q^{gas}_{fpso,t} = Q^{gas}_{fpso,t-1} + QI^{gas}_{fpso,t-l_1} + QE^{gas}_{fpso,t-l_2} \qquad \forall fpso,t \qquad (2.35)$$

Inequalities (2.36) and (2.37) restrict the installation and expansion of a FPSO facility to take place only once, respectively, while inequality (2.38) states that the connection between a FPSO facility and a field can be installed only once during the whole planning horizon. Inequality (2.39) ensures that a field can be connected to at most one FPSO facility in each time period t, while (2.40) states that at most one FPSO-field connection is possible for a field *f* during the entire planning horizon T due to engineering considerations. Constraints (2.41) and (2.42) state that the expansion in the capacity of a FPSO facility and the connection between a field and a FPSO facility, respectively, in time period t can occur only if that FPSO facility has already been installed by that time period.

$$\sum_{t \in T} b_{fpso,t} \leq 1 \qquad \forall fpso \qquad (2.36)$$

$$\sum_{t \in T} b^{ex}_{fpso,t} \leq 1 \qquad \forall fpso \qquad (2.37)$$

$$\sum_{t \in T} b^{c}_{f,fpso,t} \leq 1 \qquad \forall f, fpso \qquad (2.38)$$

$$\sum_{fpso} b^{c}_{f,fpso,t} \leq 1 \qquad \forall f, t \qquad (2.39)$$

$$\sum_{t \in T} \sum_{fpso} b^{c}_{f,fpso,t} \leq 1 \qquad \forall f \qquad (2.40)$$

$$b^{ex}_{fpso,t} \leq \sum_{\tau=1}^{t} b_{fpso,\tau} \qquad \forall fpso,t \qquad (2.41)$$

$$b^{c}_{f,fpso,t} \leq \sum_{\tau=1}^{t} b_{fpso,\tau} \qquad \forall f,fpso,t \qquad (2.42)$$

Inequality (2.43) states that the oil flow rate per well from a field *f* to a FPSO facility in time period t will be zero if that FPSO-field connection is not available in that time period. Notice that equations (2.23) and (2.43) ensure that for production from a field in time period t there must be a field-FPSO connection and at-least one well available in that field at the beginning of time period t. Constraints (2.44)-(2.49) are the upper-bounding constraints on the installation and expansion capacities for FPSO facilities in time period *t* corresponding to the three different kinds of capacities mentioned earlier.

$$x^{well}_{f,fpso,t} \leq U^{well,oil}_{f,fpso} \sum_{\tau=1}^{t} b^{c}_{f,fpso,\tau} \qquad \forall f,fpso,t \qquad (2.43)$$

$$QI^{oil}_{fpso,t} \leq U^{oil}_{fpso} b_{fpso,t} \qquad \forall fpso,t \qquad (2.44)$$

$$QI^{liq}_{fpso,t} \leq U^{liq}_{fpso} b_{fpso,t} \qquad \forall fpso,t \qquad (2.45)$$

$$QI^{gas}_{fpso,t} \leq U^{gas}_{fpso} b_{fpso,t} \qquad \forall fpso,t \qquad (2.46)$$

$$QE^{oil}_{fpso,t} \leq U^{oil}_{fpso} b^{ex}_{fpso,t} \qquad \forall fpso,t \qquad (2.47)$$

$$QE^{liq}_{fpso,t} \leq U^{liq}_{fpso} b^{ex}_{fpso,t} \qquad \forall fpso,t \qquad (2.48)$$

$$QE^{gas}_{fpso,t} \leq U^{gas}_{fpso} b^{\exp}_{fpso,t} \qquad \forall fpso,t \qquad (2.49)$$

The additional restrictions on the oil, liquid and gas expansion capacities of FPSO facilities, (2.50)-(2.52), come from the fact that these expansion capacities should be less than a certain fraction (μ) of the initial built capacities, respectively. Notice that available capacities in the previous time period can be used in the expression instead of initially built FPSO capacities given that only one installation and expansion is allowed for each of these facilities.

$$QE^{oil}_{fpso,t} \leq \mu Q^{oil}_{fpso,t-1} \qquad \forall fpso,t \qquad (2.50)$$

$$QE^{liq}_{fpso,t} \le \mu Q^{liq}_{fpso,t-1} \qquad \forall fpso,t \qquad (2.51)$$

$$QE^{gas}_{fpso,t} \le \mu Q^{gas}_{fpso,t-1} \qquad \forall fpso,t \qquad (2.52)$$

The number of wells available for the production from a field is calculated from (2.53) as the sum of the wells available at the end of previous time period and the number of wells drilled at the beginning of time period t. The maximum number of wells that can be drilled over all the fields during each time period t and in each field *f* during complete planning horizon T are restricted by respective upper bounds in (2.54) and (2.55). Notice that the important resource restriction due to the availability of drill rigs as in constraint (2.54) makes the proposed model more practical and useful. This restriction can easily be removed by relaxing this constraint if there are no drilling limitations. Moreover, the resulting model, which can be considered as a specific case of the proposed model, will most likely become easier to solve.

$$N^{well}_{f,t} = N^{well}_{f,t-1} + I^{well}_{f,t} \qquad \forall f,t \qquad (2.53)$$

$$\sum_f I^{well}_{f,t} \le UI^{well}_t \qquad \forall t \qquad (2.54)$$

$$N^{well}_{f,t} \le UN^{well}_f \qquad \forall f,t \qquad (2.55)$$

The non-convex MINLP model **(Model 1)** for offshore oilfield investment and operations planning involves constraint (2.7)-(2.55). In particular, constraints (2.17b)- (2.21) and (2.23) are nonlinear and non-convex constraints in the model that can lead to suboptimal solutions when solved with a method that assumes convexity.

In contrast to Model 1, the proposed MINLP model (**Model 2)** involves all the constraints as in Model 1 except (2.18)-(2.21) that are replaced with the reservoir profiles based on cumulative water and cumulative gas produced for each field-FPSO connection. The motivation for using polynomials for cumulative water produced and cumulative gas produced as compared to WOR and GOR is to avoid bilinear terms (2.20)-(2.21) in the formulation and allow converting the resulting MINLP model into an MILP formulation. In particular, the cumulative water and cumulative gas produced by the end of time period t from a field are represented by 4th order polynomial equations (2.56) and (2.57), respectively, in terms of fractional oil recovery by the end of time period t. Notice that these 4th order polynomials (2.56) and (2.57) correspond to the cubic equations for WOR and GOR, respectively, that are derived in Appendix A.

$$Q^{wc}_{f,fpso,t} = a_{2,f,fpso}(fc_{f,t})^4 + b_{2,f,fpso}(fc_{f,t})^3 + c_{2,f,fpso}(fc_{f,t})^2 + d_{2,f,fpso}\, fc_{f,t} \qquad \forall f, fpso, t \qquad (2.56)$$

$$Q^{gc}_{f,fpso,t} = a_{3,f,fpso}(fc_{f,t})^4 + b_{3,f,fpso}(fc_{f,t})^3 + c_{3,f,fpso}(fc_{f,t})^2 + d_{3,f,fpso}\, fc_{f,t} \qquad \forall f, fpso, t \qquad (2.57)$$

Notice that variables $Q^{wc}_{f,fpso,t}$ and $Q^{gc}_{f,fpso,t}$ will be non-zero in equations (2.56) and (2.57) if $fc_{f,t}$ is non-zero even though that particular field-FPSO connection is not present. Therefore, $Q^{wc}_{f,fpso,t}$ and $Q^{gc}_{f,fpso,t}$ represent dummy variables in equations (2.56) and (2.57) instead of actual cumulative water ( $wc_{f,fpso,t}$ ) and cumulative gas ( $gc_{f,fpso,t}$ ) recoveries due to the fact that only those cumulative water and cumulative gas produced can be non-zero that has the specific FPSO-field connection present in that time period t. Therefore, we introduce constraints (2.58)-(2.61) to equate the actual cumulative water produced, $wc_{f,fpso,t}$ , for a field-FPSO connection by the end of time period t to the corresponding dummy variable $Q^{wc}_{f,fpso,t}$ only if that field-FPSO connection is present in time period t else $wc_{f,fpso,t}$ is set to zero. Similarly, constraints (2.62)-(2.65) equate the actual cumulative gas produced, $gc_{f,fpso,t}$ , to the dummy variable $Q^{gc}_{f,fpso,t}$ only if that field-FPSO connection is present in time period t, otherwise it is set to zero. $M^{wc}_{f,fpso}$ and $M^{gc}_{f,fpso}$ correspond to maximum amount of cumulative water and gas that can be produced for a particular field and FPSO connection during the entire planning horizon, respectively. Note that the motivation for using dummy variables ( $Q^{wc}_{f,fpso,t}$ and $Q^{gc}_{f,fpso,t}$ ) for cumulative water and cumulative gas flows in equations (2.56)-(2.57) followed by big-M constraints (2.58)-(2.65), instead of using disaggregated variables for the fractional recovery in equations (2.56)-(2.57) directly, was to avoid large number of SOS1 variables while MILP reformulation of this model as explained in the next section.

$$wc_{f,fpso,t} \le Q^{wc}_{f,fpso,t} + M^{wc}_{f,fpso}(1-\sum_{\tau=1}^{t} b^{c}_{f,fpso,\tau}) \qquad \forall f,\ fpso,t \quad (2.58)$$

$$wc_{f,fpso,t} \ge Q^{wc}_{f,fpso,t} - M^{wc}_{f,fpso}(1-\sum_{\tau=1}^{t} b^{c}_{f,fpso,\tau}) \qquad \forall f,\ fpso,t \quad (2.59)$$

$$wc_{f,fpso,t} \le M^{wc}_{f,fpso}\sum_{\tau=1}^{t} b^{c}_{f,fpso,\tau} \qquad \forall f,\ fpso,t \quad (2.60)$$

$$wc_{f,fpso,t} \ge -M^{wc}_{f,fpso}\sum_{\tau=1}^{t} b^{c}_{f,fpso,\tau} \qquad \forall f,\ fpso,t \quad (2.61)$$

$$gc_{f,fpso,t} \le Q^{gc}_{f,fpso,t} + M^{gc}_{f,fpso}(1-\sum_{\tau=1}^{t} b^{c}_{f,fpso,\tau}) \qquad \forall f,\ fpso,t \quad (2.62)$$

$$gc_{f,fpso,t} \ge Q^{gc}_{f,fpso,t} - M^{gc}_{f,fpso}(1-\sum_{\tau=1}^{t} b^{c}_{f,fpso,\tau}) \qquad \forall f,\ fpso,t \quad (2.63)$$

$$gc_{f,fpso,t} \le M^{gc}_{f,fpso}\sum_{\tau=1}^{t} b^{c}_{f,fpso,\tau} \qquad \forall f,\ fpso,t \quad (2.64)$$

$$gc_{f,fpso,t} \ge -M^{gc}_{f,fpso}\sum_{\tau=1}^{t} b^{c}_{f,fpso,\tau} \qquad \forall f,\ fpso,t \quad (2.65)$$

Eq. (2.66) and (2.67) compute the water and gas flow rates in time period t from a field to FPSO facility as the difference of cumulative amounts produced by the end of current time period t and previous time period t-1 divided by the time duration of that period.

$$w_{f,fpso,t} = (wc_{f,fpso,t} - wc_{f,fpso,t-1})/\delta_t \qquad \forall f,\ fpso,t \quad (2.66)$$

$$g_{f,fpso,t} = (gc_{f,fpso,t} - gc_{f,fpso,t-1})/\delta_t \qquad \forall f,\ fpso,t \quad (2.67)$$

The non-convex MINLP model **(Model 2)** involves constraint (2.7)-(2.17) and (2.22)-(2.67) where constraints (2.17b), (2.56) and (2.57) are univariate polynomials while constraint (2.23) involves bilinear terms with integer variables. The correspondence between reservoir profiles for both the MINLP models and their comparison is presented in Appendices A and B, respectively. In the following section, we reformulate MINLP Model 2 into an MILP problem that can be solved to global optimality in an effective way. Notice that due to the presence of bilinear terms in equations (2.20) and (2.21), Model 1 cannot be reformulated into an MILP problem.

## 2.4 MILP Reformulation

The nonlinearities involved in **Model 2** include univariate polynomials (2.17b), (2.56), (2.57) and bilinear equations (2.23). In this section, we reformulate this model into an MILP model, **Model 3** using piecewise linearization and exact linearization techniques that can give the global solution of the resulting approximate problem.

To approximate the 3rd and 4th order univariate polynomials (2.17b), (2.56) and (2.57) SOS1 variables $b^{l}_{f,t}$ are introduced to select the adjacent points *l-1* and *l* for interpolation over an interval *l*. Constraints (2.68)-(2.71) represent the piecewise linear approximation for the fractional recovery and corresponding oil deliverability, cumulative water and cumulative gas produced for a field in each time period t, respectively, where $\widetilde{fc}^{l}$ , $\widetilde{Q}^{d,well,l}_{f,fpso}$ , $\widetilde{Q}^{wc,l}_{f,fpso}$ and $\widetilde{Q}^{gc,l}_{f,fpso}$ are the values of the corresponding variables at point *l* used in linear interpolation based on the reservoir profiles (2.17b), (2.56) and (2.57). Note that only $b^{l}_{f,t}$ variables are sufficient to approximate the constraints (2.17b), (2.56) and (2.57) by selecting a specific value of the fractional recovery for each field in each time period t that applies to all possible field-FPSO connections for that field. This avoids the requirement of a large number of SOS1 variables and resulting increase in the solution times that would have been required in the case if constraints

(2.56) and (2.57) were represented in terms of the disaggregated variables for fractional recovery in Model 2.

$$fc_{f,t} = \sum_{l=1}^{n} \lambda_{f,t}^{l} \tilde{fc}^{l} \qquad \forall f,t \qquad (2.68)$$

$$Q_{f,fpso,t+1}^{d,well} = \sum_{l=1}^{n} \lambda_{f,t}^{l} \tilde{Q}_{f,fpso}^{d,well,l} \qquad \forall f, fpso, t < |T| \qquad (2.69)$$

$$Q_{f,fpso,t}^{wc} = \sum_{l=1}^{n} \lambda_{f,t}^{l} \tilde{Q}_{f,fpso}^{wc,l} \qquad \forall f, fpso, t \qquad (2.70)$$

$$Q_{f,fpso,t}^{gc} = \sum_{l=1}^{n} \lambda_{f,t}^{l} \tilde{Q}_{f,fpso}^{gc,l} \qquad \forall f, fpso, t \qquad (2.71)$$

Equation (2.72) allows only one of the point *l* to be selected for which $b_{f,t}^{l}$ equals 1 while equation (2.73) states that $\lambda_{f,t}^{l}$ can be non-zero for only two consecutive points *l* and *l-1* that are used for convex combination during interpolation, eq. (2.74). Thus, the corresponding *l*th piece is used for linear interpolation as all other $\lambda_{f,t}^{l}$ are zero for a field in time period t and determines the value of the interpolated variable as a convex combination of their values at both the end of this piece *l* in equations (2.68)-(2.71).

$$\sum_{l=1}^{n-1} b_{f,t}^{l} = 1 \qquad \forall f,t \qquad (2.72)$$

$$\lambda_{f,t}^{l} \le b_{f,t}^{l-1} + b_{f,t}^{l} \qquad \forall f,t,l \qquad (2.73)$$

$$\sum_{l=1}^{n} \lambda_{f,t}^{l} = 1 \qquad \forall f,t \qquad (2.74)$$

The other nonlinear constraints (2.23) in Model 2 contain bilinear terms that can be linearized using exact linearization (Glover, 1975). To linearize constraint (2.23) we first express the integer variable, $N_{f,t}^{well}$, for the number of wells in terms of the binary variables $Z_{f,k,t}^{well}$ using eq. (2.75) where $Z_{f,k,t}^{well}$ determines the value of the *k*th term of the binary expansion.

$$N_{f,t}^{well} = \sum_k 2^{|k|-1} \cdot Z_{f,k,t}^{well} \qquad \forall f, t \qquad (2.75)$$

The bilinear term in constraint (2.23) can then be rewritten as follows,

$$x_{f,fpso,t} = \sum_k 2^{|k|-1} \cdot Z_{f,k,t}^{well} \cdot x_{f,fpso,t}^{well} \qquad \forall f, fpso, t \qquad (2.76)$$

Constraint (2.76) can be reformulated as a linear constraint (2.77) by introducing a nonnegative continuous variable $ZX_{f,fpso,k,t}^{well} = Z_{f,k,t}^{well} \cdot x_{f,fpso,t}^{well}$ which is further defined by constraints (2.78)-(2.81) by introducing an auxiliary variable $ZX1_{f,fpso,k,t}^{well}$.

$$x_{f,fpso,t} = \sum_k 2^{|k|-1} \cdot ZX_{f,fpso,k,t}^{well} \qquad \forall f, fpso, t \qquad (2.77)$$

$$ZX_{f,fpso,k,t}^{well} + ZX1_{f,fpso,k,t}^{well} = x_{f,fpso,t}^{well} \qquad \forall f, fpso, k, t \qquad (2.78)$$

$$ZX_{f,fpso,k,t}^{well} \le U_{f,fpso}^{well} Z_{f,k,t}^{well} \qquad \forall f, fpso, k, t \qquad (2.79)$$

$$ZX1_{f,fpso,k,t}^{well} \le U_{f,fpso}^{well} (1 - Z_{f,k,t}^{well}) \qquad \forall f, fpso, k, t \qquad (2.80)$$

$$ZX_{f,fpso,k,t}^{well} \ge 0, ZX1_{f,fpso,k,t}^{well} \ge 0 \qquad \forall f, fpso, k, t \qquad (2.81)$$

The reformulated MILP Model 3 involves constraints (2.7)-(2.16), (2.17a), (2.22), (2.24)-(2.55), (2.58)-(2.75) and (2.77)-(2.81) which are linear and mixed-integer linear constraints and allow to solve this approximate problem to global optimality using standard mixed-integer linear programming solvers.

**Remarks**

The previous two sections present a multiperiod MINLP model for the oilfield investment and operations planning problem for long-term planning horizon and its reformulation as an MILP model using linearization techniques. The MINLP models involve non-convexities and can yield suboptimal solutions when using an MINLP solver that relies on convexity assumptions, while the reformulated MILP model is guaranteed to be solved to global optimality using linear programming based branch and cut methods. However, given the difficulties involved in solving large scale instances of the MINLP and MILP models, especially due to the large number of binary variables, we extend these formulations by reducing the number of the binary variables. The next section describes the proposed procedure for binary reduction for MINLP and MILP formulations.

## 2.5 Reduced MINLP and MILP models

Due to the potential computational expense of solving the large scale MINLP and MILP models presented in the previous sections, we further reformulate them by removing many binary variables, namely $b^C_{f,fpso,t}$. These binary variables represent the timing of the connections between fields and FPSOs and are used for discounting the connection cost in the objective function along with some logic constraints in the proposed models. The motivation for binary reduction comes from the fact that in the solution of these models the connection cost is only ~2-3% of the total cost, and hence, this cost can be removed from the objective function as its exact discounting does not have a significant impact on the optimal solution. In particular, we propose to drop the index t from $b^C_{f,fpso,t}$, which results in a significant decrease in the number of binary variables (~33% reduction) and the solution time can be improved significantly for both the MINLP and MILP formulations.

Therefore, to formulate the reduced models that correspond to Model 2 and 3 we use the binary variables $b^R_{f,fpso}$ to represent the connection between field and FPSOs instead of using $b^C_{f,fpso,t}$ which results in a significant decrease in the number of binary variables in the model. As an example, for a field with 5 possible FPSO connections and 20 years planning horizon, the number of binary variables required can be reduced from 100 to 5. The connection cost term in the eq. (2.14) is also removed as explained above yielding constraint (2.82). Moreover, some of the constraints in the previous MINLP and MILP models that involve binary variables $b^C_{f,fpso,t}$ are reformulated to be valid for $b^R_{f,fpso}$ based reduced model, i.e. constraints (2.83)-(2.93). Notice that constraints (2.93) and

(2.23) ensure that the oil flow rate from a field to FPSO facility in time period t, $x_{f,fpso,t}$, will be non-zero only if that particular field-FPSO connection is installed and there is at-least one well available in that field for production in time period t, i.e. $b^R_{f,fpso}$ equals 1 and $N^{well}_{f,t}$ is non-zero, otherwise $x_{f,fpso,t}$ is set to zero. Moreover, it may be possible that variable $x^{well}_{f,fpso,t}$ can take non-zero value in equation (2.93) if $b^R_{f,fpso}$ equals 1 even though there is no well available in that field in time period t, but this will not have any effect on the solution given that the fractional recovery from a field and other calculations/constraints in the model are based on the actual amount of oil produced from the field, i.e. variable $x_{f,fpso,t}$ which is still zero in this case. Therefore, variable $x^{well}_{f,fpso,t}$ can be considered as a dummy variable in the reduced model.

$$CAP_t = \sum_{fpso}\left[FC_{fpso,t} b_{fpso,t} + VC^{liq}_{fpso,t}(QI^{liq}_{fpso,t} + QE^{liq}_{fpso,t}) + VC^{gas}_{fpso,t}(QI^{gas}_{fpso,t} + QE^{gas}_{fpso,t})\right] + \sum_{f} FC^{well}_{f,t} I^{well}_{f,t} \qquad \forall t \qquad (2.82)$$

$$wc_{f,fpso,t} \le Q^{wc}_{f,fpso,t} + M^{wc}_{f,fpso}(1 - b^R_{f,fpso}) \qquad \forall f, fpso, t \qquad (2.83)$$

$$wc_{f,fpso,t} \ge Q^{wc}_{f,fpso,t} - M^{wc}_{f,fpso}(1 - b^R_{f,fpso}) \qquad \forall f, fpso, t \qquad (2.84)$$

$$wc_{f,fpso,t} \le M^{wc}_{f,fpso} b^R_{f,fpso} \qquad \forall f, fpso, t \qquad (2.85)$$

$$wc_{f,fpso,t} \ge -M^{wc}_{f,fpso} b^R_{f,fpso} \qquad \forall f, fpso, t \qquad (2.86)$$

$$gc_{f,fpso,t} \le Q^{gc}_{f,fpso,t} + M^{gc}_{f,fpso}(1 - b^R_{f,fpso}) \qquad \forall f, fpso, t \qquad (2.87)$$

$$gc_{f,fpso,t} \ge Q^{gc}_{f,fpso,t} - M^{gc}_{f,fpso}(1 - b^R_{f,fpso}) \qquad \forall f, fpso, t \qquad (2.88)$$

$$gc_{f,fpso,t} \le M^{gc}_{f,fpso} b^R_{f,fpso} \qquad \forall f, fpso, t \qquad (2.89)$$

$$gc_{f,fpso,t} \geq -M^{gc}_{f,fpso} b^R_{f,fpso} \qquad \forall f, fpso, t \quad (2.90)$$

$$\sum_{fpso} b^R_{f,fpso} \leq 1 \qquad \forall f \quad (2.91)$$

$$b^R_{f,fpso} \leq \sum_{\tau=1}^{t} b_{fpso,\tau} \qquad \forall f, fpso, t \quad (2.92)$$

$$x^{well}_{f,fpso,t} \leq U^{well,oil}_{f,fpso} b^R_{f,fpso} \qquad \forall f, fpso, t \quad (2.93)$$

The non-convex MINLP **Model 2R** for offshore oilfield investment and operations planning after binary reduction involves constraints (2.7)-(2.13), (2.15)-(2.17), (2.22)-(2.37), (2.41), (2.44)-(2.57), (2.66)-(2.67) and (2.82)-(2.93). The reformulated MILP **Model 3R** after binary reduction involves constraints (2.7)-(2.13), (2.15)-(2.16), (2.17a), (2.22), (2.24)-(2.37), (2.41), (2.44)-(2.55), (2.66)-(2.75) and (2.77)-(2.93) which are linear and mixed-integer linear constraints. Similarly, **Model 1R** corresponds to the non-convex MINLP model, which is based on WOR and GOR expressions after binary reduction as described above.

The resulting reduced models with fewer binaries can be solved much more efficiently as compared to the original models. To calculate the discounted cost of connections between field and FPSOs that corresponds to the reduced model solution, we use the well installation schedule $N^{well}_{f,t}$ from the optimal solution of reduced models to find the Field-FPSO connection timing and subtract the corresponding discounted connection cost from the optimal NPV of the reduced model. The resulting NPV represents the optimal NPV of the original models in case connection costs are relatively small.

## 2.6 Numerical Results

In this section we present 3 instances of the oilfield planning problem where we consider from 3 to 10 fields while the time horizon ranges from 10 to 20 years. The maximum number of possible FPSOs is taken 3 in all the instances. We compare the computational results of the various MINLP and MILP models proposed in the previous sections for these 3 instances. Table 2.1 summarizes the main features of these MINLP and reformulated MILP models. In particular, the reservoir profiles and respective nonlinearities involved in the models are compared in the table.

Table 2.1: Comparison of the nonlinearities involved in 3 model types

| | **Model 1** | **Model 2** | **Model 3** |
|---|---|---|---|
| **Model Type** | MINLP | MINLP | MILP |
| **Oil Deliverability** | 3rd order polynomial | 3rd order polynomial | Piecewise Linear |
| **WOR** | 3rd order polynomial | - | - |
| **GOR** | 3rd order polynomial | - | - |
| **wc** | - | 4th order polynomial | Piecewise Linear |
| **gc** | - | 4th order polynomial | Piecewise Linear |
| **Bilinear Terms** | N*x<br>x*WOR<br>x*GOR | N*x | None |
| **MILP Reformulation** | Not Possible | Possible | Reformulated MILP |

### 2.6.1 Instance 1

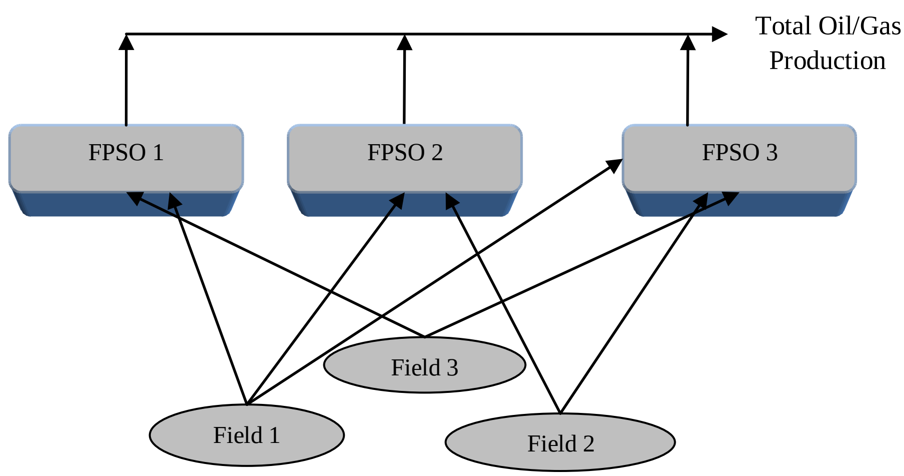


Figure 2.3: Instance 1 (3 Fields, 3 FPSOs, 10 years)

In this instance (Figure 2.3) we consider 3 oil fields that can be connected to 3 FPSOs with 7 possible connections among these fields and FPSOs. There are a total of 25 wells that can be drilled, and the planning horizon considered is 10 years, which is discretized into 10 periods of each 1 year of duration. We need to determine which of the FPSO facilities is to be installed or expanded, in what time period, and what should be its capacity of oil, liquid and gas, to which fields it should be connected and at what time, and the number of wells to be drilled in each field during each time period. Other than these installation decisions, there are operating decisions involving the flowrate of oil, water and gas from each field in each time period. The objective function is to maximize total NPV over the given planning horizon.

The problem is solved using DICOPT 2x-C solver for Models 1 and 2, and CPLEX 12.2 for Model 3. These models were implemented in GAMS 23.6.3 and run on Intel Core i7 machine. The optimal solution of this problem that corresponds to Model 2, suggests installing only FPSO 3 with a capacity of 300 kstb/d, 420.01 kstb/d and 212.09 MMSCF/d for oil, liquid and gas, respectively, at the beginning of time period 1. All the three fields are connected to this FPSO facility at time period 4 when installation of the FPSO facility is completed and a total of 20 wells are drilled in these 3 fields in that time period to start production. One additional well is drilled in field 3 in time period 5 and there are no expansions in the capacity of FPSO facility. The total NPV of this project is $6912.04 M.

Table 2.2: Performance of various solvers with Model 1 and 2 for Instance 1

| | **Model 1** | | **Model 2** | |
|---|---|---|---|---|
| Constraints | 1,357 | | 1,997 | |
| Continuous Var. | 1,051 | | 1,271 | |
| Discrete Var. | 151 | | 151 | |
| Solver | Optimal NPV (million$) | Time (s) | Optimal NPV (million$) | Time (s) |
| DICOPT | 6980.92 | 3.56 | 6912.04 | 3.07 |
| SBB | 7038.26 | 211.53 | 6959.06 | 500.64 |
| BARON 9.0.6 | 6983.65 | >36,000 | 6919.28 | >36,000 |

Table 2.2 compares the computational results of Model 1 and 2 for this instance with various MINLP solvers. Notice that based on the computational experiments, we only include those global/local MINLP solvers that were performing reasonably well as compared to the other solvers. We can observe from these results that DICOPT performs best among all the MINLP solvers in terms of computational time, while solving directly both Models 1 and 2. The number of OA iterations required is approximately 3-4 in both cases, and solving Model 2 is slightly easier than solving Model 1 directly with this solver.

However, the solutions obtained are not guaranteed to be the global solution. SBB is also reasonable in terms of solution quality but it takes much longer time to solve. BARON 9.0.6 can in principle find the global optimum solution to models 1 and 2, but it is very slow and takes more than 36,000s to be within ~23% and ~10% of optimality gap for these models, respectively. Note that we use the DICOPT solution to initialize in this case, but BARON 9.0.6 could only provide a slightly better solution (6983.65 vs. 6980.92 and 6919.28 vs. 6912.04) than DICOPT in more than 10 hours for both cases.

Table 2.3: Comparison of models 1, 2 and 3 with and without binary reduction

| | **Model 1** | **Model 1R** | **Model 2** | **Model 2R** | **Model 3** | **Model 3R** |
|---|---|---|---|---|---|---|
| Constraints | 1,357 | 1,320 | 1,997 | 1,960 | 3,094 | 3,057 |
| Continuous Var. | 1,051 | 988 | 1,271 | 1,208 | 2,228 | 2,165 |
| Discrete Var. | 151 | 109 | 151 | 109 | 219 | 177 |
| SOS1 Var. | 0 | 0 | 0 | 0 | 120 | 120 |
| NPV(million$) | 6980.92 | 7049.54 | 6912.04 | 6919.28 | 7030.90 | 7030.90 |
| Time(s) | 3.56 | 1.55 | 3.07 | 2.85 | 37.03 | 6.55 |

*Model 1 and 2 solved with DICOPT 2x-C, Model 3 solved with CPLEX 12.2

The performance of Models 1 and 2 are compared before and after reducing the binary variables for connection, i.e. Models 1R and 2R, in Table 2.3. There is one third reduction in the number of binary variables for both models. It can also be seen that there is a significant decrease in the solution time after binary reduction (for e.g. 1.55s vs. 3.56s for Model 1). Moreover, the reduced models also yield better local solutions too for both the MINLP formulations. Notice that these MINLP Models are solved with DICOPT here for comparison as it is much faster as compared to other solvers as seen from the previous results.

The MILP Model 3 and its binary reduction Model 3R that are formulated from Model 2 and Model 2R, respectively, solved with CPLEX 12.2 and results in Table 2.3 show the significant reduction in the solution time after binary reduction (6.55s vs. 37.03s) while both the models give same optimal NPV i.e. $7030.90M. Notice that these approximate MILP models are solved to global optimality in few seconds while global solution of the original MINLP formulations is much expensive to obtain. Although the higher the number of points for the approximate MILP model the better will be the solution quality, but we found that beyond 5 points at equal distance for the piecewise approximation there was not much significant change in the optimal solution, while it led to large increases in the solution time due to increase in the SOS1 variables in the model. Therefore, we use 5 equal distance points for piecewise linearization to formulate Model 3 and 3R for all the instances.

The global solution from the MILP approximation Model 3R gives a higher NPV for this example as compared to solving Model 2 directly (7030.90 vs. 6912.04). Therefore, this model can potentially be used for finding global or near optimal solution to the MINLP formulation. We fix the discrete variables coming from Model 3R in the original Models 1 and 2 (MINLPs) and solve the resulting NLPs. The local solutions obtained in this manner are significantly better for these MINLP models, i.e. 7076.62 vs. 6980.92 for Model 1 and 7004.08 vs. 6912.04 for Model 2. Notice also that no other solver could find the better solutions directly in reasonable computational time as can be seen from Table 2.2. Moreover, it is interesting to note that the discrete decisions that come from the MILPs that corresponds to Model 2 seems to be optimal for Model 1 too which ensures the close correspondence between Models 1 and 2 and its reformulations.

### 2.6.2 Instance 2

This is a slightly larger instance for oilfield planning problem than the previous one where we consider 5 oil fields that can be connected to 3 FPSOs with 11 possible connections. There are a total of 31 wells that can be drilled in all of these 5 fields and the planning horizon considered is 20 years. Table 2.4 compares the results of Model 1 and 2 with various MINLP solvers for this example. DICOPT still performs best even for this larger instance in terms of solution quality and time. SBB, which relies on a branch and bound based scheme, becomes very slow due to the increase in the number of binary variables and problem size. BARON also becomes expensive to solve this larger instance and could not improve the DICOPT solution that is used for its initialization for both cases in more than 10 hours.

Table 2.4: Comparison of various models and solvers for Instance 2

| | **Model 1** | | **Model 2** | |
|---|---|---|---|---|
| Constraints | 3,543 | | 5,543 | |
| Continuous Var. | 2,781 | | 3,461 | |
| Discrete Var. | 477 | | 477 | |
| Solver | Optimal NPV (million$) | Time (s) | Optimal NPV (million$) | Time (s) |
| DICOPT | 11412.48 | 58.53 | 11204.86 | 18.43 |
| SBB | 11376.57 | 1057.68 | 11222.34 | 3309.73 |
| BARON 9.0.6 | 11412.48 | >36,000 | 11204.86 | >36,000 |

There are significant improvements in computational times for Model 1 and 2 after binary reduction as can be seen in Table 2.5 (5.69s vs. 58.53s and 9.92s vs. 18.43s). Moreover, there are possibilities to find even better local solution too from the reduced model as in the case of Model 2. The reduced models (Model 1R and 2R) should yield the same optimal solutions as the original models (Model 1 and 2), respectively, for small connection costs but there are slight differences in the NPV values reported in Table 2.5 as these models are solved here with DICOPT that gives the local solutions. The reformulated MILP after binary reduction Model 3R becomes slightly expensive to solve as compared to finding local solutions for the original MINLP models, but the solution obtained in this case is the global one (within 2% optimality tolerance). Notice that the MILP solutions can be either lower (instance 1) or higher (instance 2) than the global optimal for MINLP models as these involve approximations of the three functions, i.e. oil deliverability, cumulative water and cumulative gas produced. Therefore, the resulting MILP can over or underestimate the original NPV function. We do not present the result of Model 3 here as it gives the same NPV as Model 3R but at a much higher computational expense since a larger number of binary variables is involved in the model.

Note that some of the binary variables are pre-fixed in all of the models considered based on the earliest installation time of the FPSO facilities and corresponding limitations on the FPSO expansions, field-FPSO connections and drilling of the wells in the fields that improves the computational performance of these models. The solution of Model 3R can also be used to fix discrete variables in the MINLPs to obtain near optimal solutions to the original problem as done for instance 1. The solutions of the NLPs obtained after fixing binary decisions in Model 1 and 2 are 11412.48 and 11356.31 respectively. We can observe that none of the solver in Table 2.4 could provide better NPV values than this case. Overall, we can say that the results for this larger instance also show similar trends as what is observed for instance 1.

Table 2.5: Comparison of models 1, 2 and 3 with and without binary reduction

| | **Model 1** | **Model 1R** | **Model 2** | **Model 2R** | **Model 3R** |
|---|---|---|---|---|---|
| Constraints | 3,543 | 3,432 | 5,543 | 5,432 | 8,663 |
| Continuous Var. | 2,781 | 2,572 | 3,461 | 3,252 | 6,103 |
| Discrete Var. | 477 | 301 | 477 | 301 | 451 |
| SOS1 Var. | 0 | 0 | 0 | 0 | 400 |
| NPV(million$) | 11412.48 | 11335.01 | 11204.86 | 11294.82 | 11259.61 |
| Time(s) | 58.53 | 5.69 | 18.43 | 9.92 | 871.80 |

*Model 1 and 2 solved with DICOPT 2x-C, Model 3 solved with CPLEX 12.2

### 2.6.3 Instance 3

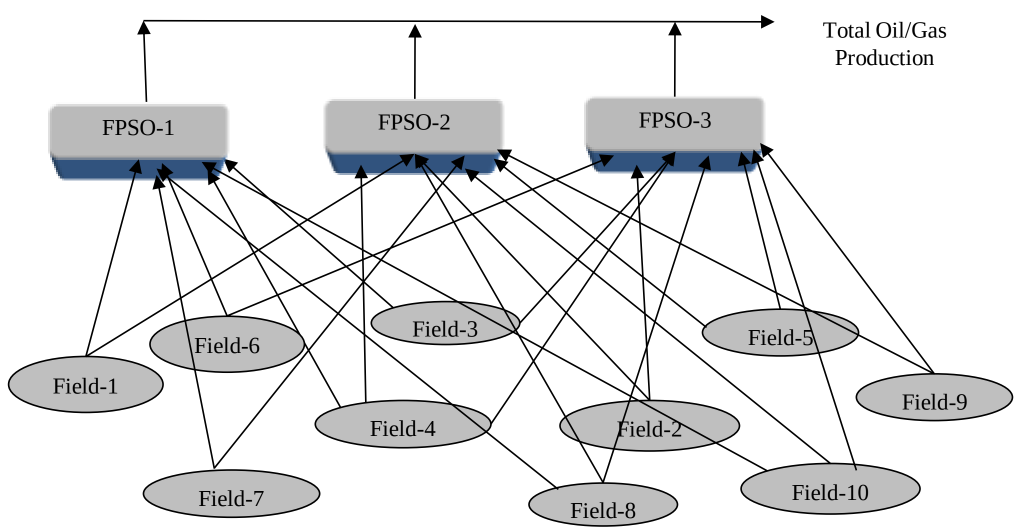


Figure 2.4: Instance 3 (10 Fields, 3 FPSOs, 20 years)

In this instance we consider 10 oil fields (Figure 2.4) that can be connected to 3 FPSOs with 23 possible connections. There are a total of 84 wells that can be drilled in all of these 10 fields and the planning horizon considered is 20 years.

The optimal solution of this problem that corresponds to Model 2R solved with DICOPT 2x-C, suggests to install all the 3 FPSO facilities in the first time period with their respective liquid (Figure 2.5-a) and gas (Figure 2.5-b) capacities. These FPSO facilities are further expanded in future when more fields come online or liquid/gas flow rates increases as can be seen from these figures.

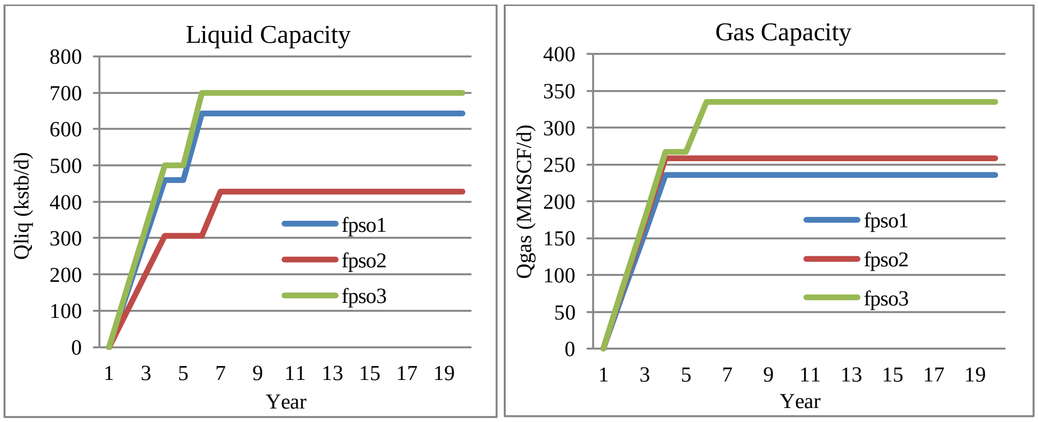


(a) Liquid capacities of FPSOs (b) Gas capacities of FPSOs

Figure 2.5: FPSO installation and expansion schedule

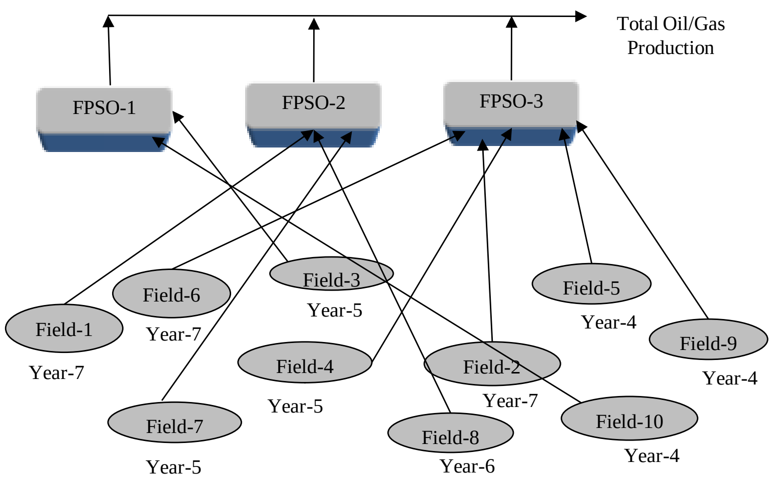


Figure 2.6: FPSO-field connection schedule

After initial installation of the FPSO facilities by the end of time period 3, these are connected to the various fields to produce oil in their respective time periods for coming online as indicated in Figure 2.6. The well drilling schedule for these fields in Figure 2.7 ensures that the maximum number of wells drilling limit and maximum potential wells in a field are not violated in each time period t.

We can observe from these results that most of the installation and expansions are in the first few time periods of the planning horizon.

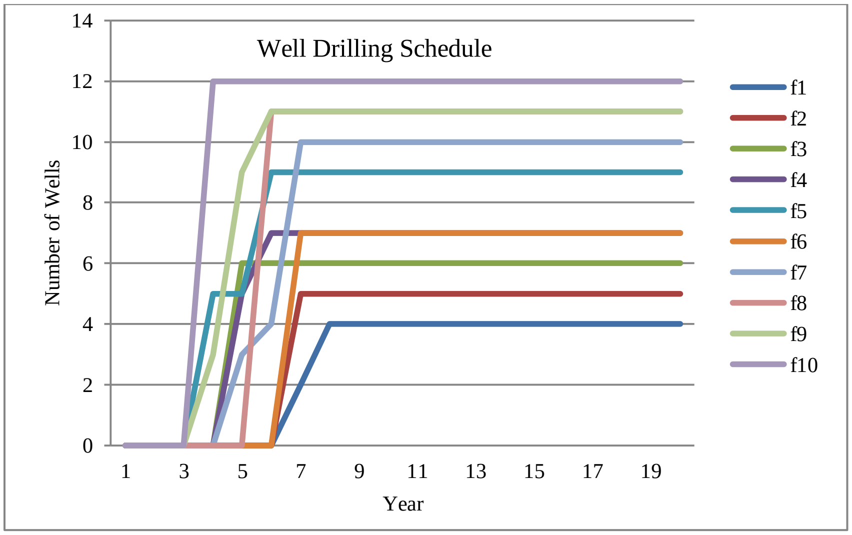


Figure 2.7: Well drilling schedule for fields

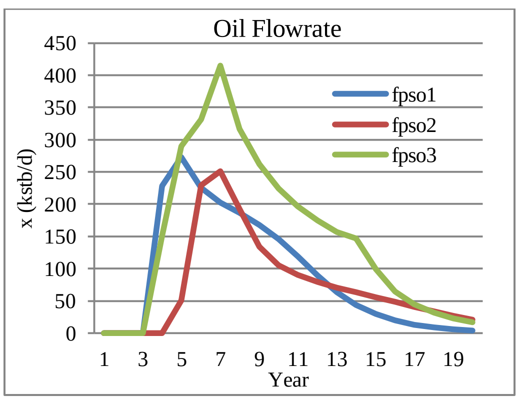


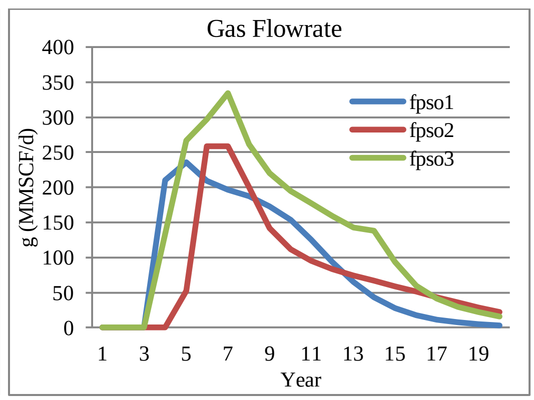


(a) Total oil flowrates from FPSO's (b) Total gas flowrates from FPSO's

Figure 2.8: Total flowrates from each FPSO facility

Other than these investment decisions, the operations decisions are the production rates of oil and gas from each of the fields, and hence, the total flow rates for the installed FPSO facilities that are connected to these fields as can be seen from Figures 2.8 (a)-(b). Notice that the oil flow rates increases initially until all the fields come online and then they start to decrease as the oil deliverability decreases when time progresses. Gas flow rate, which depends on the amount of oil produced, also follows a similar trend. The total NPV of the project is $30946.39M.

Table 2.6: Comparison of various models and solvers for Instance 3

| | **Model 1** | | **Model 2** | |
|---|---|---|---|---|
| Constraints | 5,900 | | 10,100 | |
| Continuous Var. | 4,681 | | 6,121 | |
| Discrete Var. | 851 | | 851 | |
| Solver | Optimal NPV (million$) | Time (s) | Optimal NPV (million$) | Time (s) |
| DICOPT | 31297.94 | 132.34 | 30562.95 | 114.51 |
| SBB | 30466.36 | 4973.94 | 30005.33 | 18152.03 |
| BARON 9.0.6 | 31297.94 | >72,000 | 30562.95 | >72,000 |

Table 2.7: Comparison of models 1, 2 and 3 with and without binary reduction

| | **Model 1** | **Model 1R** | **Model 2** | **Model 2R** | **Model 3R** |
|---|---|---|---|---|---|
| Constraints | 5,900 | 5,677 | 10,100 | 9,877 | 17,140 |
| Continuous Var. | 4,681 | 4,244 | 6,121 | 5,684 | 12,007 |
| Discrete Var. | 851 | 483 | 851 | 483 | 863 |
| SOS1 Var. | 0 | 0 | 0 | 0 | 800 |
| NPV(million$) | 31297.94 | 30982.42 | 30562.95 | 30946.39 | 30986.22 |
| Time(s) | 132.34 | 53.08 | 114.51 | 67.66 | 16295.26 |

*Model 1 and 2 solved with DICOPT 2x-C, Model 3 with CPLEX 12.2

Tables 2.6-2.7 represent the results for the various model types considered for this instance. We can draw similar conclusions as discussed for instances 1 and 2 based on these results. DICOPT performs best in terms of solution time and quality, even for the largest instance compared to other solvers as can be seen from Table 2.6. There are significant computational savings with the reduced models as compared to the original ones for all the model types in Table 2.7. Even after binary reduction of the reformulated MILP, Model 3R becomes expensive to solve, but yields global solutions, and provides a good discrete solution to be fixed/initialized in the MINLPs for finding better solutions.

The optimal NPV that come from the Models 1 and 2 after fixing discrete variables based on the MILP solution (even though it was solved within 10% of optimality tolerance) are $31329.81 M and $31022.48M, respectively. These are the best solutions among all other solutions obtained in Table 2.6 for the respective MINLPs. Notice that although the advantage from using the MILP formulation in terms of the NPV value is not very significant for this instance since the required solution time is large, but it does yield a global solution that is difficult to obtain for the MINLPs. In addition, when we increase the complexity of the basic deterministic model such as to fiscal contracts and/or stochastic model, the advantage of MILP formulation becomes more apparent due to the availability of the robust MILP solvers compared to MINLP.

**Remarks**

(a) The optimal NPV of both models 1 and 2 are very close (within ~1-3%) for all the instances. Moreover, the difference is even smaller when we compare the global solutions and they tend to have identical discrete decisions at the optimal solution. Hence, in principle we can use either of these models for the oilfield problem directly or with some other method. However, since Model 1 involves a large number of non-convexities because of the extra bilinear terms in equations (2.20)-(2.21), it is more prone to converging to local solutions, and may need good initializations as compared to Model 2. Moreover, as opposed to Model 2, it is not possible to convert Model 1 to an MILP model that can be solved to global optimality.

(b) Model 2 is more accurate in terms of physical representation of water and gas flow profiles than Model 1 as explained in Appendix B, especially when the length of each time period is large. Model 1 usually overestimates the NPV as it assumes constant GOR and WOR for a time period t while extracting the oil from a field during that time period, where WOR and GOR are calculated based on the fractional recovery by the end of time period t-1, i.e. point estimates are used for WOR and GOR. On the other hand, Model 2 estimates the cumulative water and gas flow rates at the end of time period t taking into account the amount of oil produced in that time period and variability of WOR and GOR during current time period t i.e. average values of WOR and GOR over the time period. Because of the general trend of increasing WOR and GOR as time progresses and hence underestimating the actual water and gas flow rates in Model 1 during each time period t due to point estimates for

WOR and GOR at the end of time t-1, it yields a slightly higher NPV as can be seen from the solutions obtained. In contrast, if WOR and GOR are estimated at the end of time period t instead t-1, the solutions from Model 1 should give lower NPV values as compared to Model 2.

## 2.7 Conclusions

In this chapter, we have proposed a new deterministic MINLP model for offshore oilfield infrastructure planning considering multiple fields, three components (oil, water and gas) explicitly in the formulation, facility expansions decisions and nonlinear reservoir profiles. The model can determine the installation and expansion schedule of facilities and respective oil, liquid and gas capacities, connection between the fields and FPSO's, well drilling schedule and production rates of oil, water and gas simultaneously in a multiperiod setting. The resulting model yields good solutions to the realistic instances when solving with DICOPT directly. Furthermore, the model is reformulated into an MILP using piecewise linearization and exact linearization techniques with which the problem can be solved to global optimality in a more consistent manner. The proposed MINLP and MILP formulations are further improved by using a binary reduction scheme resulting in the improved local solutions and more than an order of magnitude reduction in the solution times. Realistic instances involving 10 fields, 3 FPSOs and 20 years planning horizon have been solved to compare the computational performance of the proposed MINLP and MILP formulations. The models presented here are very general and can either be used for simplified cases (e.g. linear profiles for reservoir, fixed well schedule etc.) or extended to include other complexities.

## Nomenclature

### Indices

| | |
|---|---|
| *t, τ* | time periods, $t, \tau \in T$ |
| *f* | field |
| *fpso* | FPSO facility |

**Integer Variables**

| | |
|---|---|
| $I_{f,t}^{well}$ | Number of wells drilled in field *f* at the beginning of time period t |
| $N_{f,t}^{well}$ | Number of wells available in field *f* for production in time period t |

**Binary Variables**

| | |
|---|---|
| $b_{fpso,t}$ | whether or not FPSO facility *fpso* is installed at the beginning of time period *t* |
| $b_{fpso,t}^{ex}$ | whether or not FPSO facility *fpso* is expanded at the beginning of time period *t* |
| $b_{f,fpso,t}^{C}$ | whether or not a connection between field *f* and FPSO facility *fpso* is installed at the beginning of time period *t* |
| $b_{f,fpso,t}^{R}$ | whether or not a connection between field *f* and FPSO facility *fpso* is installed |

**Continuous Variables**

| | |
|---|---|
| $NPV$ | net present value |
| $REV_t$ | total revenues in time period *t* |
| $COST_t$ | total costs in time period *t* |
| $CAP_t$ | total capital costs in time period *t* |
| $OPER_t$ | total operating costs in time period *t* |
| $x_t^{tot}$ | total oil flow-rate in time period *t* |
| $w_t^{tot}$ | total water flow-rate in time period *t* |
| $g_t^{tot}$ | total gas flow-rate in time period *t* |
| $x_{f,t}$ | oil production rate from field *f* in time period *t* |
| $w_{f,t}$ | water production rate from field *f* in time period *t* |
| $g_{f,t}$ | gas production rate from field *f* in time period *t* |

$xc_{f,t}$ cumulative oil produced from field *f* by the end of time period *t*

$wc_{f,fpso,t}$ cumulative water produced from field *f* to FPSO facility *fpso* by the end of time period *t*

$gc_{f,fpso,t}$ cumulative gas produced from field *f* to FPSO facility *fpso* by the end of time period *t*

$fc_{f,t}$ fraction of oil recovered from field *f* by the end of time period *t*

$x^{well}_{f,fpso,t}$ oil flow rate per well from field *f* to FPSO facility *fpso* in time period *t*

$Q^{d,well}_{f,fpso,t}$ field deliverability (maximum oil flow rate) per well for field *f* and FPSO facility *fpso* combination in time period *t*

$Q^{wc}_{f,fpso,t}$ dummy variable for cumulative water produced from field *f* to FPSO facility *fpso* by the end of time period *t*

$Q^{gc}_{f,fpso,t}$ dummy variable for cumulative gas produced from field *f* to FPSO facility *fpso* by the end of time period *t*

$x_{fpso,t}$ total oil flow rate into FPSO facility *fpso* in time period *t*

$w_{fpso,t}$ total water flow rate into FPSO facility *fpso* in time period *t*

$g_{fpso,t}$ total gas flow rate into FPSO facility *fpso* in time period *t*

$x_{f,fpso,t}$ total oil flow rate from field *f* to FPSO facility *fpso* in time period *t*

$w_{f,fpso,t}$ total water flow rate from field *f* to FPSO facility *fpso* in time period *t*

$g_{f,fpso,t}$ total gas flow rate from field *f* to FPSO facility *fpso* in time period *t*

$Q^{oil}_{fpso,t}$ oil processing capacity of FPSO facility *fpso* in time period *t*

$Q^{liq}_{fpso,t}$ liquid (oil and water) capacity of FPSO facility *fpso* in time period *t*

$Q_{fpso,t}^{gas}$ gas capacity of FPSO facility *fpso* in time period *t*

$QI_{fpso,t}^{oil}$ oil installation capacity of FPSO facility *fpso* at the beginning of time period *t*

$QI_{fpso,t}^{liq}$ liquid installation capacity of FPSO facility *fpso* at the beginning of time period *t*

$QI_{fpso,t}^{gas}$ gas installation capacity of FPSO facility *fpso* at the beginning of time period *t*

$QE_{fpso,t}^{oil}$ oil expansion capacity of FPSO facility *fpso* at the beginning of time period *t*

$QE_{fpso,t}^{liq}$ liquid expansion capacity of FPSO facility *fpso* at the beginning of time period *t*

$QE_{fpso,t}^{gas}$ gas expansion capacity of FPSO facility *fpso* at the beginning of time period *t*

**Parameters**

$FC_{fpso,t}$ fixed capital cost for installing FPSO facility *fpso* at the beginning of time period t

$FC_{f,fpso,t}$ fixed cost for installing the connection between field *f* and FPSO facility *fpso* at the beginning of time period t

$FC_{f,t}^{well}$ fixed cost for drilling a well in field *f* at the beginning of time period t

$VC_{fpso,t}^{liq}$ variable capital cost for installing or expanding the liquid (oil and water) capacity of FPSO facility *fpso* at the beginning of time period t

$VC_{fpso,t}^{gas}$ variable capital cost for installing or expanding the gas capacity of FPSO facility *fpso* at the beginning of time period t

| | |
|---|---|
| $OC_t^{liq}$ | operating cost for per unit of liquid (oil and water) produced in time period t |
| $OC_t^{gas}$ | operating cost for per unit of gas produced in time period t |
| $REC_f$ | total amount of recoverable oil from field *f* |
| $U_{f,fpso}^{well,oil}$ | Upper bound on the oil flow rate per well from field *f* to FPSO facility *fpso* |
| $U_{fpso}^{oil}$ | Upper bound on the installation or expansion of oil capacity of a FPSO facility |
| $U_{fpso}^{liq}$ | Upper bound on the installation or expansion of liquid capacity of a FPSO facility |
| $U_{fpso}^{gas}$ | Upper bound on the installation or expansion of gas capacity of a FPSO facility |
| $UN_t^{well}$ | Maximum number of wells that can be drilled in field *f* during planning horizon *T* |
| $UI_t^{well}$ | Maximum number of wells that can be drilled during each time period t |
| $M_{f,fpso}^{wc}$ | Maximum cumulative water that can be produced for a field-FPSO connection |
| $M_{f,fpso}^{gc}$ | Maximum cumulative gas that can be produced for a field-FPSO connection |
| $l_1$ | lead time for initial installation of a FPSO facility |
| $l_2$ | lead time for expansion of an earlier installed FPSO facility |
| $\mu$ | Maximum fraction of the initial built FPSO capacities that can be expanded |
| $\alpha_t$ | price of oil in time period *t* |
| $\beta_t$ | price of gas in time period *t* |

| | |
|---|---|
| $d_t$ | discounting factor for time period $t$ |
| $\delta_t$ | number of days in time period $t$ |
| $a_{( )}, b_{( )}, c_{( )}, d_{( )}$ | coefficients for polynomials used for reservoir models |

# Chapter 3

# Modeling and computational strategies for optimal development planning of offshore oilfields under complex fiscal rules

## 3.1 Introduction

In this chapter, we address the optimal development planning of offshore oil and gas fields under complex fiscal rules considering the multi-field site deterministic model presented in chapter 2 as a basis. The proposed fiscal model considers the trade-offs between optimal investment and operating decisions that correspond to the simple NPV based model and resulting overall NPV for the oil company after paying government share, and yields improved decisions in a more realistic setting for the enterprise (see Figure 3.1).

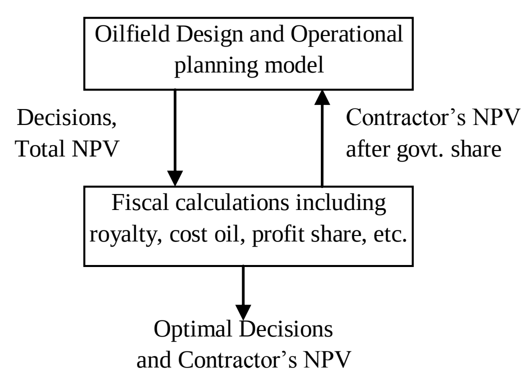


Figure 3.1: Oilfield Planning with fiscal considerations

### 3.1.1 Type of Contracts

When an oil company needs to sign a contract or agreement with the host government to explore and develop the petroleum resources in a country, there are a variety of contracts that are used in the offshore oil and gas industry (Babusiaux et al., 2007; Johnston, 1994; Sunley et al., 2002; and Tordo, 2007). Although the terms of a particular agreement are usually negotiated between both the entities in practice, these contracts can broadly be classified into two main categories:

***(i) Concessionary System***

A concessionary (or tax and royalty) system usually involves royalty, cost deduction and tax. Royalty is paid to the government at a certain percentage of the gross revenues. The net revenue after deducting costs becomes taxable income on which a pre-defined percentage is paid as tax which may include both corporate income tax and a specific profit tax. The total contractor's share involves gross revenues minus royalty and taxes in each year. The basic difference as compared to the production sharing agreement is that the oil company keeps the right to all of the oil and gas produced at the wellhead and pays royalties, bonuses, and other taxes to the government. These contracts are used in countries such as Canada, USA and the UK.

***(ii) Production Sharing Agreements (PSAs)***

The revenue flow in a typical Production Sharing Agreement can be seen as in Figure 3.2 (World Bank, 2007). First, in most cases, the company pays royalty to the government at a certain percentage of the total oil produced. After paying the royalties, some portion of the remaining oil is treated as cost oil by the oil company to recover its costs. There is a ceiling on the cost oil recovery to ensure revenues to the government as soon as production starts. The remaining part of the oil, called profit oil, is divided between oil company and the host government at a certain percentage. The oil company needs to further pay income tax on its share of profit oil. Hence, the total contractor's (oil company) share in the gross revenue comprises of cost oil and contractor's profit oil share after tax. The other important feature of a PSA is that the government keeps rights to the oil produced at wellhead, and transfers title to a portion of the extracted oil and gas to oil company that works as a contractor at an agreed delivery point. Notice that the cost oil limit is one of the key differences with a concessionary system. These contracts are used in countries such as Cambodia, China, Egypt, India, Angola and Nigeria.

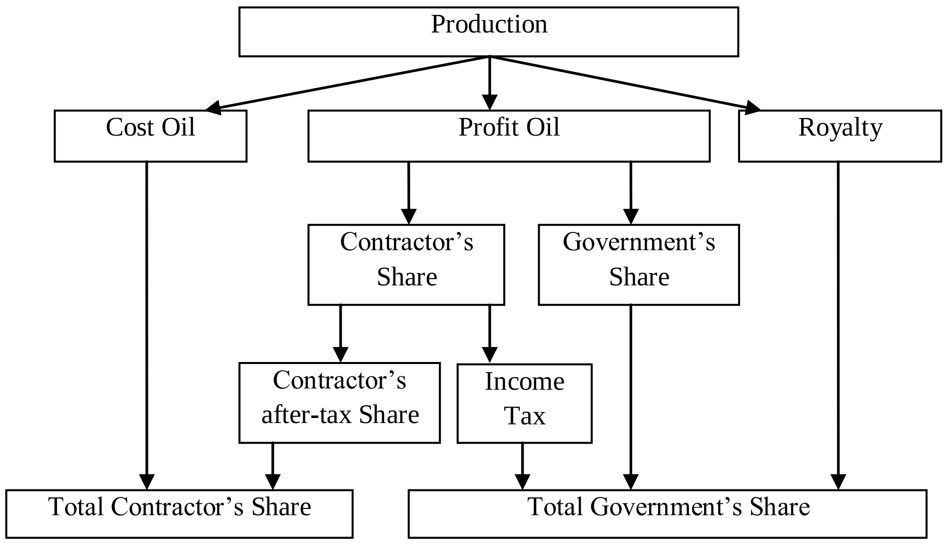


Figure 3.2: Revenue flow for a typical Production Sharing Agreement

### 3.1.2 Type of Fiscal terms for Concessionary Systems and PSA

The specific rules defined in such a contract (either concessionary or PSA, hybrid) between oil company and host government determine the profit that the oil company can keep, as well as the royalties and profit oil share that are paid to the government. These profit oil fractions, royalty rates define the fiscal terms of a particular contract and can be either of the following two types:

***(i) Regressive Fiscal Terms:***

These fiscal terms are not directly linked to the profitability of the project, e.g. fixed percentage of royalty or profit oil share for the entire planning horizon. Therefore, the so called tier structure (levels) is usually absent.

***(ii) Progressive (Sliding scale) Fiscal Terms:***

In this case fiscal terms (e.g. profit oil shares, royalty rates) are based on the profitability of the project, i.e. these terms penalize higher production rates, where cumulative oil produced, daily production, rate of return, R-factor, are the typical profitability measures that determine the tier structure (levels) for these contract terms. For instance, if the cumulative production is in the range of first tier, $0 \le xc_t \le 200$, the contractor receives 50% of the profit oil, while if the cumulative production reaches in tier 2, $200 \le xc_t \le 400$, the contractor receives 40% of the profit oil, and so on (see Figure 3.3). In practice, as we move to the higher tier, the percentage share of contractor in the total production decreases. Notice that this tier structure is a step function, which requires additional binary variables to model and makes the problem harder to solve.

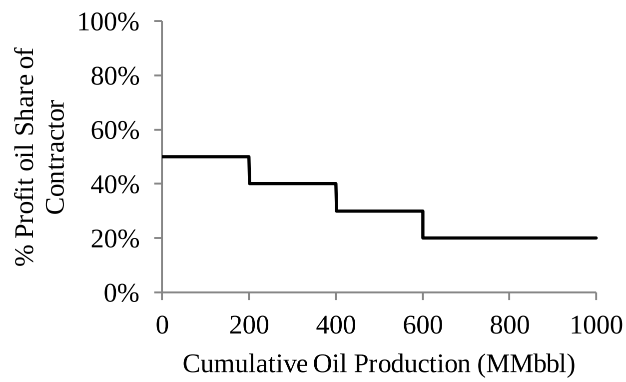


Figure 3.3: Progressive profit oil share of the contractor

### 3.1.3 Ringfencing Provisions

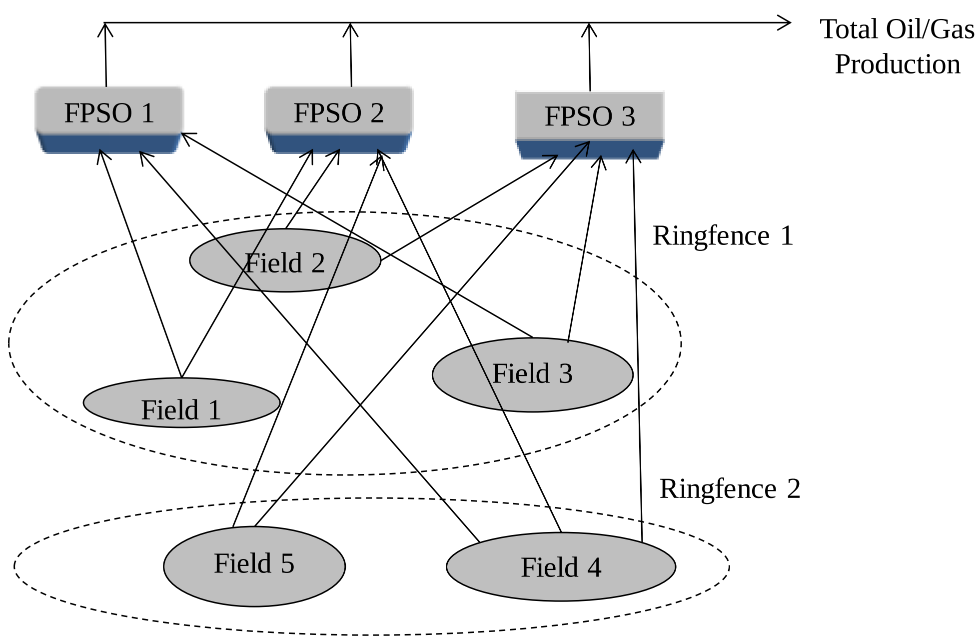


Figure 3.4: 2 Ringfences for a set of 5 Fields

Ringfencing is an important concept that is usually part of the fiscal contracts and imposed by the government, which affects the cash flows over the planning horizon. In a typical ringfencing provision, investment and operational costs for a specified group of fields or block can only be recovered from the revenue generated from those fields or block (see Figure 3.4). It means that the set of particular fields are “ringfenced”. Therefore, income derived from one contract area or project cannot be offset against losses from another contract area or project. In financial terms, a ringfencing provision basically defines the level at which all fiscal calculations need to be done, and restricts the oil companies to balance the costs and revenues across various projects/blocks for minimizing the tax burden. For example, fiscal calculations for Fields 1-3 (Ringfence 1) and Field 4-5 (Ringfence 2) in Figure 3.4 cannot be consolidated at one place. Notice that in general a field is associated to a single ringfence, while a ringfence can include more than one field. In contrast, a facility can be connected to multiple fields from different ringfences for producing oil and gas. Ringfencing provisions are more popular in production sharing contracts.

The main motivation of including ringfencing provisions by the host governments is to protect the tax revenues. However, the existence and extent of ringfencing affects the overall level of tax receipts. The more restrictive ringfencing provisions (e.g. individual field is separately ringfenced) can lead to situations that may not be economically viable to develop/operate for the oil companies. On the other hand, the relaxation of the ringfencing provisions (e.g. cost and revenues can be shared across any field for tax calculations) may lead to significant tax saving for the oil companies since revenues from the favorable fields can be used to offset the losses from other fields. Therefore, the number of ringfences and distribution of the fields among ringfences involve various trade-offs that include productivity of the field, crude quality, reservoir size, development costs etc., so that these fiscal provisions are neither very conservative nor very relaxed. Moreover, each ringfence can be assigned a different cost recovery limit, profit sharing rate etc. based on these factors.

Ringfencing provisions and income tax rates are usually legislated in the country and do not provide opportunity for negotiation, while cost recovery and profit sharing rates can be subject to negotiation. Therefore, from the perspective of the oil companies, since they have limited control over the ringfencing provisions and distribution of fields among various ringfences, they usually try to include many fields from multiple ringfences in the model for making investment and operational decisions that allows to consider the trade-offs among these fields and/or ringfences. In general, it is better to have more fiscal aspects of a contract that are subject to negotiation, since flexibility is often required to offset differences between basins, regions, and license areas within a country (Johnston, 1994) .

The above fiscal contracts, terms and ringfencing provisions are the backbone of most of the contracts that are currently used, and can have significant impact on the revenues. In addition, there can be some other fiscal considerations for a particular contract of interest, but for simplicity we only consider the important financial elements as described above. Notice that the royalties and/or government profit oil share that result from a particular contract can represent a significant amount of the gross revenues. Therefore, it is critical to consider these contract terms explicitly during the oilfield planning phase to assess the actual economic potential of such a project.

This chapter is organized as follows: we first describe the oilfield planning problem with fiscal considerations in section 3.2 and present a general model in section 3.3 that includes progressive fiscal terms and ringfencing provisions. The ways to derive a specific contract from the general model are highlighted in the next section. In section 3.5, we propose new reformulation, relaxation and approximation schemes to reduce the computational burden for the problems in this class. Numerical results of several instances of the development planning problem under complex fiscal rules are reported in section 3.6.

## 3.2 Problem Statement

We consider the offshore oilfield infrastructure as in chapter 2 that consists of a set of oil fields $F = \{1,2,\ldots\}$ for producing oil using a set of FPSO facilities, $FPSO = \{1,2,\ldots\}$ as seen in Fig. 3.4. Each oilfield consists of a number of potential wells to be drilled using drilling rigs, which are then connected to these FPSO facilities through pipelines to produce oil. We assume that the location of each potential FPSO facility and its possible connections to the given fields are known. Notice that each FPSO facility can be connected to more than one field to produce oil, while a field can only be connected to a single FPSO facility due to engineering requirements and economic viability of the offshore oilfield development projects. There can be a significant amount of water and gas that comes out with the oil during the production process that needs to be considered while planning for FPSO capacity installations and expansions. The water is usually re-injected after separation from the oil, while the gas can be sold in the market. In this case we do not consider water or gas re-injection, i.e. we consider natural depletion of the reserves. For simplicity, we only consider FPSO facilities. The proposed model can easily be extended to other facilities such as tension leg platforms (TLPs).

In addition, there are fiscal aspects that need to be accounted for. Particularly, we consider the cost recovery ceiling that is linked to gross revenues, profit oil share and taxes as the main elements of the fiscal terms (see Figure 3.2). Progressive (sliding scale) profit share of the contractor is also considered that can be linked to any of the profitability measures, e.g. cumulative oil produced, daily oil production, R-factor, IRR, where $I = \{1,2,\ldots\}$ is the set of corresponding tiers for this sliding scale. The definition of R-factor can be contract specific but in its most general form, it is calculated as the ratio of the contractor's cumulative revenue after taxes and royalty to the contractor's cumulative cost (Kaiser and Pulsipher, 2004). On the other hand, the internal rate of return (IRR) on an investment or project is defined as the "annualized effective compounded return rate" or "rate of return" that makes the net present value of the cash flows (both positive and negative) from a particular investment equal to zero. In general, as values of the above profitability measures increase, the profit oil share of the contractor decreases.

Notice that we do not consider explicit royalty provisions here as cost oil ceiling and royalties both are usually not imposed simultaneously in a PSA contract. However, including royalty provisions with cost oil ceiling is straightforward. A set of ringfences $RF = \{1,2,\ldots\}$ among the given fields is specified (see Figure 3.4) to ensure that fiscal calculations are to be done for each ringfence separately. These ringfences may or may not have the same fiscal rules. Notice that, the fiscal terms considered here collectively define a general progressive PSA with ringfencing provisions. The variety of other contracts can be derived as a special case from these rules. Notice that for simplicity, the cost recovery ceiling fraction and tax rates are assumed to be fixed percentages (no sliding scale). However, for the problems where these fiscal terms are also progressive, a similar approach as used for progressive profit oil fraction can directly be applied.

The objective is to determine the optimum investment and operation decisions to maximize the contractor's NPV for a long-term planning horizon after paying the government share based on the above fiscal considerations. The planning horizon is discretized into a number of time periods $t$, typically each with 1 year of duration. Investment decisions in each time period $t$ include, which FPSO facilities should be installed or expanded, and their respective installation or expansion capacities for oil, liquid and gas, which fields should be connected to which FPSO facility, and the number of wells that should be drilled in a particular field $f$ given the restrictions on the total number of wells that can be drilled in each time period $t$ over all the given fields. Operating decisions include the oil/gas production rates from each field $f$ in each time period $t$. It is assumed that the installation and expansion decisions occur at the beginning of each time period $t$, while operation takes place throughout the time period. There is a lead time of $l_1$ years for each FPSO facility initial installation, and a lead time of $l_2$ years for the expansion of an earlier installed FPSO facility. Once installed, we assume that the oil, liquid (oil and water) and gas capacities of a FPSO facility can be expanded only once.

Field deliverability, i.e. maximum oil flowrate from a field, water-oil-ratio (WOR) and gas-oil-ratio (GOR) are approximated by a cubic equations (a)-(c) as in the previous chapter, while cumulative water produced and cumulative gas produced from a field are represented by fourth order separable polynomials, eq. (d)-(e), in terms of the fractional oil recovered from that field, respectively. Notice that these fourth order polynomials correspond to the integration of the cubic equations for WOR and GOR as explained in chapter 2. The motivation for using polynomials for cumulative water produced and cumulative gas produced, eq. (d)-(e), as compared to WOR and GOR, eq. (b)-(c), is to avoid bilinear terms, eq. (f)-(g), in the formulation and allow converting the resulting model into an MILP formulation using piecewise linear approximations. Furthermore, all the wells in a particular field *f* are assumed to be identical for the sake of simplicity leading to the same reservoir profiles, eq. (a)-(g), for each of these wells.

$$Q_f^d = a_{1,f}(fc_f)^3 + b_{1,f}(fc_f)^2 + c_{1,f}\, fc_f + d_1 \qquad \forall f \qquad \text{(a)}$$

$$wor_f = a_{2,f}(fc_f)^3 + b_{2,f}(fc_f)^2 + c_{2,f}\, fc_f + d_{2,f} \qquad \forall f \qquad \text{(b)}$$

$$gor_f = a_{3,f}(fc_f)^3 + b_{3,f}(fc_f)^2 + c_{3,f}\, fc_f + d_{3,f} \qquad \forall f \qquad \text{(c)}$$

$$wc_f = a_{4,f}(fc_f)^4 + b_{4,f}(fc_f)^3 + c_{4,f}\, fc_f^2 + d_{4,f}\, fc_f \qquad \forall f \qquad \text{(d)}$$

$$gc_f = a_{5,f}(fc_f)^4 + b_{5,f}(fc_f)^3 + c_{5,f}\, fc_f^2 + d_{5,f}\, fc_f \qquad \forall f \qquad \text{(e)}$$

$$w_f = wor_f . x_f \qquad \forall f \qquad \text{(f)}$$

$$g_f = gor_f . x_f \qquad \forall f \qquad \text{(g)}$$

A general MINLP model for oilfield development planning with fiscal considerations is presented next based on the infrastructure, fiscal terms and reservoir characteristics described in this section.

## 3.3 Oilfield Development Planning Model

**(a) Models without fiscal considerations:**

In chapter 2, we proposed efficient multiperiod MINLP models (**Models 1 and 2**) for oilfield infrastructure planning problem described above without fiscal considerations. Model 2 is also reformulated into an MILP (**Model 3**) to solve it to global optimality. These models were further reduced (**Models 1R, 2R and 3R**) by neglecting the timing of the piping investments to improve the computational efficiency. The basic features of these models can be summarized as follows:

Model 1: MINLP based on WOR, GOR and corresponding bilinear terms

Model 2: MINLP based on separable functions for cumulative water and cumulative gas produced derived from integration of WOR and GOR expressions

Model 3: Derived from MINLP Model 2 using piecewise linearization and exact linearization techniques

Model 1R, 2R and 3R: Derived from corresponding Models 1, 2, and 3, respectively, using binary reduction scheme that relies on the fact that connection costs are much smaller as compared to other investment costs.

Based on the computational experience in the previous chapter, Model 3R is the most efficient as it can directly be solved to global optimality in reasonable time as compared to other models. Furthermore, its solution can be used to fix the design decisions in the MINLP models to obtain near optimal solutions of these models.

**(b) Proposed Models with fiscal considerations:**

In this section, we incorporate the complex fiscal rules in the above MINLP/MILP models. Particularly, we consider the progressive PSA with ringfencing provisions that is the most general form of fiscal terms. The proposed models consider the trade-offs involved between investment and operations decisions and resulting royalties, profit shares that are paid to the government, and yield the maximum overall NPV for the contractor (see Figure 3.1) due to improved decisions. The indices, variables and parameters used in the model are summarized in Appendix C.

**(i) Objective Function:** The objective function is to maximize total NPV of the contractor as in (3.1), which is the difference between discounted total contractor's gross revenue share and total cost (total capital plus operating costs) over the planning horizon (3.2). The total contractor's share in a particular time period t is the sum of the contractor's share over all the ringfences as given in equation (3.3). Similarly, constraints (3.4) and (3.5) represent the total capital and operating expenses in time period t, which is the sum of respective costs over all the ringfences in that time period.

$$Max \quad NPV \tag{3.1}$$

$$NPV = \sum_t dis_t \cdot (TotalConSh_t^{tot} - CAP_t^{tot} - OPER_t^{tot}) \tag{3.2}$$

$$TotalConSh_t^{tot} = \sum_{rf} TotalConSh_{rf,t} \qquad \forall t \tag{3.3}$$

$$CAP_t^{tot} = \sum_{rf} CAP_{rf,t} \qquad \forall t \tag{3.4}$$

$$OPER_t^{tot} = \sum_{rf} OPER_{rf,t} \qquad \forall t \tag{3.5}$$

**(ii) Capital Costs:** The overall capital expenses associated to a ringfence *rf* contains two components as given in equation (3.6), see Figure 3.4. One capital cost component, equation (3.7), is field specific and accounts for the connection costs between a field and a FPSO facility, and cost of drilling the wells for each of the field in that ringfence *rf*, i.e. set $F_{rf}$ , for each time period t. The second capital cost component for a ringfence is FPSO specific as given in equation (3.8), and it depends on the capital expenses for the corresponding FPSO facilities that are installed during the planning horizon.

$$CAP_{rf,t} = CAP1_{rf,t} + CAP2_{rf,t} \qquad \forall rf,t \tag{3.6}$$

$$CAP1_{rf,t} = \sum_{F_{rf}} \sum_{fpso} FC_{f,fpso,t} b_{f,fpso,t} + \sum_{F_{rf}} FC_{f,t}^{well} I_{f,t}^{well} \qquad \forall rf,t \tag{3.7}$$

$$CAP2_{rf,t} = \sum_{fpso} DFPSOC_{rf,fpso,t} \qquad \forall rf,t \qquad (3.8)$$

The total cost of an FPSO facility (3.9) consists of fixed installation costs, variable installation and expansion costs corresponding to liquid and gas capacities. Each FPSO facility can be connected to multiple fields from different ringfences as can seen from Figure 3.4. Therefore, to calculate the second cost component in (3.8) for a specific ringfence these FPSO costs need to be disaggregated as in (3.10) over various fields (and therefore ringfences as in (3.11)) based on the size of the fields, where set $F_{fpso}$ is the set of all the fields that can be connected to FPSO facility *fpso*. Constraint (3.12) sets the binary variable $b_{f,fpso}^{on}$ to 1 only if that field-FPSO connection comes online during the given planning horizon. This binary variable is further used in constraint (3.13) to ensure that the disaggregated FPSO cost can only be accounted for a field if that field is connected to the FPSO facility. Constraint (3.14) calculates the value of disaggregated FPSO cost for a specific field based on the ratio of the size of that field to sum of the total field sizes that are connected to that FPSO facility during given planning horizon. Notice that only those fields sizes are considered for calculations that are actually connected to that FPSO facility, i.e. for which the binary variable $b_{f,fpso}^{on}$ equals 1. In general, we consider a long planning horizon for the development planning in which the fields may not be depleted completely during this time horizon. However, the installed FPSO facilities and connections usually remain in operation until it becomes uneconomical to produce from the given fields, which may exceed few years over the time horizon considered in the planning model. Therefore, it allows us to disaggregate the FPSO costs over the various ringfences based on the recoverable volume of the oil from a field as described above to be sufficiently accurate and computationally efficient by avoiding nonlinearities.

$$FPSOC_{fpso,t} = \left[ FC_{fpso,t}^{FPSO} b_{fpso,t}^{FPSO} + VC_{fpso,t}^{liq} (QI_{fpso,t}^{liq} + QE_{fpso,t}^{liq}) + VC_{fpso,t}^{gas} (QI_{fpso,t}^{gas} + QE_{fpso,t}^{gas}) \right] \qquad \forall fpso,t \qquad (3.9)$$

$$FPSOC_{fpso,t} = \sum_{F_{fpso}} DFPSOC^{field}_{f,fpso,t} \qquad \forall fpso,t \qquad (3.10)$$

$$DFPSOC_{rf,fpso,t} = \sum_{F_{rf}} DFPSOC^{field}_{f,fpso,t} \qquad \forall rf, fpso,t \qquad (3.11)$$

$$b^{on}_{f,fpso} = \sum_{t} b_{f,fpso,t} \qquad \forall f, fpso \qquad (3.12)$$

$$DFPSOC^{field}_{f,fpso,t} \le M \cdot b^{on}_{f,fpso} \qquad \forall f, fpso,t \qquad (3.13)$$

$$DFPSOC^{field}_{f,fpso,t} = \frac{b^{on}_{f,fpso} \cdot REC_f}{\sum_{f' \in F_{fpso}} b^{on}_{f',fpso} \cdot REC_{f'}} \cdot FPSOC_{fpso,t} \qquad \forall f, fpso,t \qquad (3.14)$$

Constraint (3.14) can be re-written as constraint (3.15), which can be further simplified by setting the positive variables $ZD^{field}_{f',f,fpso,t} = b^{on}_{f',fpso} \cdot DFPSOC^{field}_{f,fpso,t}$ and $ZD_{f.fpso,t} = b^{on}_{f,fpso} \cdot FPSOC_{fpso,t}$ that yields constraint (3.16). Due to the bilinear terms involving binary variables $b^{on}_{f,fpso}$,we perform exact linearization, Glover (1975), for defining the variables $ZD^{field}_{f',f,fpso,t}$ and $ZD_{f,fpso,t}$ as in constraints (3.17)-(3.20) and (3.21)-(3.24), respectively, which in fact is equivalent to the convex hull of the corresponding disjunction of the nonlinear form.

$$\sum_{f' \in F_{fpso}} b^{on}_{f',fpso} \cdot DFPSOC^{field}_{f,fpso,t} \cdot REC_{f'} = b^{on}_{f,fpso} \cdot FPSOC_{fpso,t} \cdot REC_f$$

$$\forall f, fpso,t \qquad (3.15)$$

$$\sum_{f' \in F_{fpso}} ZD^{field}_{f',f,fpso,t} \cdot REC_{f'} = ZD_{f,fpso,t} \cdot REC_f \qquad \forall f, fpso,t \qquad (3.16)$$

$$ZD^{field}_{f',f,fpso,t} + ZD1^{field}_{f',f,fpso,t} = DFPSOC^{field}_{f,fpso,t} \qquad \forall f, fpso,t, f' \in F_{fpso} \qquad (3.17)$$

$$ZD^{field}_{f',f,fpso,t} \le U \cdot b^{on}_{f',fpso} \qquad \forall f, fpso,t, f' \in F_{fpso} \qquad (3.18)$$

$$ZD1^{field}_{f',f,fpso,t} \le U \cdot (1 - b^{on}_{f',fpso}) \qquad \forall f, fpso,t, f' \in F_{fpso} \qquad (3.19)$$

$$ZD^{field}_{f',f,fpso,t} \ge 0, ZD1^{field}_{f',f,fpso,t} \ge 0 \qquad \forall f, fpso,t, f' \in F_{fpso} \qquad (3.20)$$

$$ZD_{f,fpso,t} + ZD1_{f,fpso,t} = FPSOC_{fpso,t} \qquad \forall f, fpso, t \qquad (3.21)$$

$$ZD_{f,fpso,t} \le U \cdot b^{on}_{f,fpso} \qquad \forall f, fpso, t \qquad (3.22)$$

$$ZD1_{f,fpso,t} \le U \cdot (1 - b^{on}_{f,fpso}) \qquad \forall f, fpso, t \qquad (3.23)$$

$$ZD_{f,fpso,t} \ge 0, ZD1_{f,fpso,t} \ge 0 \qquad \forall f, fpso, t \qquad (3.24)$$

**(iii) Operating Costs:** The total operating expenses that correspond to ringfence $rf$, eq. (3.25), are the operation costs corresponding to the total amount of liquid and gas produced in each time period t from that ringfence.

$$OPER_{rf,t} = \delta_t \left[ OC^{liq}_{rf,t} (x^{tot}_{rf,t} + w^{tot}_{rf,t}) + OC^{gas}_{rf,t} g^{tot}_{rf,t} \right] \qquad \forall rf, t \qquad (3.25)$$

**(iv) Revenues:** The gross revenues (3.26) in each time period t for a ringfence *rf*, are computed based on the total amount of oil produced and its selling price, where total oil flow rate in a time period t for ringfence *rf*, is calculated as the sum of the oil production rates over all the fields in that ringfence, i.e. set $F_{rf}$, as given in equation (3.27). Given that all the fiscal terms are defined on the basis of total oil produced, for simplicity we only consider the revenue generated from the oil sales, which is much larger in general as compared to the revenue from gas. In practice, due to large transportation costs involved in shipping gas from offshore locations, it is usually re-injected or flared, if the gas revenue represents a small fraction of the oil revenues. However, extension to include the gas sales and/or fiscal terms associated is straightforward if the gas revenues are substantial.

$$REV_{rf,t} = \delta_t \alpha_t x^{tot}_{rf,t} \qquad \forall rf, t \qquad (3.26)$$

$$x^{tot}_{rf,t} = \sum_{F_{rf}} x_{f,t} \qquad \forall rf, t \qquad (3.27)$$

**(iv) Total Contractor Share:** The total contractor share that corresponds to ringfence *rf* in time period t is calculated in constraint (3.28) as the sum of contractor's profit oil share for that ringfence (after paying income tax) and the cost oil that it keeps to recover the expenses. The contractor needs to pay income-tax on its profit oil share. Therefore, the contractor's profit oil share before tax is the sum of contractor's profit oil share after tax and income tax paid as in constraint (3.29).

$$TotalConSh_{rf,t} = ConSh_{rf,t}^{aftertax} + CO_{rf,t} \qquad \forall rf, t \tag{3.28}$$

$$ConSh_{rf,t}^{beforetax} = ConSh_{rf,t}^{aftertax} + Tax_{rf,t} \qquad \forall rf, t \tag{3.29}$$

The contractor's share before tax in each time period t is some fraction of the total profit oil during that period t for ringfence *rf*. Note that we assume here that this fraction, which is called profit oil fraction( $f_{rf,i}^{po}$), is based on a decreasing sliding scale system, where *i* is the index of the corresponding tier. The sliding scale system considered here is linked to the cumulative amount of oil produced $xc_{rf,t}$ by the end of that time period t from ringfence *rf*, see Figure 3.5. The other variables for this type of sliding scale system could be for instance the contractor's IRR or R-factor. Therefore, for possible levels *i* (i.e. tiers) of cumulative amount of oil produced by the end of time period t, the corresponding contractor's profit oil share, Figure 3.6, can be calculated from disjunction (3.30). In particular, variable $Z_{rf,i,t}$ in the disjunction will be true if cumulative oil produced in time period t for a ringfence *rf*, lies between $L_{rf,i}^{oil}$ and $U_{rf,i}^{oil}$, i.e. tier *i* is active in that time period t and corresponding profit oil fraction $f_{rf,i}^{po}$ is used for calculating the contractor's profit oil share for ringfence *rf*. This disjunction (3.30) can further be rewritten as integer and mixed-integer linear constraints (3.31)-(3.38) using the convex-hull formulation (Raman and Grossmann, 1994). The solution time with the big-M formulation was much higher as compared to convex-hull formulation due to its weaker LP relaxation. Notice that the binary variables $Z_{rf,i,t}$ can also be represented as SOS1 variables. However, we did not observe any specific improvements in the computational time with this alternate approach.

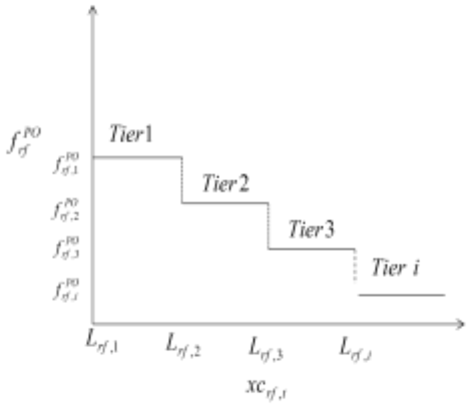


Figure 3.5: Sliding scale profit oil fraction

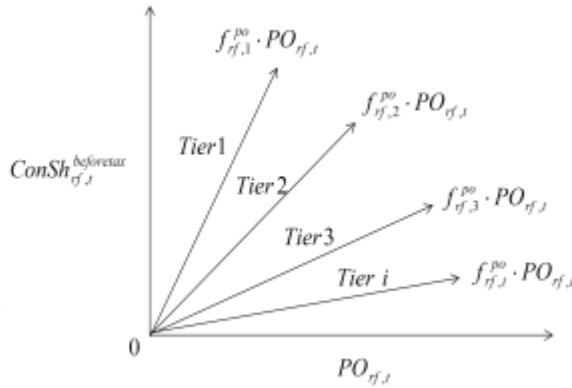


Figure 3.6: Contractor’s share of profit oil

$$\bigvee_i \begin{bmatrix} Z_{rf,i,t} \\ ConSh_{rf,t}^{beforetax} = f_{rf,i}^{PO} \cdot PO_{rf,t} \\ L_{rf,i}^{oil} \le xc_{rf,t} \le U_{rf,i}^{oil} \end{bmatrix} \qquad \forall rf,t \qquad (3.30)$$

$$ConSh_{rf,t}^{beforetax} = \sum_i DConSh_{rf,i,t}^{beforetax} \qquad \forall rf,t \qquad (3.31)$$

$$PO_{rf,t} = \sum_i DPO_{rf,i,t} \qquad \forall rf,t \qquad (3.32)$$

$$xc_{rf,t} = \sum_i Dxc_{rf,i,t} \qquad \forall rf,t \qquad (3.33)$$

$$DConSh_{rf,i,t}^{beforetax} = f_{rf,i}^{po} \cdot DPO_{rf,i,t} \qquad \forall rf,i,t \qquad (3.34)$$

$$0 \le DConSh_{rf,i,t}^{beforetax} \le M \cdot Z_{rf,i,t} \qquad \forall rf,i,t \qquad (3.35)$$

$$0 \le DPO_{rf,i,t} \le M \cdot Z_{rf,i,t} \qquad \forall rf,i,t \qquad (3.36)$$

$$L_{rf,i}^{oil} \cdot Z_{rf,i,t} \le Dxc_{rf,i,t} \le U_{rf,i}^{oil} \cdot Z_{rf,i,t} \qquad \forall rf,i,t \qquad (3.37)$$

$$\sum_i Z_{rf,i,t} = 1 \qquad \forall rf,t \qquad (3.38)$$

$$Z_{rf,i,t} \in \{0,1\}$$

The cumulative amount of oil produced from a ringfence $rf$ by the end of time period t is calculated in constraint (3.39) as the sum of the cumulative amount of oil produced by that time period from all the fields associated to that ringfence.

$$xc_{rf,t} = \sum_{F_{rf}} xc_{f,t}^{field} \qquad \forall rf, t \qquad (3.39)$$

The tax paid by the contractor on its profit oil share depends on the tax rate ( $f_{rf,t}^{tax}$ ) as in constraint (3.40), which is a given parameter assumed to have a fixed value.

$$Tax_{rf,t} = f_{rf,t}^{tax} \cdot ConSh_{rf,t}^{beforetax} \qquad \forall rf, t \qquad (3.40)$$

Constraint (3.41) states that total profit oil in time period t for a ringfence *rf*, is the portion of the gross revenue that remains after subtracting the cost oil in that period t.

$$PO_{rf,t} = REV_{rf,t} - CO_{rf,t} \qquad \forall rf, t \qquad (3.41)$$

The portion of the total revenues that the oil company can claim for cost recovery, i.e. cost oil, is normally bounded above by the so-called "cost recovery ceiling" or "cost stop". Therefore, the cost oil in time period t for a ringfence *rf*, constraint (3.42), is calculated as the minimum of the cost recovery in that time period and maximum allowable cost oil (cost recovery ceiling). The cost recovery ceiling can be a fixed fraction ( $0 \le f_{rf,t}^{CR} \le 1$ ) of the gross revenue (Kaiser and Pulsipher, 2004) or it might be based on a sliding scale system. We assume here that the fraction $f_{rf,t}^{CR}$ is independent of project economics, i.e. a fixed parameter. Constraint (3.42) can further be rewritten as mixed-integer linear constraints (3.43)-(3.48). Notice that equation (3.42) can also be represented as a disjunction and its corresponding convex-hull formulation. However, based on our computational experience, we observed that using the convex-hull instead of the big-M constraints, (3.43)-(3.48), was much slower due to additional continuous variables that were required to model the problem, whereas the LP relaxation was almost identical.

$$CO_{rf,t} = \min(CR_{rf,t}, f^{CR}_{rf,t} \cdot REV_{rf,t}) \qquad \forall rf, t \qquad (3.42)$$

$$CO_{rf,t} \le CR_{rf,t} + M(1 - b^{co}_{rf,t}) \qquad \forall rf, t \qquad (3.43)$$

$$CO_{rf,t} \ge CR_{rf,t} - M(1 - b^{co}_{rf,t}) \qquad \forall rf, t \qquad (3.44)$$

$$CO_{rf,t} \le f^{CR}_{rf,t} REV_{rf,t} + M \cdot b^{co}_{rf,t} \qquad \forall rf, t \qquad (3.45)$$

$$CO_{rf,t} \ge f^{CR}_{rf,t} REV_{rf,t} - M \cdot b^{co}_{rf,t} \qquad \forall rf, t \qquad (3.46)$$

$$CO_{rf,t} \le CR_{rf,t} \qquad \forall rf, t \qquad (3.47)$$

$$CO_{rf,t} \le f^{CR}_{rf,t} REV_{rf,t} \qquad \forall rf, t \qquad (3.48)$$

Cost recovery in time period t for a ringfence *rf*, constraint (3.49), is the sum of capital and operating costs in that period t and cost recovery carried forward from previous time period t-1. Any unrecovered cost (that is carried forward to the next period) in time period t for a ringfence *rf*, is calculated as the difference between the cost recovery and cost oil in time period t as given in constraint (3.50). Notice that constraints (3.43)-(3.50) state that any capital and operating costs that are not recovered in the form of cost oil due to cost recovery ceiling in any time period t for a ringfence *rf*, are carried forwarded to the next time period for the cost recovery purposes.

$$CR_{rf,t} = CAP_{rf,t} + OPER_{rf,t} + CRF_{rf,t-1} \qquad \forall rf, t \qquad (3.49)$$

$$CRF_{rf,t} = CR_{rf,t} - CO_{rf,t} \qquad \forall rf, t \qquad (3.50)$$

Constraints (3.1)-(3.13), (3.16)-(3.29), (3.31)-(3.41), (3.43)-(3.50) are linear and mixed-integer linear constraints that correspond to the fiscal part of the problem. Notice that we also have the non-negativity restriction on all of the variables involved in these constraints, except NPV, as revenues, costs, tax, profit share, etc., that cannot be less than zero in any time period. These fiscal constraints can be included in either of the MINLP/MILP formulations in the previous chapter which corresponds to the reservoir constraints, field-FPSO flow constraints, FPSO capacity constraints, well drilling limitations and logic constraints.

The resulting oilfield infrastructure planning models with fiscal considerations (Models 1F, 2F and 3F) correspond to MINLP (for Models 1 and 2) or MILP (for Model 3) based on the type of reservoir profiles or their approximations used, which are described in chapter 2. Table 3.1 summarizes the main features of the proposed MINLP and MILP models with fiscal considerations. Notice that Models 1-3 are the simple NPV based models in Figure 3.1, while Models 1F-3F consider the fiscal aspects described above and associated trade-offs during planning.

Table 3.1: Comparison of the proposed oilfield planning models

| | **Model 1F** | **Model 2F** | **Model 3F** |
|---|---|---|---|
| **Model Type** | MINLP | MINLP | MILP |
| **Oil Deliverability** | 3rd order polynomial | 3rd order polynomial | Piecewise Linear |
| **WOR** | 3rd order polynomial | - | - |
| **GOR** | 3rd order polynomial | - | - |
| **wc** | - | 4th order polynomial | Piecewise Linear |
| **gc** | - | 4th order polynomial | Piecewise Linear |
| **Bilinear Terms** | N*x<br>x*WOR<br>x*GOR | N*x | None |
| **MILP Reformulation** | Not Possible | Possible | Reformulated MILP |
| **Fiscal Calculations** | Yes | Yes | Yes |

It should be noted that the fiscal part of the problem only involves calculations as in constraints (3.1)-(3.13), (3.16)-(3.29), (3.31)-(3.41), (3.43)-(3.50) for a given set of investment and operational decisions. In particular, all fiscal variables (cost oil, profit oil, tax etc.) are dependent variables that are pre-defined functions of costs and revenues (or flows) as can also be seen from Figure 3.1, and hence the total contractor's share is also a function of costs and revenues, eq. (3.51). However, including the fiscal part in the problem provides a way to make investment and operations decisions that are also optimal in terms of fiscal aspects.

$$TotalConSh_{rf,t} = f(COST_{rf,1}, COST_{rf,2}, \ldots. COST_{rf,t}; REV_{rf,1}, REV_{rf,2}, \ldots REV_{rf,t}) \quad \forall rf, t \qquad (3.51)$$

***Remarks:***

The proposed non-convex MINLP models (Model 1F and 2F) for offshore oilfield planning with fiscal rules involves nonlinear non-convex constraints due to reservoir profiles that can lead to suboptimal solutions when solved with an MINLP method that assumes convexity (e.g. branch and bound, outer-approximation; see Grossmann, 2002). However, the MILP formulation (Model 3F) corresponds to Model 3 with fiscal constraints and can be solved to global optimality. The computational efficiency of the proposed MINLP and MILP models can be further improved by neglecting the timing of the piping investments. In particular, Model 1RF, 2RF and 3RF can be derived from corresponding Models 1R, 2R, and 3R, respectively, that are described in the previous chapter by including the fiscal constraints, (3.1)-(3.13), (3.16)-(3.29), (3.31)-(3.41) and (3.43)-(3.50).

In summary, **Model 3RF**, which is an MILP and derived from Model 3R, corresponds to the oilfield planning with fiscal considerations after binary reduction, is most efficient as it can be directly solved to global optimality in reasonable time as compared to other models described above. Moreover, its solution can also be used to fix the investment decisions in the MINLP models to obtain the near optimal solution of the original problem. Therefore, we use **Model 3RF** as a basis for the proposed reformulations, solution strategies and computational experiments presented in the next sections. Notice that these approaches are directly applicable to the other models, but it would be much expensive to either solve (e.g. Model 3F) or obtain good quality solutions (Model 1F, 1RF, 2F, 2RF) for these models directly as compared to Model 3RF as per the computational experience on the respective non-fiscal models in chapter 2.

The deterministic models with fiscal considerations proposed here are very general, and can either be used for simplified cases (e.g. linear profiles for reservoir, fixed well schedule, single field site, etc.), or be extended to include other complexities such as uncertainties, or more details of the specific contracts.

## 3.4 Deriving Specific Contracts from the Proposed Model

In the previous section, we proposed a general oilfield planning model with fiscal rules (Model 3RF). The model is an extension of the Model 3R (MILP) from chapter 2 to include progressive PSA terms with ringfencing provisions that encapsulates a variety of contracts and fiscal terms that are used in practice. Therefore, the fiscal models for specific cases based on the type of contracts, fiscal terms and other provisions can be derived from this general formulation. For instance, we reduce the general model (Model 3RF) to a variety of specific cases as follows:

**(a) No-ringfencing Provisions:** The fiscal terms without ringfencing provisions can be trivially considered as the specific case of the proposed model with only 1 ringfence. In financial terms, it represents the consolidation of the fiscal calculations for the various fields at one place. Therefore, constraints (3.1)-(3.50) can be written without index for ringfence *rf* in this case. Moreover, as all the given fields belong to the same ringfence, the costs and revenues over various ringfences need not be disaggregated. In particular, constraints (3.6)-(3.24) reduce to the simple total capital cost equation (3.52) which is same as it was used in the models without fiscal calculations.

$$CAP_t = \left[FC_{fpso,t}^{FPSO} b_{fpso,t}^{FPSO} + VC_{fpso,t}^{liq}(QI_{fpso,t}^{liq} + QE_{fpso,t}^{liq}) + VC_{fpso,t}^{gas}(QI_{fpso,t}^{gas} + QE_{fpso,t}^{gas})\right] + \sum_{F_{rf}} \sum_{fpso} FC_{f,fpso,t} b_{f,fpso,t} + \sum_{F_{rf}} FC_{f,t}^{well} I_{f,t}^{well} \qquad \forall t \qquad (3.52)$$

**(b) Concessionary System:** The fiscal rules in a typical concessionary system can be considered as the specific case of PSA where we do not have any cost oil recovery limit and profit oil share. Therefore, only royalties, cost deduction and taxes are involved. Royalties can be calculated as a certain fraction ( $f_{rf,t}^{Royal}$ ) of the gross revenues, i. e. eq. (3.53). There are no cost ceiling provisions; and therefore, cost oil ceiling fraction is one in equation (3.42) (i.e. $f_{rf,t}^{CR} = 1$), which yields equation (3.54). Notice that it allows to consider the total oil produced in a given year to be recovered for the capital and operating expenses after paying royalty. Equation (3.54) can further be rewritten as mixed-integer linear constraints similar to (3.43)-(3.48) where $f_{rf,t}^{CR} = 1$. Notice that the cost recovery term $CR_{rf,t}$ used in eq. (3.54) has the same definition as in PSA model described earlier. Therefore, it can be represented by the constraints (3.49)-(3.50). The remaining part of the oil after royalties and cost oil becomes profit, eq. (3.55).

$$Royalty_{rf,t} = f_{rf,t}^{royal} REV_{rf,t} \qquad \forall rf,t \qquad (3.53)$$

$$CO_{rf,t} = \min(CR_{rf,t}, REV_{rf,t}) \qquad \forall rf,t \qquad (3.54)$$

$$PO_{rf,t} = REV_{rf,t} - Royalty_{rf,t} - CO_{rf,t} \qquad \forall rf,t \qquad (3.55)$$

In addition, due to the absence of profit oil split layer in the fiscal calculation (Figure 3.2), for concessionary system, the contractor's share before tax can be set as equal to the profit oil, equation (3.56), which corresponds to the profit oil fraction as one, ( $f_{rf,i,t}^{PO} = 1$). Therefore, disjunction (3.30) is not required. The company needs to pay tax on its profit, eq. (3.57), where an effective tax rate may involve income tax and a specific profit tax, eq. (3.58), which are assumed to have a fixed value. The resulting tax is used to calculate the contractor's after tax share in eq. (3.59).

$$ConSh_{rf,t}^{beforetax} = PO_{rf,t} \qquad \forall rf,t \qquad (3.56)$$

$$Tax_{rf,t} = f_{rf,t}^{eff,taxrate} ConSh_{rf,t}^{beforetax} \qquad \forall rf,t \qquad (3.57)$$

$$f_{rf,t}^{eff,taxrate} = f_{rf,t}^{tax} + f_{rf,t}^{profittax} \qquad \forall rf,t \qquad (3.58)$$

$$ConSh_{rf,t}^{aftertax} = ConSh_{rf,t}^{beforetax} - Tax_{rf,t} \qquad \forall rf,t \qquad (3.59)$$

Notice that a particular concessionary system can also have a sliding scale royalty rates and/or sliding scale profit tax rates to penalize the production over a certain threshold. However, including those fiscal considerations is straightforward based on the modeling approach presented in the previous section for profit oil share in a typical PSA.

**(c) Regressive fiscal terms:** It can be considered as a specific case of the progressive fiscal terms with only one tier. In particular, disjunction (3.30) and its corresponding reformulation (3.31)-(3.38) is not required in the model. Therefore, the contractor's share in the profit oil can directly be written in terms of the given profit oil fraction for ringfence *rf* without index for tier *i*, constraint (3.60). Notice that since the binary variables corresponding to the disjunction are eliminated from the model for regressive fiscal terms, the model is likely to solve much faster than the progressive fiscal terms.

$$ConSh_{rf,t}^{beforetax} = f_{rf}^{po} \cdot PO_{rf,t} \qquad \forall rf,t \qquad (3.60)$$

**(d) Different Sliding scale variables:** The variables that define the tier structure for sliding scale can be contract specific. For instance, cumulative oil produced, R-factor or IRR. Therefore, a sliding scale variable $SV_{rf,t}$ for the fiscal system of interest can be used in disjunction (3.30) that yields disjunction (3.61), with its corresponding definition in eq. (3.62). Notice that depending on the definition of the sliding scale variable $SV_{rf,t}$ in eq. (3.62), there is the possibility that additional nonlinearities be introduced in the model, e.g. IRR as a sliding scale variable.

$$\underset{i}{\vee}\begin{bmatrix} Z_{rf,i,t} \\ ConSh_{rf,t}^{beforetax} = f_{rf,i}^{PO} \cdot PO_{rf,t} \\ L_{rf,i}^{oil} \le SV_{rf,t} \le U_{rf,i}^{oil} \end{bmatrix} \qquad \forall rf,t \qquad (3.61)$$

$$SV_{rf,t} = f_{rf,t}(xc_{rf,t}, COST_{rf,t}, REV_{rf,t}, \ldots) \qquad \forall rf,t \qquad (3.62)$$

In some cases, for instance sliding scale royalties where average daily oil production is the sliding scale variable, higher royalty rates are only applicable on the oil production rate that is above the given threshold value in each year, i.e. incremental sliding scale. Therefore, an effective overall royalty should be used in disjunction (3.61) for each tier i in each time period t instead of higher royalty rate on the total oil production. This situation mainly occurs in the concessionary systems.

**Discussions:**

1. Including fiscal rules in simple NPV based development planning models are traditionally assumed to be very expensive. However, this may not always be the case. For instance regressive (only 1 tier) fiscal terms may improve the computational performance of the model without any fiscal terms (e.g. regressive Model 3RF vs. Model 3R, see Table 3.9), or at least perform in the similar way. The progressive fiscal terms (tier structure as the disjunction in (3.30)) are usually the ones most responsible for increasing the computational time when we include the fiscal terms (see sections 3.6.2 and 3.6.3). This is due to the additional binary variables and resulting weak relaxation, as good bounds on the revenue, cost oil, profit oil for each time period are not known a priori. However, due to the importance of explicitly considering the fiscal aspects for planning optimization (see sections 3.6.1 and 3.6.2), it may be a worthwhile effort despite the increase in the solution time.
2. The model with ringfencing provisions is usually much more expensive to solve (see sections 3.6.2 and 3.6.3) than the model without any ringfence, as binary variables for tiers as in constraints (3.31)-(3.38) are required for each ringfence separately. In addition, the relaxation becomes even worse due to the cost disaggregation over each ringfence and additional binary variables as in constraints (3.6)-(3.24). Therefore, the computational efficiency of the fiscal model with many ringfences will rely on the efficiency of solving the model without any ringfence or just with few ringfences.
3. Concessionary or PSA fiscal system should have similar computational complexity as the solution time is associated to the progressive (tier) vs. regressive terms and ringfencing provisions that can be part of either of these contracts. For example, a regressive PSA model can be orders of magnitude faster than a progressive Concessionary system.
4. Although the proposed Model 3RF is a general formulation, the computational time requirements may vary significantly depending on the variables that define tiers in disjunction (3.30). Furthermore, additional nonlinearities may be introduced in some cases, for instance the IRR as a sliding scale variable,

that may require expensive global optimization based approaches for solving the resulting non-convex MINLP model. However, these rules are not very common in practice.

## 3.5 Computational Strategies

In this section, we propose some reformulation/approximation techniques and solution strategies to overcome the computational expense that can arise from incorporating the fiscal part in planning, specifically the models where progressive fiscal terms are present. Notice that the proposed approaches and results are presented taking **Model 3RF** (MILP) as a basis, where tiers are defined on the basis of cumulative oil produced for profit oil share, disjunction (3.30), that are widely used in practice. However, these approaches can directly be extended to other models that are proposed and a different sliding scale variable. Notice also that the proposed strategies are independent of ringfencing provisions.

**Reformulation/Approximation Techniques**

The following reformulation/approximation techniques in the proposed Model 3RF can improve its computational performance significantly:

***(i) Tighter Formulation using additional Logic Constraints and Valid Inequalities***

The additional logic constraints (3.63) and (3.64) can be included in Model 3RF if the sliding scale variable is a monotonically increasing function as time evolves, e.g. cumulative oil produced. In particular, constraints (3.63) ensure that once tier i is active in current period t, earlier tiers (i'< i) cannot be active in the future. Similarly, constraints (3.64) state that higher tiers (i'> i) cannot to be active before time period t if tier i is active in that period.

$$Z_{rf,i,t} \Rightarrow \bigwedge_{\tau=t}^{T} \neg Z_{rf,i',\tau} \qquad \forall rf, i, i' < i, t \qquad (3.63)$$

$$Z_{rf,i,t} \Rightarrow \bigwedge_{\tau=1}^{t} \neg Z_{rf,i',\tau} \qquad \forall rf, i, i' > i, t \qquad (3.64)$$

These logic constraints (3.63) and (3.64) can be expressed as integer linear inequalities, (3.65) and (3.66), respectively, (Raman and Grossmann, 1991).

$$Z_{rf,i,t} + Z_{rf,i',\tau} \le 1 \qquad \forall rf, i, i' < i, t, t \le \tau \le T \qquad (3.65)$$

$$Z_{rf,i,t} + Z_{rf,i',\tau} \le 1 \qquad \forall rf, i, i' > i, t, 1 \le \tau \le t \qquad (3.66)$$

In addition, we derive the following valid inequalities (3.67), see Appendix D (Proposition 3.1) for derivation, that can also be included in Model 3RF where cumulative oil produced is the sliding scale variable. The LHS of the inequality represents the cumulative contractor share in the profit oil by the end of time period *t* in terms of the oil volume, where $\alpha_t$ is the price of oil. Since, profit oil in a given year, eq. (3.41), is the difference of total oil produced in that year less cost oil that contractor used to recover its costs. Therefore, the RHS in (3.67) corresponds to an upper bound on the cumulative contractor's share in the cumulative profit oil by the end of time period t based on the sliding scale profit oil share and cost oil that has been recovered. In particular, the first term in RHS of inequality (3.67) accounts for the amount of the cumulative oil that contractor can receive by the end of time period t if tier i is active in the current time period t, based on the given tier thresholds without considering the impact of the cost oil. On the other hand, the second term in RHS is used to include the impact of cost oil recovery in the profit oil calculation to provide the tighter bound on cumulative contractor's share, where profit oil fraction of the last tier $f^{PO}_{rf,i^{end}}$ with minimum value is used so that it yields a valid upper bound for any tier i. Notice that these inequalities act as tight dynamic bounds on the cumulative contractor share that appears in the objective function for the corresponding value of the cumulative oil produced by the end of current year t. Therefore, this leads to a much tighter formulation than Model 3RF.

$$\sum_{\tau \le t} (Contsh^{beforetax}_{rf,\tau} / \alpha_\tau) \le \sum_{i'=1}^{i' \le i} (f^{PO}_{rf,i'} - f^{PO}_{rf,i'-1}) \cdot (xc_{rf,t} - L_{rf,i'}) - f^{PO}_{rf,i^{end}} \cdot \sum_{\tau \le t} (CO_{rf,\tau} / \alpha_\tau)$$
$$\forall rf, i, t \qquad (3.67)$$

We observed more than threefold improvement in the fullspace solution time with these additional mixed-integer linear constraints and valid inequalities, i.e. constraints (3.65)-(3.67) in Model 3RF, which we refer **Model 3RF-L**. This is due to the improved relaxation and significant reduction in the total number of nodes needed in the branch and bound search tree.

Notice that the same logic constraints (3.65)-(3.66) can be used for any other problem where sliding scale variable is monotonically increasing function as time progresses. A different set of logic constraints can be derived for a particular case of interest where this condition does not hold. Moreover, it is straightforward to derive similar inequalities (3.67) for other tier variables (e.g. daily oil produced), see Appendix D (Proposition 3.2). The general rule is that as long as we can represent the contractor's share (or cumulative one) as a direct fraction of gross revenues in the current period (or cumulative revenue) and the sliding scale variable is the daily oil produced (or cumulative oil), it is easy to generate similar inequalities. However, in some cases like with the IRR might require additional effort.

**(ii)** ***Alternate formulation: Sliding scale Fiscal Rules without Binary Variables***

Model 3RF, that relies on disjunction (3.30) and corresponding binary variables to represent the sliding scale fiscal terms, usually becomes expensive to solve for large instances. These instances may still be intractable even after we include the above logic constraints and valid inequalities. Therefore, in this section we present an alternative formulation of development planning Model 3RF with progressive fiscal terms that does not use disjunctions to represent the tier structure. Notice that although we consider the cumulative oil produced as the sliding scale variable, but the reformulation can also be used for a variety of other sliding scale variables.

In particular, the proposed **Model 3RI** is formulated from Model 3RF using valid inequalities described above (3.67), without considering the constraints (3.31)-(3.38) that correspond to the disjunction (3.30). This alternate Model 3RI may yield the optimal solution to a typical concessionary system or some special cases of PSAs, for which the valid inequalities (3.67) reduce to the simpler ones, (see Appendix E for more details).

However, for the general case of progressive PSA that has cost oil limit provisions, the proposed Model 3RI yields the relaxation of the original disjunctive Model 3RF as constraints (3.31)-(3.38) are not present. Therefore, we outline the following two possibilities to use this alternate model for general PSA fiscal terms that can be considered as a good heuristics to obtain the near optimal solution to realistic instances of the fiscal problem:

**Case 1: Relaxed Model (Model 3RI)**

In this case, the valid inequalities are directly used in Model 3RF as described earlier, i.e. constraints (3.67) in place of constraints (3.31)-(3.38) that correspond to the disjunction (3.30)**.** This yields a relaxed solution to the original problem, and therefore an upper bound. However, its solution can be used to generate a lower bound by fixing the discrete decisions in the original model. Furthermore, this model can be used in either a bi-level decomposition, disjunctive branch and bound, or branch-and-cut solution algorithm to close the gap between the upper and lower bounds. In general, this relaxed model provides reasonable bounds, and good discrete decisions in orders of magnitude less time than the disjunctive formulation used for sliding scales in Model 3RF.

**Case 2: Approximate Model (Model 3RI-A)**

In this case, the valid inequalities (3.67) are defined in Model 3RI such that they yield an approximate solution to the original problem, i.e. these are replaced with constraints (3.68). Notice that the inequalities (3.67) and (3.68) that are used in Models 3RI and 3RI-A, respectively, only differ in the second term in RHS. In the first case (eq. 3.67), as we use the least value of this term ( $f^{PO}_{rf,i^{end}}$ ) for it to be valid for all tiers, so it turns out to be the relaxation. On the other hand, in eq. (3.68) we use the highest value of this term ( $f^{PO}_{rf,1}$ ) to approximate the initial tiers as close to reality as possible when costs are high yielding near optimal solutions. Since, Model 3RI-A is an approximate model, neither an upper or lower bound is guaranteed from this model, but in practice, it yields the solution within 2-3% of accuracy based on our computational experiments. Moreover, its solution can be used to generate a near optimal solution to the original problem in orders of magnitude less time than the disjunctive approach used in Model 3RF. The detailed description of the correspondence between these two different set of inequalities, (3.67) vs. (3.68), and derivation of inequalities (3.68) is explained in Appendix F.

$$\sum_{\tau \le t} (Contsh_{rf,\tau}^{beforetax} / \alpha_\tau) \le \sum_{i'=1}^{i' \le i} (f_{rf,i'}^{PO} - f_{rf,i'-1}^{PO}) \cdot (xc_{rf,t} - L_{rf,i'}) - f_{rf,1}^{PO} \cdot \sum_{\tau \le t} (CO_{rf,\tau} / \alpha_\tau) \quad \forall rf, i, t \qquad (3.68)$$

**Remarks:**

1. The advantage of using Model 3RI and Model 3RI-A is that these are orders of magnitude faster to solve than other fiscal models relying on the disjunctive constraints, and even 3-4 times faster than solving the models without any fiscal terms (i.e. Model 3R) as observed by the computational experiments. The extreme instances of the oilfield planning problem with fiscal terms, i.e. progressive PSA with ringfencing, are solved in reasonable time using these alternate models which were intractable for Model 3RF.
2. Notice that the alternate Model 3RI and its approximation Model 3RI-A are defined for the tier structure that is assumed to be linked to the cumulative oil produced. Other sliding scale variables, e.g. daily oil produced, R-factor are also used in practice. The similar approaches as described in the chapter can be explored to model these fiscal considerations without explicitly using disjunctions and corresponding binary variables.

These reformulation/approximation techniques can be used for the other models directly. Tables 3.2 and 3.3 summarize all of the proposed models (MINLP and MILP) for oilfield development planning problem with and without fiscal considerations. In particular, Table 3.2 involves basic models 1, 2 and 3 with their fiscal counterparts considering detailed investment timing for the pipeline connections. Whereas, Table 3.3 represents the respective reduced models that are obtained by removing a large fraction of binary variables that represent connection timings to improve the computational efficiency without significant loss in the solution quality.

Table 3.2: Comparison of the proposed oilfield planning models (detailed connections)

| | **MINLP** | **MINLP** | **MILP** |
|---|---|---|---|
| Basic Model | Model 1 | Model 2 | Model 3 |
| Basic model with fiscal terms (using Disjunctions (3.30)) | Model 1F | Model 2F | Model 3F |
| Basic model with fiscal terms (using Disjunctions (3.30), Logic constraints (3.65)-(3.66) and valid Inequalities (3.67)) | Model 1F-L | Model 2F-L | Model 3F-L |
| Basic model with fiscal terms (no binary variables for sliding scales i.e. using only valid Inequalities (eq. (3.67) for relaxed/exact model or eq. (3.68) for approximate model)) | Model 1I (relaxed/exact) | Model 2I (relaxed/exact) | Model 3I (relaxed/exact) |
| | Model 1I-A (approximate) | Model 2I-A (approximate) | Model 3I-A (approximate) |

Table 3.3: Comparison of the proposed oilfield planning models (neglecting piping investments)

| | **MINLP** | **MINLP** | **MILP** |
|---|---|---|---|
| Basic Model with binary reduction | Model 1R | Model 2R | Model 3R |
| Basic model with binary reduction and fiscal terms (using Disjunctions (3.30)) | Model 1RF | Model 2RF | **Model 3RF** |
| Basic model with binary reduction and fiscal terms (using Disjunctions (3.30), Logic constraints (3.65)-(3.66) and valid Inequalities (3.67)) | Model 1RF-L | Model 2RF-L | **Model 3RF-L** |
| Basic model with binary reduction and fiscal terms (no binary variables for sliding scales i.e. using only valid Inequalities (eq. (3.67) for relaxed/exact model or eq. (3.68) for approximate model)) | Model 1RI (relaxed/exact) | Model 2RI (relaxed/exact) | **Model 3RI (relaxed/exact)** |
| | Model 1RI-A (approximate) | Model 2RI-A (approximate) | **Model 3RI-A (approximate)** |

## 3.6 Numerical Results

In this section, we consider three instances of the oilfield planning problem with fiscal considerations where ringfencing provisions may or may not be present, and examine the efficiency of the proposed models and solution strategies.

### 3.6.1 Instance 1

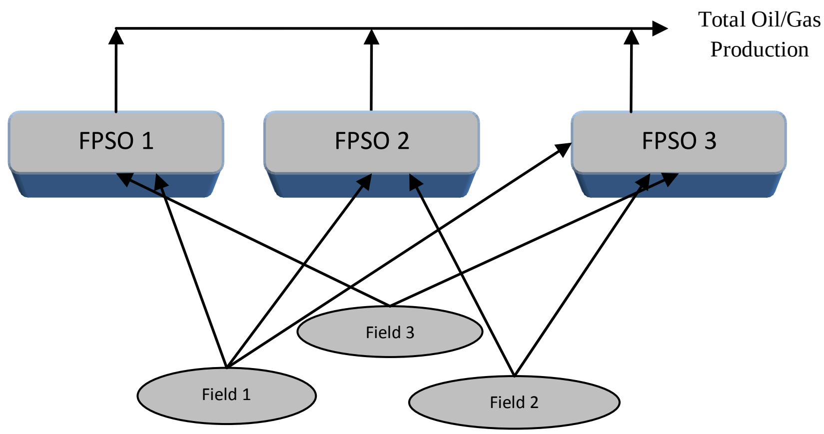


Figure 3.7: Instance 1 (3 Fields, 3 FPSO, 15 years, No Ringfencing)

In this instance (Figure 3.7) we consider 3 oil fields that can be connected to 3 FPSOs with 7 possible connections among these fields and FPSOs. There are a total of 25 wells that can be drilled, and the planning horizon considered is 15 years, which is discretized into 15 periods of each 1 year of duration. Table 3.4 represents the data corresponding to the field sizes and their initial deliverability per well for a particular field-FPSO connection. There is a cost recovery ceiling of 50% and 3 tiers that are defined for profit oil split between the contractor and the host government, and are linked to cumulative oil production as seen in Table 3.5. This represents the fiscal terms of a typical progressive Production Sharing Agreement without ringfencing provisions.

We need to determine which of the FPSO facilities is to be installed or expanded, in what time period, and what should be its capacity, to which fields it should be connected and at what time, and the number of wells to be drilled in each field during each time period. Other than these installation decisions, there are operating decisions involving the flowrate of oil, water and gas from each field in each time period. The problem is solved to maximize the NPV of the contractor's share after paying taxes, and corresponding optimal investment and operations decisions over the planning horizon.

Table 3.4: Field characteristics for instance 1

| **Fields** | **Field Size (MMbbl)** | **Initial Oil derivability per well (kstb/d)** | | |
|---|---|---|---|---|
| | | **FPSO 1** | **FPSO 2** | **FPSO 3** |
| Field 1 | 230 | 16 | 18 | 16 |
| Field 2 | 280 | - | 18 | 20 |
| Field 3 | 80 | 15 | - | 12 |

Table 3.5: Sliding scale Contractor's profit oil share for instance 1

| **Tiers** | **Cumulative Oil Produced** | **Contractor's Share in Profit Oil** |
|---|---|---|
| Tier 1 | 0-150 MMbbl | 50% |
| Tier 2 | 150-325 MMbbl | 40% |
| Tier 3 | >325 MMbbl | 20% |

The models are implemented in GAMS 23.6.3 and run on Intel Core i7, 4GB RAM machine using CPLEX 12.2. The optimal solution of this problem is presented in Table 3.6, that corresponds to Model 3F involving detailed connections, suggests installing only FPSO 3 with a capacity 297.75 kstb/d and 161.90 MMSCF/d for liquid and gas, respectively, at the beginning of year 1. It takes 3 years for this FPSO to be available for production. Fields 1 and 2 are connected to this FPSO at the beginning of year 4, where 7 wells are drilled in Field 1 and 6 wells are drilled in Field 2 to start the production. These fields are preferred compared to Field 3 due to their large sizes and deliverabilities. Liquid capacity of FPSO 3 facility is expanded by 103.93 kstb/d in year 5 that becomes available in year 6 due to 1 year of lead time involved. Field 3 that is smaller in size comes online at the beginning of year 6 when deliverability of fields 1 and 2 decreases, where 3 wells are drilled in this field with an additional well in year 9 when production goes down. There are no further expansions and well drillings after year 9. Notice that most of the investments occur in early stages of the project. The total NPV of this project is $ 1497.69M after paying government share.

Table 3.6: Optimal Installation and Drilling Schedule for instance 1

| **Year** | 1 | 2 | 3 | 4 | 5 | 6 | 7 | 8 | 9 | 10-15 |
|---|---|---|---|---|---|---|---|---|---|---|
| **Facility Installations** | Install FPSO3 | - | - | - | Expand FPSO3 | - | - | - | - | - |
| **Field 1** | - | - | - | Drill 7 wells | - | - | - | - | - | - |
| **Field 2** | - | - | - | Drill 6 wells | Drill 1 well | Drill 2 wells | - | - | - | - |
| **Field 3** | - | - | - | - | - | Drill 3 wells | - | - | Drill 1 well | - |

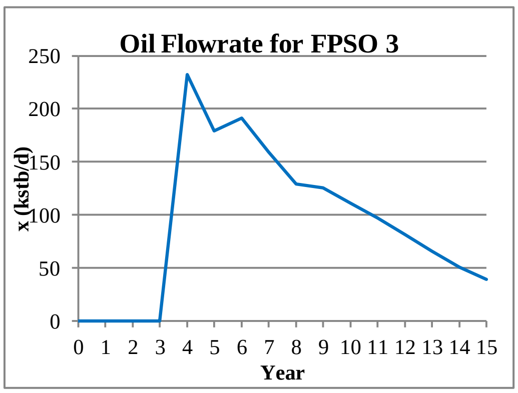


Figure 3.8: Total oil flowrate for FPSO 3

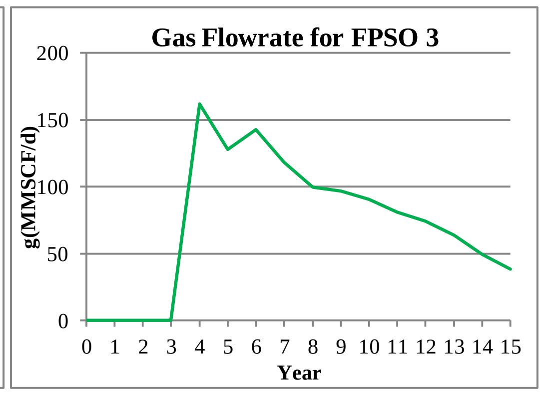


Figure 3.9: Total gas flowrate for FPSO 3

Figures 3.8-3.9 represent the total oil and gas flow rates for the FPSO facility during the planning horizon considered. Given that the timing of the particular tier activation depends upon the cumulative oil production for this instance (Table 3.5) Tier 2 becomes active after fifth year while Tier 3 is active after the eighth year involving less share in profit oil for contractor, see Figure 3.10.

In contrast, the sequential approach that first maximizes NPV i.e. Model 3, without considering the impact of the fiscal terms, and then calculates the contractor share based on these decisions and fiscal rules, yields a very different solution. The optimum in this case suggests installing FPSO3 with a large capacity (liquid 445.54 kstb/d and gas 211.65 MMSCF/d) at the beginning of the planning horizon without any future expansions. The drilling decisions are also front ended compared to the solution of the fiscal model, Model 3F. However, the total NPV of the contractor's share in the sequential case turns out to be $ 1362.67M, which is significantly lower than the optimal solution ($ 1497.69M) of the model with fiscal considerations (Model 3F). These results represent the optimistic nature of the sequential approach that tries to generate as much revenue as possible at the beginning of the planning horizon neglecting the trade-offs that are associated to the fiscal part. Therefore, it may lead to the decisions that can incur large losses in the long term after considering the impact of the fiscal calculations.

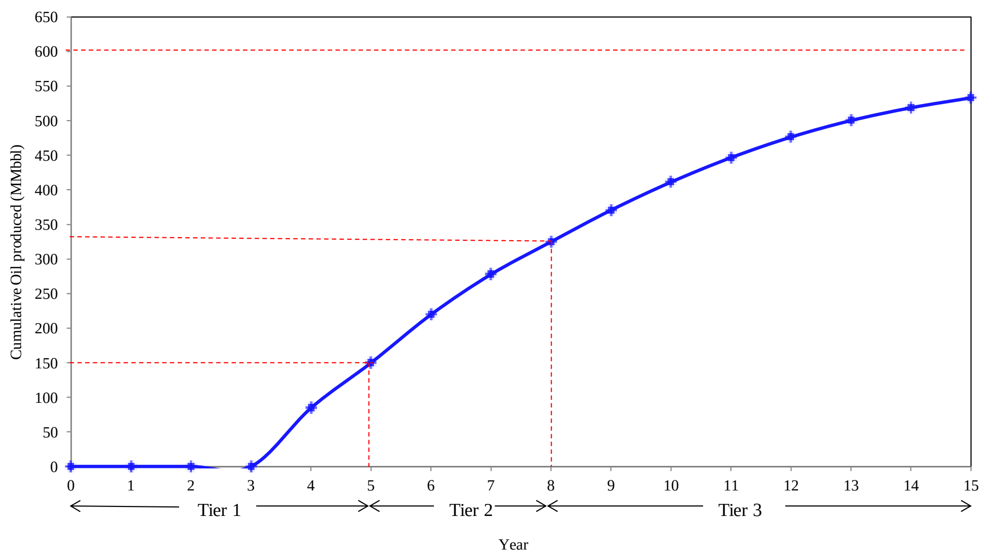


Figure 3.10: Cumulative Oil Produced vs. Timing of Tier activation

Table 3.7: Comparison of the computational performance of various models for instance 1

| Model | Solver | # of constraints | # of continuous variables | # of discrete variables | NPV ($Million) | Time (s) |
|---|---|---|---|---|---|---|
| Model 2F (MINLP) | BARON 9.0.6 | 3,557 | 2,236 | 345 | 1,198.44 (<60% gap) | >36,000 |
| Model 3F (MILP) | CPLEX 12.2 | 5,199 | 3,668 | 399 | 1,497.69 | 3,359 |
| Model 3RF (MILP) | CPLEX 12.2 | 5,147 | 3,570 | 322 | 1,497.69 | 337 |

Table 3.7 compares the computational performance of the various models. In particular, Model 3RF which is obtained after binary reduction from Model 3F yields the same solution in an order of magnitude less time (337s vs. 3,359s), when solved to optimality. In contrast, solving the corresponding MINLP formulation Model 2F with BARON 9.0.6 can only provide a solution having NPV of $ 1198.44M with a 60% gap in more than 10 hours. Moreover, we observe that solving Model 2F directly with DICOPT requires a good initialization due to the additional binary variables and constraints that are added in this fiscal model compared to Model 2. Therefore, the optimal solution from corresponding MILP formulations (Model 3F and Model 3RF) provides a way to obtain a near optimal solution of the original Model 2F. We fixed the design decisions in Model 2F from the optimal solution of Model 3RF and solved the resulting NLP problem that yields an NPV of $1496.26 M, which shows that the accuracy of the MILP solution is within 0.1% of the MINLP formulation. Therefore, the proposed MILP formulations are computationally efficient and provide near optimal solutions. In the next section, we will use these MILP models as the basis and examine the performance of the proposed computational strategies for the larger instances.

### 3.6.2 Instance 2

**(i) PSA without ringfencing provisions for Instance 2**

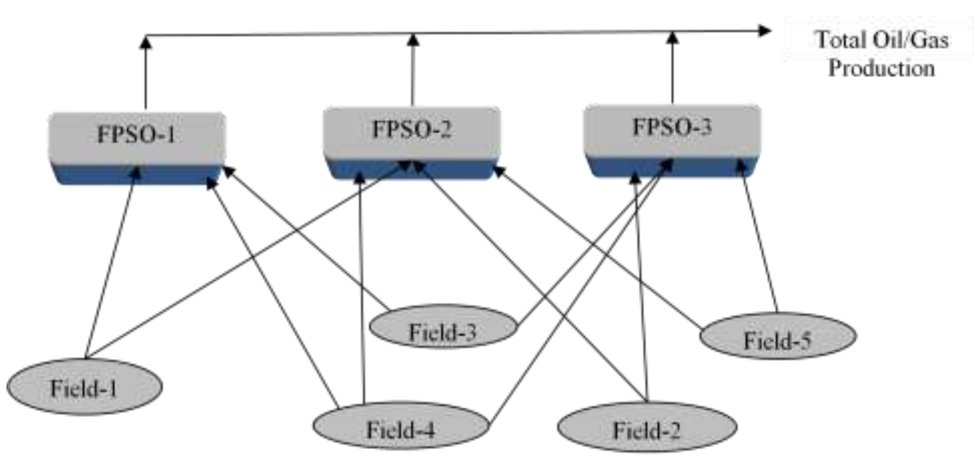


Figure 3.11: Instance 2 (5 Fields, 3 FPSOs, 20 years, No ringfencing)

In this instance, we consider 5 oilfields that can be connected to 3 FPSOs with 11 possible connections, see Figure 3.11. There are a total of 31 wells that can be drilled in these 5 fields, and the planning horizon considered is 20 years. There is a cost recovery ceiling of 50% and 4 tiers (see Fig. 3.3) that are defined for profit oil fraction between the contractor and host government based on the cumulative oil production. The problem is solved to maximize the NPV of the contractor's share after paying taxes and the corresponding optimal investment/operations decisions.

Table 3.8 compares the performance of the MILP (Model 3F) involving detailed connections and reduced MILP model (Model 3RF) that are the extension of the Models 3 and 3R, respectively, with progressive PSAs. The models are implemented in GAMS 23.6.3 and run on Intel Core i7, 4GB RAM machine using CPLEX 12.2. We can observe that there is significant increase in the computational time with fiscal consideration for the MILP formulation Model 3F with this larger instance, which takes more than 10 hours with a 14% of optimality gap as compared to the reduced MILP model (Model 3RF), which terminates the search with a 2% gap in reasonable time.

Table 3.8: Computational Results for Instance 2 (Model 3F vs. Model 3RF)

| **Model** | **# of constraints** | **# of continuous variables** | **# of discrete variables** | **NPV ($Million)** | **Time (s)** | **Optimality Gap** |
|---|---|---|---|---|---|---|
| Model 3F | 9,474 | 6,432 | 727 | 2,183.63 | >36,000 | <14% |
| Model 3RF | 9,363 | 6,223 | 551 | 2,228.94 | 1,164 | <2% |

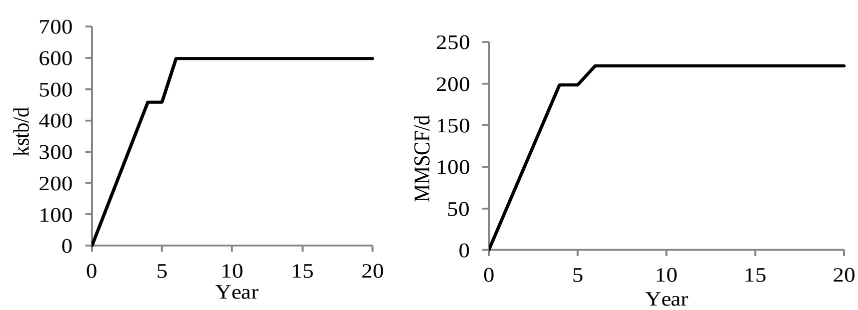


(a) Liquid capacity (b) Gas capacity

Figure 3.12. Optimal liquid and gas capacities of FPSO 3 facility for Instance 2

The optimal solution from Model 3RF suggests installing 1 FPSO facility (FPSO3) with expansions in the future (see Fig. 3.12), while Fig. 3.13 represents the well drilling schedule for this example. The tiers 2, 3 and 4 for profit oil split become active in years 6, 8 and 12, respectively, based on the cumulative oil production profile during the given planning horizon. Notice that the optimal solution of this problem fails to develop field 1, which is not intuitive. The reason for not developing field 1 is that the size of the field 1 is quite small as compared to the other fields and the superstructure we consider does not allow connecting field 1 to FPSO 3, which is the only FPSO that is installed. Therefore, based on the superstructure and field size, it is not worth to install an additional FPSO to produce from this field after paying government share. In contrast, the solution from the sequential approach suggests exploring field 1 as well since it is worth in that case to install 2 small FPSO facilities and also produce from field 1 given that the trade-offs due to fiscal rules are neglected. Whereas, the total NPV of the contractor's share in this case is lower than the optimal solution of Model 3RF ($1,914.71M vs. $2,228.94M ).Therefore, we can observe that incorporating fiscal terms within development planning can yield significantly different investment and operations decisions compared to a simple NPV based optimization.

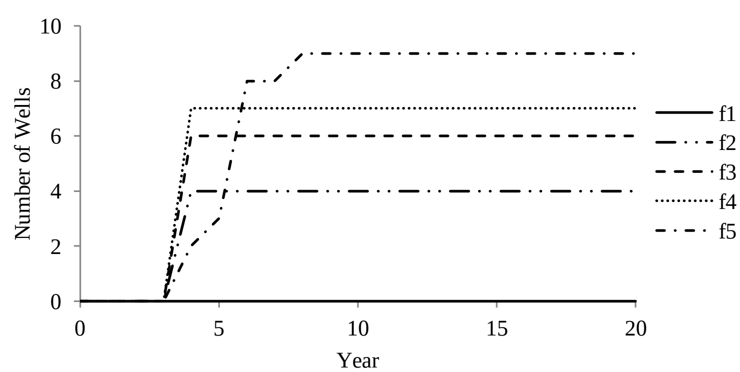

Figure 3.13. Optimal well drilling schedule for Instance 2

Note that fiscal terms without tier structure, for instance fixed percentage of profit share, royalty rates, often reduces the computational expense of solving the deterministic model directly without any fiscal terms instead. Surprisingly, the problem with flat 35% of the profit share of contractor is solved in 73s which is even smaller than the solution time for deterministic case without any fiscal terms (190s). On the other hand, the problem with 2 tiers instead of 4 as considered above is solved in 694s which is more than the model without fiscal terms and less than the model with 4 tiers as can be seen in Table 3.9. Therefore, the increase in computational time while including fiscal rules within development planning, is directly related to the number of tiers (levels) that are present in the model to determine the profit oil shares or royalties.

Table 3.9: Comparison of number of tiers vs. solution time for Model 3RF

| # of tiers | Time (s) |
|---|---|
| 4 | 1,164 |
| 2 | 694 |
| 1 | 73 |
| No fiscal rules | 190 |

Table 3.10 compares the further improvements in the solution time for Model 3RF (1,164s) after using the reformulation/approximation techniques and strategies that are proposed. In particular, the tighter formulation Model 3RF-L that is obtained after including logic constraint and valid inequalities, (3.65)-(3.67), is solved in one fourth of the time than Model 3RF. Notice that these MILP models are solved with a 2% of optimality tolerance yielding a slightly different objective values for Model 3RF and Model 3RF-L. Model 3RI, which relaxes the disjunction (3.30), can be solved more than 20 times faster than the original Model 3RF. Although the solution obtained is a relaxed one (upper bound of 2,591.10), it gives the optimal investment decisions that result in the same solution as we obtained from solving Model 3RF directly. The approximate version of this Model 3RI-A, takes only 82s as compared to Model 3RF (1164s) and yields the optimal solution after we fix the decisions from this model in the original one. Notice that the quality of the approximate solution itself is very good (~1.5% accurate) and both relaxed/approximate models are even ~3 times faster than the model without any fiscal terms (Model 3R) that takes 190s.

Table 3.10: Results for Instance 2 after using various solution strategies

| Model | # of constraints | # of continuous variables | # of discrete variables | NPV ($Million) | NPV after fixing decisions in Model 3RF ($Million) | Time (s) |
|---|---|---|---|---|---|---|
| Model 3RF | 9,363 | 6,223 | 551 | 2,228.94 | - | 1,164 |
| Model 3RF-L | 11,963 | 6,223 | 551 | 2,222.40 | - | 275 |
| Model 3RI-A | 8,803 | 5,903 | 471 | 2,197.63 | 2,228.94 | 82 |
| Model 3RI | 8,803 | 5,903 | 471 | 2,591.10 | 2,228.94 | 48 |

**(ii) PSA with ringfencing provisions for Instance 2**

In this case, we consider two ringfences for the above Instance 2 (see Figure 3.4) where progressive PSA terms are defined for each of these ringfences separately. Based on the computational performance of the Model 3RF as compared to Model 3F in the previous case, we only show the results for Model 3RF, which is more efficient.

Table 3.11: Results for Instance 2 with ringfencing provisions

| Model | # of constraints | # of continuous variables | # of discrete variables | NPV ($Million) | NPV after fixing decisions in Model 3RF ($Million) | Time (s) | % gap |
|---|---|---|---|---|---|---|---|
| Model 3RF | 14,634 | 9,674 | 651 | 2,149.39 | - | >36,000 | <15.4% |
| Model 3RF-L | 19,834 | 9,674 | 651 | 2,161.27 | - | 3,334 | <2% |
| Model 3RI-A | 13,514 | 9,034 | 491 | 2,148.90 | 2,142.75 | 134 | <2% |
| Model 3RI | 13,514 | 9,034 | 491 | 2,533.06 | 2,151.75 | 112 | <2% |

Table 3.11 compares the results for various models for this case. We can observe that including ringfencing provisions makes Model 3RF expensive to solve (>10 hrs), compared to the previous instance without any ringfences that required only 1,164s. This is due to the additional binary variables that are required in the model for each of the two ringfences, their trade-offs and FPSO cost disaggregation. In contrast, since Models 3RI and 3RI-A do not need binary variable for the sliding scale in disjunction (3.30), they solve much faster than Model 3RF (>300 times faster) and Model 3RF-L (~30 times faster). Notice that even after including ringfencing provisions, these two models are faster than the

simple NPV based Model 3R. This is due to the trade-off from the fiscal part in the simple NPV based model without binary variables for the sliding scale.

Notice that Model 3RI and 3RI-A are solved here in one of the most general forms of the fiscal terms where the solutions may not be the global optimal, but the relaxed Model 3RI, which provides a valid upper bound, also allows to compare the solution quality. The optimal NPV after ringfencing provisions is lower as compared to the earlier case without ringfencing provisions due to the additional restrictions it imposes on the revenue and cash flows.

In addition, we also consider a bi-level decomposition approach (see Appendix G) to solve this ringfencing instance. The algorithm considers an aggregate fiscal model at upper level by neglecting the ringfencing provisions that yields an upper bound ($2,222.40 M) as can be seen in Table 3.12. The lower level detailed fiscal model is solved for the infrastructure selected from the upper level problem to yield the feasible solution ($2,161.27 M). In the next iteration, the upper level problem is solved with additional integer cuts that avoid the same investment decisions to be selected. The objective value of this model ($2,040.23 M) becomes smaller than the lower bound obtained during the first iteration and the algorithm stops. The MILP models are solved in this instance with a 2% of optimality tolerance and total solution time is 869s. Based on these preliminary results, the algorithm can be considered as an alternative to solve the oilfield problems involving ringfencing provisions. However, the efficiency of the algorithm relies on the efficiency of solving the lower and upper level problems which may itself become expensive to solve for the large instances and/or may need several iterations to close the gap.

Table 3.12: Bi-level decomposition for Instance 2 with ringfencing provisions

| **Iteration** | **UB ($Million)** | **LB ($Million)** | **Optimality gap (%)** |
|---|---|---|---|
| 1 | 2,222.40 | 2,161.27 | 2.75% |
| 2 | 2,040.23 | - | 0.00% |

### 3.6.3 Instance 3

### (i) PSA without ringfencing provisions for Instance 3

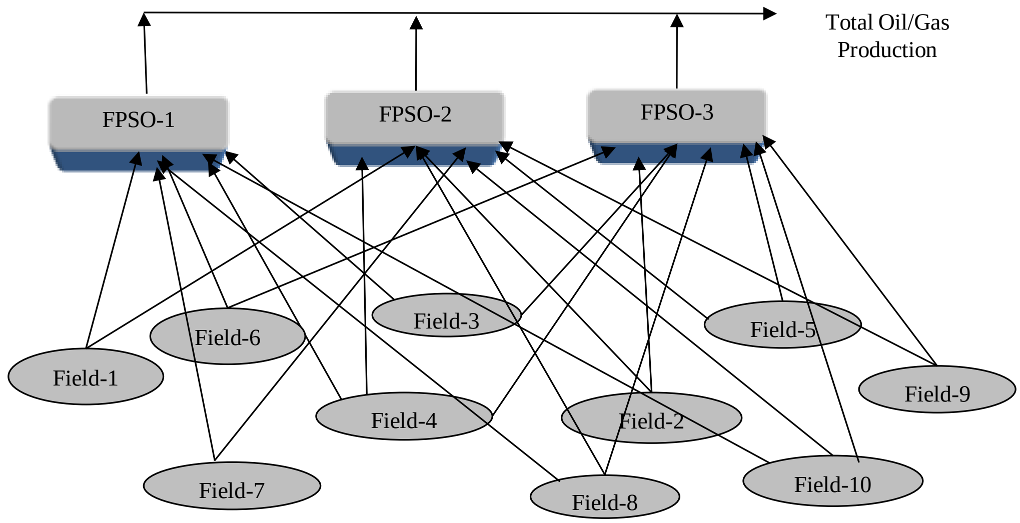


Figure 3.14: Instance 3 with 10 Fields, 3 FPSO, 20 years

In this case, we consider a larger instance of the oilfield planning problem with fiscal considerations. There are 10 oil fields (Figure 3.14) that can be connected to 3 FPSOs with 23 possible connections. There are a total of 84 wells that can be drilled in all of these 10 fields and the planning horizon considered is 20 years. There is a cost recovery ceiling of 50% and 4 tiers are defined for profit oil split between the contractor and host government that are linked to cumulative oil production. The objective is to maximize the NPV of the contractor's share after paying taxes and corresponding optimal investment/operations decisions.

Table 3.13: Results for Instance 3 after using various solution strategies

| Model | # of constraints | # of continuous variables | # of discrete variables | NPV ($Million) | NPV after fixing decisions in Model 3RF ($Million) | Time (s) | % gap |
|---|---|---|---|---|---|---|---|
| Model 3RF | 17,640 | 11,727 | 963 | 6,440.58 | - | >72,000 | <22% |
| Model 3RF-L | 20,240 | 11,727 | 963 | 6,498.45 | - | 22,500 | <10% |
| Model 3RI-A | 17,080 | 11,407 | 883 | 6,355.00 | 6,452.36 | 2,035 | <10% |
| Model 3RI | 17,080 | 11,407 | 883 | 7,319.60 | 6,484.12 | 1,569 | <10% |

Table 3.13 compares the solution time required for Model 3RF with the proposed reformulation/approximation techniques. We can observe that even Model 3RF without any ringfences becomes expensive to solve for this larger instance as compared to instance 2. Moreover, it takes more than 20hrs to reach within 22% of optimality for Model 3RF, whereas the relaxed Model 3RI can be solved in less than half an hour within 10% of optimality. The solution that is obtained after fixing the design decisions in the original formulation is also better than Model 3RF. Model 3RI-A, which is an approximation, also performs similar to the relaxed model and gives an even improved solution than Model 3RF with a ~2% of accuracy. Both models are more than 20 times faster than even the tighter formulation Model 3RF-L involving logic constraints and valid inequalities. Surprisingly, these models perform again better than the model without any fiscal terms, i.e. the simple NPV based model (Model 3R) takes more than 12,000s to reach within 10% of optimality gap due to the trade-off that is missing between production and fiscal part.

Notice that the times reported in Table 3.13 for Model 3RI-A and 3RI are the times to solve Models 3RI-A and 3RI only. We did not include the time required to solve Model 3RF with fixed decisions in all the examples considered since it was negligible as compared to solution time of Models 3RI-A, 3RI and 3RF. For instance, it is ~2 orders of magnitude smaller than the solution time required for Model 3RI-A (25s vs. 2035s) for this case. It is due to the fact that the critical discrete variables that represent the infrastructure and well drilling are fixed in the model and most of the remaining decisions correspond to the continuous operational decisions.

**(ii) PSA with ringfencing provisions for Instance 3**

In this case, we consider three ringfences for the above Instance 3 with 10 fields (see Figure 3.14) where Table 3.14 and 3.15 represent data corresponding to the field sizes, ringfencing provisions and sliding scale profit oil divisions.

Table 3.14: Field Sizes and Ringfencing Provisions for Instance 3

| Field | F-1 | F-2 | F-3 | F-4 | F-5 | F-6 | F-7 | F-8 | F-9 | F-10 |
|---|---|---|---|---|---|---|---|---|---|---|
| Field Size (MMbbl) | 60 | 100 | 170 | 230 | 280 | 80 | 200 | 320 | 400 | 500 |
| Corresponding Ringfence | RF-1 | RF-1 | RF-1 | RF-2 | RF-2 | RF-2 | RF-3 | RF-3 | RF-3 | RF-1 |

Table 3.15: Fiscal data for Instance 3 with ringfencing provisions

(i) Sliding scale Contractor's Profit Oil share

| | Ringfences: RF-1, RF-2, RF-3 | |
|---|---|---|
| | Cumulative oil Produced | Contractor's Profit Oil Share |
| Tier-1 | 0 - 200 MMbbl | 50% |
| Tier-2 | 200 - 400 MMbbl | 40% |
| Tier-3 | 400 - 600 MMbbl | 30% |
| Tier-4 | > 600 MMbbl | 20% |

(ii) Tax rates and Cost Oil Ceilings

| Ringfence | Income Tax Rate ( % of Contractor's Profit Oil Share) | Cost Recovery Ceiling (% of Gross Revenues from the Ringfence) |
|---|---|---|
| RF-1 | 30% | 50% |
| RF-2 | 30% | 50% |
| RF-3 | 30% | 50% |

Table 3.16 compares the computational results of various models for this case of instance 3. It can be observed that including ringfencing provisions for this largest instance makes even both Model 3RF and Model 3RF-L very expensive compared to the previous case without any ringfences. This is due to the additional binary variables that are required in the model for each of the three ringfences separately and resulting weak relaxations.

Table 3.16: Results for Instance 3 with Ringfencing provisions

| Model | # of constraints | # of continuous variables | # of discrete variables | NPV ($Million) | NPV after fixing decisions in Model 3RF ($Million) | Time (s) | % gap |
|---|---|---|---|---|---|---|---|
| Model 3RF | 33,403 | 22,150 | 1,163 | 6,382.46 | - | >72,000 | <57% |
| Model 3RF-L | 41,203 | 22,150 | 1,163 | 6,469.30 | - | >72,000 | <22% |
| Model 3RI-A | 31,723 | 21,190 | 923 | 6,273.59 | 6,442.68 | 3,383 | <10% |
| Model 3RI | 31,723 | 21,190 | 923 | 7,166.70 | 6,349.99 | 4,003 | <10% |

In contrast, since Models 3RI and 3RI-A do not require binary variables for sliding scales, they perform much better than Model 3RF and its tighter version Model 3RF-L as observed in the earlier cases. Model 3RI is a relaxation and yields a reasonable upper bound, while Model 3RI-A yields an approximate solution within 3% of accuracy.

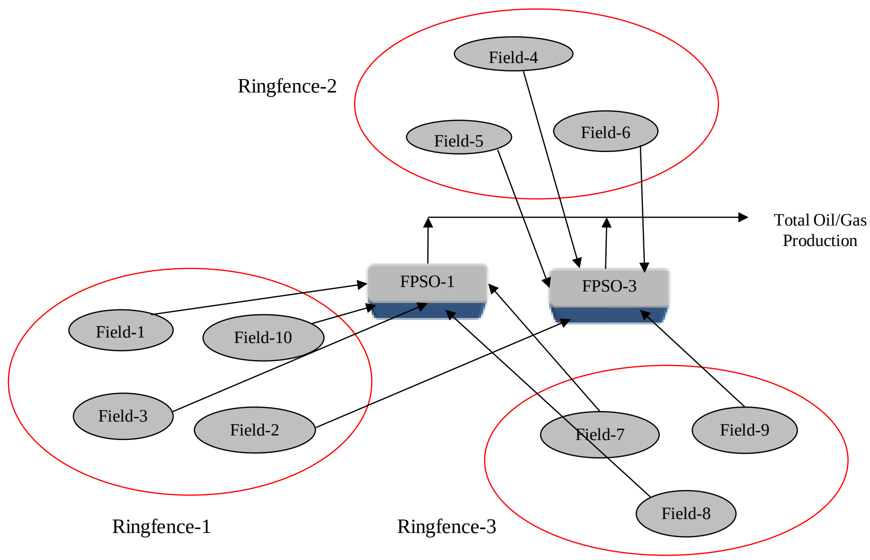


Figure 3.15: Optimal Solution for Instance 3 with Ringfencing provisions

Figure 3.15 represents the optimal installation and connections between fields and FPSO for this problem, where we can observe that each of the installed FPSO (1 and 3) is connected to a total of 5 fields that do not belong to the same ringfence. The optimal cumulative oil production profile for various ringfences is shown in Figure 3.16, and the sliding scale rules in Table 3.15(i), results in the different times of higher tier activations for these three ringfences as shown in Table 3.17. Notice that ringfence 3, which involves larger size fields, enters into higher tier (Tier 4) sooner as compared to the other ringfences. Moreover, in ringfence 2 which has smaller fields, only 3 tiers become active.

Table 3.17: Optimal timings of Tier activations for various Ringfences

| **Ringfence** | **Tier-1** | **Tier-2** | **Tier-3** | **Tier-4** |
|---|---|---|---|---|
| RF-1 | Year 1- Year 6 | Year 7- Year 8 | Year 9- Year 12 | Year 13- Year 20 |
| RF-2 | Year 1- Year 6 | Year 7- Year 10 | Year 11- Year 20 | - |
| RF-3 | Year 1- Year 6 | Year 7- Year 8 | Year 9- Year 11 | Year 12- Year 20 |

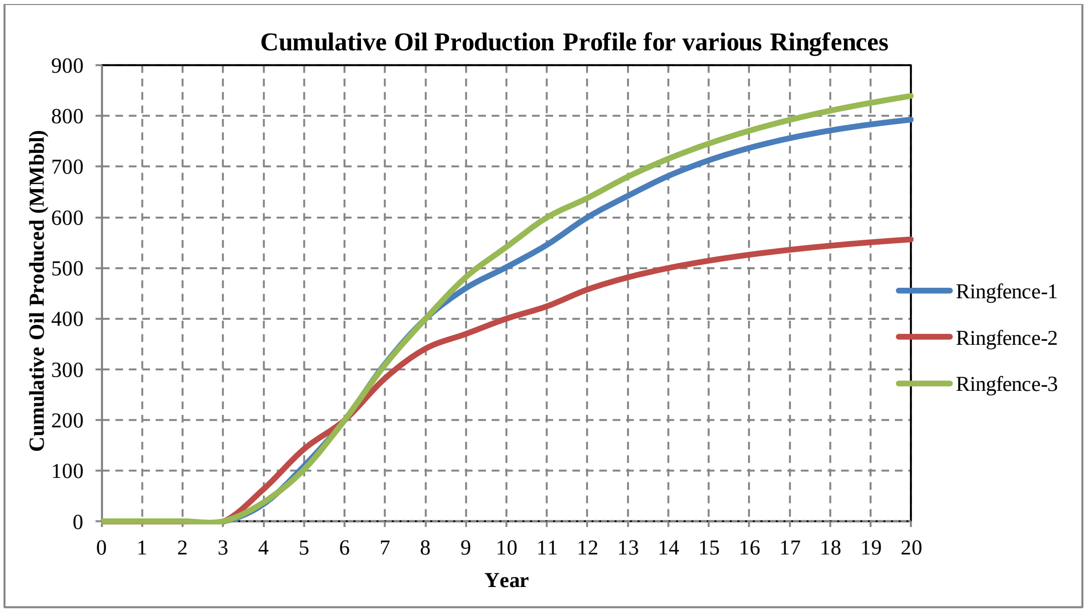


Figure 3.16: Optimal Cumulative Oil production for Instance 3 with Ringfencing provisions

It is important to note that the performance of Models 3RI and 3RI-A is independent of the number of ringfences that are present in the fiscal terms, as it can be seen that the increase in solution time is negligible compared to the previous case without ringfencing provisions. This is due to the fact that increasing ringfences in these models only increases the number of continuous variables and linear constraints, except a few binary variables that are required for cost oil recovery calculation. In contrast, the complexity of Models 3RF and 3RF-L that rely on disjunction (3.30) increases exponentially with an increase in the number of ringfences or tiers. Moreover, it is also interesting to note that even after including one of the extreme cases of the fiscal term (progressive PSA with ringfencing) for a large instance involving 10 fields, the proposed relaxed/approximate models still perform extremely well, and they are in fact even 3-4 times better than the simple NPV based Model 3R without fiscal considerations.

## 3.7 Conclusions

In this chapter, we have introduced the fiscal aspects within offshore oil and gas field planning problem. These fiscal considerations are usually either ignored or considered in an ad-hoc manner, which may have a very large impact on the planning decisions. In particular, we have proposed a general model for the multi-field site problems that accounts for the fiscal calculations in the objective functions and constraints explicitly. The model is an extension of the strategic/tactical planning model presented in the previous chapter to progressive PSAs involving ringfencing provisions. Few simpler cases of the fiscal contracts have also been derived from the proposed general model as an illustration. The model yields investment and operating decisions that are not only optimal in the sense of NPV after taxes for the project at hand, but also provides a more appropriate basis to compare a portfolio of different projects involving different fiscal contracts and other details. However, as the computational expense can be a serious issue with the incorporation of fiscal terms for some particular contract, we have also proposed a tighter formulation using additional logic constraints and valid inequalities, two heuristic approaches yielding good solutions to the large instances, and a bi-level decomposition approach. Numerical results in realistic examples show that these models and solution strategies are quite efficient, and reduce the solution time orders of magnitude than using the MILP for the disjunctive formulation. We hope that this work has shown that explicit consideration of the fiscal rules is important for oilfield infrastructure planning, and that the models/methods described here can serve as the basis for further extensions and improvements in the computational effort.

# Chapter 4

# Solution strategies for multistage stochastic programming with endogenous uncertainties in the planning of process networks

## 4.1 Introduction

In this chapter, we consider a general multistage stochastic mixed-integer linear programming model for multiperiod planning problems where optimization decisions determine the times when the uncertainties in some of the parameters will be resolved, i.e. decision-dependent uncertainty (Jonsbraten et al., 1998; Goel and Grossmann, 2006; and Tarhan and Grossmann, 2008). To address the issue of computational expense in solving these endogenous uncertainty problems, we also present several solution strategies and apply them to process network examples having uncertainty in the process yields which can only be revealed once an investment is made in the process.

The outline of this chapter is as follows. First, in sections 4.2 and 4.3 we present the problem statement for the endogenous uncertainty problems under consideration and the corresponding multistage stochastic programming model, respectively. In section 4.4, three theoretical properties are identified for the model and used to formulate a reduced model in the subsequent section. To solve the large instance of the problems in this class a *k*-stage constraint solution approach, NAC relaxation strategy, and a Lagrangean decomposition algorithm are proposed in section 4.6. The proposed models and solution strategies are then applied to two process network problems under uncertain yields in section 4.7 to illustrate the advantages of these approaches.

## 4.2 Problem Statement

In the class of problems under consideration, the time horizon is represented by the discrete set of time periods $T = \{1, 2, \ldots\}$. Set $I = \{1, 2, \ldots\}$ represents the set of "sources" of endogenous uncertainty, while $\theta_i$ represents the endogenous uncertain parameter associated with source $i \in I$. The discrete set of possible realizations for $\theta_i$ is represented by $\Phi_i$. The resolution of uncertainty in $\theta_i$ depends on the binary decision variables $b_{i,t}$. Specifically, the uncertainty in $\theta_i$ will be resolved in time period $t$ if binary decision $b_{i,t} = 1$ and $b_{i,\tau} = 0, \ \forall \tau < t$. Note that the parameters $\theta_i$ represent intrinsic properties of source $i$ and are assumed to be independent and time invariant. Besides the decisions represented by variables $b_{i,t}$, other decisions to be made in time period $t$ are represented by variables $y_t$ and $x_t$ where these are decisions made at the beginning and end of the corresponding time period $t$.

The sequence of events in each time period is as follows. Decisions $y_t$ and $b_{i,t}$ are implemented at the beginning of time period $t$. This is followed by the resolution of uncertainty in the endogenous parameter $\theta_i$ for source $i$ if $b_{i,t} = 1$ and $b_{i,\tau} = 0 \ \forall \tau < t$. The state variables ($w_t$) are calculated based on the decision variables that are selected, while the recourse variables ($x_t$) are decisions implemented at the end of each period.

In general, the variables $b_{i,t}$ may represent investment decisions associated with source $i$. In the gas field problem considered by Goel et al. (2006), these variables represent whether or not investment is made at field $i$ in time period $t$. The uncertainty associated with a field is resolved in time period $t$ only if investment is carried out at that field in time period $t$, while no investments have been made at that field in the past. Similarly, for capacity expansion planning problems these decisions represent whether or not unit $i$ is installed in time period $t$. However, in this case we assume that the uncertainty associated with a process gets resolved as soon as initial investment is made in that process and it is independent of the plant capacity.

Note that for ease of exposition, we assume that there is only one endogenous uncertain parameter associated with source $i$ for all $i \in I$. Thus, $\theta_i$ is a scalar for all $i \in I$. Moreover, the problem statement presented here is the specific case of the one that is described in Goel and Grossmann (2006).

## 4.3 Model

The multistage stochastic programming model (MSSP$^0$) with endogenous uncertainty can be represented as a mixed-integer linear disjunctive programming model as described in Goel and Grossmann (2006).

**(MSSP$^0$)**
$$\min \sum_{s \in S} p^s \sum_{t \in T} \left( c_t^{ws} w_t^s + c_t^{xs} x_t^s + c_t^{ys} y_t^s + \sum_{i \in I} c_{i,t}^{bs} b_{i,t}^s \right) \tag{4.1}$$

$$s.t. \sum_{\substack{\tau \in T, \\ \tau \le t}} \left( A_{\tau,t}^{ws} w_\tau^s + A_{\tau,t}^{xs} x_\tau^s + A_{\tau,t}^{ys} y_\tau^s + \sum_{i \in I} A_{i,\tau,t}^{bs} b_{i,\tau}^s \right) \le a_t^s \qquad \forall s \in S, \forall t \in T \tag{4.2}$$

$$b_{i,1}^s = b_{i,1}^{s'} \qquad \forall s, s' \in S, \forall i \in I, s \neq s' \tag{4.3a}$$

$$y_1^s = y_1^{s'} \qquad \forall s, s' \in S, s \neq s' \tag{4.3b}$$

$$Z_t^{s,s'} \Leftrightarrow \bigwedge_{i \in D(s,s')} \left[ \bigwedge_{\tau=1}^{t} \neg (b_{i,\tau}^s) \right] \qquad \forall s, s' \in S, \forall t \in T, s \neq s' \tag{4.4}$$

$$\begin{bmatrix} Z_t^{s,s'} \\ x_t^s = x_t^{s'} \\ b_{i,t+1}^s = b_{i,t+1}^{s'} \quad \forall i \in I \\ y_{t+1}^s = y_{t+1}^{s'} \end{bmatrix} \vee \left[ \neg Z_t^{s,s'} \right] \qquad \forall s, s' \in S, \forall t \in T, s \neq s' \tag{4.5}$$

$$w_t^s \in W_t^s, x_t^s \in X_t^s, y_t^s \in Y_t^s, b_{i,t}^s \in \{0,1\} \quad \forall s \in S, \forall t \in T, \forall i \in I$$

$$Z_t^{s,s'} \in \{True, False\} \qquad \forall s, s' \in S, \forall t \in T$$

The objective function (4.1) in the above model (MSSP$^0$) minimizes the expectation of an economic criterion. For a particular scenario, inequality (4.2) represents constraints that govern decisions in time period $t$ and link decisions across time periods. First time period non-anticipativity (NA) constraints are given by equations (4.3a) and (4.3b), while conditional NA constraints that are written for the later time periods in terms of decisions $b_{i,t}^{s}$ are given by (4.4) and (4.5). Note that the set *D(s,s')* that is used in the equation (4.4) is defined as follows:

$$D(s,s') = \left\{ i \,\middle|\, i \in I, \theta_i^s \neq \theta_i^{s'} \right\}$$

The idea of non-anticipativity is that the decisions at time *t* can only be affected by the decisions ($y_t^s, b_{i,t}^s$) made before time period *t*. These constraints state that if two scenarios *s* and *s'* are indistinguishable in time period *t* (i.e. they are the same), then decisions for these scenarios in time period *t* should be the same. It should also be noted that problem ($\text{MSSP}^0$) can be reformulated as an MILP as described in Goel and Grossmann (2006) by replacing the equations (4.4) and (4.5) with integer and mixed-integer constraints, respectively.

## 4.4 Model Reduction Scheme

NA constraints like the ones in (4.3a), (4.3b) and (4.5) are essential in multistage stochastic programming to ensure that our current decisions do not anticipate future outcomes. When the model ($\text{MSSP}^0$) is reformulated as an MILP problem, the difficulty is that the NA constraints typically represent around 80% of the total constraints and grow quadratically in the number of scenarios, making real-world size problems intractable. To overcome this limitation, we present three theoretical properties that allow us to formulate significantly reduced MSSP models.

Let us assume that there are $p$ uncertain parameters ($\theta_1$, $\theta_2$, $\theta_3$,.........., $\theta_p$) each of which has $k$ realizations ($\ell_1$, $\ell_2$, $\ell_3$,.........., $\ell_k$). Then the total number of combinations of realizations of these parameters will be $k^p$ each of which will define a scenario *s*. For these $S = k^p$ scenarios there will be a total of $S(S-1)$ scenario pairs *(s, s')* each of which corresponds to a NA constraint in each time period *t*. The following properties significantly reduce the problem size by reducing the number of these scenario pairs *(s, s')* and the corresponding NA constraints. The first two properties were proposed by Goel and Grossmann (2006).

**Property 1.** *If scenario pair (s, s') is indistinguishable at stage t, so is (s', s). Therefore, we have to consider only one of these scenario pairs (i. e. (s, s') such that s < s').*

*Proof. See Goel and Grossmann (2006).*

**Property 2.** *It is sufficient to express NA constraints for the pairs of scenarios (s, s') that differ in the outcome of only one uncertain parameter.*

*Proof. See Goel and Grossmann (2006).*

Property 1 is based on the symmetry of the scenario pairs *(s, s')* and prevents duplication of the NA constraints for the same pair of scenarios *(s, s')* in the model. On the other hand, Property 2 exploits the fact that the NA constraints between those scenarios which differ in the realizations of more than one uncertain parameter is implicitly enforced by considering the NA constraints for the one that differ in realization of only one uncertain parameter. Therefore, it is sufficient to include a subset of scenario pairs corresponding to those that differ in realization of one uncertain parameter. Properties 1 and 2 are further illustrated by a small example in the next section. Although, these two properties significantly reduce the number of scenario pairs for the NA constraints, there are still many of these scenario pairs that are connected implicitly and that can be removed. This motivates us to find these scenario pairs systematically to further reduce the size of the problem and establish a new Property 3.

Property 3 basically exploits transitivity relationship among scenario pairs *(s, s')* that results after applying Properties 1-2, and is an extension of Property 2 to those cases where uncertain parameters have more than two realizations (i.e. $k > 2$). In that case, according to the Property 2 all the scenario pairs that differ in just one uncertain parameter will be included in the model for the NA constraints and there will be multiple links among those scenarios pairs that corresponds to a single uncertain parameter. Some of these multiple links among scenarios are not needed because of the fact that many of these scenarios that corresponds to a single uncertain parameter are such that they can be only realized at the same time irrespective of any decisions taken during the planning horizon and hence, we can take advantage of the transitivity relation among these scenarios.

Therefore, the new property establishes that for an endogenous uncertainty problem with *p* uncertain parameters and each having *k* realizations, it is sufficient to express NA constraints only for those scenario pairs *(s, s')* such that $(s,s') \in (s_1, s_2, ...., s_k)$, where $(s_1, s_2, ...., s_k) \in L_p$ for each uncertain parameter $\theta_p$ and *s, s'* are the consecutive elements in this set. The required set $L_p$ is defined as follows:

$$L_p = \begin{Bmatrix} (s_1, s_2, \ldots, s_k) \left| s_1, s_2, \ldots, s_k \in S, s_1 < s_2 < \ldots < s_k, \right. \\ D(s,s') = \{p\} \ \forall (s,s') \in (s_1, s_2, \ldots, s_k) \end{Bmatrix} \quad \forall p$$

The *k* scenarios within each of these $(s_1, s_2, ...., s_k)$ sets can only be realized at the same time irrespective of the other realizations during the given time horizon because they differ in the realization of the same uncertain parameter $\theta_p$. Therefore, unique linking among only these scenarios will be sufficient to enforce non-anticipativity. Specifically, Property 3 can be stated as follows:

**Property 3.** *For an endogenous uncertainty problem having* $p$ *uncertain parameters and* $S$ *scenarios, the maximum number of scenario pairs (s, s') required to represent the non-anticipativity are* $p(|S| - |S|^{p-1/p})$.

*Proof.* Suppose that for an endogenous uncertainty problem,

$p$ is the number of uncertain parameters = ($\theta_1$**,** $\theta_2$**,** $\theta_3$**,.........,** $\theta_p$)

$k$ is the number of realizations of each uncertain parameter

= ($\ell_1$**,** $\ell_2$**,** $\ell_3$**,.........,** $\ell_k$)

Therefore, the total number of scenarios are $S = k^p$

For each uncertain parameter $\theta_p$, there will be a total of $k^{p-1}$ number of scenario sets $(s_1, s_2, ...., s_k)$, i.e. $|L_p| = k^{p-1}$, each having $k$ scenarios. The characteristic of these *k* scenarios within a set $(s_1, s_2, ...., s_k) \in L_p$ is that uncertainty in these scenarios can be realized at the same time irrespective of the other realization during the specified time horizon because these scenarios have the same realizations for all the uncertain parameters except for that particular uncertain parameter $\theta_p$. In other words, the $k$ scenarios in a set $(s_1, s_2, ...., s_k) \in L_p$ differ only in the realization of the uncertain parameter $\theta_p$ and can be realized at the same time irrespective of other realizations. Also, according to Property 2, it is sufficient to express NA constraints for those scenario pairs that differ in the realization of only one uncertain parameter. Therefore, we do not need to include scenario pairs *(s, s')* that differ in realization of more than one uncertain parameter. As the uncertainty in these $k$ scenarios in a set $(s_1, s_2, ...., s_k)$ is realized at same time, it is sufficient to express non-anticipativity uniquely in these $k$ scenarios only. Hence, $k-1$ scenario pairs *(s, s')* will be required to link $k$ scenarios in each of these sets $(s_1, s_2, ...., s_k)$, i.e. $k-1$ equations are required to represent non-anticipativity for each of these $k^{p-1}$ number of sets for a particular uncertain parameter $\theta_p$. Therefore, the total number of scenario pairs *(s, s')* required for non-anticipativity are $pk^{p-1}(k-1)$ or $p(|S| - |S|^{p-1/p})$ . □

The proposed Property 3 can be used in addition to earlier Properties 1 and 2 to reduce the model size as explained in the next section with a small example. Qualitatively, the end result of using these 3 properties is that they lead to the minimum number of independent links between the scenarios to represent the NA constraints.

## 4.5 Reduced Model Formulation

In this section we apply the three properties described above in order to reduce the size of the model (MSSP$^0$). Let us define,

$P$: Set of scenario pairs *(s, s')* for NACs in the model (MSSP$^0$)

$P_1$: Set of scenario pairs *(s, s')* for NACs after applying Property 1

$P_2$: Set of scenario pairs *(s, s')* for NACs after applying Properties 1 and 2

$P_3$: Set of scenario pairs *(s, s')* for NACs after applying Properties 1,2 and 3

Therefore,

$$P = \{(s, s') | s, s' \in S, s \neq s'\}$$

$$P_1 = \{(s, s') | s, s' \in S, s < s'\}$$

$$P_2 = \{(s, s') | s, s' \in S, s < s', |D(s, s')| = 1\}$$

$$P_3 = \left\{ (s_1, s_2), (s_2, s_3), ...., (s_{k-1}, s_k) \middle| (s_1, s_2, ..., s_k) \in L_p \ \forall p \right\}$$

The relation between these sets can be stated as, $P_3 \subseteq P_2 \subseteq P_1 \subseteq P$.

The reduced model (MSSP$^R$) that is formulated from the original model (MSSP$^0$) by considering NA constraints for scenario pairs *(s, s')* within the set $P_3$ for the equations (4.3a), (4.3b), (4.4) and (4.5) is given as follows:

**(MSSP$^R$)**

$$\min \sum_{s \in S} p^s \sum_{t \in T} \left( c_t^{ws} w_t^s + c_t^{xs} x_t^s + c_t^{ys} y_t^s + \sum_{i \in I} c_{i,t}^{bs} b_{i,t}^s \right) \tag{4.1}$$

$$s.t. \sum_{\substack{\tau \in T, \\ \tau \le t}} \left( A_{\tau,t}^{ws} w_\tau^s + A_{\tau,t}^{xs} x_\tau^s + A_{\tau,t}^{ys} y_\tau^s + \sum_{i \in I} A_{i,\tau,t}^{bs} b_{i,\tau}^s \right) \le a_t^s \qquad \forall s \in S, \forall t \in T \tag{4.2}$$

$$b_{i,1}^s = b_{i,1}^{s'} \qquad \forall (s, s') \in P_3, \forall i \in I \tag{4.6a}$$

$$y_1^s = y_1^{s'} \qquad \forall (s, s') \in P_3 \tag{4.6b}$$

$$Z_t^{s,s'} \Leftrightarrow \bigwedge_{i \in D(s,s')} \left[ \bigwedge_{\tau=1}^{t} \neg (b_{i,\tau}^s) \right] \qquad \forall (s, s') \in P_3, \forall t \in T \tag{4.7}$$

$$\begin{bmatrix} Z_t^{s,s'} \\ x_t^s = x_t^{s'} \\ b_{i,t+1}^s = b_{i,t+1}^{s'} \quad \forall i \in I \\ y_{t+1}^s = y_{t+1}^{s'} \end{bmatrix} \vee \left[ \neg Z_t^{s,s'} \right] \qquad \forall (s, s') \in P_3, \forall t \in T \tag{4.8}$$

$$w_t^s \in W_t^s, x_t^s \in X_t^s, y_t^s \in Y_t^s, b_{i,t}^s \in \{0,1\} \qquad \forall s \in S, \forall t \in T, \forall i \in I$$

$$Z_t^{s,s'} \in \{True, False\} \qquad \forall s, s' \in S, \forall t \in T$$

**Theorem 4.1.** *The optimum solution of the Reduced model (MSSP$^R$) is the same as the optimum solution of the Original Model (MSSP$^0$).*

The proof follows trivially from applying Properties 1-3. To illustrate the effect of the proposed properties on the problem size, we consider a case of endogenous uncertainty problem having 2 uncertain parameters, *i.e.* ($\theta_1, \theta_2$). Each of these uncertain parameters has three realizations ($\ell_1$, $\ell_2$, $\ell_3$) which give rise to a total of 9 scenarios shown in Table 4.1.

Table 4.1: 9 Scenarios for the given example

| Scenario (s) | 1 | 2 | 3 | 4 | 5 | 6 | 7 | 8 | 9 |
|---|---|---|---|---|---|---|---|---|---|
| $\theta_1$ | $\ell_1$ | $\ell_2$ | $\ell_3$ | $\ell_1$ | $\ell_2$ | $\ell_3$ | $\ell_1$ | $\ell_2$ | $\ell_3$ |
| $\theta_2$ | $\ell_1$ | $\ell_1$ | $\ell_1$ | $\ell_2$ | $\ell_2$ | $\ell_2$ | $\ell_3$ | $\ell_3$ | $\ell_3$ |

According to the original model ($MSSP^0$), a total of 72 scenario pairs will be required to represent non-anticipativity in the above problem as shown in Table 4.2(a) where each element in the table represent the indices of uncertain parameters, ($\theta_1$, $\theta_2$) that differentiate the corresponding scenarios s and s', i.e. set *D(s, s')*.

However, if we use Property 1 (i.e. (s, s') such that s < s') the number of scenario pairs reduces to 36 from 72 due to the symmetry of the scenario pairs as seen in Table 4.2(b). Now, if we apply Property 2 (i.e. consider the scenario pairs which differ in realization of only one uncertain parameter) then (s, s') becomes 18 by removing those scenario pairs have more than one element in the set *D(s, s')* as seen in Table 4.2(c). But out of these 18 scenario pairs, only 12 are sufficient as seen in Table 4.2(d) to uniquely define the non-anticipativity that also satisfies the requirement of Property 3. This is due to the transitivity relation among the scenarios pairs corresponding to a single uncertain parameter and their characteristic of being realized at the same time irrespective of the other decisions as explained in the previous section. Hence, there is 83.33% reduction (i.e. from 72 to 12) in the scenario pairs (or problem size) on using the three theoretical properties. Note that for this example $L_1 = \{(s_1, s_2, s_3), (s_4, s_5, s_6), (s_7, s_8, s_9)\}$ and $L_2 = \{(s_1, s_4, s_7), (s_2, s_5, s_8), (s_3, s_6, s_9)\}$ according to the definition of these sets described earlier.

Table 4.2: Scenario pairs and corresponding differentiating set *D(s, s')* for the 9 scenario example

(a) 72 Scenario pairs in the original model ($MSSP^0$)

| ***D(s,s')*** | **1** | **2** | **3** | **4** | **5** | **6** | **7** | **8** | **9** |
|---|---|---|---|---|---|---|---|---|---|
| **1** | | 1 | 1 | 2 | 1,2 | 1,2 | 2 | 1,2 | 1,2 |
| **2** | 1 | | 1 | 1,2 | 2 | 1,2 | 1,2 | 2 | 1,2 |
| **3** | 1 | 1 | | 1,2 | 1,2 | 2 | 1,2 | 1,2 | 2 |
| **4** | 2 | 1,2 | 1,2 | | 1 | 1 | 2 | 1,2 | 1,2 |
| **5** | 1,2 | 2 | 1,2 | 1 | | 1 | 1,2 | 2 | 1,2 |
| **6** | 1,2 | 1,2 | 2 | 1 | 1 | | 1,2 | 1,2 | 2 |
| **7** | 2 | 1,2 | 1,2 | 2 | 1,2 | 1,2 | | 1 | 1 |
| **8** | 1,2 | 2 | 1,2 | 1,2 | 2 | 1,2 | 1 | | 1 |
| **9** | 1,2 | 1,2 | 2 | 1,2 | 1,2 | 2 | 1 | 1 | |

(b) 36 Scenario pairs after using Property 1

| ***D(s,s')*** | **1** | **2** | **3** | **4** | **5** | **6** | **7** | **8** | **9** |
|---|---|---|---|---|---|---|---|---|---|
| **1** | | 1 | 1 | 2 | 1,2 | 1,2 | 2 | 1,2 | 1,2 |
| **2** | | | 1 | 1,2 | 2 | 1,2 | 1,2 | 2 | 1,2 |
| **3** | | | | 1,2 | 1,2 | 2 | 1,2 | 1,2 | 2 |
| **4** | | | | | 1 | 1 | 2 | 1,2 | 1,2 |
| **5** | | | | | | 1 | 1,2 | 2 | 1,2 |
| **6** | | | | | | | 1,2 | 1,2 | 2 |
| **7** | | | | | | | | 1 | 1 |
| **8** | | | | | | | | | 1 |
| **9** | | | | | | | | | |

(c) 18 Scenario pairs after using Properties 1-2

| ***D(s,s')*** | **1** | **2** | **3** | **4** | **5** | **6** | **7** | **8** | **9** |
|---|---|---|---|---|---|---|---|---|---|
| **1** | | 1 | 1 | 2 | | | 2 | | |
| **2** | | | 1 | | 2 | | | 2 | |
| **3** | | | | | | 2 | | | 2 |
| **4** | | | | | 1 | 1 | 2 | | |
| **5** | | | | | | 1 | | 2 | |
| **6** | | | | | | | | | 2 |
| **7** | | | | | | | | 1 | 1 |
| **8** | | | | | | | | | 1 |
| **9** | | | | | | | | | |

(d) 12 Scenario pairs after using Properties 1-3

| ***D(s,s')*** | **1** | **2** | **3** | **4** | **5** | **6** | **7** | **8** | **9** |
|---|---|---|---|---|---|---|---|---|---|
| **1** | | 1 | | 2 | | | | | |
| **2** | | | 1 | | 2 | | | | |
| **3** | | | | | | 2 | | | |
| **4** | | | | | 1 | | 2 | | |
| **5** | | | | | | 1 | | 2 | |
| **6** | | | | | | | | | 2 |
| **7** | | | | | | | | 1 | |
| **8** | | | | | | | | | 1 |
| **9** | | | | | | | | | |

The graphical illustration of the model reduction scheme for the above 9 scenario example can be seen in Figure 4.1. Property 1 basically removes one of the two links between scenarios 1 and 2 in the figure. Scenarios 1 and 5 differ in both the uncertain parameters and due to the implicit connection between these scenarios through links 1-2 and 2-5 each of which corresponds to a single uncertain parameter, Property 2 can be used to remove the link 1-5. Because scenarios 1, 4 and 7 differ in the realization of just the second uncertain parameter $\theta_2$ and can only be realized simultaneously, they can be expressed by unique link among them. Therefore, Property 3 removes the link 1-7 and still allowing scenarios 1 and 7 to take non-anticipative decisions through the links 1-4 and 4-7. The other similar links removed by these properties are not shown in the figure for clarity.

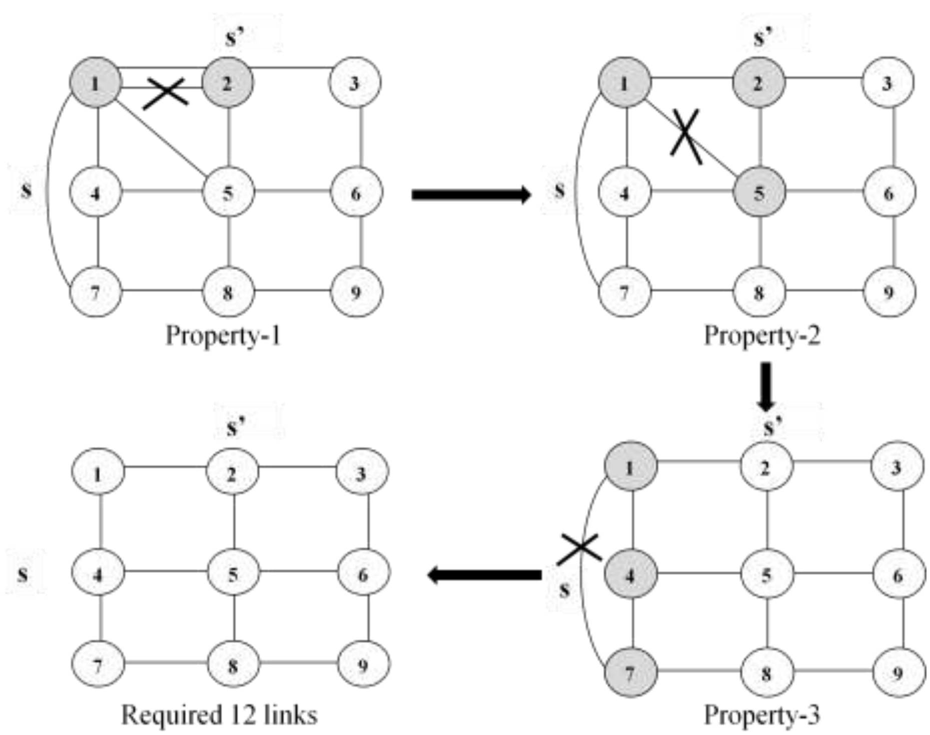


Figure 4.1: Model Reduction Scheme for 9 scenario example

Property 3 can be easily extended to the cases where there is a different number of realizations for each uncertain parameter. In that case, we need to create some dummy realizations for some of the uncertain parameters to make the same number of realizations for all the uncertain parameters and apply Property 3 to find out the least number of scenario links required for this new scenario set.

Finally, we can remove those scenario pairs from the NA constraints set that involve dummy realizations of the uncertain parameters leading to the least number of NA constraints for the given realizations.

Note that the number of scenario pairs using Properties 1-3 will be smaller compared to using Properties 1-2 only if the number of realization of uncertain parameters is more than two. Otherwise we will get the same number of scenarios in both cases. Therefore, in contrast to the earlier properties by Goel and Grossmann (2006), the proposed Property 3 can be regarded as the extension of the Property 2 to the cases where uncertain parameters have more than two realizations. Moreover, the effect of these properties on the problem size and solution time becomes very significant for the problems having large number of scenarios and/or having many realizations of each uncertain parameter.

## 4.6 Solution Strategies

Although the model formulation in the previous section greatly reduces the size of the multistage stochastic programs with endogenous uncertainties, given the exponential increase in the problem size with the number of uncertain parameters and its realizations, these problems may not be solvable in reasonable computational time. Hence, we may need some special solution techniques to solve large-scale problems in this class as discussed in this section.

### 4.6.1 *k*-stage Constraint Strategy

We know that NA constraints play a major role in the size of any multistage stochastic program and most of them are inactive at the optimum solution of the problem, particularly in the later time periods since investments tend to take place in the earlier periods. This observation motivates us to include only the subset of these constraints, corresponding up to the first $k$-stages of the problem which are assumed to be critical for defining the optimum solution of the problem. By defining $ST$ as the set of $k$ initial stages for which NA constraints are to be included, the proposed $k$-stage constraint formulation that is obtained from the reduced model by replacing the set $T$ with $ST$ in equations (4.7) and (4.8) is as follows:

$$\textbf{(MSSP}^{\textbf{SC}}\textbf{)} \qquad \min \sum_{s \in S} p^s \sum_{t \in T} \left( c_t^{ws} w_t^s + c_t^{xs} x_t^s + c_t^{ys} y_t^s + \sum_{i \in I} c_{i,t}^{bs} b_{i,t}^s \right) \tag{4.1}$$

$$s.t. \sum_{\substack{\tau \in T, \\ \tau \le t}} \left( A_{\tau,t}^{ws} w_\tau^s + A_{\tau,t}^{xs} x_\tau^s + A_{\tau,t}^{ys} y_\tau^s + \sum_{i \in I} A_{i,\tau,t}^{bs} b_{i,\tau}^s \right) \le a_t^s \qquad \forall s \in S, \forall t \in T \tag{4.2}$$

$$b_{i,1}^s = b_{i,1}^{s'} \qquad \forall (s,s') \in P_3, \forall i \in I \tag{4.6a}$$

$$y_1^s = y_1^{s'} \qquad \forall (s,s') \in P_3 \tag{4.6b}$$

$$Z_t^{s,s'} \Leftrightarrow \bigwedge_{i \in D(s,s')} \left[ \bigwedge_{\tau=1}^{t} \neg (b_{i,\tau}^s) \right] \qquad \forall (s,s') \in P_3, \forall t \in ST \tag{4.9}$$

$$\begin{bmatrix} Z_t^{s,s'} \\ x_t^s = x_t^{s'} \\ b_{i,t+1}^s = b_{i,t+1}^{s'} \quad \forall i \in I \\ y_{t+1}^s = y_{t+1}^{s'} \end{bmatrix} \vee \left[ \neg Z_t^{s,s'} \right] \qquad \forall (s,s') \in P_3, \forall t \in ST \tag{4.10}$$

$$w_t^s \in W_t^s, x_t^s \in X_t^s, y_t^s \in Y_t^s, b_{i,t}^s \in \{0,1\} \qquad \forall s \in S, \forall t \in T, \forall i \in I$$
$$Z_t^{s,s'} \in \{True, False\} \qquad \forall s, s' \in S, \forall t \in T$$

The above model can be solved successively by starting with a fixed number of stages (say *k=2*) with NA constraints and increasing the number of stages, i.e. the value of *k*, if NA constraints of those stages greater than *k* are violated. The following two propositions are established to implement the proposed *k*-stage constraint strategy:

**Proposition 4.1.** *The k-stage constraint model (MSSP$^{SC}$) provides a valid lower bound on the Original Model (MSSP$^{0}$) and the Reduced Model (MSSP$^{R}$).*

*Proof*. It can be seen from Reduced Model (MSSP$^{R}$) and the stage constraint model (MSSP$^{SC}$) that they are identical except the constraints that corresponds to the conditional NA constraints. More specifically, equations (4.9) and (4.10) are written for the subset of stages *ST* instead of all the stages *T* in equations (4.7) and (4.8) respectively. Therefore, the *k*-stage constraint model (MSSP$^{SC}$) can be regarded as the relaxation of the Reduced Model (MSSP$^{R}$) where we neglect the conditional NA constraints for the stages that are not the elements of the set *ST*. Hence, the *k*-stage constraint model ($MSSP^{SC}$) provides a valid lower bound on the Reduced Model ($MSSP^{R}$). As models ($MSSP^{R}$) and ($MSSP^{0}$) are equivalent, the *k*-stage constraint model ($MSSP^{SC}$) also provides a valid lower bound on the Original Model ($MSSP^{0}$). □

**Proposition 4.2.** *The k-stage constraint model ($MSSP^{SC}$) provides the optimum solution to the Original Model ($MSSP^{0}$) and the Reduced Model ($MSSP^{R}$), if there is no realization of any of the endogenous uncertain parameter after specified stages in the solution that is obtained.*

*Proof.* The proof follows from the fact that if there is no realization of any of the uncertain parameter after specified stage *k* in the solution, then there will be no new information available to any scenario from period $k+1$ to end of the planning horizon *T*. Therefore, the state of the system corresponding to each scenario will be the same from period *k* to *T*. Moreover, the scenario pairs that have already being distinguished within the first *k* stages according to the logic condition of the non-anticipativity, there will not be any need to include NA constraints for these scenario pairs. On the other hand, if there are some scenario pairs that have not been distinguished until stage *k*, and as there in no further realization of uncertainty, these scenarios will have the same information from period 1 to *T* and will have the same decisions. Hence, the NA constraints from period $k+1$ to *T* will automatically be satisfied for these scenario pairs. Given that the reduced model ($MSSP^{R}$) and the stage constraint model ($MSSP^{SC}$) are identical except the conditional NA constraints that were relaxed, i.e. from period $k+1$ to *T* in the stage constraint model, and because the NA from period $k+1$ to *T* are satisfied in the solution of *k* stage constraint model if there is no realization of uncertain parameter after stage *k* as discussed earlier, the solution of the stage constraint model corresponding to the current stage *k* will be the optimum solution for the reduced model ($MSSP^{R}$). As models ($MSSP^{R}$) and ($MSSP^{0}$) are equivalent, the *k*-stage constraint model ($MSSP^{SC}$) also provides an optimal solution to the Original Model ($MSSP^{0}$) if the above condition is satisfied. □

The step-by-step procedure to implement the proposed *k*-stage constraint strategy is as follows:

***Step 1:*** *Set the effective number of stages k (usually k=2) and lower bound to -∞.*

***Step 2:*** *Include NA constraints for the specified number of stages k in the model ($MSSP^{SC}$) and solve.*

***Step 3:*** *If Proposition 4.2 is satisfied, i.e. there is no realization of any of the uncertain parameter after the current stage k, Stop. Optimal solution is found; else go to Step 4.*

***Step 4:*** *If Proposition 4.2 is not satisfied, update the lower bound using the solution of the model ($MSSP^{SC}$) for the specified value of k. Set k=k+1 and go to Step 2.*

The following remarks can be made about the proposed *k*-stage constraint strategy:

1. There are two cases involved while checking whether Proposition 4.2 holds in step 3 of the above procedure. In the first case, if there is neither investment nor expansion decision in the later stages in the solution, then we can ensure that Proposition 4.2 is satisfied and the solution obtained is optimal by inspection. In case that there are expansions in the later stages and no new investments, then the NA constraints corresponding to the later stages are also satisfied, i.e. Proposition 4.2 holds true and the solution is optimal.

2. The lower bounds obtained from the above procedure are generally very tight and the corresponding solution is very close to the feasible solution to the original problem. Therefore, this solution can be used to obtain a good feasible solution, i.e. upper bound, and one can also evaluate the quality of the solution that is obtained.

3. In case that the iterations during the above solution procedure are computationally expensive, one can use the solution of the previous iteration to determine a good value of *k* that can be used in the next iteration to fix the number of stages instead of increasing *k* value by just 1 in each iteration. Therefore, one can skip the expensive calculations for those values of *k* that are less likely to be optimum.

The proposed $k$-stage constraint strategy can be quite effective for the investment planning models because the trend in problems of this class is that their optimum solution involves investments in the earlier stages of the project. The reason behind this is the effect of economies of scale, as in general, it pays to make investments only once and earlier because of the fixed cost charges. Second, if one expands the capacity, it is better to do it early as otherwise one will not take full advantage of the investment. This implies that the investment and operation decisions in the early stages of planning horizon are critical for these problems and require enforcing the NA constraints in these stages, while the ones for later stages can be ignored making the large-scale investment planning problems easier to solve. Specific examples for these problems are process network planning, or oil and gas fields infrastructure planning problems.

### 4.6.2 NAC Relaxation Strategy

The $k$-stage constraint strategy presented in the previous section involves the solution of the reduced model for the specified number of stages iteratively and has advantage for the investment planning problems where only first few stages involve uncertainty realization. This is due to the economies of scale in these problems as explained earlier. On the other hand, if there are endogenous uncertainties that are revealed later in the planning horizon, then the stage constraint approach can become expensive for finding the optimal solution due to the solution of MILP problems for multiple times, although a strong lower bound to the problem can still be obtained.

Therefore, for the more general problems we propose a NAC relaxation strategy. This strategy is motivated by the fact that very few inequality NA constraints become active at the optimal solution of the problem (e.g. see Colvin and Maravelias, 2010). In this strategy (Figure 4.2), we divide the solution procedure in two phases, Phase I and Phase II. Phase I involves removing all inequality NA constraints from the reduced model ($MSSP^R$) and solving its LP relaxation ($LP\text{-}MSSP^R$). Then we check the feasibility of the NA constraints and add the violated NA constraints in the LP relaxation and solve iteratively until there is no violation of the NA constraints in the LP relaxation. In Phase II of the

NAC relaxation strategy, the resulting model from Phase I with the added cuts is solved as an MILP problem to obtain a lower bound that is usually very tight. The upper bound is obtained by fixing the binary decisions in the reduced model ($MSSP^R$) using the solution of the lower bounding MILP problem such that NA constraints are not violated and solving the problem in fullspace. If the gap between lower and upper bounds is more than the specified tolerance, we check the feasibility of the NA constraints for the MILP solution in the current iteration and solve the new MILP problem with violated NA constraints that serve as added cuts in the next iteration. The procedure of solving lower and upper bounding problems in Phase II continues until the gap between upper and lower bound is within the specified optimality tolerance.

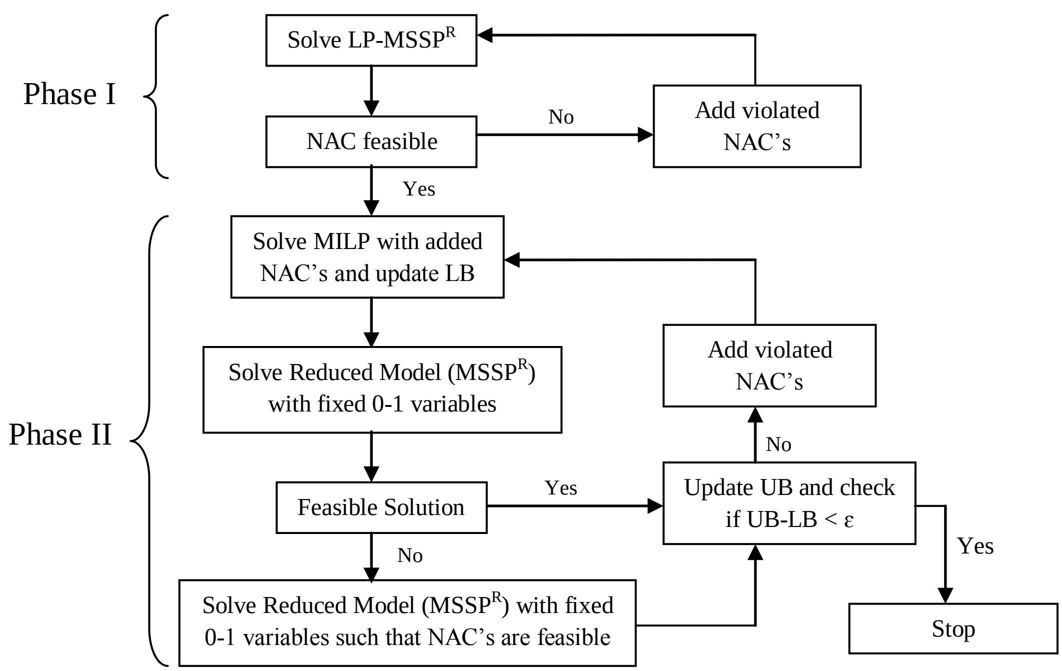


Figure 4.2: NAC Relaxation Strategy

Note that in comparison to the branch and cut solution method by Colvin and Maravelias (2010), the proposed NAC relaxation strategy is much easier to implement directly using the available commercial solvers, although there might be some trade-offs between these solution strategies in terms of the solution times. Furthermore, it has been observed that very few inequality NA constraints (~6-7% of the total inequality NA constraints in the reduced model) are added as cuts in the complete solution procedure and most of the violated NA constraints as cuts are added in Phase I itself which is very fast compared to Phase II. Although, the most expensive part of this procedure is the solution of the MILP problems during the Phase II iterations, it has been observed in most of the cases that only one or two iterations are required in Phase II to obtain a strong lower bound as well as the to generate the optimal solution from it. Moreover, due to the very small problem size compared to the reduced model, the solution of the MILP problems in Phase II are significantly faster during these iterations.

### 4.6.3 Lagrangean Decomposition Algorithm

The solution strategies presented in the previous two sections basically require the solution of a fullspace model and do not take the advantage of the decomposable structure of the model by scenarios. We should notice that the reduced model ($MSSP^R$) is composed of scenario subproblems connected through initial and conditional NA constraints. If these NA constraints are relaxed or dualized, then the problem decomposes by scenarios, and each sub-problem can be solved independently within an iterative scheme for the multipliers as described in Carøe and Schultz (1999) and in Goel and Grossmann (2006). In this way, we can effectively decompose the large scale problems in this class.

In the Lagrangean Decomposition algorithm (Figure 4.3) the lower bound (LB) is obtained by solving the Lagrangean problem with fixed multipliers that is obtained from the reduced model ($MSSP^R$) by relaxing the conditional NA constraints and dualizing the first time period NA constraints as penalty terms in the objective. Each sub-problem in the following Lagrangean problem ($LR^R$-$MSSP^R$) corresponds to a scenario:

**($LR^R$ -$MSSP^R$)**
$$\min \sum_{s\in S} p^s \sum_{t\in T}\left( c_t^{ws} w_t^s + c_t^{xs} x_t^s + c_t^{ys} y_t^s + \sum_{i\in I} c_{i,t}^{bs} b_{i,t}^s \right) + \sum_{(s,s')\in P_3} \sum_{i\in I} \left( \lambda_{b,i,1}^{s,s'} \left( b_{i,1}^s - b_{i,1}^{s'} \right)\right) + \sum_{(s,s')\in P_3} \left( \lambda_{y,1}^{s,s'} \left( y_1^s - y_1^{s'} \right)\right) \quad (4.11)$$

$$s.t. \sum_{\substack{\tau\in T,\\ \tau\le t}} \left( A_{\tau,t}^{ws} w_\tau^s + A_{\tau,t}^{xs} x_\tau^s + A_{\tau,t}^{ys} y_\tau^s + \sum_{i\in I} A_{i,\tau,t}^{bs} b_{i,\tau}^s \right) \le a_t^s \quad \forall s\in S, \forall t\in T \quad (4.2)$$

$$w_t^s \in W_t^s, x_t^s \in X_t^s, y_t^s \in Y_t^s, b_{i,t}^s \in \{0,1\}$$
$$\forall s \in S, \forall t \in T, \forall i \in I$$

The upper bound (UB) is generated by using a heuristic based on the solution of the Lagrangean problem. In this heuristic, we fix the decisions obtained from the above problem ($LR^R$- $MSSP^R$) in the reduced problem ($MSSP^R$) such that there is no violation of NA constraints and solve it to obtain the upper bound. The sub-gradient method by Fisher (1985) is used during each iteration to update the multipliers for the Lagrangean problem. The algorithm stops when either a maximum iteration limit is reached, or the difference between the bounds LB and UB is less than a pre-specified tolerance.

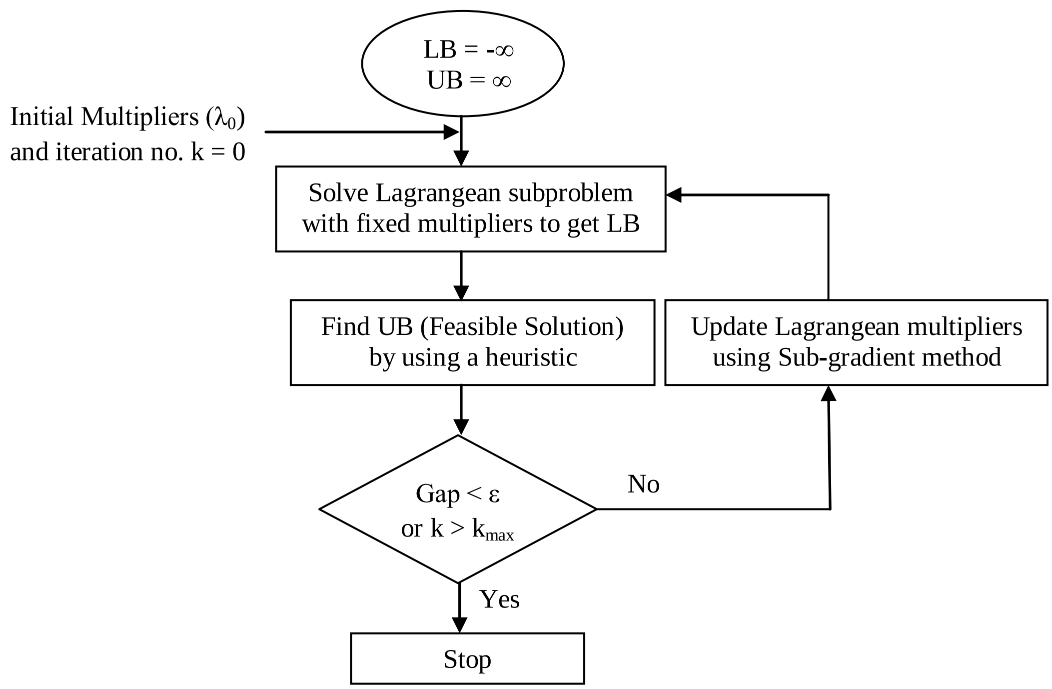


Figure 4.3: Lagrangean Decomposition algorithm

The major advantage with the above Lagrangean decomposition algorithm for endogenous uncertainty problems is that it provides good bounds on the optimal solution at the root node by taking advantage of the decomposable structure of the problem. Notice that in contrast to the method presented by Goel and Grossmann (2006), no branch and bound method is performed here with which the dual gap may not be closed for the problem. Therefore, if the gap between lower and upper bounds is large then in principle we would have to also incorporate a branch and bound procedure to reduce this gap. In our experience, however, we have observed for problems in this class that a good feasible solution within a small optimality tolerance is often found at the root node with this algorithm.

It should be noted that as opposed to the *k*-stage constraint method described earlier, in both the NAC relaxation strategy and Lagrangean decomposition algorithm, it is possible to assess the quality of the solution obtained (UB) with the lower bound at each iteration. On the other hand, in the *k*-stage constraint strategy we obtain the solution with optimal number of stages *k*.

## 4.7 Numerical Results

In this section we apply the proposed solution strategies to two process network examples and examine their performance compared to the original and reduced models.

### 4.7.1 Example 1

To illustrate the application of the various solution strategies for multistage stochastic programming with endogenous uncertainties, we consider the following problem from Goel and Grossmann (2006). Given is a process network (Figure 4.4) that is used to produce product A. Currently, the production of A takes place only in Process III with installed capacity of 3 tons/hour that consumes an intermediate product B that is purchased. If needed, the final product A can also be purchased so as to maintain its inventory. The demand for the final product, which is known, must be satisfied for all time periods over the given time horizon. Two new technologies (Process I and Process II) are considered for producing the intermediate B from two different raw materials C and D. These new technologies have uncertainty in the yields. The yield of Process I and Process II can be (0.67,0.69,0.81,0.83,0.84) and (0.62,0.65,0.85,0.88,0.89), respectively, with equal probability of 0.2. These five realizations of yield for each of Process I and Process II give rise to a total of 25 scenarios.

The problem consists of finding the optimum expansion and operation decisions for this process network for a 10 year planning horizon to minimize the total expected cost of the project. Applying the original model ($MSSP^0$) and solving it with XPRESS 20.00, we obtain the results shown in Figures 4.5(a)-(e).

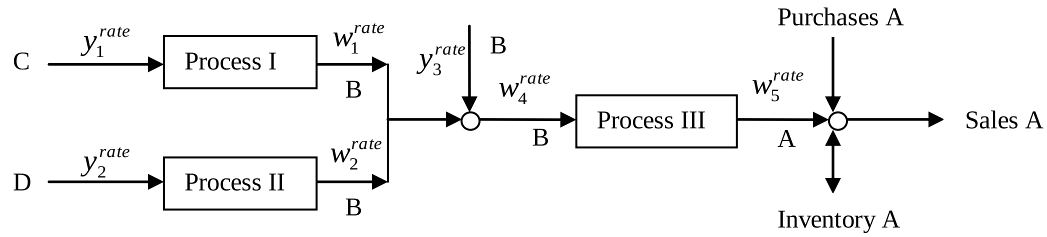


Figure 4.4: Process Network Example 1

The total expected cost is \$369,124 and the solution suggests to install Process II with a capacity of 1 tons/hr and expand the existing Process III from a capacity of 3 tons/hr to 6.914 tons/hr in the first year. If the yield of Process II turns out to be low, i.e. 0.65 (Figure 4.5-a) or 0.62 (Figure 4.5-b), then in the second year it is not expanded and the new Process I is installed. On the other hand, if yield of Process II turns out to be high, i.e. 0.89, (Figure 4.5-c), 0.88 (Figure 4.5-d) or 0.85 (Figure 4.5-e), then Process II is expanded in the second year to slightly different capacities close to 8 tons/hr in each of these three cases and there is no installation of Process I. There are no further installations or expansions of any of the processes.

It is interesting to note that the solution of the two-stage stochastic model of this example that considers no expansions, i.e. no recourse actions for the investment decisions of the processes, yields an expected cost of \$379,706 or about 3% higher than the multistage model. In this case the solution suggests to install Process I and Process II with capacities of 4.246 tons/hr, and 4.541 tons/hr respectively, and expand Process III to a capacity of 7.384 tons/hr in the first year. The savings in the expected cost using the multistage stochastic model are due to the fact that multistage stochastic solution takes advantage of favorable scenarios corresponding to the high yields of Process II, while minimizing the losses due to the low yield of Process II by taking appropriate recourse action in the future on the basis of the outcome of the yield of Process II. It can be seen from the Figures 4.5 (c)-(e), that there is no investment made in Process-I for the scenarios corresponding to the high yields of Process II and from Figures 4.5(a)-(b), that there is installation of Process I for the scenarios corresponding to low yields of Process II.

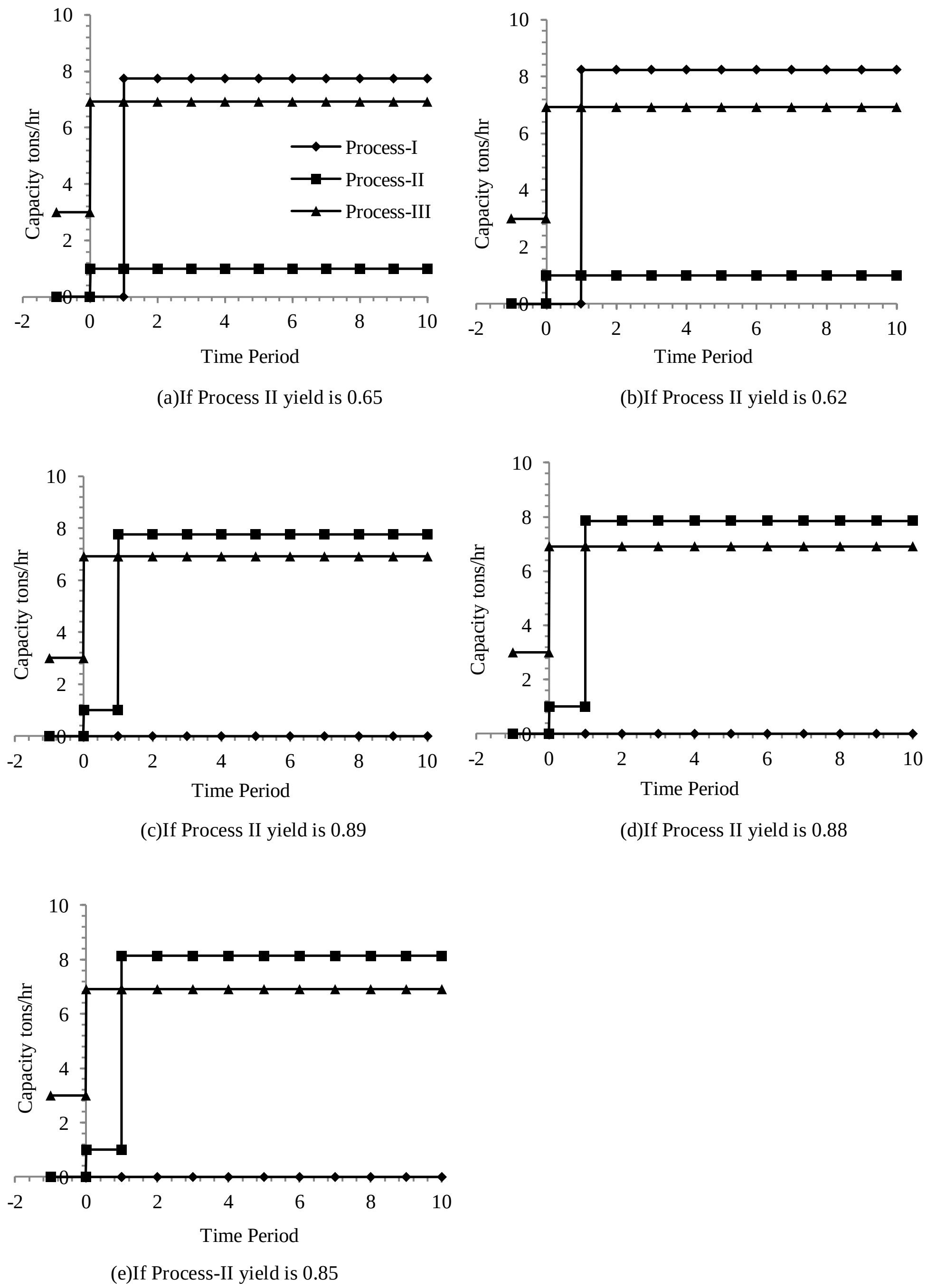


Figure 4.5: Installation Schedule for the Process Network Example 1

If we reformulate the original ($MSSP^0$) and reduced ($MSSP^R$) models into MILP problems (see Goel and Grossmann, 2006) for this example, the comparison of problem sizes and solution times between these models using XPRESS 20.00 solver is given in Table 4.3. It can be seen that problem size has reduced approximately 90% using Properties 1-3. Therefore, the advantage of including the new Property 3 with the earlier Properties 1 and 2 is very significant for this problem.

Table 4.3: Comparison of the various solution strategies for Example 1

| **Problem Type** | **Expected Cost ($\$10^3$)** | **Number of Constraints** | **Continuous Variables** | **Binary Variables** | **Solution Time(s)** |
|---|---|---|---|---|---|
| Original Model ($MSSP^0$) | 369.12 | 192,376 | 11,026 | 750 | 243.33 |
| Reduced Model: Property 1 | 369.12 | 98,576 | 8,026 | 750 | 224.79 |
| Reduced Model: Properties 1-2 | 369.12 | 32,376 | 6,026 | 750 | 56.76 |
| Reduced Model ($MSSP^R$): | 369.12 | 15,816 | 5,426 | 750 | 35.94 |
| *k*-stage constraint Model for | 369.12 | 7,096 | 5,106 | 750 | 8.36 |
| NAC Relaxation Strategy | 369.12 | 8,187* | 5,426* | 750* | 12.00 |

**Size of the last MILP with NA constraints in Phase II.*

*** Solved using XPRESS 20.00 solver in GAMS 23.0 on an Intel Pentium-IV machine with 3 GB of RAM.*

The comparison of the *k*-stage constraint strategy with the original ($MSSP^0$) and the reduced ($MSSP^R$) models for this 3 process network is also given in Table 4.3 where it can be seen that the global optimum is obtained using the *k*-stage constraint strategy and the solution time is greatly decreased to only 8.4s. We should note that the problem was solved with 2-stages initially and was stopped after the first iteration itself because there was no installation in time periods after $k=2$, and therefore Proposition 4.2 is satisfied. When the NAC relaxation strategy is applied to this problem, it provides the optimal solution significantly faster compared to the fullspace model as seen in Table 4.3, and its performance is slightly slower than the *k*-stage constraint strategy. The problem size of the MILP in the last iteration with this strategy after adding the violated NA constraints is also comparable to the size of the *k*-stage model.

The Lagrangean decomposition algorithm was also used for solving the process network Example 1 using the reduced model. The results in Table 4.4 show that with the Lagrangean decomposition algorithm the problem can be solved within 1% of optimality at the root node in just 27 s compared to 243 s in the case of the original model. Note that the global optimum is also obtained in this case. To further reduce the gap one may have to incorporate a branch and bound method.

Table 4.4: Iterations during Lagrangean Decomposition

| **Sub-gradient Iteration No.** | **Lower Bound ($\$10^3$)** | **Upper Bound ($\$10^3$)** | **% Gap** |
|---|---|---|---|
| 1* | 360.408 | 369.124 | 2.361 |
| 2* | 362.594 | 369.124 | 1.769 |
| 3* | 363.795 | 369.124 | 1.444 |
| 4 | 363.795 | 369.124 | 1.444 |
| 5* | 364.244 | 369.124 | 1.322 |
| 6 | 364.789 | 369.124 | 1.174 |
| 7* | 364.816 | 369.124 | 1.167 |
| 8 | 364.883 | 369.124 | 1.149 |
| 9 | 364.883 | 369.124 | 1.149 |
| 10* | 365.374 | 369.124 | 1.016 |
| 27 | 366.135 | 369.124 | 0.810 |
| Time(s) | 21.95 | 5.18 | 0.810 |

*problem solved for upper bound generation

Table 4.5: Comparison of the original and reduced models for Example 1 considering different scenarios

| **Number of Scenarios** | **Solution Time(s) Original Model*** | **Solution Time(s) Reduced Model*** | **% Optimality Gap** |
|---|---|---|---|
| 4 | 1.30 | 0.96 | 0 |
| 9 | 19.38 | 4.98 | 0 |
| 16 | 133.09 | 14.71 | 0 |
| 25 | 243.33 | 35.94 | 0 |
| 36 | 731.37 | 42.26 | < 0.5% |
| 64 | 2516.709 | 102.04 | < 0.5% |
| 81 | NA | 105.03 | < 0.5% |
| 100 | NA | 120.19 | < 0.5% |

**Problems are solved in fullspace.*

Furthermore, to investigate the impact of the model reduction using Properties 1-3, we also consider other cases for this example where the number of realization of uncertain yields are changed for Process I and Process II from 2 to 10, and the results are shown in Table 4.5. It is clear that the problem size is reduced significantly and hence the solution time for all the cases. Also, note that we can solve all the problems with the reduced model, while the larger ones cannot be solved with the original model. The main reason is the much smaller size of the reduced model as can be seen in Figure 4.6.

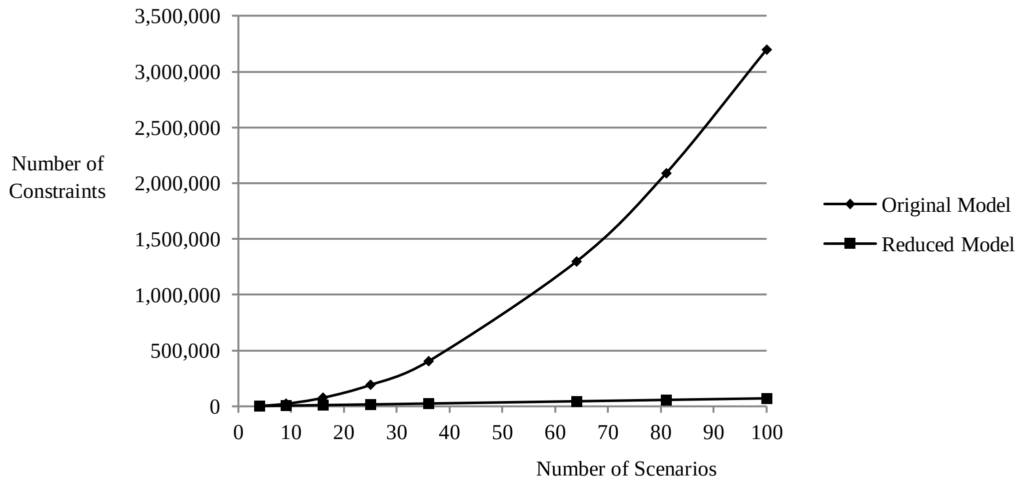


Figure 4.6: Comparison of constraints in Original and Reduced Models for Example 1 considering different scenarios

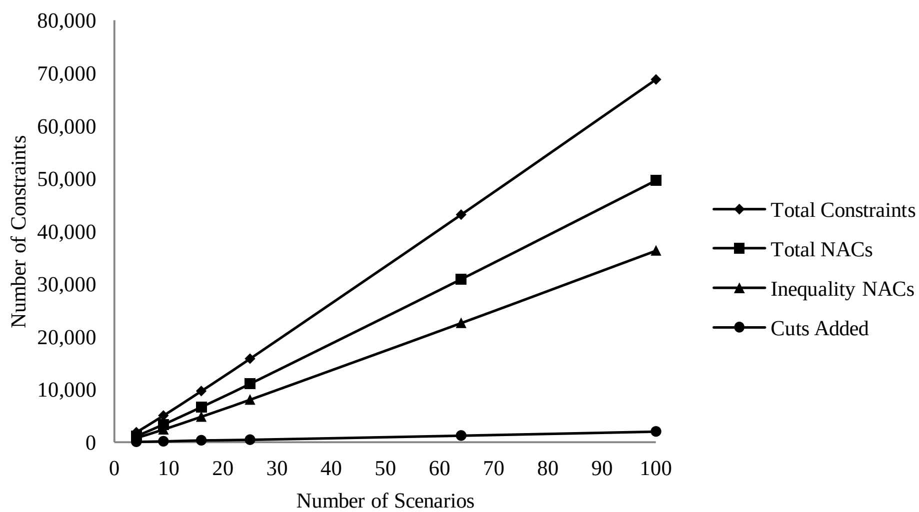


Figure 4.7: Cuts Added vs. Total Constraints in the Reduced Model for NAC Relaxation Strategy

As discussed earlier, the number of active NA constraints at the optimal solution of these problems is very small. It can be observed from Figure 4.7 that very few (~6-7%) inequality NA constraints of the reduced model are added as cuts during the NAC relaxation strategy for all scenario instances of Example 1. Also, the computational advantage of this strategy can be seen in Table 4.6. It should be noted that very few Phase II iterations are needed to obtain the optimal solution.

Table 4.6: Reduced Model vs. NAC-Relaxation Strategy for various scenario instances

| Number of Scenarios | Optimal Solution ($\$10^3$) | Gap % | Phase I Iterations | Phase II Iterations | Solution Time (s) NAC Relaxation Strategy | Solution Time(s) Reduced Model |
|---|---|---|---|---|---|---|
| 4 | 379.072 | 0.000 | 3 | 1 | 1.136 | 0.96 |
| 9 | 390.944 | 0.012 | 3 | 1 | 3.701 | 4.98 |
| 16 | 377.364 | 0.002 | 3 | 1 | 10.837 | 14.71 |
| 25 | 369.124 | 0.002 | 3 | 1 | 12.005 | 35.94 |
| 64 | 376.824 | 0.000 | 5 | 2 | 51.577 | 102.04 |
| 100 | 376.747 | 0.003 | 3 | 1 | 76.537 | 120.19 |

### 4.7.2 Example 2

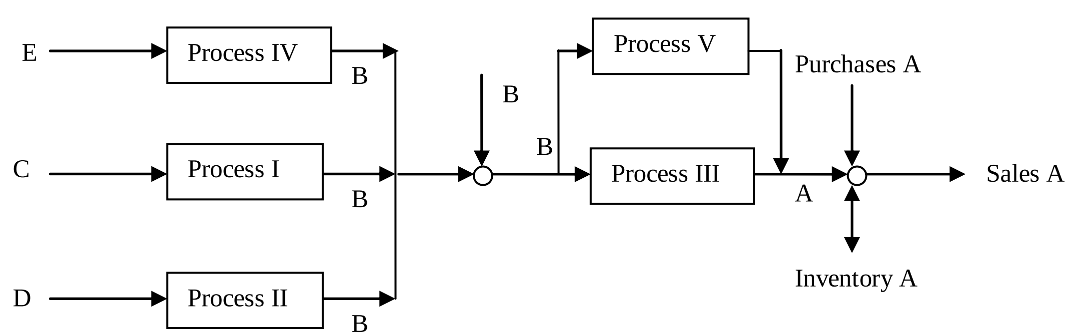


Figure 4.8: Process Network Example 2

To illustrate the solution of a larger instance, we consider a 5 process network (Figure 4.8) having 4 uncertain parameters, i.e. yield of Process I, Process II, Process IV and Process V. Notice that here we consider 2 new additional processes compared to the previous example in which Process IV converts E into B and Process V that converts B into final product A. Each of the uncertain yields has 3 realizations and gives rise to a total of 81 scenarios with equal probabilities. The problem consists of finding the expansion and operation decisions for this process network over a 10 year planning horizon to minimize the total expected cost of the project.

The optimum installation schedule of the processes for this problem can be seen in Figure 4.9. Only one node in time period 1 in Figure 4.9 corresponds to the initial state of the system when there is no realization of any of the uncertain yields. The uncertain Process II, Process IV and Process V are installed in the first year with small capacities in all the scenarios and due to the 3 possible realizations of the yield of each of these 3 processes, there are total 27 nodes at time period 2 in the scenario tree (Figure 4.9) that correspond to the 27 possible states of the system at the beginning of the second year. On the basis of these yield realizations, the recourse actions involve installation of the new Process I for low yield scenarios and expansion of the already installed processes for high yield scenarios. Note that in Figure 4.9, the number of nodes (states) in time period 3 is greater than the ones in period 2 due to the installation of Process I in some of the states in the second year and its corresponding 3 possible yield realizations for each of these new installations. From period 3 to end of the planning horizon there is no further realization of uncertainty in any of the scenarios and no new branches appeared as can be seen from Figure 4.9. Moreover, we can observe from this solution that the structure of the scenario tree for these problems depends on our decisions, i.e. decision-dependent scenario tree as explained earlier.

Table 4.7: Comparison of the various solution strategies for Example 2

| **Problem Type** | **Expected Cost ($\$10^3$)** | **Number of Constraints** | **Continuous Variables** | **Binary Variables** | **Solution Time(s)** |
|---|---|---|---|---|---|
| Original Model ($MSSP^0$) | - | 3,158,272 | 90,802 | 4,050 | NA |
| Reduced Model: Property 1 | - | 1,591,732 | 58,402 | 4,050 | NA |
| Reduced Model: Properties 1-2 | 369.590 | 151,552 | 29,242 | 4,050 | 1627.51 |
| Reduced Model ($MSSP^R$): | 368.972 | 109,432 | 28,162 | 4,050 | 1160.34 |
| *k*-Stage Constraint Model fo*r* | 368.916 | 44,200 | 26,434 | 4,050 | 371.53 |
| NAC Relaxation Strategy | 368.650 | 45,797* | 28,162* | 4,050* | 250.64 |

**Size of the last MILP with NA constraints in Phase II.*

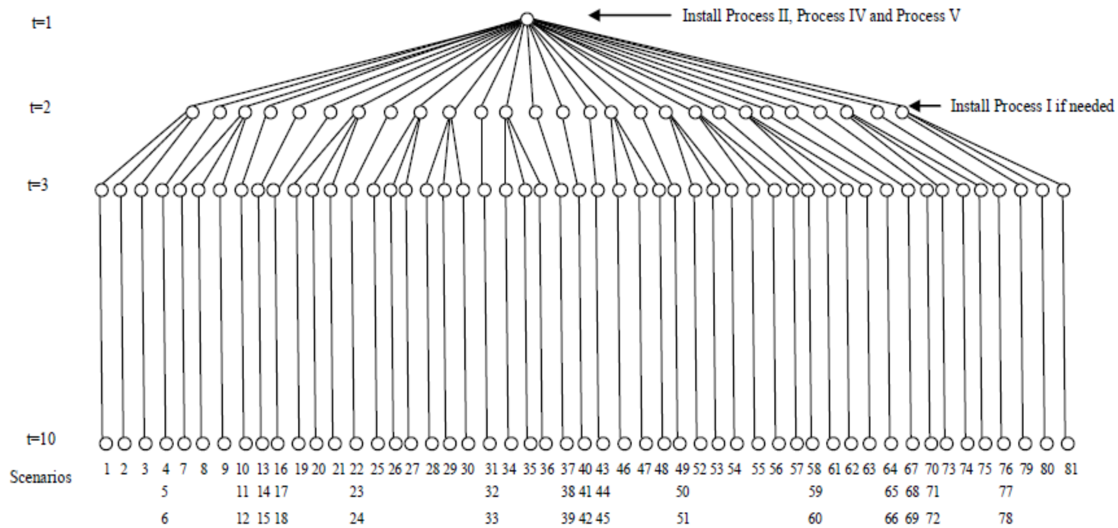


Figure 4.9: Optimal Solution (Example 2)

The results for this problem are compared in Table 4.7 for the original ($MSSP^0$), reduced ($MSSP^R$), *k*-stage constraint ($MSSP^{sc}$) models and NAC relaxation strategy. The problem was solved within 0.5% optimally tolerance in all the cases which gives slightly different optimal values. It can be seen that the problem cannot be solved in the fullspace for the original model and even after using Property 1, while using the reduced model with Properties 2 and 3, we can solve it. The solution time for only considering Properties 1-2 is 1.5 times more than the solution time from considering Properties 1-3, which is expected due to a factor of around the same order in the number of scenario pairs included in these models.

The *k*-stage constraint model was initially solved for two stages ($k = 2$) and it gives the optimal solution to the problem as there was no realization of any uncertain parameter after $k=2$. Because of the inherent property of these problems, the proposed *k*-stage constraint model does not need many iterations and performs better than the reduced model. On the other hand, the NAC relaxation strategy works well in all the cases because of its generality. As it can be seen in Table 4.7, the optimal solution obtained from the NAC relaxation strategy has a slightly lower cost than the other strategies, and it is also significantly faster than the reduced model and comparable to the *k*-stage model.

Table 4.8: Iterations during Lagrangean Decomposition

| Sub-gradient Iteration No. | Lower Bound ($\$10^3$) | Upper Bound ($\$10^3$) | % Gap |
|---|---|---|---|
| 1* | 351.577 | 371.579 | 5.383 |
| 2* | 352.517 | 371.579 | 5.130 |
| 3* | 354.426 | 371.579 | 4.616 |
| 4* | 354.426 | 371.579 | 4.616 |
| 5* | 354.869 | 371.579 | 4.497 |
| 6* | 354.869 | 371.579 | 4.497 |
| 7* | 354.929 | 371.579 | 4.481 |
| 8* | 354.929 | 371.579 | 4.481 |
| 9 | 355.235 | 371.579 | 4.399 |
| 10 | 355.235 | 371.579 | 4.399 |
| 30 | 358.361 | 371.579 | 3.557 |
| Time(s) | 167.19 | 13.63 | 3.557 |

*problem solved for upper bound generation

The Lagrangean decomposition algorithm was also applied to this 5 process network problem using the reduced model. The results in Table 4.8 show that using Lagrangean decomposition algorithm with the reduced model, the problem can be solved within about 3.5% of optimality gap at the root node after 30 iterations. The solution obtained (UB) at the root node has a higher cost than the solution obtained from the NAC relaxation strategy ($371,579 vs. $368, 650). On the other hand, it is faster than the NAC relaxation strategy (181s vs. 251s).

The Lagrangean decomposition strategy has the advantage that if the problem size is too large to be generated for all the scenarios at once, the model can be decomposed by scenarios. The *k*-stage constraint and NAC relaxation strategies will not work in this case as they need to be solved for all scenarios at once. It is only in smaller to moderate size problems that the *k*-stage constraint strategy and the NAC relaxation strategy may perform better than Lagrangean decomposition strategy because of the tight lower bounds and corresponding better solutions obtained in these cases. These trends can be clearly seen from the two examples considered.

It is also interesting to note that the two-stage stochastic model corresponding to this example gives about 5% higher total expected cost ($387,421 vs. $368,650) and suggests to invest in all the processes in period 1. Similar to the Example 1, in the two-stage case the higher cost occurs due to the absence of appropriate recourse for the investment decisions in the model. Furthermore, the larger savings compared to the previous example indicate the advantage of using the multistage stochastic model. Also, note that the total expected cost is about 3-6 % higher for the expected value problem (EVP) in comparison to the multistage stochastic programming model for all the cases considered.

The numerical results presented in this section are very encouraging to solve multistage stochastic programming problems with endogenous uncertainty using the proposed solution strategies in reasonable computational time. Although there are several trade-offs involved in using a particular solution strategy for a particular class of the problems under uncertainty, the proposed solution strategies are fairly general and can be applied to many problems classes, specifically to all the problems that involve endogenous uncertain parameters.

## 4.8 Conclusions

In this chapter, we have proposed several solution strategies for multistage stochastic programming problems with endogenous uncertainty. We have identified a new Property 3 for the models in this class that together with two properties previously presented by Goel and Grossmann (2006), significantly reduce the problem size and the solution time. To solve the large instance of these problems, we have proposed a *k*-stage constraint strategy that yields the global optimum in particular cases and is useful for problems where endogenous uncertainty is revealed during the first few time periods of the planning horizon. To solve the more general problems of large size, we also proposed a NAC relaxation strategy based on relaxing the NA constraints and adding them if they are violated. Finally, we described a Lagrangean Decomposition algorithm that can predict the rigorous lower bounds for the solution obtained. The proposed solution strategies have been successfully applied to two process network problems. Moreover, these strategies are applicable to a wide range of problems having endogenous uncertainty in some of the parameters.

# Chapter 5

# Multistage stochastic programming approach for offshore oilfield infrastructure planning under production sharing agreements and endogenous uncertainties

## 5.1 Introduction

In this chapter, we present a general multistage stochastic programming model for multiperiod investment and operations planning of offshore oil and gas field infrastructure. The model considers the deterministic models proposed in chapter 2 and 3 as a basis to extend to the stochastic programming using the modeling framework presented in chapter 4 for endogenous (decision-dependent) uncertainty problems. In terms of the fiscal contracts, we consider progressive production sharing agreements, whereas the endogenous uncertainty (type 2) in the field parameters i.e. field size, oil deliverability, water-oil ratio and gas-oil ratio is considered, that can only be revealed once an investment is made in the field and production is started in it. Compared to the conventional models where either fiscal rules or uncertainty in the field parameters are taken into account, the proposed model is the first one in the literature that also allows considering both of these complexities simultaneously. To solve large instances of the problem, the Lagrangean decomposition approach similar to chapter 4, allowing parallel solution of the scenario subproblems, is implemented in the GAMS grid computing environment.

The outline of this chapter is as follows. First, in section 5.2 we present a detailed problem description for offshore oilfield development planning under production sharing agreements and endogenous uncertainties. The corresponding multistage stochastic programming model is presented in extensive as well as compact forms in sections 5.3 and 5.4, respectively. The Lagrangean decomposition algorithm adapted from chapter 4 is explained in section 5.5 to solve large instances of the stochastic oilfield planning model. The proposed model and solution approach are then applied to multiple instances of the two oilfield development problems in section 5.6 to illustrate their performances.

## 5.2 Problem statement

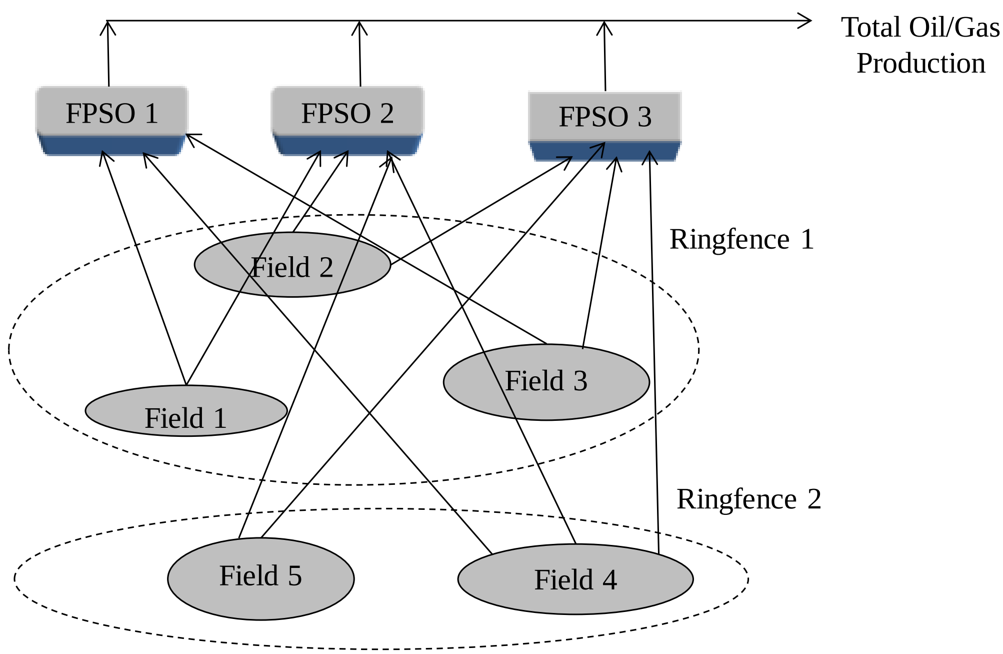


Figure 5.1: A typical offshore oilfield infrastructure representation

In this chapter, we consider the development planning of an offshore oil and gas field infrastructure under complex fiscal rules and endogenous uncertainties. In particular, a multi-field site, $F = \{1,2,\ldots\}$, with potential investments in floating production storage and offloading (FPSO) facilities, $FPSO = \{1,2,\ldots\}$ with continuous capacities and ability to expand them in the future is considered (Figure 5.1), as in the previous chapters. The connection of a field to an installed FPSO facility and a number of wells need to be drilled to produce oil from these fields for the given planning horizon. The planning horizon is discretized into T time periods, typically each with one year duration. The location of each FPSO facility and its possible connections to the given fields are assumed to be known. Notice that each FPSO facility can be connected to more than one field to produce oil, while a field can only be connected to a single FPSO facility due to engineering requirements and economic viability of the project. For simplicity, we only consider FPSO facilities. The proposed model can easily be extended to other facilities such as tension leg platforms (TLPs). The water produced with the oil is usually re-injected after separation, while the gas can be sold in the market. In this case, we consider natural depletion of the reserves, i.e. no water or gas re-injection. Notice that for convenience to the reader, we included the detailed problem statement and model in this chapter which contain few common elements from the previous chapters.

There are three major complexities in the problem considered here:

**5.2.1 Nonlinear Reservoir Profiles:** We consider three components (oil, water and gas) explicitly during production from a field. Field deliverability, i.e. maximum oil flowrate from a field, water-oil-ratio (WOR) and gas-oil-ratio (GOR) are approximated by cubic equations (a)-(c) (see Figure 5.2), while cumulative water produced and cumulative gas produced from a field are represented by fourth order separable polynomials, eqs. (d)-(e), that are derived in Appendix A. The motivation for using the polynomials for cumulative water produced and cumulative gas produced in eqs. (d)-(e) as compared to WOR and GOR in eqs. (b)-(c) is to avoid bilinear terms, eqs. (f)-(g), in the formulation and allow converting the resulting model into an MILP formulation using piecewise linear approximations. All the wells in a particular field *f* are assumed to be identical for the sake of simplicity leading to the same reservoir profiles, eqs. (a)-(g), for each of these wells.

$$\hat{Q}_f^d = a_{1,f}(fc_{f,t})^3 + b_{1,f}(fc_f)^2 + c_{1,f}\, fc_f + d_1 \qquad \forall f \qquad \text{(a)}$$

$$w\hat{o}r_f = a_{2,f}(fc_f)^3 + b_{2,f}(fc_f)^2 + c_{2,f}\, fc_f + d_{2,f} \qquad \forall f \qquad \text{(b)}$$

$$g\hat{o}r_f = a_{3,f}(fc_f)^3 + b_{3,f}(fc_f)^2 + c_{3,f}\, fc_f + d_{3,f} \qquad \forall f \qquad \text{(c)}$$

$$\hat{w}c_f = a_{4,f}(fc_f)^4 + b_{4,f}(fc_f)^3 + c_{4,f}\, fc_f^2 + d_{4,f}\, fc_f \qquad \forall f \qquad \text{(d)}$$

$$\hat{g}c_f = a_{5,f}(fc_f)^4 + b_{5,f}(fc_f)^3 + c_{5,f}\, fc_f^2 + d_{5,f}\, fc_f \qquad \forall f \qquad \text{(e)}$$

$$w_f = w\hat{o}r_f . x_f \qquad \forall f \qquad \text{(f)}$$

$$g_f = g\hat{o}r_f . x_f \qquad \forall f \qquad \text{(g)}$$

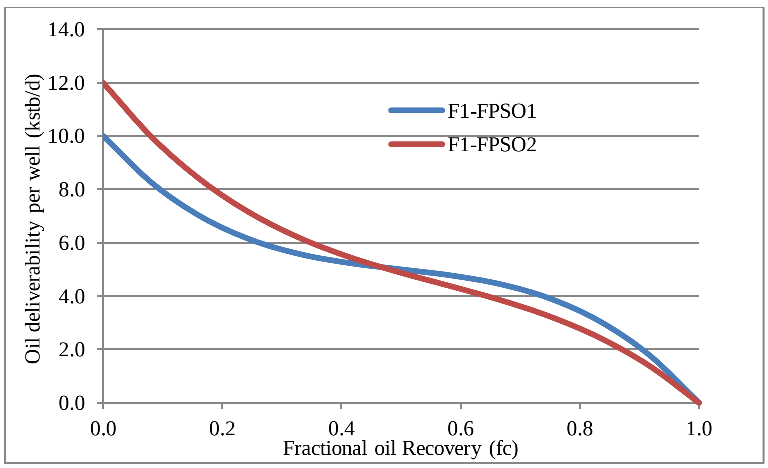


(a) Oil Deliverability per well for field (F1)

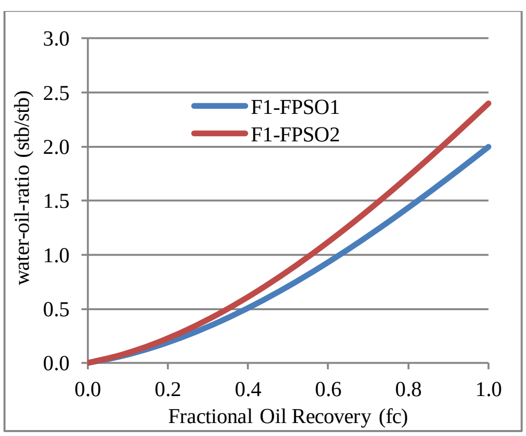


(b) Water to oil ratio for field (F1)

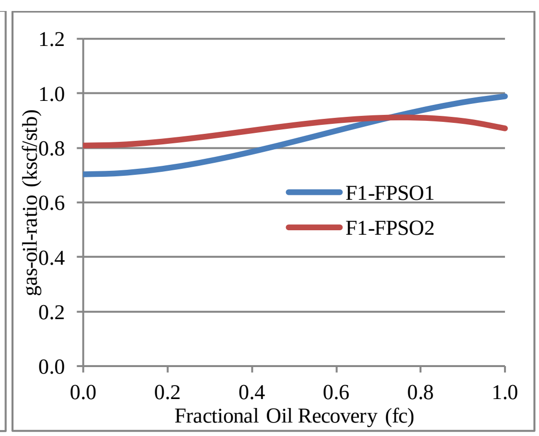


(c) Gas to oil ratio for field (F1)

Figure 5.2: Nonlinear Reservoir Characteristics for field (F1) for 2 FPSOs (FPSO 1 and 2)

**5.2.2 Production Sharing Agreements:** There are fiscal contracts with the host government that need to be accounted for during development planning. In particular, we consider progressive (sliding scale) production sharing agreements with ringfencing provisions, which are widely used in several countries. The revenue flow in a typical production sharing agreement (PSA) can be seen as in Figure 5.3 (World Bank, 2007). First, in most cases, the company pays royalty to the government at a certain percentage of the total oil produced. After paying the royalties, some portion of the remaining oil is treated as cost oil by the oil company to recover its costs. There is a ceiling on the cost oil recovery to ensure revenues to the government as soon as production starts. The remaining part of the oil, called profit oil, is divided between oil company and the host government at a certain percentage. The oil company needs to further pay income tax on its share of profit oil. Hence, the total contractor's (oil company) share in the gross revenue is comprised of cost oil and contractor's profit oil share after tax.

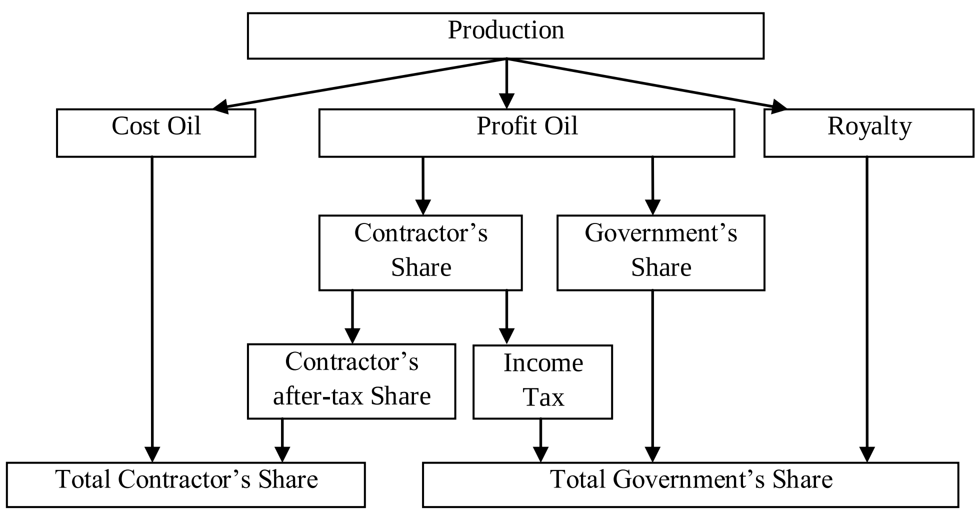


Figure 5.3: Revenue flow for a typical Production Sharing Agreement

In this work, we consider a sliding scale profit oil share of the contractor linked to the cumulative oil produced. For instance, if the cumulative production (in MMbbl) is in the range of first tier, $0 \le xc_t \le 200$, the contractor receives 50% of the profit oil, while if the cumulative production (in MMbbl) reaches in tier 2, $200 \le xc_t \le 400$, the contractor receives 40% of the profit oil, and so on (see Figure 5.4). Notice that this tier structure is a step function, which requires additional binary variables to model and makes the problem harder to solve. Moreover, the cost recovery ceiling is considered to be a fraction of the gross revenues in each time period t. For simplicity, the cost recovery ceiling fraction and income tax rates are assumed to be a fixed percentages (no sliding scale), and there are no explicit royalty provisions which is a straightforward extension.

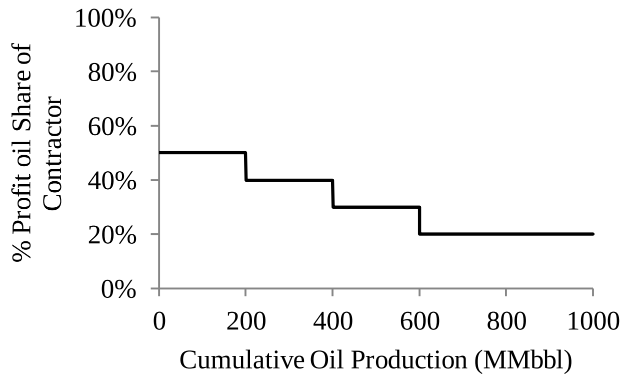


Figure 5.4: Progressive profit oil share of the contractor

A set of ringfences *RF = {1,2,...}* among the given fields is specified (see Figure 5.1) to ensure that fiscal calculations are to be done for each ringfence separately (see chapter 3 for details). For example, the fiscal calculations for Fields 1-3 (Ringfence 1) and Field 4-5 (Ringfence 2) in Figure 5.1 cannot be consolidated in one place. These ringfences may or may not have the same fiscal rules. Qualitatively, a typical ringfencing provision states that the investment and operational costs for a specified group of fields or block can only be recovered from the revenue generated from those fields or block. Notice that in general a field is associated to a single ringfence, while a ringfence can include more than one field. In contrast, a facility can be connected to multiple fields from different ringfences for producing oil and gas.

### 5.2.3 Endogenous Uncertainties:

**(a) Uncertain Field Parameters:** We consider here the uncertainty in the field parameters, i.e. field size, oil deliverability per well, water-oil ratio and gas-oil ratio. These are endogenous uncertain parameters since investment and operating decisions affect the stochastic process (Jonsbraten et al., 1998; Goel et al., 2006; Tarhan et al., 2009; and Gupta and Grossmann, 2011a). In particular, the uncertainty in the field parameters can only be resolved when an investment is made in that field and production is started in it. Therefore, optimization decisions determine the timing of uncertainty realization, i.e. decision-dependent uncertainty (type 2).

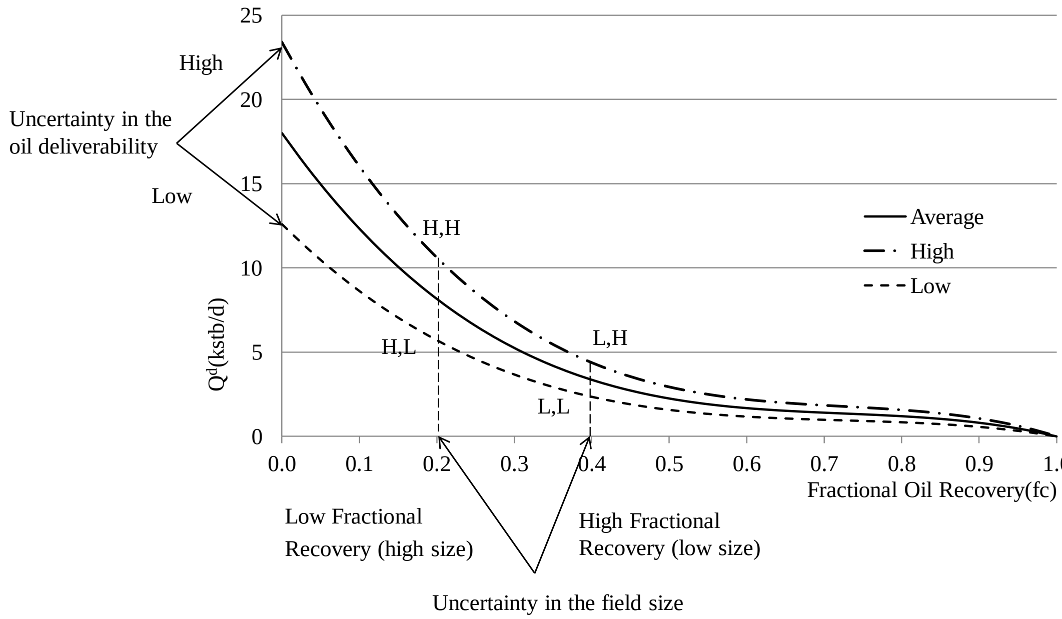


$$fc \propto \frac{1}{REC_f}$$

Figure 5.5: Oil deliverability per well for a field under uncertainty

The average profile in Figure 5.5 represents the oil deliverability per well for a field as a nonlinear polynomial in terms of the fractional oil recovery (eq. (a)) under perfect information. However, due to the uncertainty in the oil deliverability, the actual profile is assumed to be either the lower or upper side of the average profile with a given probability. In particular, eq. (h) represents the oil deliverability per well for a field under uncertainty where parameter $\alpha_{f,oil}$ is used to characterize this uncertainty.

$$Q_f^d = \alpha_{f,oil} \cdot \hat{Q}_f^d \qquad \forall f \qquad \text{(h)}$$

For instance, if $\alpha_{f,oil} > 1$, then we have a higher oil deliverability than expected ($\alpha_{f,oil} = 1$), whereas for $\alpha_{f,oil} < 1$ a lower than expected oil deliverability is observed. Since, the uncertain field size (recoverable oil volume, $REC_f$) is an inverse function of the fraction oil recovery, a higher field size will correspond to the low fractional oil recovery, whereas a small field size will correspond to the higher fractional oil recovery for a given amount of the cumulative oil production.

Similarly, eqs. (i) and (j) correspond to the uncertain field profiles for water-oil-ratio and gas-oil-ratio that are characterized by the uncertain parameters $\alpha_{f,wor}$ and $\alpha_{f,gor}$, respectively. Notice that since the cumulative water produced (eq. (d)) and the cumulative gas produced (eq. (e)) profiles are used in the model, instead of water-oil-ratio (eq. (b)) and gas-oil-ratio (eq. (c)), the uncertainty in the parameters $\alpha_{f,wor}$ and $\alpha_{f,gor}$ can be transformed into the corresponding uncertainty in the parameters $\alpha_{f,wc}$ and $\alpha_{f,gc}$ as in eqs. (k) and (l), respectively. In particular, we use the correspondence among the coefficients of these two sets of the polynomials (see Appendix A) for this transformation.

$$wor_f = \alpha_{f,wor} \cdot \hat{wor}_f \qquad \forall f \qquad \text{(i)}$$

$$gor_f = \alpha_{f,gor} \cdot \hat{gor}_f \qquad \forall f \qquad \text{(j)}$$

$$wc_f = \alpha_{f,wc} \cdot \hat{wc}_f \qquad \forall f \qquad \text{(k)}$$

$$gc_f = \alpha_{f,gc} \cdot \hat{gc}_f \qquad \forall f \qquad \text{(l)}$$

Moreover, the uncertain parameters for every field, i.e. $\theta_f = \{REC_f, \alpha_{f,oil}, \alpha_{f,wor}, \alpha_{f,gor}\}$ are considered to have a number of possible discrete realizations $\tilde{\theta}_f^k$ with a given probability. Therefore, all the possible combinations of these realizations yield a set of scenarios $s \in S^{\sup}$ where each scenario has the corresponding probability $p^s$.

**(b) Correlation among the uncertain parameters:** If the uncertain parameters are considered to be independent, the total number of scenarios in set $S^{\sup}$ grows exponentially with the number of uncertain parameters and their possible realizations, which makes the problem intractable. For instance, if there are only 2 fields, then 4 uncertain parameters for each field having 2 realizations will require 256 scenarios. Therefore, it becomes difficult to solve a multi-field site problem with independent uncertainties in the set $\theta_f = \{REC_f, \alpha_{f,oil}, \alpha_{f,wor}, \alpha_{f,gor}\}$. Since in practice normally uncertainties are not independent, we can overcome this limitation by considering that there are correlations among the uncertain parameters for each individual field. In particular, the uncertain parameters for a field $\theta_f = \{REC_f, \alpha_{f,oil}, \alpha_{f,wor}, \alpha_{f,gor}\}$ are considered to be dependent. Therefore, only a subset of the possible scenarios $S \subset S^{\sup}$ is sufficient to represent the uncertainty. For instance, based on the practical considerations, we can assume that if a field is of lower size than expected, then the oil deliverability is also lower ($\alpha_{f,oil} < 1$). Therefore, the scenarios with a combinations of higher oil deliverability ($\alpha_{f,oil} > 1$) and lower field size are not included in the reduced scenario set and vice-versa. Similarly, correlations for the water-oil ratio and gas-oil ratio can be considered to substantially reduce the original scenario set $S^{\sup}$. Therefore, the problem can be considered as selecting a sample of the scenarios for each field, where a scenario for that field will be equivalent to the selected combinations of the realizations of the uncertain parameters $\theta_f = \{REC_f, \alpha_{f,oil}, \alpha_{f,wor}, \alpha_{f,gor}\}$.

In the computational experiments, we only consider the extreme cases of the scenarios assuming perfect correlations, i.e. all uncertain parameters for a field have either low, medium or high realizations. Note that these assumptions on correlation among the field parameters are flexible and can be modified depending on the problem at hand. In addition to the correlation among the uncertain parameters for each individual field, one can also take into account the correlation among the fields based on the available information for a particular oilfield development site to further reduce the total number of scenarios. Notice also that the model and solution method presented in the chapter is irrespective of whether a reduced scenario set $S$ is considered or the complete one ($S^{\sup}$).

**(c) Uncertainty Resolution Rules**: Instead of assuming that the uncertainties are resolved as soon as a well is drilled in the field, i.e. immediate resolution, we assume that several wells need to be drilled and production has to be started from the field for this purpose. Moreover, since the uncertain parameters for a field $\theta_f = \{REC_f, \alpha_{f,oil}, \alpha_{f,wor}, \alpha_{f,gor}\}$ are assumed to be correlated as described above, the timing of uncertainty resolution in these parameters is also considered to the same. This allows solving much larger multi-field site instances without losing much in terms of the quality of the solution.

In contrast, Tarhan et al. (2009) considered a single field at a detailed level where no correlations among the uncertain parameters of the field were considered, and these parameters were allowed to be revealed independently at different time periods in the planning horizon. However, the resulting scenario tree even for a single field became very complex to model and solve. Therefore, we assume that the uncertainty in all the field parameters $\theta_f = \{REC_f, \alpha_{f,oil}, \alpha_{f,wor}, \alpha_{f,gor}\}$ is resolved if at-least $N_1$ number of wells have been drilled in the field, and production has been performed from that field for a duration of at-least $N_2$ years. Notice that these assumptions on uncertainty resolution rules are flexible and can be adapted depending on the field information that is available. Moreover, the model can also be extended to the case where each parameter for a field is allowed to be revealed in different years based on the work of Tarhan et al. (2009) that will result in a significant increase in the computation expense.

**(d) Decision-dependent scenario trees**: The multiperiod planning horizon and the discrete set of the selected scenarios for each field with given probabilities can be represented by scenario trees. However, since the timing of the uncertainty realization for a field (or its corresponding scenarios) depends on the drilling and operating decisions, the resulting scenario tree is also decision-dependent as was seen in chapter 4. For instance, if we consider a set of two uncertain fields $F = \{1,2\}$ and the selected scenario set based on the parameter correlations for each field has 2 elements, $\{\tilde{\theta}_f^1, \tilde{\theta}_f^2\}$, with equal probability. Therefore, the problem involves the following 4 scenarios each with a probability of 0.25:

$$S = \{1:(\tilde{\theta}_1^1, \tilde{\theta}_2^1);\ 2:(\tilde{\theta}_1^1, \tilde{\theta}_2^2);\ 3:(\tilde{\theta}_1^2, \tilde{\theta}_2^1);\ 4:(\tilde{\theta}_1^2, \tilde{\theta}_2^2)\}$$

Notice that each of these elements, $\{\tilde{\theta}_f^1, \tilde{\theta}_f^2\}$, is equivalent to a selected combination of the realization of the corresponding uncertain parameters, for example $\tilde{\theta}_f^1 = \{REC_f^1, \alpha_{f,oil}^1, \alpha_{f,wor}^1, \alpha_{f,gor}^1\}$. Figure 5.6 represents the scenario tree for this problem, where the uncertainty in the first field is resolved at the end of first year, since we drill $N_1$ wells in the field at the beginning of year 1 and produce from this field during that year ($N_2$ =1). The system can be in two different states in year 2 depending on the realized value of the uncertain parameter $\tilde{\theta}_1^k$. Similarly, uncertainty in the field 2 is resolved in year 4 under the scenarios 3 and 4 due to drilling and operating decisions, whereas it remains uncertain in the scenarios 1 and 2. Therefore, the resulting scenario tree depends on the optimization decisions, which are not known a priori, requiring modeling a superstructure of the all possible scenario trees that can occur based on our decisions. Notice that the scenario-tree also allows considering the cases where the number of wells drilled in a field is less than the one required for the uncertainty resolution (i.e. $N_1$ wells), and therefore, the corresponding scenarios remain indistinguishable.

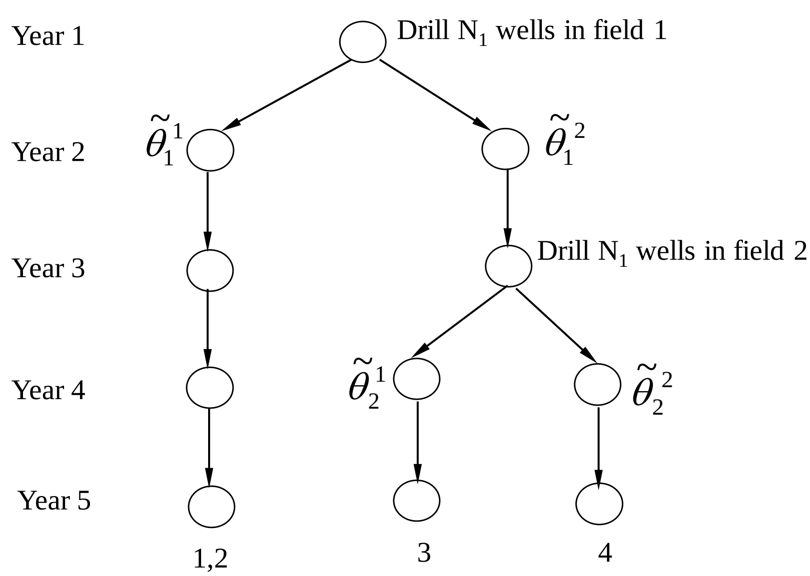


Figure 5.6: Decision-dependent scenario tree for two fields

An alternate representation of the decision-dependent scenario-tree (chapter 4) is used to model the problem as a multistage stochastic program in which the scenarios are treated independently and related through the non-anticipativity constraints for states of different scenarios that are identical (see Goel and Grossmann, 2006; and Gupta and Grossmann, 2011a).

The problem is to determine the optimal investment and operating decisions to maximize the contractor's expected NPV for a given planning horizon considering the above production sharing agreements and endogenous uncertainties. In particular, investment decisions in each time period *t* and scenario s include FPSO facilities installation or expansion, and their respective installation or expansion capacities for oil, liquid and gas, fields-FPSO connections, and the number of wells that need to be drilled in each field *f* given the restrictions on the total number of wells that can be drilled in each time period *t* over all the given fields. Operating decisions include the oil/gas production rates from each field *f* in each time period *t* under every scenario s.

It is assumed that the installation and expansion decisions occur at the beginning of each time period *t*, while operations take place throughout the time period. There is a lead time of $l_1$ years for each FPSO facility initial installation, and a lead time of $l_2$ years for the expansion of an earlier installed FPSO facility. Once installed, we assume that the oil, liquid (oil and water) and gas capacities of a FPSO facility can only be expanded once. These assumptions are made for the sake of simplicity, and both the model and the solution approaches are flexible enough to incorporate more complexities. In the next section, we propose a multistage stochastic programming model for oilfield development planning with production sharing agreements and decision-dependent uncertainty in the field parameters as described.

## 5.3 Multistage Stochastic Programming Model

In this section, we present a general multistage stochastic programming model for offshore oilfield development planning. The proposed model considers the trade-offs involved between investment and operating decisions, uncertainties in the field parameters and profit share with the government while maximizing the overall expected NPV for the contractor. Notice that the model is intended to be solved every year in a rolling horizon manner with updated information, not just once for the entire planning horizon. The constraints involved in the model are as follows:

**(i) Objective Function:** The objective function is to maximize the total expected NPV of the contractor as in (5.1), which is the summation of the NPVs over all the scenarios having probabilities $p^s$. The NPV of a particular scenario s is the difference between discounted total contractor's gross revenue share and total cost over the planning horizon (5.2). The total contractor's share in a particular time period t and scenario s is the sum of the contractor's share over all the ring-fences (*rf*) as given in equation (5.3). Similarly, constraints (5.4) and (5.5) represent the total capital and operating expenses for each scenario s in time period t.

$$Max \quad ENPV \tag{5.1}$$

$$ENPV = \sum_s p^s \sum_t dis_t \cdot (TotalConSh_t^{tot,s} - CAP_t^{tot,s} - OPER_t^{tot,s}) \tag{5.2}$$

$$TotalConSh_t^{tot,s} = \sum_{rf} TotalConSh_{rf,t}^s \qquad \forall t,s \tag{5.3}$$

$$CAP_t^{tot,s} = \sum_{rf} CAP_{rf,t}^s \qquad \forall t,s \tag{5.4}$$

$$OPER_t^{tot,s} = \sum_{rf} OPER_{rf,t}^s \qquad \forall t,s \tag{5.5}$$

**(ii) Cost Calculations:** The total capital expenses in scenario s for a ring-fence *rf* contains two components as given in equation (5.6). One is field specific (eq. 5.7) that accounts for the connection costs between a field and a FPSO facility, and cost of drilling the wells for each of the field in that ring-fence *rf*. The other cost component is FPSO specific (eq. 5.8) that includes the capital expenses for the corresponding FPSO facilities. Eq. (5.9) calculates the total cost of an FPSO facility in time period t for scenario s which is disaggregated in eq. (5.10) over various fields (and therefore ring-fences as in (5.11)). The cost disaggregation is done on the basis of the field sizes to which the FPSO is connected (eq. (5.12)-(5.14)), where set $F_{fpso}$ is the set of all the fields that can be connected to FPSO facility *fpso* and the binary variable $b^{on,s}_{f,fpso}$ represents the potential connections. Notice that there is an uncertainty in the recoverable oil volume of the field ( $REC^s_f$ ) used in eq. (5.14) that multiplies the binary variable $b^{on,s}_{f,fpso}$. To linearize the bilinear terms in eq. (5.14), we use exact linearization technique (Glover, 1975) by introducing the positive variables ( $ZD^{field,s}_{f',f,fpso,t}, ZD1^{field,s}_{f',f,fpso,t}$ ) and ( $ZD^s_{f,fpso,t}, ZD1^s_{f,fpso,t}$ ) that results in the constraints (5.15)-(5.23).

$$CAP^s_{rf,t} = CAP1^s_{rf,t} + CAP2^s_{rf,t} \qquad \forall rf,t,s \qquad (5.6)$$

$$CAP1^s_{rf,t} = \sum_{F_{rf}} \sum_{fpso} FC_{f,fpso,t} b^s_{f,fpso,t} + \sum_{F_{rf}} FC^{well}_{f,t} I^{well,s}_{f,t} \qquad \forall rf,t,s \qquad (5.7)$$

$$CAP2^s_{rf,t} = \sum_{fpso} DFPSOC^s_{rf,fpso,t} \qquad \forall rf,t,s \qquad (5.8)$$

$$FPSOC^s_{fpso,t} = \left[ FC^{FPSO}_{fpso,t} b^{FPSO,s}_{fpso,t} + VC^{liq}_{fpso,t} (QI^{liq,s}_{fpso,t} + QE^{liq,s}_{fpso,t}) + VC^{gas}_{fpso,t} (QI^{gas,s}_{fpso,t} + QE^{gas,s}_{fpso,t}) \right]$$
$$\forall rf,t,s \qquad (5.9)$$

$$FPSOC^s_{fpso,t} = \sum_{F_{fpso}} DFPSOC^{field,s}_{f,fpso,t} \qquad \forall rf,t,s \qquad (5.10)$$

$$DFPSOC^s_{rf,fpso,t} = \sum_{F_{rf}} DFPSOC^{field,s}_{f,fpso,t} \qquad \forall rf, fpso,t,s \qquad (5.11)$$

$$b^{on,s}_{f,fpso} = \sum_t b^s_{f,fpso,t} \qquad \forall f, fpso, s \qquad (5.12)$$

$$DFPSOC^{field,s}_{f,fpso,t} \le M \cdot b^{on,s}_{f,fpso} \qquad \forall f, fpso,t,s \qquad (5.13)$$

$$DFPSOC^{field,s}_{f,fpso,t} = \frac{b^{on,s}_{f,fpso} \cdot REC^s_f}{\sum_{f' \in F_{fpso}} b^{on,s}_{f',fpso} \cdot REC^s_{f'}} \cdot FPSOC^s_{fpso,t} \qquad \forall f, fpso,t,s \qquad (5.14)$$

$$\sum_{f' \in F_{fpso}} ZD^{field,s}_{f',f,fpso,t} \cdot REC^s_{f'} = ZD^s_{f,fpso,t} \cdot REC^s_f \qquad \forall f, fpso,t,s \qquad (5.15)$$

$$ZD^{field,s}_{f',f,fpso,t} + ZD1^{field,s}_{f',f,fpso,t} = DFPSOC^{field,s}_{f,fpso,t} \qquad \forall f, fpso,t, f' \in F_{fpso}, s \qquad (5.16)$$

$$ZD_{f',f,fpso,t}^{field,s} \leq U \cdot b_{f',fpso}^{on,s} \qquad \forall f,\ fpso,t,\ f' \in F_{fpso}, s \quad (5.17)$$

$$ZD1_{f',f,fpso,t}^{field,s} \leq U \cdot (1 - b_{f',fpso}^{on,s}) \qquad \forall f,\ fpso,t,\ f' \in F_{fpso}, s \quad (5.18)$$

$$ZD_{f',f,fpso,t}^{field,s} \geq 0, ZD1_{f',f,fpso,t}^{field,s} \geq 0 \qquad \forall f,\ fpso,t,\ f' \in F_{fpso}, s \quad (5.19)$$

$$ZD_{f,fpso,t}^{s} + ZD1_{f,fpso,t}^{s} = FPSOC_{fpso,t}^{s} \qquad \forall f,\ fpso,t,s \quad (5.20)$$

$$ZD_{f,fpso,t}^{s} \leq U \cdot b_{f,fpso}^{on,s} \qquad \forall f,\ fpso,t,s \quad (5.21)$$

$$ZD1_{f,fpso,t}^{s} \leq U \cdot (1 - b_{f,fpso}^{on,s}) \qquad \forall f,\ fpso,t,s \quad (5.22)$$

$$ZD_{f,fpso,t}^{s} \geq 0, ZD1_{f,fpso,t}^{s} \geq 0 \qquad \forall f,\ fpso,t,s \quad (5.23)$$

The total operating expenses for scenario s in time period t for ring-fence $rf$, eq. (5.24), are the operation costs corresponding to the total amount of liquid and gas produced.

$$OPER_{rf,t}^{s} = \delta_t \left[ OC_{rf,t}^{liq} (x_{rf,t}^{tot,s} + w_{rf,t}^{tot,s}) + OC_{rf,t}^{gas} g_{rf,t}^{tot,s} \right] \quad \forall rf,t,s \quad (5.24)$$

**(iii) Total Contractor Share Calculations:** The total contractor share in scenario s for ring-fence $rf$ in time period t, eq. (5.25), is the sum of contractor's after-tax profit oil share for that ring-fence and the cost oil that it keeps to recover the expenses. The contractor's profit oil share after tax in scenario s is the difference of the contractor's profit oil share before tax and income tax paid as in constraint (5.26). The tax paid by the contractor on its profit oil share depends on the given tax rate ( $f_{rf,t}^{tax}$ ) as in constraint (5.27).

$$TotalConSh_{rf,t}^{s} = ConSh_{rf,t}^{aftertax,s} + CO_{rf,t}^{s} \qquad \forall rf,t,s \quad (5.25)$$

$$ConSh_{rf,t}^{aftertax,s} = ConSh_{rf,t}^{beforetax,s} - Tax_{rf,t}^{s} \qquad \forall rf,t,s \quad (5.26)$$

$$Tax^{s}_{rf,t} = f^{tax}_{rf,t} \cdot ConSh^{beforetax,s}_{rf,t} \qquad \forall rf,t,s \qquad (5.27)$$

The contractor's share before tax for scenario s in each time period t is some fraction of the total profit oil during that period t for ring-fence *rf*. Note that we assume here that this profit oil fraction, $f^{po}_{rf,i}$, is based on a decreasing sliding scale system that is linked to the cumulative amount of oil produced $xc^{s}_{rf,t}$, where *i* is the index of the corresponding tier. Therefore, for possible levels *i* (i.e. tiers) of cumulative amount of oil produced by the end of time period t in scenario s, the corresponding contractor's profit oil share can be calculated using disjunction (5.28) where the boolean variable $Z_{rf,i,t}$ is true if the cumulative oil produced lies between the tier i threshold. This disjunction (5.28) can further be rewritten as integer and mixed-integer linear constraints (5.29)-(5.36) using the convex-hull formulation (Raman and Grossmann, 1994).

$$\bigvee_{i} \begin{bmatrix} Z^{s}_{rf,i,t} \\ ConSh^{beforetax,s}_{rf,t} = f^{PO}_{rf,i} \cdot PO^{s}_{rf,t} \\ L^{oil}_{rf,i} \le xc^{s}_{rf,t} \le U^{oil}_{rf,i} \end{bmatrix} \qquad \forall rf,t,s \qquad (5.28)$$

$$ConSh^{beforetax,s}_{rf,t} = \sum_{i} DConSh^{beforetax,s}_{rf,i,t} \qquad \forall rf,t,s \qquad (5.29)$$

$$PO^{s}_{rf,t} = \sum_{i} DPO^{s}_{rf,i,t} \qquad \forall rf,t,s \qquad (5.30)$$

$$xc^{s}_{rf,t} = \sum_{i} Dxc^{s}_{rf,i,t} \qquad \forall rf,t,s \qquad (5.31)$$

$$DConSh^{beforetax,s}_{rf,i,t} = f^{po}_{rf,i} \cdot DPO^{s}_{rf,i,t} \qquad \forall rf,i,t,s \qquad (5.32)$$

$$0 \le DConSh^{beforetax,s}_{rf,i,t} \le M \cdot Z^{s}_{rf,i,t} \qquad \forall rf,i,t,s \qquad (5.33)$$

$$0 \le DPO^{s}_{rf,i,t} \le M \cdot Z^{s}_{rf,i,t} \qquad \forall rf,i,t,s \qquad (5.34)$$

$$L^{oil}_{rf,i} \cdot Z^{s}_{rf,i,t} \le Dxc^{s}_{rf,i,t} \le U^{oil}_{rf,i} \cdot Z^{s}_{rf,i,t} \qquad \forall rf,i,t,s \qquad (5.35)$$

$$\sum_{i} Z_{rf,i,t}^{s} = 1 \qquad \forall rf, t, s \qquad (5.36)$$

$$Z_{rf,i,t}^{s} \in \{0,1\}$$

The cumulative amount of oil produced from a ring-fence *rf* by the end of time period t in scenario s is calculated as the sum of the cumulative amount of oil produced by that time period from all the fields associated to that ring-fence, eq. (5.37). Constraint (5.38) represents the total profit oil in time period t for a ring-fence *rf* as the difference between gross revenue and the cost oil for scenario s. The gross revenues (5.39) in each time period t for a ring-fence *rf* in scenario s, are computed based on the total amount of oil produced and its selling price, where total oil flow rate in a time period t for ring-fence *rf*, is calculated as the sum of the oil production rates over all the fields in that ring-fence, i.e. set $F_{rf}$, in equation (5.40). For simplicity, we only consider the revenue generated from the oil sales, which is much larger in general as compared to the revenue from gas.

$$xc_{rf,t}^{s} = \sum_{F_{rf}} xc_{f,t}^{field,s} \qquad \forall rf, t, s \qquad (5.37)$$

$$PO_{rf,t}^{s} = REV_{rf,t}^{s} - CO_{rf,t}^{s} \qquad \forall rf, t, s \qquad (5.38)$$

$$REV_{rf,t}^{s} = \delta_t \alpha_t x_{rf,t}^{tot,s} \qquad \forall rf, t, s \qquad (5.39)$$

$$x_{rf,t}^{tot,s} = \sum_{F_{rf}} x_{f,t}^{s} \qquad \forall rf, t, s \qquad (5.40)$$

The cost oil in time period t for a ring-fence *rf*, constraint (5.41), is calculated as the minimum of the cost recovery in that time period and maximum allowable cost oil (cost recovery ceiling) in scenario s. Eq. (5.41) can further be rewritten as mixed-integer linear constraints (5.42)-(5.47). Cost recovery in time period t for a ring-fence *rf* in scenario s, constraint (5.48), is the sum of capital and operating costs in that period t and cost recovery carried forward from previous time period t-1. Any unrecovered cost (that is carried forward to the next period) in time period t for a ring-fence *rf*, is calculated as the difference between the cost recovery and cost oil in time period t for a scenario s (eq. (5.49)).

$$CO^{s}_{rf,t} = \min(CR^{s}_{rf,t}, f^{CR}_{rf,t} \cdot REV^{s}_{rf,t}) \qquad \forall rf,t,s \qquad (5.41)$$

$$CO^{s}_{rf,t} \le CR^{s}_{rf,t} + M(1 - b^{co,s}_{rf,t}) \qquad \forall rf,t,s \qquad (5.42)$$

$$CO^{s}_{rf,t} \ge CR^{s}_{rf,t} - M(1 - b^{co,s}_{rf,t}) \qquad \forall rf,t,s \qquad (5.43)$$

$$CO^{s}_{rf,t} \le f^{CR}_{rf,t} REV^{s}_{rf,t} + M \cdot b^{co,s}_{rf,t} \qquad \forall rf,t,s \qquad (5.44)$$

$$CO^{s}_{rf,t} \ge f^{CR}_{rf,t} REV^{s}_{rf,t} - M \cdot b^{co,s}_{rf,t} \qquad \forall rf,t,s \qquad (5.45)$$

$$CO^{s}_{rf,t} \le CR^{s}_{rf,t} \qquad \forall rf,t,s \qquad (5.46)$$

$$CO^{s}_{rf,t} \le f^{CR}_{rf,t} REV^{s}_{rf,t} \qquad \forall rf,t,s \qquad (5.47)$$

$$CR^{s}_{rf,t} = CAP^{s}_{rf,t} + OPER^{s}_{rf,t} + CRF^{s}_{rf,t-1} \qquad \forall rf,t,s \qquad (5.48)$$

$$CRF^{s}_{rf,t} = CR^{s}_{rf,t} - CO^{s}_{rf,t} \qquad \forall rf,t,s \qquad (5.49)$$

**(iv) Tightening Constraints:** The logic constraints (5.50) and (5.51) that defines the tier sequencing are included in the model to tighten its relaxation. These constraints can be expressed as integer linear inequalities, (5.52) and (5.53), respectively, (Raman and Grossmann, 1991). In addition, the valid inequalities (5.54), are also included that bounds the cumulative contractor's share in the cumulative profit oil by the end of time period t based on the sliding scale profit oil share and cost oil that has been recovered (see chapter 3 for details).

$$Z^{s}_{rf,i,t} \Rightarrow \bigwedge_{\tau=t}^{T} \neg Z^{s}_{rf,i',\tau} \qquad \forall rf,i,i'<i,t,s \qquad (5.50)$$

$$Z^{s}_{rf,i,t} \Rightarrow \bigwedge_{\tau=1}^{t} \neg Z^{s}_{rf,i',\tau} \qquad \forall rf,i,i'>i,t,s \qquad (5.51)$$

$$Z^{s}_{rf,i,t} + Z^{s}_{rf,i',\tau} \le 1 \qquad \forall rf,i,i'<i,t,t \le \tau \le T,s \qquad (5.52)$$

$$Z^{s}_{rf,i,t} + Z^{s}_{rf,i',\tau} \le 1 \qquad \forall rf,i,i'>i,t,1 \le \tau \le t,s \qquad (5.53)$$

$$\sum_{\tau \le t}(Contsh^{beforetax,s}_{rf,\tau} / \alpha_\tau) \le \sum_{i'=1}^{i' \le i}( f^{PO}_{rf,i'} - f^{PO}_{rf,i'-1}) \cdot (xc^s_{rf,t} - L_{rf,i'}) - f^{PO}_{rf,i^{end}} \cdot \sum_{\tau \le t}(CO^s_{rf,\tau} / \alpha_\tau)$$

$$\forall rf, i, t, s \qquad (5.54)$$

**(v) Reservoir Constraints:** Constraints (5.55)-(5.58) predict the reservoir behavior for each field *f* in each time period t for a scenario s. In particular, constraint (5.55) restricts the oil flow rate from each well for a particular FPSO-field connection in time period t to be less than the deliverability of that field per well in scenario s. Equation (5.56) represents the field deliverability per well in scenario s at the beginning of time period t+1 for a particular FPSO-field connection as the cubic equation in terms of the fractional oil recovered by the end of time period t from that field. In particular, (5.56a) corresponds to the oil deliverability in time period 1, while (5.56b) corresponds to the rest of the time periods in the planning horizon. Notice that the uncertainty in the oil deliverability profile is characterized by the uncertain parameter $\alpha^s_{oil}$. Constraints (5.57) and (5.58) represent the separable polynomials for the cumulative water and cumulative gas produced by the end of time period t for a specific field-FPSO connection in scenario s, where $\alpha^s_{wc}$ and $\alpha^s_{gc}$ are the respective uncertain parameters. The motivation for using polynomials for cumulative water produced and cumulative gas produced as compared to WOR and GOR is to avoid bilinear terms in the formulation, and allow converting the resulting MINLP model into an MILP formulation as explained in the chapter 2.

$$x^{well,s}_{f,fpso,t} \le Q^{d,well,s}_{f,fpso,t} \qquad \forall f, fpso, t, s \qquad (5.55)$$

$$Q^{d,well,s}_{f,fpso,1} = \alpha^s_{oil} \cdot d_{1,f,fpso} \qquad \forall f, fpso, s \qquad (5.56a)$$

$$Q^{d,well,s}_{f,fpso,t+1} = \alpha^s_{oil} \cdot [a_{1,f,fpso}(fc^s_{f,t})^3 + b_{1,f,fpso}(fc^s_{f,t})^2 + c_{1,f,fpso} fc^s_{f,t} + d_{1,f,fpso}]$$

$$\forall f, fpso, t < |T|, s \qquad (5.56b)$$

$$Q^{wc,s}_{f,fpso,t} = \alpha^s_{wc} \cdot [a_{2,f,fpso}(fc^s_{f,t})^4 + b_{2,f,fpso}(fc^s_{f,t})^3 + c_{2,f,fpso}(fc^s_{f,t})^2 + d_{2,f,fpso} fc^s_{f,t}]$$

$$\forall f, fpso, t, s \qquad (5.57)$$

$$Q^{gc,s}_{f,fpso,t} = \alpha^s_{gc} \cdot [a_{3,f,fpso}(fc^s_{f,t})^4 + b_{3,f,fpso}(fc^s_{f,t})^3 + c_{3,f,fpso}(fc^s_{f,t})^2 + d_{3,f,fpso} fc^s_{f,t}] \quad \forall f, fpso, t, s \qquad (5.58)$$

Notice that variables $Q^{wc,s}_{f,fpso,t}$ and $Q^{gc,s}_{f,fpso,t}$ will be non-zero in equations (5.57) and (5.58) if $fc^s_{f,t}$ is non-zero even though that particular field-FPSO connection is not present. Therefore, additional constraints (5.59)-(5.66) need to be included to equate the actual cumulative water produced ( $wc^s_{f,fpso,t}$ ) and cumulative gas produced ( $gc^s_{f,fpso,t}$ ) for a field-FPSO connection by the end of time period t to the corresponding dummy variables $Q^{wc,s}_{f,fpso,t}$ and $Q^{gc,s}_{f,fpso,t}$ only if that field-FPSO connection is present in time period t, else it is zero. Note that the motivation for using dummy variables ( $Q^{wc,s}_{f,fpso,t}$ and $Q^{gc,s}_{f,fpso,t}$ ) for cumulative water and cumulative gas flows in equations (5.57)-(5.58) followed by big-M constraints (5.59)-(5.66), instead of using disaggregated variables for the fractional recovery in equations (5.57)-(5.58) directly, is to avoid large number of SOS1 variables while MILP reformulation of this model, as explained in chapter 2.

$$wc^s_{f,fpso,t} \le Q^{wc,s}_{f,fpso,t} + M^{wc,s}_{f,fpso}(1 - \sum_{\tau=1}^{t} b^s_{f,fpso,\tau}) \qquad \forall f, fpso, t, s \qquad (5.59)$$

$$wc^s_{f,fpso,t} \ge Q^{wc,s}_{f,fpso,t} - M^{wc,s}_{f,fpso}(1 - \sum_{\tau=1}^{t} b^s_{f,fpso,\tau}) \qquad \forall f, fpso, t, s \qquad (5.60)$$

$$wc^s_{f,fpso,t} \le M^{wc,s}_{f,fpso} \sum_{\tau=1}^{t} b^s_{f,fpso,\tau} \qquad \forall f, fpso, t, s \qquad (5.61)$$

$$wc^s_{f,fpso,t} \ge -M^{wc,s}_{f,fpso} \sum_{\tau=1}^{t} b^s_{f,fpso,\tau} \qquad \forall f, fpso, t, s \qquad (5.62)$$

$$gc^s_{f,fpso,t} \le Q^{gc,s}_{f,fpso,t} + M^{gc,s}_{f,fpso}(1 - \sum_{\tau=1}^{t} b^s_{f,fpso,\tau}) \qquad \forall f, fpso, t, s \qquad (5.63)$$

$$gc^s_{f,fpso,t} \ge Q^{gc,s}_{f,fpso,t} - M^{gc,s}_{f,fpso}(1 - \sum_{\tau=1}^{t} b^s_{f,fpso,\tau}) \qquad \forall f, fpso, t, s \qquad (5.64)$$

$$gc^{s}_{f,fpso,t} \leq M^{gc,s}_{f,fpso} \sum_{\tau=1}^{t} b^{s}_{f,fpso,\tau} \qquad \forall f, fpso, t, s \qquad (5.65)$$

$$gc^{s}_{f,fpso,t} \geq -M^{gc,s}_{f,fpso} \sum_{\tau=1}^{t} b^{s}_{f,fpso,\tau} \qquad \forall f, fpso, t, s \qquad (5.66)$$

Eq. (5.67) and (5.68) compute the water and gas flow rates in time period t from a field to FPSO facility in scenario s as the difference of cumulative amounts produced by the end of current time period t and previous time period t-1 divided by the time duration of that period.

$$w^{s}_{f,fpso,t} = (wc^{s}_{f,fpso,t} - wc^{s}_{f,fpso,t-1}) / \delta_t \qquad \forall f, fpso, t, s \qquad (5.67)$$

$$g^{s}_{f,fpso,t} = (gc^{s}_{f,fpso,t} - gc^{s}_{f,fpso,t-1}) / \delta_t \qquad \forall f, fpso, t, s \qquad (5.68)$$

**(vi) Field-FPSO flow constraints:** The total oil flow rate in (5.69) from each field *f* in time period t for a scenario s is the sum of the oil flow rates that are directed to FPSO facilities in that time period t, whereas oil that is directed to a particular FPSO facility from a field *f* in scenario s is calculated as the multiplication of the oil flow rate per well and number of wells available for production in that field (eq. (5.70)). Eq. (5.71) computes the cumulative amount of oil produced from field *f* by the end of time period *t* in scenario s, while (5.72) represents the fractional oil recovery by the end of time period *t*. The cumulative oil produced in scenario s is also restricted in (5.73) by the recoverable amount of oil from the field. Eqs. (5.74)-(5.76) compute the total oil, water and gas flow rates into each FPSO facility, respectively, in time period t from all the given fields in each scenario s. The total oil, water and gas flowrates in each time period t for scenario s are calculated as the sum of the production rate of these components over all the FPSO facilities in equations (5.77)-(5.79), respectively.

$$x^{s}_{f,t} = \sum_{fpso} x^{s}_{f,fpso,t} \qquad \forall f, t, s \qquad (5.69)$$

$$x^{s}_{f,fpso,t} = N^{well,s}_{f,t} \cdot x^{well,s}_{f,fpso,t} \qquad \forall f, fpso, t, s \qquad (5.70)$$

$$xc_{f,t}^{s} = \sum_{\tau=1}^{t}(x_{f,\tau}^{s}\delta_{\tau}) \qquad \forall f,t,s \qquad (5.71)$$

$$fc_{f,t}^{s} = \frac{xc_{f,t}^{s}}{REC_{f}^{s}} \qquad \forall f,t,s \qquad (5.72)$$

$$xc_{f,t}^{s} \le REC_{f}^{s} \qquad \forall f,t,s \qquad (5.73)$$

$$x_{fpso,t}^{s} = \sum_{f} x_{f,fpso,t}^{s} \qquad \forall fpso,t,s \qquad (5.74)$$

$$w_{fpso,t}^{s} = \sum_{f} w_{f,fpso,t}^{s} \qquad \forall fpso,t,s \qquad (5.75)$$

$$g_{fpso,t}^{s} = \sum_{f} g_{f,fpso,t}^{s} \qquad \forall fpso,t,s \qquad (5.76)$$

$$x_{t}^{tot,s} = \sum_{fpso} x_{fpso,t}^{s} \qquad \forall t,s \qquad (5.77)$$

$$w_{t}^{tot,s} = \sum_{fpso} w_{fpso,t}^{s} \qquad \forall t,s \qquad (5.78)$$

$$g_{t}^{tot,s} = \sum_{fpso} g_{fpso,t}^{s} \qquad \forall t,s \qquad (5.79)$$

**(vii) FPSO Capacity Constraints:** Eqs. (5.80)-(5.82) restrict the total oil, liquid and gas flow rates into each FPSO facility to be less than its corresponding capacity in each time period t, respectively. These three different kinds of capacities of a FPSO facility in time period *t* are computed by equalities (5.83)-(5.85) as the sum of the corresponding capacity at the end of previous time period t-1, installation capacity at the beginning of time period $t$-$l_1$ and expansion capacity at the beginning of time period $t$-$l_2$, where $l_1$ and $l_2$ are the lead times for FPSO installation and expansions, respectively.

$$x^{s}_{fpso,t} \le Q^{oil,s}_{fpso,t} \qquad \forall fpso,t,s \qquad (5.80)$$

$$x^{s}_{fpso,t} + w^{s}_{fpso,t} \le Q^{liq,s}_{fpso,t} \qquad \forall fpso,t,s \qquad (5.81)$$

$$g^{s}_{fpso,t} \le Q^{gas,s}_{fpso,t} \qquad \forall fpso,t,s \qquad (5.82)$$

$$Q^{oil,s}_{fpso,t} = Q^{oil,s}_{fpso,t-1} + QI^{oil,s}_{fpso,t-l_1} + QE^{oil,s}_{fpso,t-l_2} \qquad \forall fpso,t,s \qquad (5.83)$$

$$Q^{liq,s}_{fpso,t} = Q^{liq,s}_{fpso,t-1} + QI^{liq,s}_{fpso,t-l_1} + QE^{liq,s}_{fpso,t-l_2} \qquad \forall fpso,t,s \qquad (5.84)$$

$$Q^{gas,s}_{fpso,t} = Q^{gas,s}_{fpso,t-1} + QI^{gas,s}_{fpso,t-l_1} + QE^{gas,s}_{fpso,t-l_2} \qquad \forall fpso,t,s \qquad (5.85)$$

**(viii) Logic Constraints:** Inequalities (5.86) and (5.87) restrict the installation and expansion of a FPSO facility to take place only once, respectively, while inequality (5.88) states that the connection between a FPSO facility and a field can be installed only once during the whole planning horizon. Inequality (5.89) ensures that a field can be connected to at most one FPSO facility in each time period t, while (5.90) states that at most one FPSO-field connection is possible for a field *f* during the entire planning horizon under each scenario s. Constraints (5.91) and (5.92) state that the expansion in the capacity of a FPSO facility and the connection between a field and a FPSO facility, respectively, in time period t can occur only if that FPSO facility has already been installed by that time period.

$$\sum_{t \in T} b^{s}_{fpso,t} \le 1 \qquad \forall fpso,s \qquad (5.86)$$

$$\sum_{t \in T} b^{ex,s}_{fpso,t} \le 1 \qquad \forall fpso,s \qquad (5.87)$$

$$\sum_{t \in T} b^{c,s}_{f,fpso,t} \le 1 \qquad \forall f, fpso,s \qquad (5.88)$$

$$\sum_{fpso} b^{c,s}_{f,fpso,t} \le 1 \qquad \forall f,t,s \qquad (5.89)$$

$$\sum_{t \in T} \sum_{fpso} b^{c,s}_{f,fpso,t} \le 1 \qquad \forall f,s \qquad (5.90)$$

$$b^{ex,s}_{fpso,t} \le \sum_{\tau=1}^{t} b^{s}_{fpso,\tau} \qquad \forall fpso,t,s \qquad (5.91)$$

$$b^{c,s}_{f,fpso,t} \le \sum_{\tau=1}^{t} b^{s}_{fpso,\tau} \qquad \forall f, fpso,t,s \qquad (5.92)$$

**(ix) Upper bounding constraints:** Inequality (5.93) states that the oil flow rate per well from a field *f* to a FPSO facility in time period t will be zero if that FPSO-field connection is not available in that time period in a scenario s. Constraints (5.94)-(5.99) are the upper-bounding constraints on the installation and expansion capacities for FPSO facilities in time period *t* for each scenario s. The additional upper bounds on the oil, liquid and gas expansion capacities of FPSO facilities, (5.100)-(5.102), come from the fact that these expansion capacities should be less than a certain fraction (μ) of the initial built capacities, respectively.

$$x^{well,s}_{f,fpso,t} \le U^{well,oil}_{f,fpso} \sum_{\tau=1}^{t} b^{c,s}_{f,fpso,\tau} \qquad \forall f, fpso,t,s \qquad (5.93)$$

$$QI^{oil,s}_{fpso,t} \le U^{oil}_{fpso} b^{s}_{fpso,t} \qquad \forall fpso,t,s \qquad (5.94)$$

$$QI^{liq,s}_{fpso,t} \le U^{liq}_{fpso} b^{s}_{fpso,t} \qquad \forall fpso,t,s \qquad (5.95)$$

$$QI^{gas,s}_{fpso,t} \le U^{gas}_{fpso} b^{s}_{fpso,t} \qquad \forall fpso,t,s \qquad (5.96)$$

$$QE^{oil,s}_{fpso,t} \le U^{oil}_{fpso} b^{ex,s}_{fpso,t} \qquad \forall fpso,t,s \qquad (5.97)$$

$$QE^{liq,s}_{fpso,t} \le U^{liq}_{fpso} b^{ex,s}_{fpso,t} \qquad \forall fpso,t,s \qquad (5.98)$$

$$QE^{gas,s}_{fpso,t} \le U^{gas}_{fpso} b^{ex,s}_{fpso,t} \qquad \forall fpso,t,s \qquad (5.99)$$

$$QE^{oil,s}_{fpso,t} \le \mu Q^{oil,s}_{fpso,t-1} \qquad \forall fpso,t,s \qquad (5.100)$$

$$QE^{liq,s}_{fpso,t} \le \mu Q^{liq,s}_{fpso,t-1} \qquad \forall fpso,t,s \qquad (5.101)$$

$$QE^{gas,s}_{fpso,t} \le \mu Q^{gas,s}_{fpso,t-1} \qquad \forall fpso,t,s \qquad (5.102)$$

**(x) Well drilling limitations:** The number of wells available for production from a field in scenario s is calculated from (5.103) as the sum of the wells available at the end of previous time period and the number of wells drilled at the beginning of time period t. The maximum number of wells that can be drilled over all the fields during each time period t and in each field $f$ during complete planning horizon are restricted by the respective upper bounds in (5.104) and (5.105).

$$N_{f,t}^{well,s} = N_{f,t-1}^{well,s} + I_{f,t}^{well,s} \qquad \forall f,t,s \qquad (5.103)$$

$$\sum_{f} I_{f,t}^{well,s} \le UI_t^{well} \qquad \forall t,s \qquad (5.104)$$

$$N_{f,t}^{well,s} \le UN_f^{well} \qquad \forall f,t,s \qquad (5.105)$$

**(xi) Initial Non-anticipativity Constraints:** In addition to the above constraints (5.1)-(5.105) that are equivalent to the constraints for the deterministic model with fiscal rules for each scenario s as in chapter 3, we need the initial non-anticipativity constraints, eqs. (5.106)-(5.115), for time periods $T_I \subset T$ where the set $T_I$ may include only first or few initial time periods. These constraints ensure that we make the same decisions (FPSO installations, expansions and their oil, liquid, gas capacities; well drilling schedule and field-FPSO connections) in scenarios s and s' until uncertainty in the any of the parameters cannot be revealed.

$$b_{fpso,t}^{FPSO,s} = b_{fpso,t}^{FPSO,s'} \qquad \forall fpso, s, s', t \in T_I \qquad (5.106)$$

$$b_{fpso,t}^{ex,s} = b_{fpso,t}^{ex,s'} \qquad \forall fpso, s, s', t \in T_I \qquad (5.107)$$

$$b_{f,fpso,t}^{s} = b_{f,fpso,t}^{s'} \qquad \forall f,\ fpso, s, s', t \in T_I \qquad (5.108)$$

$$I_{f,t}^{well,s} = I_{f,t}^{well,s'} \qquad \forall f, s, s', t \in T_I \qquad (5.109)$$

$$QI_{fpso,t}^{oil,s} = QI_{fpso,t}^{oil,s'} \qquad \forall fpso, s, s', t \in T_I \qquad (5.110)$$

$$QI_{fpso,t}^{liq,s} = QI_{fpso,t}^{liq,s'} \qquad \forall fpso, s, s', t \in T_I \qquad (5.111)$$

$$QI_{fpso,t}^{gas,s} = QI_{fpso,t}^{gas,s'} \qquad \forall fpso, s, s', t \in T_I \qquad (5.112)$$

$$QE_{fpso,t}^{oil,s} = QE_{fpso,t}^{oil,s'} \qquad \forall fpso, s, s', t \in T_I \qquad (5.113)$$

$$QE_{fpso,t}^{liq,s} = QE_{fpso,t}^{liq,s'} \qquad \forall fpso, s, s', t \in T_I \qquad (5.114)$$

$$QE_{fpso,t}^{gas,s} = QE_{fpso,t}^{gas,s'} \qquad \forall fpso, s, s', t \in T_I \qquad (5.115)$$

**(xii) Conditional Non-anticipativity Constraints:** To determine the scenario pairs (s, s') that are indistinguishable at the beginning of time period t, we consider the uncertainty resolution rule as explained in section 5.2.3. In particular, we assume that the uncertainty in all the parameters of a field is revealed if we drill at-least $N_1$ number of wells in the field, and produce from that field for at-least $N_2$ number of years. Therefore, eq. (5.116) is used relate the number of wells in the field to the binary variable $w_{f,t}^{1,s}$ such that the variable $w_{f,t}^{1,s}$ is true if and only if the number of wells drilled in the field are less than $N_1$. Similarly, the production from the field *f* has been made for less than $N_2$ years, if and only if $w_{f,t}^{2,s}$ is true as represented in eqs. (5.117)-(5.118). The logic constraint (5.119) sets the value of the binary variable $w_{f,t}^{3,s}$ to be true if and only if either of $w_{f,t}^{1,s}$ or $w_{f,t}^{2,s}$ are true, i.e. uncertainty in the field *f* has not been revealed in scenario s at the beginning of time period t.

$$w_{f,t}^{1,s} \Leftrightarrow (N_{f,t-1}^{well,s} \le N_1 - 1) \qquad \forall f,t,s \tag{5.116}$$

$$w_{f,t}^{2,s} \Leftrightarrow (\sum_{\tau=1}^{t-1} b_{f,\tau}^{prod,s} \le N_2 - 1) \qquad \forall f,t,s \tag{5.117}$$

$$b_{f,t}^{prod,s} \Leftrightarrow (x_{f,t}^{s} \ge \varepsilon) \qquad \forall f,t,s \tag{5.118}$$

$$w_{f,t}^{3,s} \Leftrightarrow w_{f,t}^{1,s} \vee w_{f,t}^{2,s} \qquad \forall f,t,s \tag{5.119}$$

Based on the above value of the variable $w_{f,t}^{3,s}$ equation (5.120) determines the value of the boolean variable $Z_t^{s,s'}$. In particular, two scenarios (s, s') will be indistinguishable at the beginning of time period *t* if and only if for each field *f* that distinguishes those scenarios (i.e. $f \in D(s,s')$), $w_{f,t}^{3,s}$ is true. Therefore, eqs. (5.116)-(5.120) can be used to determine the indistinguishable scenarios at the beginning of time period t based on the decisions that have been implemented before that time period. Notice that as a special case, where either well drilling or production from the field is sufficient to observe the uncertainty, then one only needs to consider eq. (5.116) or eqs. (5.117)-(5.118), respectively, and eq. (5.120) without introducing the additional variable $w^{3,s}_{f,t}$.

$$Z^{s,s'}_t \Leftrightarrow \bigwedge_{f \in D(s,s')} w^{3,s}_{f,t} \qquad \forall s,s',t \tag{5.120}$$

The conditional non-anticipativity constraints in disjunction (5.121) equate the decisions in scenarios s and s' for the later time periods $T_C \subset T$, if these scenarios are indistinguishable at the beginning of time period t, i.e. for which $Z^{s,s'}_t$ is true calculated in eq. (5.120).

$$\begin{bmatrix} Z^{s,s'}_t & \\ b^{FPSO,s}_{fpso,t} = b^{FPSO,s'}_{fpso,t} & \forall fpso \\ b^{ex,s}_{fpso,t} = b^{ex,s'}_{fpso,t} & \forall fpso \\ b^{s}_{f,fpso,t} = b^{s'}_{f,fpso,t} & \forall f, fpso \\ I^{well,s}_{f,t} = I^{well,s'}_{f,t} & \forall f \\ QI^{oil,s}_{fpso,t} = QI^{oil,s'}_{fpso,t} & \forall fpso \\ QI^{liq,s}_{fpso,t} = QI^{liq,s'}_{fpso,t} & \forall fpso \\ QI^{gas,s}_{fpso,t} = QI^{gas,s'}_{fpso,t} & \forall fpso \\ QE^{oil,s}_{fpso,t} = QE^{oil,s'}_{fpso,t} & \forall fpso \\ QE^{liq,s}_{fpso,t} = QE^{liq,s'}_{fpso,t} & \forall fpso \\ QE^{gas,s}_{fpso,t} = QE^{gas,s'}_{fpso,t} & \forall fpso \end{bmatrix} \vee \left[ \neg Z^{s.s'}_t \right] \qquad \forall s,s',t \in T_C \tag{5.121}$$

The multistage stochastic mixed-integer nonlinear disjunctive programming model **(MSSP-ND)** for offshore oilfield investment and operations planning involves constraints (5.1)-(5.13), (5.15)-(5.27), (5.29)-(5.40), (5.42)-(5.49), (5.52)-(5.121) that consider endogenous uncertainty in the field parameters and sliding scale production sharing agreements with ringfencing provisions. In particular, constraints (5.56b)- (5.58) and (5.70) are nonlinear and non-convex constraints in the model. These constraints can be linearized using exact linearization and piecewise linear approximation techniques described in chapter 2 to convert the nonlinear model **(MSSP-ND)** to a linear one **(MSSP-LD).** Notice that the resulting model will be an extension of the deterministic MILP fiscal model (Model 3F) in chapter 3 to the stochastic case using the modeling framework presented in chapter 4.

## 5.4 Compact representation of the multistage stochastic model

The proposed multistage stochastic mixed-integer linear disjunctive programming model **(MSSP-LD)** in the previous section can be represented in the following compact form:

**(MD)**

$$\max \quad z = \sum_{s \in S} p^s \sum_{t \in T} c_t x_t^s \tag{5.122}$$

$$s.t. \quad \sum_{\tau \le t} A_\tau^s x_\tau^s \le a_t^s \qquad \forall t, s \tag{5.123}$$

$$x_t^s = x_t^{s'} \quad \forall t \in T_I, \forall s, s' \in S \tag{5.124}$$

$$Z_t^{s,s'} \Leftrightarrow F(x_1^s, x_2^s \ldots x_{t-1}^s) \quad \forall t \in T_C, \forall s, s' \in S \tag{5.125}$$

$$\begin{bmatrix} Z_t^{s,s'} \\ \\ x_t^s = x_t^{s'} \end{bmatrix} \vee \begin{bmatrix} \neg Z_t^{s,s'} \\ \\ \end{bmatrix} \qquad \forall t \in T_C, \forall s, s' \in S \tag{5.126}$$

$$x_{jt}^s \in I \qquad \forall t, s, \forall j \in J' \tag{5.127}$$

$$x_{jt}^s \in R \qquad \forall t, s, \forall j \in J \setminus J' \tag{5.128}$$

The objective function (5.122) in the above model (MD) maximizes the expectation of an economic criterion over the set of scenarios $s \in S$, and over a set of time periods $t \in T$, which is equivalent to eq. (5.1). For a particular scenario s, inequality (5.123) represents constraints that govern decisions $x_t^s$ in time period $t$ and link decisions across time periods. These individual scenario constraints correspond to the eqs. (5.2)-(5.13), (5.15)-(5.27), (5.29)-(5.40), (5.42)-(5.49) and (5.52)-(5.105), where the nonlinear and non-convex constraints (5.56b)- (5.58) and (5.70) have been linearized using exact linearization and piecewise linear approximation techniques described in chapter 2.

Non-anticipativity (NA) constraints for initial time periods $T_I \subset T$ are given by equations (5.124) for each scenario pair (s,s') to ensure the same decisions in all the scenarios, which are the compact representation for constraints (5.106)-(5.115). The conditional NA constraints are written for the later time periods $T_C \subset T$ in terms of logic propositions (5.125) and disjunctions (5.126). Notice that the set of initial time periods $T_I$ may include first few years of the planning horizon until uncertainty cannot be revealed, while $T_C$ represents the rest of the time periods in the planning horizon. The function $F(x_1^s, x_2^s \ldots x_{t-1}^s)$ in eq. (5.125) is an uncertainty resolution rule for a given pair of scenarios s and s' that determines the value of the corresponding boolean variable $Z_t^{s,s'}$ based on the decisions that have been implemented so far as shown in eqs. (5.116)-(5.120). The variable $Z_t^{s,s'}$ is further used in disjunction (5.126) to ensure the same decisions in scenarios s and s' if these are still indistinguishable in time period t, which is similar to the disjunctions (5.121). Equations (5.127)-(5.128) define the domain of the discrete and continuous variables in the model.

Notice that the model with a reduced number of scenario pairs (s,s') that are sufficient to represent the non-anticipativity constraints can be obtained from model (MD) after applying the three properties presented in chapter 4. These properties are defined on the basis of symmetry, adjacency and transitivity relationship among the scenarios. The reduced model **(MDR)** can be formulated from (MD) as follows, where $P_3$ is the set of minimum number of scenario pairs that are required to represent non-anticipativity in each time period t,

(MDR) $$\max \quad z = \sum_{s \in S} p^s \sum_{t \in T} c_t x_t^s \tag{5.122}$$

$$s.t. \quad \sum_{\tau \le t} A_\tau^s x_\tau^s \le a_t^s \qquad \forall t, s \tag{5.123}$$

$$x_t^s = x_t^{s'} \quad \forall t \in T_I, \forall (s,s') \in P_3 \tag{5.129}$$

$$Z_t^{s,s'} \Leftrightarrow F(x_1^s, x_2^s \ldots x_{t-1}^s) \quad \forall t \in T_C, \forall (s,s') \in P_3 \tag{5.130}$$

$$\begin{bmatrix} Z_t^{s,s'} \\ x_t^s = x_t^{s'} \end{bmatrix} \vee \begin{bmatrix} \neg Z_t^{s,s'} \end{bmatrix} \quad \forall t \in T_C, \forall (s,s') \in P_3 \tag{5.131}$$

$$x_{jt}^s \in I \qquad \forall t, s, \forall j \in J' \tag{5.127}$$

$$x_{jt}^s \in R \qquad \forall t, s, \forall j \in J \setminus J' \tag{5.128}$$

The mixed-integer linear disjunctive model (MDR) can be further converted to a mixed-integer linear programming model **(MLR)**. First, the logic constraints (5.130) are re-written as the mixed-integer linear constraints eq. (5.132) based on the uncertainty resolution rule where $z_t^{s,s'}$ is a binary variable that takes a value of 1 if scenario pair (s,s') is indistinguishable in time period t, else it is zero. The disjunction (5.131) can then be converted to mixed-integer linear constraints (5.133) and (5.134) using the big-M formulation. The resulting mixed-integer linear model (MLR) includes constraints (5.122), (5.123), (5.129), (5.132), (5.133), (5.134), (5.127) and (5.128).

$$B_t^s x_t^s + C_t^s z_t^{s,s'} \le d_t^s \qquad \forall t \in T_C, \forall (s,s') \in P_3 \tag{5.132}$$

$$-M(1 - z_t^{s,s'}) \le x_t^s - x_t^{s'} \quad \forall t \in T_C, \forall (s,s') \in P_3 \tag{5.133}$$

$$M(1 - z_t^{s,s'}) \ge x_t^s - x_t^{s'} \quad \forall t \in T_C, \forall (s,s') \in P_3 \tag{5.134}$$

Figure 5.7 represents the block angular structure of model (MLR), where we can observe that the initial (eq. (5.129)) and conditional (eqs. (5.132), (5.133) and (5.134)) non-anticipativity constraints link the scenario subproblems. Therefore, these are the complicating constraints in the model. However, this structure allows decomposing the fullspace problem into smaller subproblems by relaxing the linking constraints as in chapter 4. It should be noted that the NACs (especially conditional NACs) represent a large fraction of the total constraints in the model. For clarity, we use this compact representation (MLR) in the next section to describe the solution approach instead of the detailed model **(MSSP-LD)** presented in the previous section.

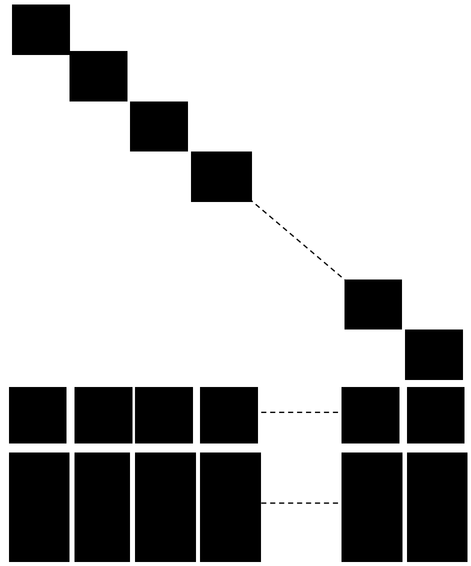


Figure 5.7: Structure of a typical Multistage Stochastic Program with Endogenous uncertainties

## 5.5 Solution Approach

The reduced model (MLR) is composed of scenario subproblems connected through the initial (eq. (5.129)) and conditional (eqs. (5.132), (5.133) and (5.134)) non-anticipativity (NA) constraints. If these NA constraints are either relaxed or dualized using Lagrangean decomposition, then the problem decomposes into smaller subproblems that can be solved independently for each scenario within an iterative scheme for the multipliers as described in Carøe and Schultz (1999) and in Gupta and Grossmann (2011a). In this way, we can effectively decompose and solve the large-scale oilfield development planning instances. The Lagrangean decomposition algorithm of Figure 5.8 for MSSP with endogenous uncertainties as proposed in chapter 4 involves obtaining the upper bound (UB) by solving the Lagrangean problem **(L1-MLR)** with fixed multipliers $\lambda_t^{s,s'}$. The Lagrangean problem (L1-MLR) is formulated from the mixed-integer linear reduced model (MLR) by relaxing all the conditional NA constraints (5.132), (5.133) and (5.134), and dualizing all the initial NA constraints (5.129) as penalty terms in the objective function. This gives rise to the subproblems for each scenario $s \in S$, **(L1-MLR$^s$)** that can be solved in parallel.

$$\textbf{(L1-MLR)} \qquad \max \sum_{s\in S} p^s \sum_{t\in T} c_t x_t^s + \sum_{t\in T_1} \sum_{(s,s')\in P_3} \lambda_t^{s,s'} (x_t^s - x_t^{s'}) \tag{5.135}$$

$$s.t. \quad \sum_{\tau \le t} A_\tau^s x_\tau^s \le a_t^s \qquad \forall t, s \tag{5.136}$$

$$x_{jt}^s \in \{0,1\} \qquad \forall t, s, \forall j \in J' \tag{5.137}$$

$$x_{jt}^s \in R \qquad \forall t, s, \forall j \in J \setminus J' \tag{5.138}$$

$$\textbf{(L1-MLR}^{s}\textbf{)} \qquad \max \sum_{t\in T} p^s c_t x_t^s + \sum_{t\in T_1} x_t^s \Big( \sum_{\substack{(s,s')\in P_3 \\ s<s'}} \lambda_t^{s,s'} - \sum_{\substack{(s',s)\in P_3 \\ s>s'}} \lambda_t^{s',s} \Big) \tag{5.139}$$

$$s.t. \quad \sum_{\tau \le t} A_\tau^s x_\tau^s \le a_t^s \qquad \forall t \tag{5.140}$$

$$x_{jt}^s \in \{0,1\} \qquad \forall t, \forall j \in J' \tag{5.141}$$

$$x_{jt}^s \in R \qquad \forall t, \forall j \in J \setminus J' \tag{5.142}$$

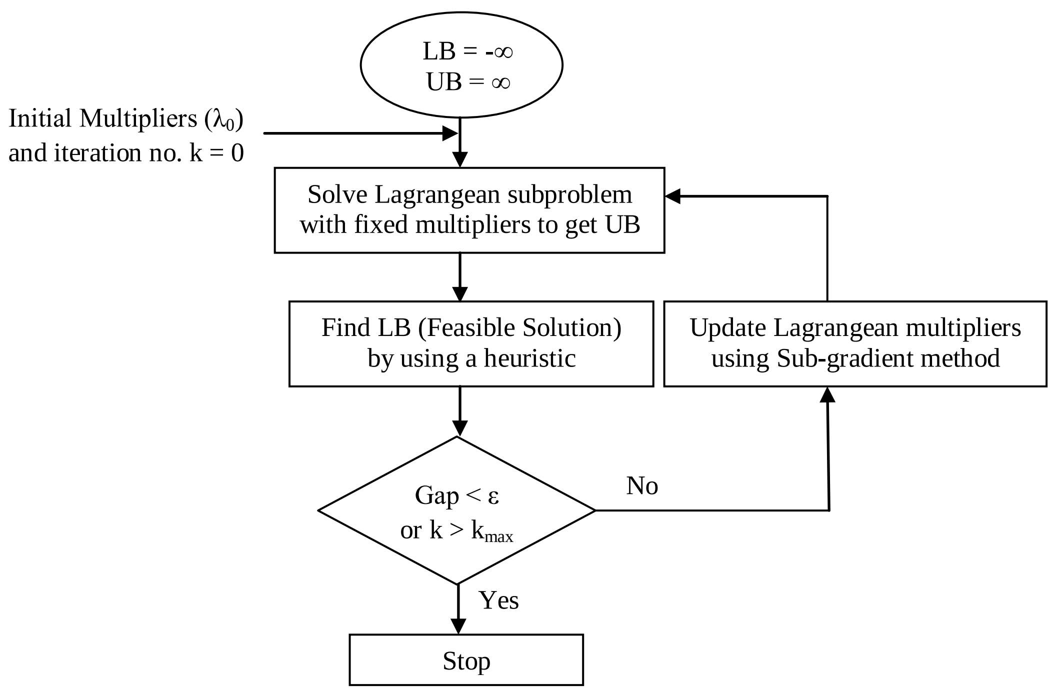


Figure 5.8: Lagrangean Decomposition algorithm

The lower bound (LB) or feasible solution is generated by using a heuristic based on the solution of the Lagrangean problem (L1-MLR). In this heuristic, we fix the decisions obtained from the above problem (L1-MLR) in the reduced problem (MLR) such that there is no violation of NA constraints and solve it to obtain the lower bound. The sub-gradient method by Fisher (1985) is used during each iteration to update the Lagrangean multipliers. The algorithm stops when either a maximum iteration/time limit is reached, or the difference between the lower and upper bounds, LB and UB, is less than a pre-specified tolerance.

Notice that the extended form of this method relying on duality based branch and bound search, has also been proposed in Goel and Grossmann (2006), Tarhan et al. (2009), and Tarhan et al. (2011) to close the gap between the upper and the lower bounds. Moreover, a new Lagrangean decomposition algorithm is proposed in the next chapter 6 to further improve the quality of the dual bound at the root node.

## 5.6 Numerical results

In this section, we present computational results for the offshore oilfield development planning examples under endogenous uncertainty in the field parameters, which resolves as a function of investment and operating decisions as described before. Moreover, we consider a case where progressive production sharing agreements are also present. The multistage stochastic MILP model **(MLR)** presented in section 5.4 is considered that maximizes the expected NPV value over the given planning horizon. The model is implemented in GAMS 23.6.3 and run on an Intel Core i7, 4GB RAM machine using CPLEX 12.2 solver for all the instances.

### 5.6.1 3 Oilfield Planning Example

**Case (i): Uncertainty in the field size only (4 scenarios)**

In this instance, we consider 3 oilfields and 3 potential FPSO's that can be installed. There are a total of 9 possible connections among field-FPSO (Figure 5.9), and 30 wells can be drilled in the fields over the planning horizon of 10 years. Field 3 has a recoverable oil volume (field size) of 500 MMbbls. However, there is uncertainty in the size of fields 1 and 2, where each one has two possible realizations (low, high) with equal probability. Therefore, there are a total of 4 scenarios each with a probability of 0.25 (see Table 5.1). Notice that for simiplicity we only consider the cases with same probabilities for all the scenarios thoughout this chapter. In our future paper, if it would be possible, we will include more realistic probability values for the examples.

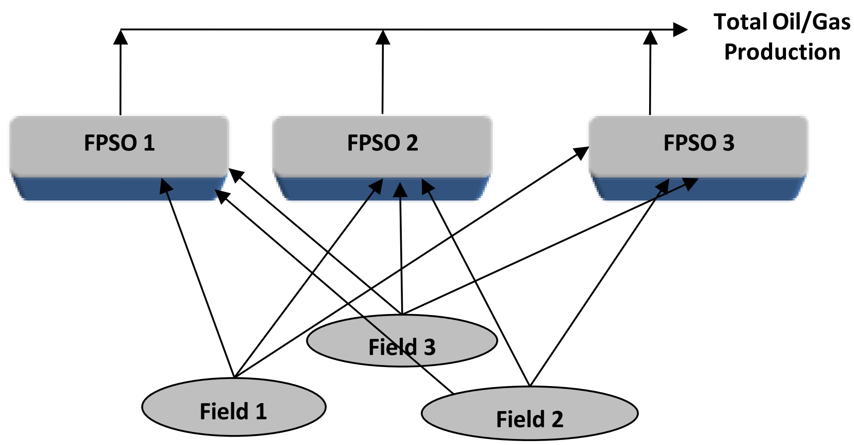


Figure 5.9: 3 oilfield planning example

Table 5.1: 3 oilfield planning example, case (i)

| Scenarios | s1 | s2 | s3 | s4 |
|---|---|---|---|---|
| Field 1 Size (MMbbls) | 57 | 403 | 57 | 403 |
| Field 2 Size (MMbbls) | 80 | 80 | 560 | 560 |
| Scenario Probability | 0.25 | 0.25 | 0.25 | 0.25 |

It is assumed that the uncertainty in field 1 size is revealed after drilling 3 wells ($N_1$= 3) in the field and producing for 1 year ($N_2$= 1) from it. Whereas, field 2 needs at-least 4 wells to be drilled ($N_1$= 4) and one year of production ($N_2$= 1) for this purpose. The problem is to determine the optimum investment (FPSO installations and expansions, field-FPSO connections and well drilling) and operating decisions (oil production rate) with an objective to maximize the total expected NPV (ENPV) over the planning horizon.

Table 5.2: Model statistics for the 3 oilfield example, case (i)

| Problem Type | Number of Constraints | Continuous Variables | Discrete Variables | SOS1 Variables |
|---|---|---|---|---|
| Reduced Model (MLR) | 16,473 | 9,717 | 876 | 240 |
| Individual Scenario | 3,580 | 2,390 | 179 | 60 |

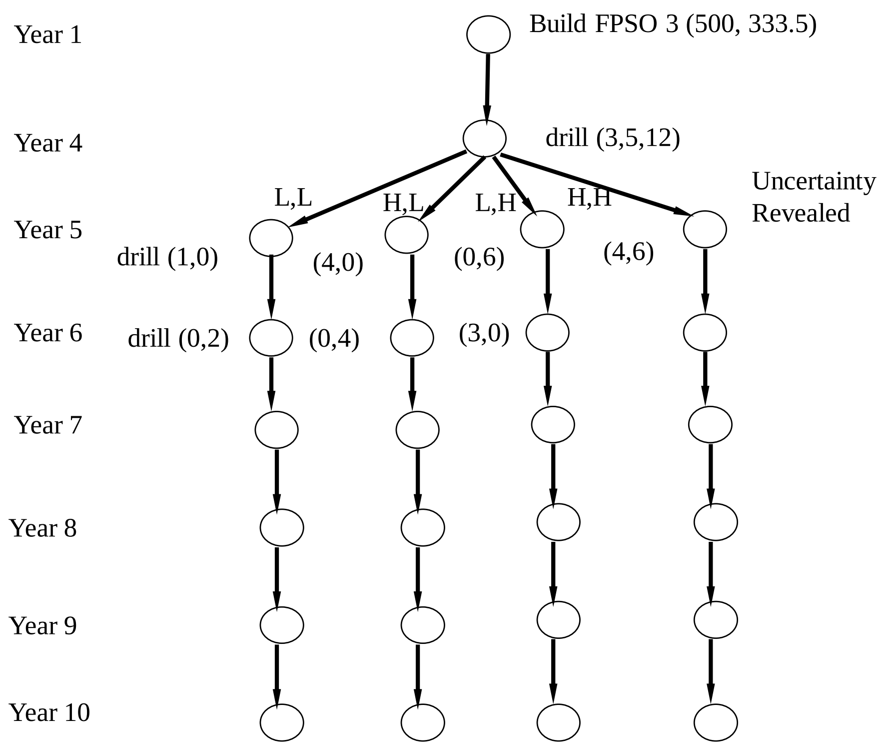


Figure 5.10: Optimal solution for 3 oilfield example, case (i)

The optimal ENPV for the problem is \$11.50 x$10^9$ when the reduced model (MLR) is solved in fullspace using CPLEX 12.2 solver requiring 1184s. Table 5.2 presents the model statistics for this instance. The solution suggests installing only FPSO 3 in the first year (see Figure 5.10) with a capacity of 500 kstb/d and 333.5 MMSCF/d for liquid and gas, respectively. The facility is available to produce at the beginning of year 4 due to a lead time of three years. Then, we drill 3, 5 and 12 wells in fields 1,2 and 3, respectively, given the drilling-rig limitation of a total 20 wells in a year. Since, fields 1 and 2 have uncertainties, based on the realization of the uncertainty in their field sizes, more wells are drilled in these fields in the future for the favorable scenarios compared to the unfavorable outcomes, whereas no more wells are drilled in field 3. In particular, the favorable scenarios for field 1 are scenarios 2 and 4, where a total of 7 wells are drilled in the field. On the other hand, field 2 has favorable scenarios 3 and 4, where a total of 11 wells are drilled in the field. Due to the different drilling and production decisions in different scenarios based on the uncertainty realizations, the capacity of FPSO3 is expanded in year 5 for scenarios 2, 3 and 4, whereas no expansion is made in the FPSO3 capacity in scenario 1. We can observe that the optimal scenario-tree is decision-dependent which is not known a-priori (Figure 5.10).

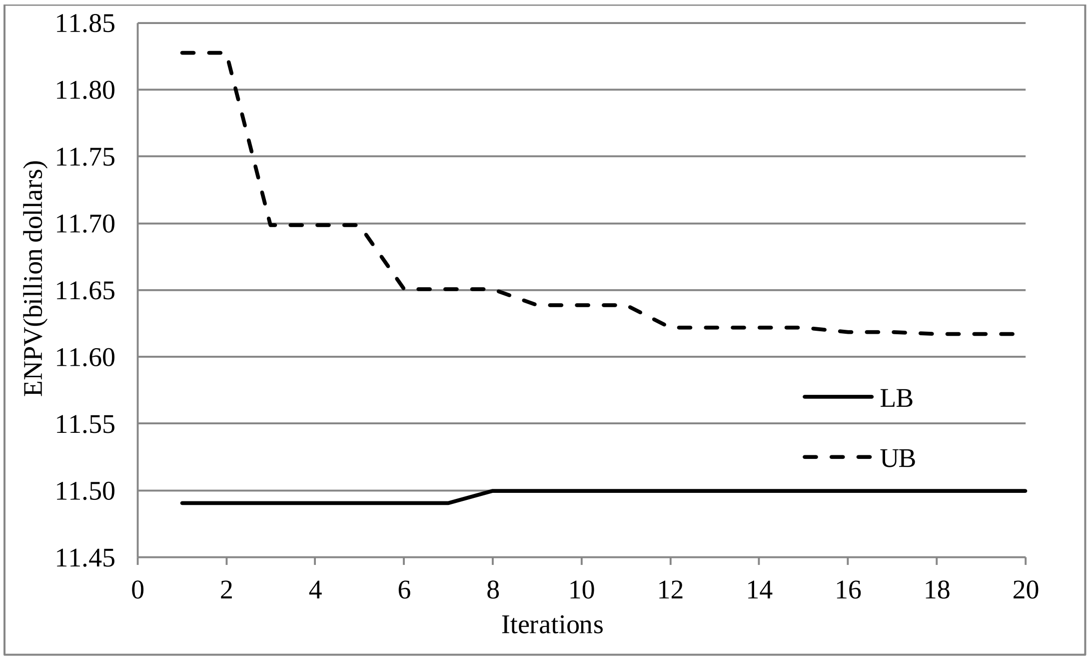


Figure 5.11: Lagrangean decomposition results for 3 oilfield example, case (i)

The multistage stochastic model (MLR) is also solved using the Lagrangean decomposition algorithm presented in the previous section that relies on dualizing the initial NACs and removing the conditional NACs. Figure 5.11 demonstrates the progress of the bounds obtained at the root node using this decomposition approach. A termination criterion of either 1% gap or 20 sub-gradient iterations is used. We can observe that the problem can be solved in ~1% optimality tolerance in only 466s for the sequential implementation compared to the fullspace model that takes 1184s. Moreover, the parallel implementation of the Lagrangean decomposition algorithm in GAMS with 8 processors only takes 259s. Therefore, the proposed strategy reduces the solution time for this 4 scenario instance by more than 75% compared to the fullspace model. It is also important to note that the reformulation of the MINLP model (Model 2) to MILP approximation (Model 3) in chapter 2 allows us to use this decomposition strategy with valid upper and lower bounds on the objective function value, without solving the non-convex MINLP model to global optimality which is quite expensive. Notice that the solution of the expected value problem considering the mean value of the field sizes is \$11.28 $\times 10^9$. Therefore, the value of the stochastic solution for this case is \$220 $\times 10^6$ or ~2%.

**Case (ii): Uncertainty in the field size, oil deliverability, WOR and GOR (4 scenarios)**

In this case, we consider uncertainty in the field size, oil deliverability, water-oil ratio (WOR) and gas-oil-ratio (GOR) for oilfields 1 and 2. Notice that oil deliverability, WOR and GOR are represented by the univariate polynomials in terms of the fractional oil recovery as shown in equations (5.143)-(5.145), respectively.

$$Q^d = \alpha_o \cdot g(fc) \tag{5.143}$$

$$wor = \alpha_w \cdot g(fc) \tag{5.144}$$

$$gor = \alpha_g \cdot g(fc) \tag{5.145}$$

The uncertainty in oil deliverability, WOR and GOR is characterized by the uncertainty in corresponding parameters $\alpha_o$, $\alpha_w$ and $\alpha_g$. We assume that the uncertain parameters for a field are correlated, and that uncertainty in these parameters is resolved at the same time as explained earlier. This allows us to reduce a large number of scenarios in the problem. The two possible combinations of these parameters for each field results in a total of 4 scenarios each with a probability of 0.25 as can be seen in Table 5.3. The data for the rest of the problem are as in case (i) presented above.

Table 5.4 summarizes the computational results for this case, and we can observe the similar trends as in the previous case. In particular, the fullspace multistage stochastic model using CPLEX 12.2 takes >10,000s to solve the problem to optimality and it yields an expected NPV value of \$11.95 $\times 10^9$. The sequential and parallel implementations (8 processors) of the proposed

Lagrangean decomposition approach provide a solution of $\$11.94 \times 10^9$ with more than an order of magnitude reduction in solution times. To further reduce the gap between the upper and the lower bounds, the algorithm can be extended to the duality based branch and bound search procedure as proposed in Goel and Grossmann (2006). In addition, an improved Lagrangean decomposition approach that yields a tighter dual bound at the root node is also presented in the next chapter.

Table 5.3: 3 oilfield planning example, case (ii)

| Scenarios | | s1 | s2 | s3 | s4 |
|---|---|---|---|---|---|
| Field 1 | Size (MMbbls) | 57 | 403 | 57 | 403 |
| | $\alpha_o$ | 0.75 | 1.25 | 0.75 | 1.25 |
| | $\alpha_w$ | 0.75 | 1.25 | 0.75 | 1.25 |
| | $\alpha_g$ | 0.75 | 1.25 | 0.75 | 1.25 |
| Field 2 | Size (MMbbls) | 80 | 80 | 560 | 560 |
| | $\alpha_o$ | 0.75 | 0.75 | 1.25 | 1.25 |
| | $\alpha_w$ | 0.75 | 0.75 | 1.25 | 1.25 |
| | $\alpha_g$ | 0.75 | 0.75 | 1.25 | 1.25 |
| Scenario Probability | | 0.25 | 0.25 | 0.25 | 0.25 |

Table 5.4: Computational results for 3 oilfield example, case (ii)

| | Fullspace | Lagrangean Decomposition | |
|---|---|---|---|
| | | Sequential | Parallel |
| UB ($\$10^9$) | 11.95 | 12.14 | 12.14 |
| LB ($\$10^9$) | 11.95 | 11.94 | 11.94 |
| Solution Time (s) | 10390 | 438 | 257 |
| % Gap | 0% | 1.66% | 1.66% |
| Subgradient iterations | - | 20 | 20 |

**Case (iii): Uncertainty in the field size and progressive production sharing agreements**

We also extend the 3 oilfield example to the case where we include the progressive production sharing agreements and a planning horizon of 15 years.

Table 5.5 represents the sliding scale profit share of the contactor involving 3 tiers that are defined on the basis of the cumulative oil production. The cost recovery ceiling of 50% of the gross revenue every year and an income tax rate of 30% is also considered. There is uncertainty in the field sizes (field 1 and 2) with a total of 4 scenarios as described in Table 5.1.

Table 5.5: Sliding scale contractor's profit oil share for the 3 oilfield example, case (iii)

| **Tiers** | **Cumulative Oil Produced** | **Contractor's Share in Profit Oil** |
|---|---|---|
| Tier 1 | 0-350 MMbbl | 50% |
| Tier 2 | 350-700 MMbbl | 40% |
| Tier 3 | >700 MMbbl | 20% |

Table 5.6: Computational results for 3 oilfield example, case (iii)

| Fullspace Model | | | | | Lagrangean Decomposition | | |
|---|---|---|---|---|---|---|---|
| # Constraints | # Dis. Var. | # Cont. Var. | ENPV ($\$10^9$) | Time (s) | ENPV ($\$10^9$) | Sequential Time (s) | Parallel Time (s) |
| 27,113 | 1,536 | 15,857 | $2.97 (>21%) | >36,000 | $3.04 (0.7%) | 8,990 | 4,002 |

The multistage stochastic model becomes very difficult to solve for this instance in fullspace due to the complexities introduced in the model by the non-anticipativity constraints, and the disjunction for representing the sliding scale fiscal rules. In particular, the best solution obtained after 10 hours in fullspace using CPLEX 12.2 solver is $\$2.97 \times 10^9$ with more than 21% of optimality gap (see Table 5.6). On the other hand, the proposed Lagrangean decomposition can solve this problem in approximately 2 hrs for the sequential implementation of the scenario subproblem solutions, and in about 1 hr for the parallel implementation (8 processors). Both the cases yield a higher ENPV $\$3.04 \times 10^9$ within a 0.7% of optimality tolerance. Therefore, this example illustrates the importance of the decomposition algorithm, and its parallel implementation, as more complexities are added to the problem, such as the progressive fiscal rules.

### 5.6.2 5 Oilfield Planning Example

**Case (i): Uncertainty in the field size only (8 scenarios)**

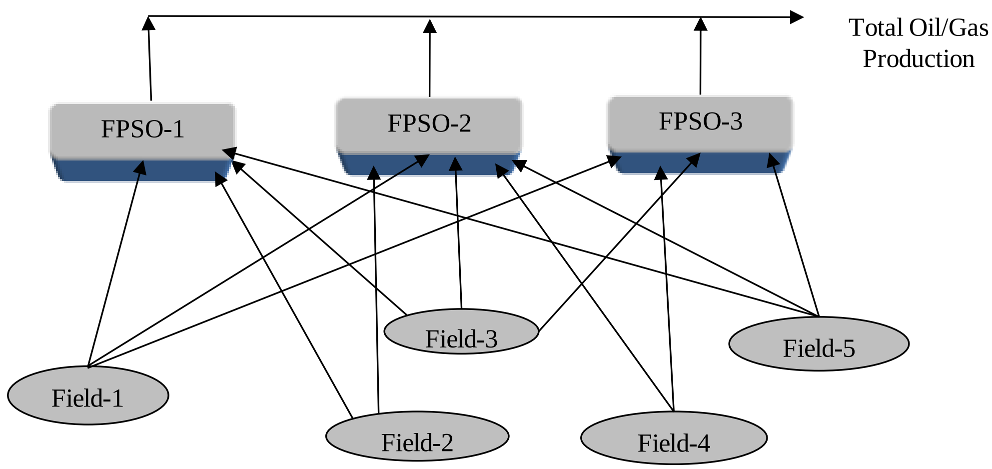


Figure 5.12: 5 oilfield planning example

This is a larger example for oilfield planning problem under uncertainty than the previous one, where we consider 5 oilfields that can be connected to 3 FPSOs with 13 possible connections (Figure 5.12). A total of 51 wells can be drilled in the fields over the planning horizon of 20 years. There is uncertainty in the size of fields 1, 3 and 5, where each one has two possible realizations (low, high) with equal probability. Therefore, there are a total of 8 scenarios each with a probability of 0.125 (see Table 5.7). Fields 2 and 4 have known recoverable oil volumes of 200 and 400 MMbbls, respectively.

It is assumed that the uncertainty in field 1 size is revealed after drilling 3 wells ($N_1$= 3) in the field and producing for 1 year ($N_2$= 1) from it. Fields 3 and 5 need at-least 4 wells to be drilled ($N_1$= 4) and one year of production ($N_2$= 1) for this purpose. The problem is to determine the optimum investment (FPSO installations and expansions, field-FPSO connections and well drilling) and operating decisions (oil production rate) with an objective to maximize the total expected NPV (ENPV) over the planning horizon.

Table 5.7: 5 oilfield planning example, case (i)

| Scenarios | s1 | s2 | s3 | s4 | s5 | s6 | s7 | s8 |
|---|---|---|---|---|---|---|---|---|
| Field 1 Size (MMbbls) | 57 | 403 | 57 | 403 | 57 | 403 | 57 | 403 |
| Field 3 Size (MMbbls) | 80 | 80 | 560 | 560 | 80 | 80 | 560 | 560 |
| Field 5 Size (MMbbls) | 125 | 125 | 125 | 125 | 875 | 875 | 875 | 875 |
| Scenario Probability | 0.125 | 0.125 | 0.125 | 0.125 | 0.125 | 0.125 | 0.125 | 0.125 |

Table 5.8: Model statistics for the 5 oilfield example, case (i)

| Problem Type | Number of Constraints | Continuous Variables | Discrete Variables | SOS1 Variables |
|---|---|---|---|---|
| Reduced Model (MLR) | 94,837 | 54,537 | 5,144 | 1600 |
| Individual Scenario | 9,986 | 6,688 | 513 | 200 |

Table 5.8 compares the size of the fullspace multistage stochastic MILP model with the individual scenario where a significant number of constraints and variables can be observed in the former. Therefore, the fullspace model becomes very difficult to solve directly using CPLEX 12.2 which takes more than 10 hours to reach 32% of the optimality tolerance with an expected NPV value of $\$20.27 \times 10^9$. The solution of the sequential implementation of the proposed Lagrangean decomposition approach also becomes expensive, but provides a solution with 3.1% higher ENPV than the fullspace model ($\$20.91 \times 10^9$ vs. $\$20.27 \times 10^9$) in 31,350s with 2.1% of the optimality gap. The parallel implementation is the most efficient, and takes only 9,340s to yield the same objective function value as the sequential approach. Table 5.9 summarizes the computational results for this case, and we can observe that the impact of decomposition becomes more prominent for the larger instances. To further reduce the gap between the upper and the lower bounds, the algorithm can be

extended to the duality based branch and bound search procedure as proposed in Goel and Grossmann (2006).

Table 5.9: Computational results for 5 oilfield example, case (i)

| | Fullspace | Lagrangean Decomposition | |
|---|---|---|---|
| | | Sequential | Parallel |
| UB ($\$10^9$) | 26.78 | 21.37 | 21.37 |
| LB ($\$10^9$) | 20.27 | 20.91 | 20.91 |
| Solution Time (s) | >36,000 | 31,350 | 9,340 |
| % Gap | >32% | 2.1% | 2.1% |
| Subgradient iterations | - | 20 | 20 |

**Case (ii): Uncertainty in the field size, oil deliverability, WOR and GOR (8 scenarios)**

In this case, we consider uncertainty in the field size, oil deliverability, water-oil ratio (WOR) and gas-oil-ratio (GOR) for oilfields 1, 3 and 5 in Figure 5.12. The uncertainty in oil deliverability, water-oil ratio (WOR) and gas-oil-ratio (GOR) is characterized by the corresponding parameters, $\alpha_o$, $\alpha_w$ and $\alpha_g$ in equations (5.143)-(5.145), respectively. Two possible combinations of these parameters for each uncertain field results in a total of 8 scenarios, each with a probability of 0.125 as can be seen in Table 5.10. The data for the rest of the problem are similar to the case (i) presented above for 5 oilfield example.

Table 5.11 represents the computational results for this case. The fullspace multistage stochastic model can only provide a solution with ENPV of $\$21.26 \times 10^9$ in 10hrs when solved using CPLEX 12.2. The sequential as well as parallel implementation of the proposed Lagrangean decomposition approach provide a higher ENPV $\$21.78 \times 10^9$ and a significantly tighter upper bound than the fullspace model (2.5% gap vs. >28% gap) in less time. Overall, the results in this case also emphasize the efficiency of the proposed Lagrangean decomposition compared to the fullspace model solved with a state-of-art commercial solver.

Table 5.10: 5 oilfield planning example, case (ii)

| Scenarios | | s1 | s2 | s3 | s4 | s5 | s6 | s7 | s8 |
|---|---|---|---|---|---|---|---|---|---|
| Field 1 | Size (MMbbls) | 57 | 403 | 57 | 403 | 57 | 403 | 57 | 403 |
| | $\alpha_o$ | 0.75 | 1.25 | 0.75 | 1.25 | 0.75 | 1.25 | 0.75 | 1.25 |
| | $\alpha_w$ | 0.75 | 1.25 | 0.75 | 1.25 | 0.75 | 1.25 | 0.75 | 1.25 |
| | $\alpha_g$ | 0.75 | 1.25 | 0.75 | 1.25 | 0.75 | 1.25 | 0.75 | 1.25 |
| Field 3 | Size (MMbbls) | 80 | 80 | 560 | 560 | 80 | 80 | 560 | 560 |
| | $\alpha_o$ | 0.75 | 0.75 | 1.25 | 1.25 | 0.75 | 0.75 | 1.25 | 1.25 |
| | $\alpha_w$ | 0.75 | 0.75 | 1.25 | 1.25 | 0.75 | 0.75 | 1.25 | 1.25 |
| | $\alpha_g$ | 0.75 | 0.75 | 1.25 | 1.25 | 0.75 | 0.75 | 1.25 | 1.25 |
| Field 5 | Size (MMbbls) | 125 | 125 | 125 | 125 | 875 | 875 | 875 | 875 |
| | $\alpha_o$ | 0.75 | 0.75 | 0.75 | 0.75 | 1.25 | 1.25 | 1.25 | 1.25 |
| | $\alpha_w$ | 0.75 | 0.75 | 0.75 | 0.75 | 1.25 | 1.25 | 1.25 | 1.25 |
| | $\alpha_g$ | 0.75 | 0.75 | 0.75 | 0.75 | 1.25 | 1.25 | 1.25 | 1.25 |
| Scenario Probability | | 0.125 | 0.125 | 0.125 | 0.125 | 0.125 | 0.125 | 0.125 | 0.125 |

Table 5.11: Computational results for 5 oilfield example, case (ii)

| | Fullspace | Lagrangean Decomposition | |
|---|---|---|---|
| | | Sequential | Parallel |
| UB ($\$10^9$) | 27.31 | 22.34 | 22.34 |
| LB ($\$10^9$) | 21.26 | 21.78 | 21.78 |
| Solution Time (s) | >36,000 | 36,000 | 14,872 |
| % Gap | >28% | 2.5% | 2.5% |
| Subgradient iterations | - | 20 | 20 |

## 5.7 Conclusions

A general multistage stochastic programming model has been presented for offshore oil and gas field infrastructure planning considering endogenous uncertainties in the field parameters and progressive production sharing agreements. Discrete probability distribution functions of the uncertain parameters, i.e. field size, oil deliverability, water-oil-ratio and gas-oil ratio, are considered to represent the scenarios where uncertainty in these parameters can only be revealed once an investment is made in the field. The resulting decision-dependent scenario tree is modeled using initial and conditional non-anticipativity constraints considering the basic oilfield models developed in chapters 2 and 3. The model yields optimum investment and operating decisions while maximizing the expected NPV. Correlations among the endogenous uncertain parameters of a field are considered, which reduce the dimensionality of the model for large instances. The Lagrangean decomposition algorithm proposed in chapter 4 is adapted to the corresponding multistage stochastic model for oilfield development with parallel solution of the scenario subproblems. Numerical results on the two oilfield development planning examples show that the proposed Lagrangean decomposition algorithm, either sequential or parallel implementation, is efficient as compared to the fullspace method, and allows the solution of intractable instances of the problem. The model and solution approach can be further used as a basis to incorporate additional complexities such as exogenous uncertainties in oil/gas prices.

# Chapter 6

# A new decomposition algorithm for multistage stochastic programs with endogenous uncertainties

## 6.1 Introduction

In this chapter, we focus on type 2 of endogenous uncertainty for the multiperiod planning problems where decisions are used to gain more information, and resolve uncertainty either immediately or in a gradual manner. Therefore, the resulting scenario tree is decision-dependent that requires modeling a superstructure of all possible scenario trees that can occur based on the timing of the decisions as observed in chapters 4 and 5. In this context, we focus here on a general multistage stochastic programming framework to model the problems in this class in which special disjunctive constraints with propositional logic are considered to enforce the conditional non-anticipativity constraints that define the decision-dependent scenario tree.

In general, these multistage stochastic programs (MSSP) become very difficult to solve directly as deterministic equivalent since the problem size (constraints and variables) increases with the number of scenarios, whereas the solution time increases exponentially. Therefore, special solution techniques are used to solve problems in this class. Several fullspace based approaches for the medium-size problems exploiting the properties of the model and the optimal solution have been proposed. In particular, Colvin and Maravelias (2010) developed a branch-and-cut framework, while in chapter 4 we proposed a NAC relaxation strategy to solve these MSSP problems under the assumption that only few non-anticipativity constraints be active at the optimal solution.

Lagrangean decomposition is a widely used technique to solve large-scale problems that have decomposable structure as in stochastic programs (Fisher, 1985; Ruszczynski, 1997; Carøe and Schultz, 1999; Guignard, 2003; Conejo et al. 2006). It addresses problems where a set of constraints links several smaller subproblems. If these constraints are removed by dualizing them, the resulting subproblems can be solved independently. In the case of multistage stochastic programs with endogenous uncertainty initial and conditional non-anticipativity constraints are the linking constraints, while each subproblem corresponds to the problem for a given scenario. Therefore, the model has the decomposable structure that is amenable to Lagrangean decomposition approaches. In this context, a Lagrangean decomposition algorithm based on dualizing all the initial NACs and relaxing all the conditional NACs that allow parallel solution of the scenario subproblems has been proposed in chapter 4. An extended form of this decomposition approach relying on the duality based branch and bound search is also presented in Goel and Grossmann (2006), Tarhan et al. (2009), and Tarhan et al. (2011) to close the gap between the upper and lower bounds. Solak (2007) used a sample average approximation method for solving the problems in this class, where the sample problems were solved through Lagrangean relaxation and heuristics. However, there are several limitations with these methods including a weak dual bound at the root node, a large number of iterations to converge at each node, and many nodes that may be required during the branch and bound search to close the gap depending on the branching rules and variables. Moreover, the number of subproblems to be solved during each iteration at every node grows linearly with the number of scenarios. In this chapter, we propose a new decomposition scheme for solving these multistage stochastic programs that overcomes some of the limitations of the standard approaches.

The outline of this chapter is as follows. First, in section 6.2 we introduce the problem statement with particular focus on the problems where timing of uncertainty realization depends on the optimization decisions. Then, a general multistage stochastic mixed-integer linear disjunctive programming model for endogenous uncertainty problems is presented in section 6.3. Several Lagrangean decomposition approaches that have been used and their limitations are identified next. To overcome these limitations, in section 6.5 we propose a new Lagrangean decomposition scheme that relies on the concept of scenario group partitions. In section 6.6, we present the computational results on process network and oilfield planning problems adapted from chapters 4 and 5, respectively, to compare the various decomposition approaches.

## 6.2 Problem Statement

We consider multiperiod planning problems that have endogenous uncertainty in some the parameters (type 2), i.e. where timing of uncertainty realization depends on optimization decisions. In particular, the time horizon is represented by the discrete set of time periods $T$ = {1, 2, . . . . }. The set of endogenous uncertain parameters $\Theta = \{\theta_1, \theta_2, ....\}$ is considered where each parameter has a discrete set of possible realizations. Therefore, a scenario $s$ represents the possible combination of the realizations of these uncertain parameters with a probability $p^s$. Note that when some of the parameters $\theta_p$ are correlated as they may belong to a particular uncertainty source, then the resulting scenario set will be smaller (see chapter 5). The timing of uncertainty resolution in each uncertain parameter depends on the decisions $x_t^s$ (both discrete and continuous) that have been implemented so far. Furthermore, the uncertainty resolution rule can be immediate (Goel and Grossmann, 2006) or gradual (Tarhan et al., 2009) depending on the problem at hand. Therefore, the resulting scenario tree is decision-dependent, and hence we need to use a superstructure of all possible scenario-trees that can occur based on the decisions. In particular, we use logic propositions and disjunctions as in chapter 4 (Goel and Grossmann, 2006; and Gupta and Grossmann, 2011a) to represent the scenario-tree for the problems in this class. The uncertainty realizations for each parameter $\theta_p$ are assumed to be time invariant. In the next section, we present a MSSP model corresponding to this description.

## 6.3 Model

A multistage stochastic mixed-integer linear disjunctive program with endogenous uncertainties can be represented in the following compact form:

**(MD)**

$$\min \quad z = \sum_{s \in S} p^s \sum_{t \in T} c_t x_t^s \tag{6.1}$$

$$s.t. \quad \sum_{\tau \le t} A_\tau^s x_\tau^s \le a_t^s \qquad \forall t, s \tag{6.2}$$

$$x_t^s = x_t^{s'} \quad \forall t \in T_I, \forall s, s' \in S \tag{6.3}$$

$$Z_t^{s,s'} \Leftrightarrow F(x_1^s, x_2^s \ldots x_{t-1}^s) \quad \forall t \in T_C, \forall s, s' \in S \tag{6.4}$$

$$\begin{bmatrix} Z_t^{s,s'} \\ \\ x_t^s = x_t^{s'} \end{bmatrix} \vee \begin{bmatrix} \neg Z_t^{s,s'} \end{bmatrix} \qquad \forall t \in T_C, \forall s, s' \in S \tag{6.5}$$

$$x_{jt}^s \in \{0,1\} \qquad \forall t, s, \forall j \in J' \tag{6.6}$$

$$x_{jt}^s \in R \qquad \forall t, s, \forall j \in J \setminus J' \tag{6.7}$$

The objective function (6.1) in the above model **(MD)** minimizes the expectation of an economic criterion over the set of scenarios $s \in S$ , and over a set of time periods $t \in T$ . For a particular scenario *s*, inequality (6.2) represents constraints that govern decisions $x_t^s$ in time period *t* and link decisions across time periods. Non-anticipativity (NA) constraints for initial time periods $T_I \subset T$ are given by equations (6.3) for each scenario pair *(s,s')* to ensure the same decisions in all the scenarios. The conditional NA constraints are written for the later time periods $T_C \subset T$ in terms of logic propositions (6.4) and disjunctions (6.5). Notice that the set of initial time periods $T_I$ may include the first few years of the planning horizon until uncertainty cannot be revealed, while $T_C$ represents the rest of the time periods in the planning horizon. The function $F(x_1^s, x_2^s \ldots x_{t-1}^s)$ in eq. (6.4) is an uncertainty resolution rule for a given pair of scenarios *s* and *s'* that determines the value of the corresponding boolean variable $Z_t^{s,s'}$ based on the decisions that have been implemented so far. The variable $Z_t^{s,s'}$ is further used in disjunction (6.5) to ensure the same decisions in scenarios *s* and *s'* if these are still indistinguishable in time period *t*. Eqs. (6.6)-(6.7) define the domain of the discrete and continuous variables in the model.

Notice that the model with reduced number of scenario pairs *(s,s')* that are sufficient to represent the non-anticipativity constraints can be obtained from model (MD) after applying the three properties presented in the chapter 4. These properties are defined on the basis of symmetry, adjacency and transitivity relationship among the scenarios. The reduced model **(MDR)** can be formulated as follows, where $P_3$ is the set of minimum number of scenario pairs that are required to represent non-anticipativity in each time period *t*,

**(MDR)**

$$\min \quad z = \sum_{s \in S} p^s \sum_{t \in T} c_t x_t^s \tag{6.1}$$

$$s.t. \quad \sum_{\tau \le t} A_\tau^s x_\tau^s \le a_t^s \qquad \forall t, s \tag{6.2}$$

$$x_t^s = x_t^{s'} \quad \forall t \in T_I, \forall (s,s') \in P_3 \tag{6.3a}$$

$$Z_t^{s,s'} \Leftrightarrow F(x_1^s, x_2^s \ldots x_{t-1}^s) \quad \forall t \in T_C, \forall (s,s') \in P_3 \tag{6.4a}$$

$$\begin{bmatrix} Z_t^{s,s'} \\ x_t^s = x_t^{s'} \end{bmatrix} \vee \begin{bmatrix} \neg Z_t^{s,s'} \end{bmatrix} \qquad \forall t \in T_C, \forall (s,s') \in P_3 \tag{6.5a}$$

$$x_{jt}^s \in \{0,1\} \qquad \forall t, s, \forall j \in J' \tag{6.6}$$

$$x_{jt}^s \in R \qquad \forall t, s, \forall j \in J \setminus J' \tag{6.7}$$

We then define the following sets,

$$L_p = \left\{ \begin{matrix} (s_1, s_2, \ldots, s_k) \middle| s_1, s_2, \ldots, s_k \in S, s_1 < s_2 < \ldots < s_k, \\ D(s,s') = \{p\} \ \forall (s,s') \in (s_1, s_2, \ldots, s_k) \end{matrix} \right\} \quad \forall \theta_p \in \Theta \tag{6.8}$$

$$D(s,s') = \left\{ p \middle| \theta_p \in \Theta, \hat{\theta}_p^s \ne \hat{\theta}_p^{s'} \right\} \tag{6.9}$$

$$P_3 = \{(s_1, s_2), (s_2, s_3), \ldots, (s_{k-1}, s_k) | (s_1, s_2, \ldots, s_k) \in L_p \ \forall \theta_p \in \Theta\} \tag{6.10}$$

Notice that the minimum scenario pair set $(s, s') \in P_3$ can be obtained by first defining a scenario group set $(s_1, s_2, \ldots, s_k) \in L_p$ for each uncertain parameter $\theta_p \in \Theta$ with $k$ realizations (eq. 6.8) such that the $k$ scenarios in each of these $(s_1, s_2, \ldots, s_k)$ set can only be realized at the same time irrespective of the other realizations during the given time horizon. The basic idea to identify such scenario sets $(s_1, s_2, \ldots, s_k)$ is that all the scenarios in each of these sets only differ in the realization of the uncertain parameter $\theta_p$ for which the corresponding set is defined. Therefore, for any scenario pair $(s, s') \in (s_1, s_2, \ldots, s_k)$, the value of $D(s, s') = \{p\}$ where $D(s, s')$ represents the index of the uncertain parameter $\theta_p \in \Theta$ in eq. (6.9) that distinguish the two scenarios *s* and *s'* having values $\hat{\theta}_p^s$ and $\hat{\theta}_p^{s'}$ , respectively. The required minimum scenario pair set $P_3$ (eq. 6.10) then corresponds to the consecutive elements in the scenario group sets $(s_1, s_2, \ldots, s_k) \in L_p$ for each uncertain parameter $\theta_p \in \Theta$. The cardinality of the set $P_3$ is $|\Theta|(|S| - |S|^{|\Theta|-1/|\Theta|})$ as shown in chapter 4. For instance, if there are 2 uncertain parameters, *i.e.* ($\theta_1, \theta_2$). Each of these uncertain parameters has three realizations (L, M, H) which give rise to a total of 9 scenarios. The original model (MD) requires a total of 72 scenario pairs to represent the non-anticipativity, while the reduced model (MDR) only requires 12 scenario pairs, i.e. $|P_3| = 12$ in each time period *t* (see Gupta and Grossmann (2011a) for details).

The mixed-integer linear disjunctive model (MDR) can further be converted to a mixed-integer linear programming model **(MLR)**. First, the logic constraints (6.4a) are re-written as the mixed-integer linear constraints eq. (6.4b) based on the uncertainty resolution rule, where $z_t^{s,s'}$ is a binary variable that takes a value of 1 if scenario pair *(s,s')* is indistinguishable in time period *t*, and zero otherwise. The disjunction (6.5a) can then be converted to mixed-integer linear constraints (6.5b) and (6.5c) using the big-M formulation. The resulting mixed-integer linear model

(MLR) includes constraints (6.1), (6.2), (6.3a), (6.4b), (6.5b), (6.5c), (6.6) and (6.7).

$$B_t^s x_t^s + C_t^s z_t^{s,s'} \le d_t^s \qquad \forall t \in T_C, \forall (s,s') \in P_3 \tag{6.4b}$$

$$-M(1-z_t^{s,s'}) \quad \le x_t^s - x_t^{s'} \quad \forall t \in T_C, \forall (s,s') \in P_3 \tag{6.5b}$$

$$M(1-z_t^{s,s'}) \quad \ge x_t^s - x_t^{s'} \quad \forall t \in T_C, \forall (s,s') \in P_3 \tag{6.5c}$$

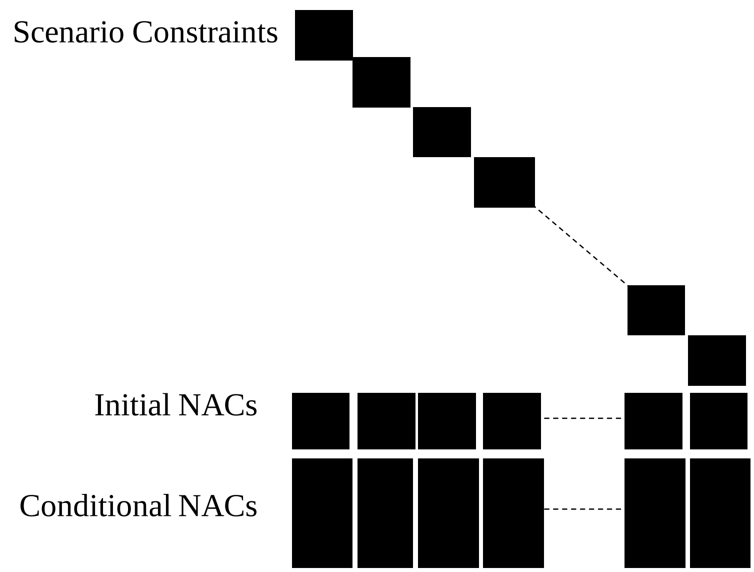


Figure 6.1: Structure of a typical Multistage Stochastic Program with Endogenous uncertainties

Figure 6.1 represents the block angular structure of model (MLR), where we can observe that the initial (eq. (6.3a)) and conditional (eqs. (6.4b), (6.5b) and (6.5c)) non-anticipativity constraints link the scenario subproblems (eq. (6.2)), i.e. these are the complicating constraints in the model. However, this structure allows decomposing the fullspace problem into smaller subproblems by relaxing the linking constraints. It should be noted that the NACs (especially conditional NACs) represent a large fraction of the total constraints in the model.

## 6.4 Conventional Lagrangean Decomposition Algorithms

The reduced model (MLR) is composed of scenario subproblems connected through initial (eq. (6.3a)) and conditional (eq. (6.4b), (6.5b) and (6.5c)) NA constraints. If these NA constraints are either relaxed or dualized using

Lagrangean decomposition, then the problem decomposes into smaller subproblems that can be solved independently for each scenario within an iterative scheme for the multipliers as described in Carøe and Schultz (1999) and in chapter 4. In this way, we can effectively decompose the large scale problems in this class. However, there are several decomposition schemes that can be used for this structure (Figure 6.1) as described below:

**6.4.1 Lagrangean Decomposition based on relaxing conditional NACs (Standard approach):** In the decomposition algorithm of Figure 6.2 for MSSP with endogenous uncertainties as proposed in chapter 4, the lower bound (LB) is obtained by solving the Lagrangean problem with fixed multipliers $\lambda_t^{s,s'}$,

**(L1-MLR)** $$\min \sum_{s\in S} p^s \sum_{t\in T} c_t x_t^s + \sum_{t\in T_1} \sum_{(s,s')\in P_3} \lambda_t^{s,s'}(x_t^s - x_t^{s'}) \qquad (6.1a)$$

$$s.t. \quad \sum_{\tau\le t} A_\tau^s x_\tau^s \le a_t^s \qquad \forall t,s \qquad (6.2)$$

$$x_{jt}^s \in \{0,1\} \qquad \forall t,s,\forall j\in J' \qquad (6.6)$$

$$x_{jt}^s \in R \qquad \forall t,s,\forall j\in J\setminus J' \qquad (6.7)$$

which gives rise to the subproblems for each scenario $s\in S$,

**(L1-MLR$^s$)** $$\min \sum_{t\in T} p^s c_t x_t^s + \sum_{t\in T_1} x_t^s \Big( \sum_{\substack{(s,s')\in P_3\\ s<s'}} \lambda_t^{s,s'} - \sum_{\substack{(s',s)\in P_3\\ s>s'}} \lambda_t^{s',s} \Big) \qquad (6.1b)$$

$$s.t. \quad \sum_{\tau\le t} A_\tau^s x_\tau^s \le a_t^s \qquad \forall t \qquad (6.2a)$$

$$x_{jt}^s \in \{0,1\} \qquad \forall t,\forall j\in J' \qquad (6.6a)$$

$$x_{jt}^s \in R \qquad \forall t,\forall j\in J\setminus J' \qquad (6.7a)$$

In particular, the Lagrangean problem **(L1-MLR)** is formulated from the mixed-integer linear reduced model (MLR) by relaxing all the conditional NA constraints (6.4b), (6.5b) and (6.5c) and dualizing all the initial NA constraints (6.3a) as penalty terms in the objective function. Figure 6.3 represents the structure of the resulting model (L1-MLR). Notice that the each sub-problem

**(L1-MLR$^s$)** in the Lagrangean problem (L1-MLR) corresponds to a scenario that can be solved in parallel.

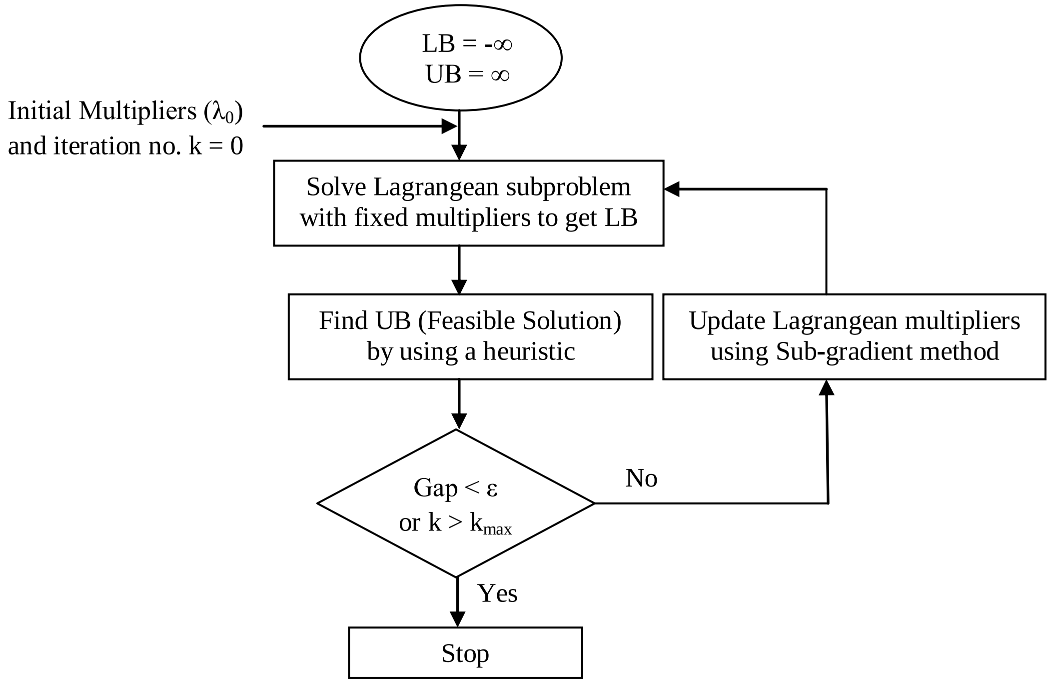


Figure 6.2: Lagrangean Decomposition algorithm

The upper bound (UB) is generated by using a heuristic based on the solution of the Lagrangean problem (L1-MLR). In this heuristic, we fix the decisions obtained from the above problem (L1-MLR) in the reduced problem (MLR) such that there is no violation of NA constraints and solve it to obtain the upper bound. The sub-gradient method by Fisher (1985) or an alternative update scheme (see Mouret et al., 2011; Oliveira et al., 2013; and Tarhan et al. 2013) is used during each iteration to update the Lagrangean multipliers. The algorithm stops when either a maximum iteration/time limit is reached, or the difference between the lower and upper bounds, LB and UB, is less than a pre-specified tolerance. Notice that the extended form of this method relying on duality based branch and bound search has also been proposed in Goel and Grossmann (2006); Tarhan et al. (2009), and Tarhan et al. (2011) to close the gap between the upper and the lower bounds.

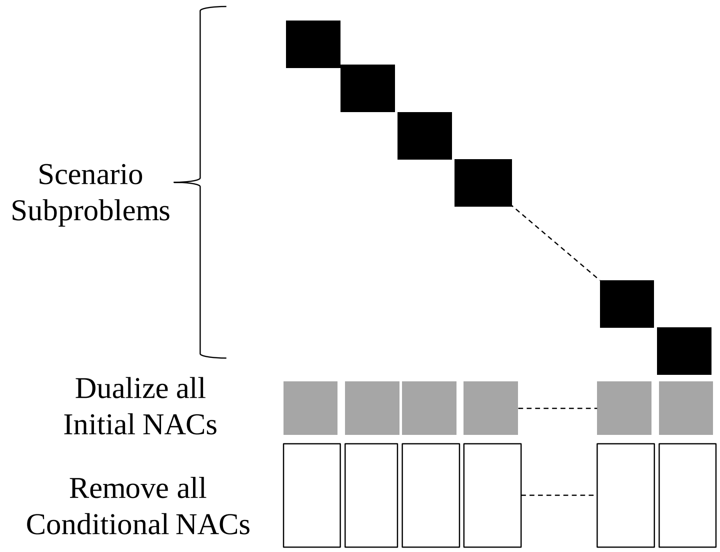

Figure 6.3: Lagrangean Decomposition based on relaxing conditional NACs

**Limitations:** We can observe from Figure 6.3 that the major limitation of this Lagrangean Decomposition algorithm for endogenous uncertainty problems (Gupta and Grossmann, 2011a; Goel and Grossmann, 2006; Tarhan et al., 2009; and Tarhan et al., 2011) is that all the conditional non-anticipativity constraints (6.4b), (6.5b) and (6.5c) are removed while formulating the scenario subproblems at the root node. These constraints represent a large fraction of the total constraints in the model and can have significant impact on the decisions. For instance, in Figure 6.4, the scenario tree for the later time periods $T_C$ (conditional NACs) can be constructed in several ways even though the initial NACs (for time periods $T_I$ ) are satisfied.

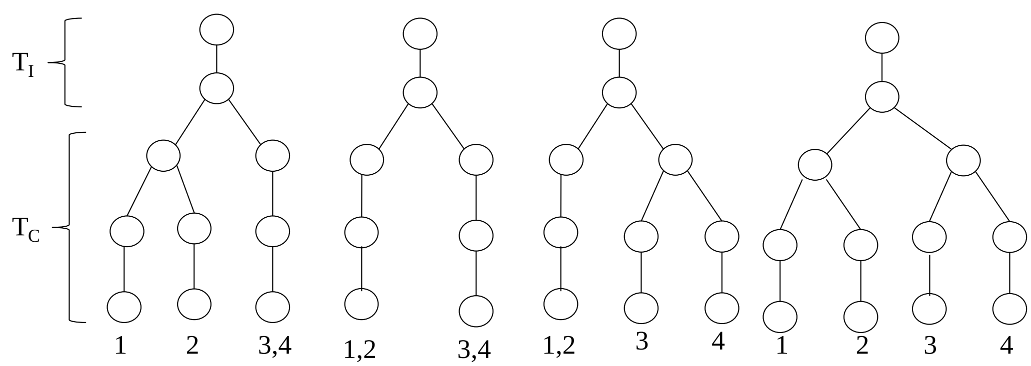

Figure 6.4: Impact of conditional NACs on the scenario tree structure

Therefore, there can be several undesired consequences that can occur with this relaxation approach:

1. The dual bound at root node can be significantly weaker since a large amount of information from the conditional NACs is ignored. In particular, only the initial NAC are considered (dualized) while formulating the subproblems at the root node, which represent only a first few time periods in the model. This means that the dynamics of the problem corresponding to the later periods is completely relaxed.
2. It is theoretically impossible to obtain a dual bound that is stronger than the optimal solution of the model without all conditional NACs at the root node.
3. The total number of nodes in the branch and bound search tree and the number of iterations required at each node can be very large.
4. Since many constraints are relaxed form the model, a good heuristic is needed to generate a feasible solution based on the solution of the dual problem.
5. The number of subproblems grows with the number of uncertain parameters and their realizations in an exponential manner.
6. It is problem specific and non-intuitive to define the branching rules/variables in the tree search since there are several alternatives.

### 6.4.2 Lagrangean Decomposition based on dualizing all the NACs:

**(i)** In this decomposition approach, we dualize all the NACs (both initial (6.3a) and conditional (6.5b) and (6.5c)) in the objective function directly while formulating the lower bounding Lagrangean problem **(L2-MLR)**, which is still decomposable into individual scenarios. Notice that since (6.5b) and (6.5c) are inequality constraints, the corresponding Lagrangean multipliers $\lambda_{tg}^{s,s'}$ and $\lambda_{tl}^{s,s'}$ need to be non-negative.

**(L2-MLR)**

$$\begin{aligned}\min\ & \sum_{s\in S} p^s \sum_{t\in T} c_t x_t^s + \sum_{t\in T_1}\sum_{(s,s')\in P_3} \lambda_t^{s,s'}(x_t^s - x_t^{s'}) \\ & + \sum_{t\in T_C}\sum_{(s,s')\in P_3} \lambda_{tg}^{s,s'}(x_t^{s'} - x_t^s - M(1-z_t^{s,s'})) \\ & + \sum_{t\in T_C}\sum_{(s,s')\in P_3} \lambda_{tl}^{s,s'}(x_t^s - x_t^{s'} - M(1-z_t^{s,s'}))\end{aligned} \tag{6.1c}$$

$$s.t. \quad \sum_{\tau \le t} A_\tau^s x_\tau^s \le a_t^s \qquad \forall t, s \tag{6.2}$$

$$B_t^s x_t^s + C_t^s z_t^{s,s'} \le d_t^s \qquad \forall t \in T_C, \forall (s,s') \in P_3 \tag{6.4b}$$

$$x_{jt}^s \in \{0,1\} \qquad \forall t, s, \forall j \in J' \tag{6.6}$$

$$x_{jt}^s \in R \qquad \forall t, s, \forall j \in J \setminus J' \tag{6.7}$$

Figure 6.5 represents the structure of the model (L2-MLR) where **L2-MLR$^{\mathbf{s}}$** correspond to the scenario sub-problems in this decomposed model.

**(L2-MLR$^{\mathbf{s}}$)**

$$\min \quad \sum_{t \in T} p^s c_t x_t^s + \sum_{t \in T_1} x_t^s \Big( \sum_{\substack{(s,s') \in P_3 \\ s < s'}} \lambda_t^{s,s'} - \sum_{\substack{(s',s) \in P_3 \\ s > s'}} \lambda_t^{s',s} \Big)$$

$$+ \sum_{t \in T_C} x_t^s \Big[ \sum_{\substack{(s,s') \in P_3 \\ s < s'}} (\lambda_{tl}^{s,s'} - \lambda_{tg}^{s,s'}) - \sum_{\substack{(s',s) \in P_3 \\ s > s'}} (\lambda_{tl}^{s',s} - \lambda_{tg}^{s',s}) \Big] \tag{6.1d}$$

$$- \sum_{t \in T_C} \sum_{\substack{(s,s') \in P_3 \\ s < s'}} [(1 - z_t^{s,s'}).(\lambda_{tg}^{s,s'} + \lambda_{tl}^{s,s'}).M)$$

$$s.t. \quad \sum_{\tau \le t} A_\tau^s x_\tau^s \le a_t^s \qquad \forall t \tag{6.2a}$$

$$B_t^s x_t^s + C_t^s z_t^{s,s'} \le d_t^s \qquad \forall t \in T_C, \forall (s,s') \in P_3, s < s' \tag{6.4c}$$

$$x_{jt}^s \in \{0,1\} \qquad \forall t, \forall j \in J' \tag{6.6a}$$

$$x_{jt}^s \in R \qquad \forall t, \forall j \in J \setminus J' \tag{6.7a}$$

It is important to observe that we assign the shared binary variable $z_t^{s,s'}$ and its corresponding constraints (6.4b) and objective function term to the scenario problem *s* for all $(s,s') \in P_3$ where ($s < s'$). This allows to decompose the problem into independent scenarios. For instance in the case of 4 scenarios, the minimum scenario pair set $P_3 = \{(1,2),(1,3),(2,4),(3,4)\}$ and, therefore, the corresponding shared variables $z_t^{1,2}, z_t^{1,3}$ are assigned to scenarios 1; $z_t^{2,4}$ to scenario 2; and $z_t^{3,4}$ to scenario 3. As an alternative, one can also create a copy of the shared variable $z_t^{s,s'}$ as $z_t^{s',s}$ and its corresponding constraints (6.4b), (6.5b) and (6.5c) for all

$(s,s')\in P_3$ that will allow to keep these variables in both the sub-problems *s* and *s'*. However, the performance of the two alternative decomposition approaches should not be very different.

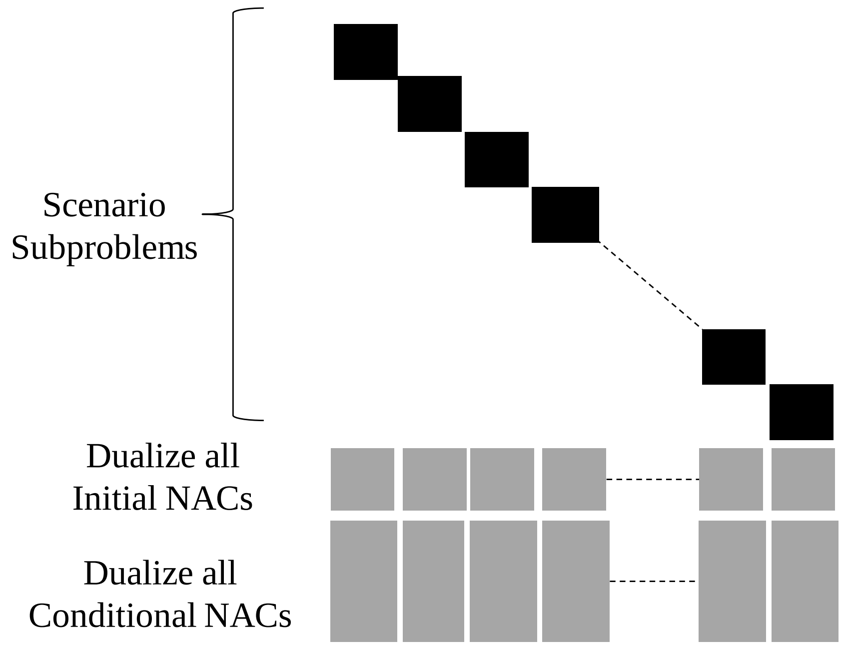


Figure 6.5: Lagrangean Decomposition based on dualizing all NACs directly

**(ii)** Another way to decompose the model (MLR) while considering all the NACs, is based on first reformulating the constraints (6.3a), (6.5b) and (6.5c) as (6.3b), (6.5d) and (6.5e) respectively, where $\tilde{x}_t^{s,s'}$ represents the value of the variable $x_t^{s'}$ for $\forall t\in T\ ,\forall(s,s')\in P_3$.

$$x_t^s=\tilde{x}_t^{s,s'}\quad \forall t\in T_I,\forall(s,s')\in P_3 \tag{6.3b}$$

$$-M(1-z_t^{s,s'})\quad \le x_t^s-\tilde{x}_t^{s,s'}\quad \forall t\in T_C,\forall(s,s')\in P_3 \tag{6.5d}$$

$$M(1-z_t^{s,s'})\quad \ge x_t^s-\tilde{x}_t^{s,s'}\quad \forall t\in T_C,\forall(s,s')\in P_3 \tag{6.5e}$$

$$x_t^{s'}=\tilde{x}_t^{s,s'}\quad \forall t\in T,\forall(s,s')\in P_3,s<s' \tag{6.5f}$$

In addition, eq. (6.5f) is required to ensure that all the copy variables $\tilde{x}_t^{s,s'}$ for $x_t^{s'}$ have the same values in all the scenario pairs it occurs. Notice that the reformulated model ($MLR^C$) includes constraints (6.1), (6.2), (6.3b), (6.4b), (6.5d), (6.5e), (6.5f), (6.6) and (6.7). Model ($MLR^C$) can now be decomposed into individual scenarios by dualizing only constraints (6.5f) as can be seen in Figure 6.6. **L3-MLR$^{\mathbf{C}}$** and **L3-MLR$^{\mathbf{Cs}}$** represent the Lagrangean problem and scenario sub-problems for this indirect decomposition approach, respectively.

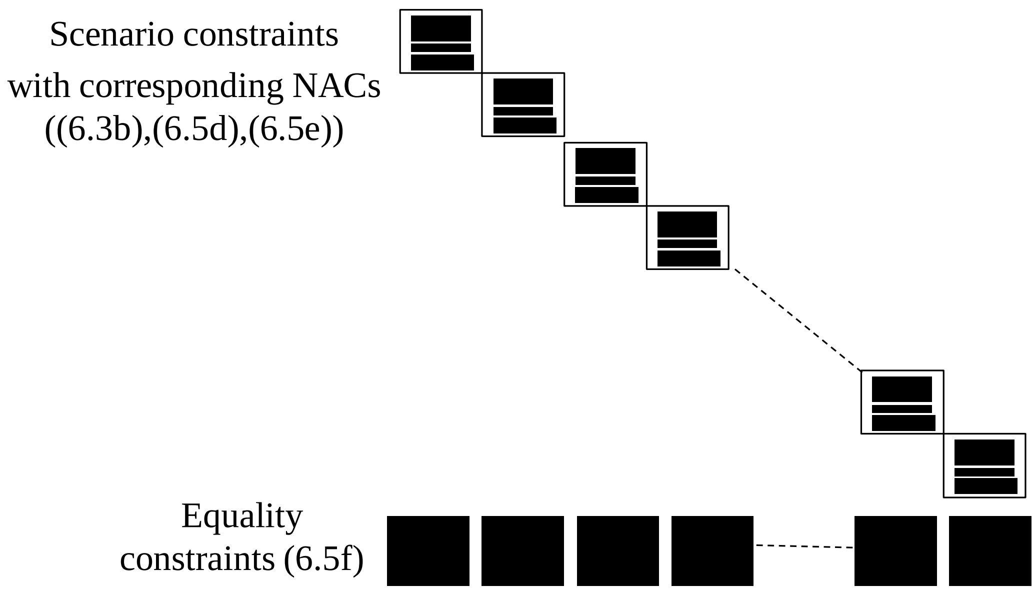


Figure 6.6: Structure of the Reduced Model after reformulation ($MLR^C$)

(**L3-MLR$^{\mathbf{C}}$**)

$$\min \sum_{s\in S} p^s \sum_{t\in T} c_t x_t^s + \sum_{t\in T} \sum_{\substack{(s,s')\in P_3 \\ s<s'}} \lambda_t^{s,s'} (x_t^{s'} - \tilde{x}_t^{s,s'}) \qquad (6.1e)$$

$$s.t. \quad \sum_{\tau \le t} A_\tau^s x_\tau^s \le a_t^s \qquad \forall t, s \qquad (6.2)$$

$$x_t^s = \tilde{x}_t^{s,s'} \qquad \forall t \in T_I, \forall (s,s') \in P_3 \qquad (6.3b)$$

$$-M(1 - z_t^{s,s'}) \le x_t^s - \tilde{x}_t^{s,s'} \qquad \forall t \in T_C, \forall (s,s') \in P_3 \qquad (6.5d)$$

$$M(1 - z_t^{s,s'}) \ge x_t^s - \tilde{x}_t^{s,s'} \qquad \forall t \in T_C, \forall (s,s') \in P_3 \qquad (6.5e)$$

$$B_t^s x_t^s + C_t^s z_t^{s,s'} \le d_t^s \qquad \forall t \in T_C, \forall (s,s') \in P_3 \qquad (6.4b)$$

$$x_{jt}^s \in \{0,1\} \qquad \forall t, s, \forall j \in J' \qquad (6.6)$$

$$x_{jt}^s \in R \qquad \forall t, s, \forall j \in J \setminus J' \qquad (6.7)$$

$$\textbf{(L3-MLR}^{\textbf{Cs}}\textbf{)} \quad \min \sum_{t \in T} p^s c_t x_t^s + \sum_{t \in T} [x_t^s \sum_{\substack{(s',s) \in P_3 \\ s > s'}} \lambda_t^{s',s} - \sum_{\substack{(s,s') \in P_3 \\ s < s'}} \lambda_t^{s,s'} \tilde{x}_t^{s,s'}] \qquad (6.1f)$$

$$s.t. \quad \sum_{\tau \le t} A_\tau^s x_\tau^s \le a_t^s \qquad \forall t \qquad (6.2a)$$

$$x_t^s = \tilde{x}_t^{s,s'} \quad \forall t \in T_I, \forall (s,s') \in P_3, s < s' \qquad (6.3c)$$

$$-M(1 - z_t^{s,s'}) \quad \le x_t^s - \tilde{x}_t^{s,s'} \quad \forall t \in T_C, \forall (s,s') \in P_3, s < s' \qquad (6.5g)$$

$$M(1 - z_t^{s,s'}) \quad \ge x_t^s - \tilde{x}_t^{s,s'} \quad \forall t \in T_C, \forall (s,s') \in P_3, s < s' \qquad (6.5h)$$

$$B_t^s x_t^s + C_t^s z_t^{s,s'} \le d_t^s \qquad \forall t \in T_C, \forall (s,s') \in P_3, s < s' \qquad (6.4c)$$

$$x_{jt}^s \in \{0,1\} \qquad \forall t, s, \forall j \in J' \qquad (6.6a)$$

$$x_{jt}^s \in R \qquad \forall t, s, \forall j \in J \setminus J' \qquad (6.7a)$$

Notice that once the scenario subproblems L2-MLR$^s$ and L3-MLR$^{Cs}$ corresponding to the direct and indirect approaches, (i) and (ii), are formulated, the rest of the algorithmic steps are similar to as we have seen in the previous section (Figure 6.2).

**Limitations:** Based on the computational experiments, approach (ii) performs slightly better than the approach (i). However, the main limitation with both of these decomposition approaches (i) and (ii) is that the number of Lagrangean multipliers becomes very large since the conditional NACs represent a very large fraction of the total constraints in the problem. In addition, these constraints appear as big-M constraints in the model where only a small fraction of these constraints become active at the optimal solution, so the improvement in the resulting lower bound is usually very slow and one may need several iterations to converge. Overall, the performance with the decomposition approaches that rely on considering all the conditional NACs can even be worse than the decomposition approach presented in section 6.4.1 which relaxes all of these constraints.

However, for the problems with exogenous uncertainties, there is no big-M involved in the NACs. Therefore, on dualizing these NACs (all time periods) for scenario decomposition, the quality of the lower bound is usually strengthened.

## 6.5 Proposed Lagrangean Decomposition Algorithm

The decomposition approaches presented in the previous section may perform reasonably well for a certain class of problems with a given set of data. However, as we mentioned these methods also have some limitations. To overcome them, we propose a new decomposition scheme that neither relaxes nor dualizes all the conditional NACs. The basic idea relies on decomposing the fullspace model into scenario group subproblems instead of individual scenarios. This allows keeping a subset of the NACs in the subproblems as constraints, while dualizing and relaxing the rest of the NACs. Therefore, it can be considered as a partial decomposition approach. Since, the formulation of the scenario groups is a key element in the proposed decomposition algorithm, we first describe the methodology to construct these scenario groups for the MSSP with endogenous uncertainties.

**6.5.1 Formulating the Scenario Groups:** The proposed algorithm divides the reduced model (MLR) into scenario group subproblems as explained in this section. Let us consider that there are two endogenous uncertain parameters $\{\theta_1, \theta_2\}$ where each one has 2 possible realizations (L, H). Therefore, there are 4 scenarios (1: LL, 2: HL, 3: LH, 4: HH). The scenario pairs *(s,s')* required to represent the NA constraints in each time period *t* based on the three properties in chapter 4 are {(1,2),(1,3),(2,4),(3,4)} as can be seen in Figure 6.7(a). Notice that the double line between scenario pairs is used to emphasize the fact that there are initial as well as conditional NACs between each of these scenario pairs, whereas each node represents the index of an individual scenario. The dash lines correspond to the dualized NA constraints.

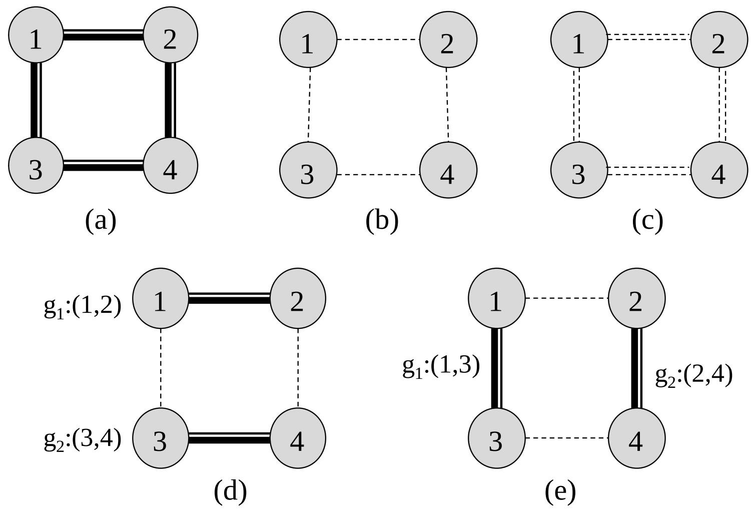


Figure 6.7: An illustration for the 4 Scenarios and its scenario group decomposition (top view)

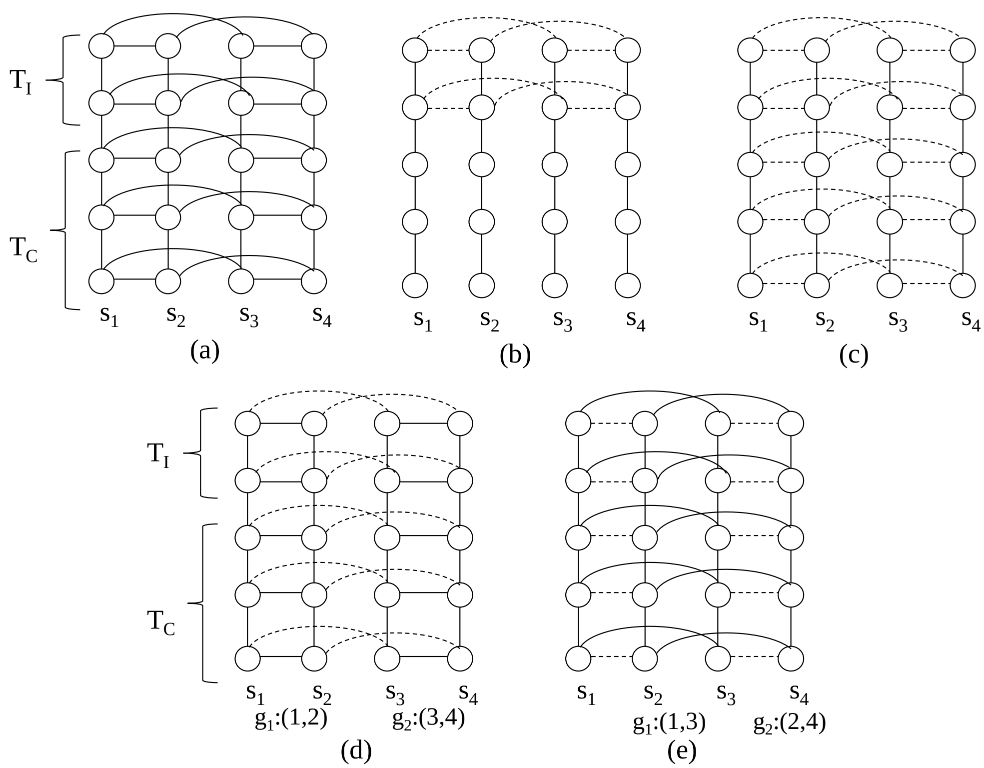


Figure 6.8: An illustration for the 4 Scenarios and its scenario group decomposition (front view)

The Lagrangean decomposition scheme corresponding to the section 6.4.1 is represented by Figure 6.7(b) where we remove all the conditional NACs and dualize all the initial NACs. Figure 6.7(c) corresponds to the scenario decomposition scheme presented in section 6.4.2 that relies on dualizing all the NACs (initial and conditional) either directly (i) or after reformulation (ii). In contrast, the proposed algorithm decomposes the fullspace model into scenario groups as shown in Figures 6.7(d) or 6.7(e). In particular, Figure 6.7(d) corresponds to the two scenario group problems {$g_1$: (1,2), $g_2$: (3,4)} where 6.7(e) represents the scenario group problems { $g_1$: (1,3), $g_2$: (2,4)}. Notice that Figures 6.7(a)-(e) correspond to the top view of the scenario-tree representation in Figures 6.8(a)-(e), respectively. Each node in Figures 6.8(a-e) represents the state of the system in a given time period *t* while the linking lines correspond to the NA constraints.

The rules to formulate the scenario groups for the proposed algorithm are as follows:

1. Each scenario *s* occurs in only one of the scenario group $S_g$ and every scenario is included in at-least one of the groups $G$. All the scenario groups $S_g \in G$ have equal number of scenarios. Therefore, the total number of scenarios equal to the number of scenario groups times the number of scenarios in each group i.e., $|S| = |G| \cdot |S_g|$. Notice that here we assume the symmetry of the scenario groups to formulate the subproblems that have almost similar complexity. However, we can always consider an asymmetric approach as shown in Figure 6.9 for the 4 scenario instance described above. Specifically, Figure 6.9(a) and 6.9(b) decompose the problem into two scenario groups {$g_1$: (1,2,3), $g_2$: (4)} and {$g_1$: (1,3,4), $g_2$: (2)}, respectively, where the subproblems with 3 scenarios should be more expensive to solve than the one with a single scenario.

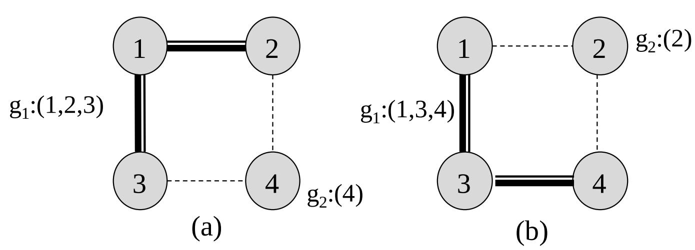


Figure 6.9: Asymmetric scenario group decomposition

2. Scenario groups $S_g$ are formulated by first selecting an endogenous uncertain parameter and then taking those scenarios in a group which differ in the realization of only that particular uncertain parameter. For instance, in Figure 6.7(a), we first select parameter $\{\theta_1\}$ and write only those scenario groups that differ in the realization of this uncertain parameter, i.e. {(1,2),(3,4)} which results in the scenario groups as in Figure 6.7(d). Similarly, the uncertain parameter $\{\theta_2\}$ leads to the scenario groups {(1,3),(2,4)} in Figure 6.7(e). Notice that these scenario groups are nothing but the scenario sets $(s_1, s_2, ...., s_k) \in L_p$ (eq. 6.8) that are required to formulate the reduced model (MLR).
3. Since there can be many uncertain parameters $\{\theta_p\}$ each with its own scenario set $(s_1, s_2, ...., s_k) \in L_p$, the selection of a particular set of scenario groups is not unique.
   (i) Ideally, one may consider selecting a scenario group set that provides the tightest initial bound compared to the others. However, in general unless all the combinations are tested, it is not obvious how to select such a scenario group set.
   (ii) A relatively simpler approach can be to first solve each scenario independently, and selecting the scenario group set corresponding to that uncertain parameter, which has the largest total difference in the objective function values of the corresponding scenarios. This is due to the fact that most likely the corresponding NACs for those scenarios will be active at the optimal solution. Therefore, keeping these NACs in the subproblem as constraints should yield a tighter bound. For instance, select 7(e) if scenario group set corresponding to $\theta_2$ exhibits larger total variation in the objective function value than the scenario group set for uncertain parameter $\theta_1$. In other words, this idea relies on the sensitivity of the objective function value for an uncertain parameter and its possible realizations.

Notice that for simplicity we only consider the cases with same probabilities for all the scenarios during this work. If it would be possible, the impact of different scenario probability values on scenario group partitions will be addressed in our future paper.

4. Even after selecting a scenario group set that corresponds to an uncertain parameter $\{\theta_p\}$, it may still be difficult to solve the resulting scenario group subproblems. For instance if a parameter has many realizations, then each scenario group subproblem will have that many scenarios which may increase the computational expense. Therefore, one may further divide the scenario groups into subgroups and solve the resulting smaller problems.

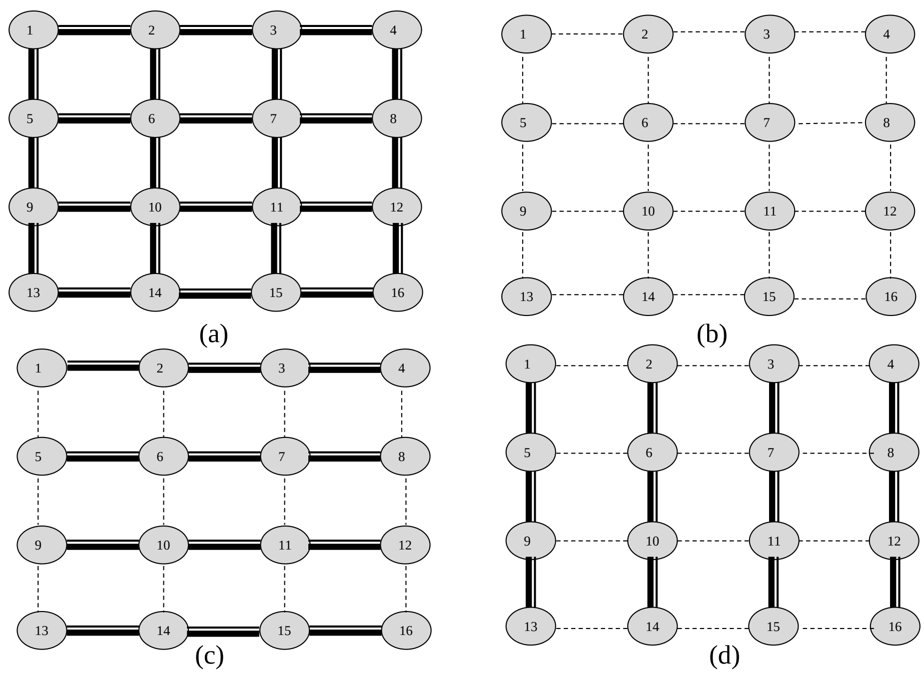


Figure 6.10: 2 parameters, 16 scenarios and its scenario/scenario group decomposition

As an example, say if we have 2 uncertain parameters and 4 realizations of each parameter, there are a total of 16 scenarios. There are two possibilities of the scenario groups {(1,2,3,4), (5,6,7,8), (9,10,11,12), (13,14,15,16)} (Figure 6.10(c)) and {(1,5,9,13), (2,6,10,14), (3,7,11,15), (4,8,12,16)} (Figure 6.10 (d)) according to the rules 1-3. Based on the problem characteristics, it may be difficult to solve each scenario group subproblem with 4 scenarios. Therefore, these groups can be further decomposed into a total of 8 scenario groups each with 2 scenarios, respectively (Figure 6.11(a) and 11(b)). However, the quality of the bound may deteriorate since the corresponding conditional NACs need to be relaxed. Therefore, there is a trade-off between the quality of the bound and the complexity of solving a scenario group problem.

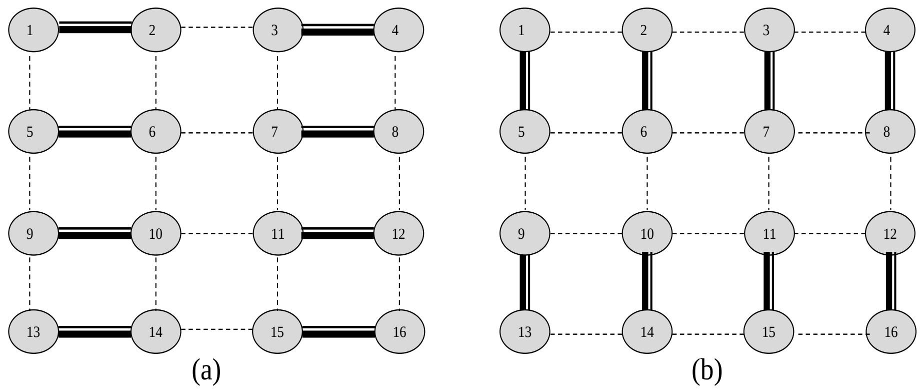


Figure 6.11: Decomposition of the scenario groups into subgroups

5. In general, if the problem is expensive to solve for each scenario, it is better to use scenario groups each with only few scenarios. On the other hand, if individual scenarios are not expensive to solve, then one may consider more scenarios in each group to improve the quality of the bound.

The above rules are general and can be applied to a problem with any number of uncertain parameters and many realizations of each uncertain parameter. For instance, Figure 6.12(a) represents the extension to three uncertain parameter case where each parameter has 2 realizations (total 8 scenarios).

There are 6 possibilities to formulate the scenario groups in symmetric form:

(a) Taking 4 scenarios in each group:

{(1,2,3,4), (5,6,7,8)} i.e. Figure 6.12(c)

{(1,2,5,6), (3,4,7,8)} i.e. Figure 6.12(d)

{(1,3,5,7), (2,4,6,8)} i.e. Figure 6.12(e)

(b) Taking 2 scenarios in each group:

{(1,2),(3,4), (5,6),(7,8)} i.e. Figure 6.12(f)

{(1,5),(2,6), (3,7),(4,8)} i.e. Figure 6.12(g)

{(1,3),(2,4), (5,7),(6,8)} i.e. Figure 6.12(h)

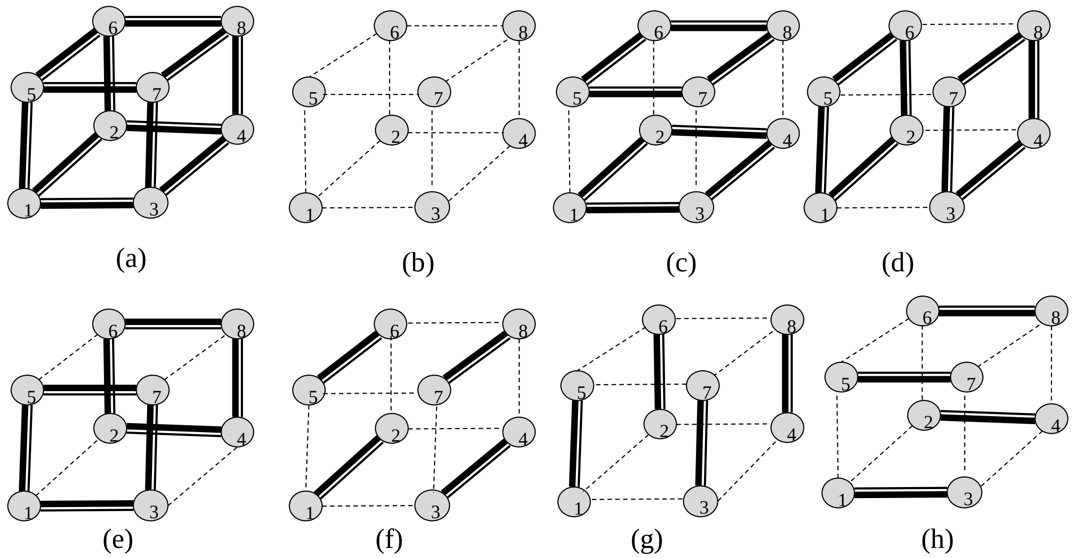


Figure 6.12: 3 parameters, 8 scenarios and its scenario/scenario group decomposition

**6.5.2 Decomposition Algorithm:** Based on the scenario groups that are constructed in the previous section, we now first present the corresponding reformulated Reduced (MILP) model. Notice that these scenario group partitions will be used to decompose the resulting reduced model into scenario group subproblems during the proposed Lagrangean decomposition algorithm.

Let us consider that $G$ is the set of scenario groups $S_g \in G$ that are selected based on the rules presented in the previous section, where each of these scenario groups $S_g$ may have 1 or more scenarios. The reduced model (MLR) can now be represented as an equivalent model (**MLR$^{\mathbf{G}}$)** in terms of the scenario groups $S_g \in G$ where we disaggregate the total NACs for the scenario pairs that corresponds to the same scenario group $(s,s') \in S_g$ (i.e. eqs. (6.3i), (6.4i),(6.5i),(6.5j)) with those which belong to the different scenario groups $(s \in S_g) \wedge (s' \notin S_g)$ (i.e. eqs. (6.3j), (6.4j),(6.5k),(6.5l)).

**(MLR$^{\mathbf{G}}$)** $$\min \sum_{S_g \in G} \left\{ \sum_{s \in S_g} p^s \sum_{t \in T} c_t x_t^s \right\} \qquad (6.1i)$$

$$s.t. \quad \sum_{\tau \le t} A_\tau^s x_\tau^s \le a_t^s \qquad \forall t, s \in S_g \in G \tag{6.2i}$$

$$x_t^s = x_t^{s'} \quad \forall t \in T_I, \forall (s,s') \in P_3,\ s,s' \in S_g \in G \tag{6.3i}$$

$$B_t^s x_t^s + C_t^s z_t^{s,s'} \le d_t^s \qquad \forall t \in T_C, \forall (s,s') \in P_3, s,s' \in S_g \in G \tag{6.4i}$$

$$-M(1 - z_t^{s,s'}) \quad \le x_t^s - x_t^{s'} \quad \forall t \in T_C, \forall (s,s') \in P_3, s,s' \in S_g \in G \tag{6.5i}$$

$$M(1 - z_t^{s,s'}) \quad \ge x_t^s - x_t^{s'} \quad \forall t \in T_C, \forall (s,s') \in P_3, s,s' \in S_g \in G \tag{6.5j}$$

$$x_t^s = x_t^{s'} \quad \forall t \in T_I, \forall (s,s') \in P_3, (s \in S_g) \wedge (s' \notin S_g), S_g \in G \tag{6.3j}$$

$$B_t^s x_t^s + C_t^s z_t^{s,s'} \le d_t^s \qquad \forall t \in T_C, \forall (s,s') \in P_3, (s \in S_g) \wedge (s' \notin S_g), S_g \in G \tag{6.4j}$$

$$-M(1 - z_t^{s,s'}) \quad \le x_t^s - x_t^{s'} \quad \forall t \in T_C, \forall (s,s') \in P_3, (s \in S_g) \wedge (s' \notin S_g), S_g \in G \tag{6.5k}$$

$$M(1 - z_t^{s,s'}) \quad \ge x_t^s - x_t^{s'} \quad \forall t \in T_C, \forall (s,s') \in P_3, (s \in S_g) \wedge (s' \notin S_g), S_g \in G \tag{6.5l}$$

$$x_{jt}^s \in \{0,1\} \qquad \forall t, \forall s \in S_g \in G, \forall j \in J' \tag{6.6i}$$

$$x_{jt}^s \in R \qquad \forall t, \forall s \in S_g \in G, \forall j \in J \setminus J' \tag{6.7i}$$

The Lagrangean problem (**L4-MLR$^G$**) corresponding to the model (MLR$^G$) can be formulated by dualizing only those initial NAC constraints for the pairs of scenarios *(s,s')* that link the two scenario groups, i.e. eq. (6.3j), and removing the corresponding conditional NACs (eqs. (6.4j),(6.5k) and (6.5l)). Therefore, the initial and conditional NACs (eq. 6.3(i), 6.4(i), 6.5(i) and 6.5(j)) among the scenario pairs *(s,s')* that belong to the same scenario group remain in the Lagrangean problem as explicit constraints.

(**L4-MLR$^G$)**

$$\min \quad \sum_{S_g \in G} \left\{ \sum_{s \in S_g} p^s \sum_{t \in T} c_t x_t^s + \sum_{t \in T_1} \sum_{\substack{(s,s') \in P_3 \\ s.t.\ (s \in S_g) \wedge (s' \notin S_g)}} \lambda_t^{s,s'} (x_t^s - x_t^{s'}) \right\} \tag{6.1j}$$

$$s.t. \quad \sum_{\tau \le t} A_\tau^s x_\tau^s \le a_t^s \qquad \forall t, s \in S_g \in G \tag{6.2i}$$

$$x_t^s = x_t^{s'} \quad \forall t \in T_I, \forall (s,s') \in P_3,\ s,s' \in S_g \in G \tag{6.3i}$$

$$B_t^s x_t^s + C_t^s z_t^{s,s'} \le d_t^s \qquad \forall t \in T_C, \forall (s,s') \in P_3, s,s' \in S_g \in G \tag{6.4i}$$

$$-M(1 - z_t^{s,s'}) \quad \le x_t^s - x_t^{s'} \quad \forall t \in T_C, \forall (s,s') \in P_3, s,s' \in S_g \in G \tag{6.5i}$$

$$M(1 - z_t^{s,s'}) \quad \ge x_t^s - x_t^{s'} \quad \forall t \in T_C, \forall (s,s') \in P_3, s,s' \in S_g \in G \tag{6.5j}$$

$$x_{jt}^s \in \{0,1\} \qquad \forall t, \forall s \in S_g \in G, \forall j \in J' \tag{6.6i}$$

$$x_{jt}^s \in R \qquad \forall t, \forall s \in S_g \in G, \forall j \in J \setminus J' \tag{6.7i}$$

In contrast to the previous approaches, we can observe that the main idea in the proposed decomposition approach is that instead of removing all the conditional NACs from the model (as in section 6.4.1) or dualizing all the conditional NACs either directly or in an indirect manner (as in section 6.4.2), we only remove a subset of conditional NACs from the model and dualize a subset of the initial NACs in the objective function instead of dualizing all the initial NACs while formulating the Lagrangean problem (L4-MLR$^G$). This results in the decomposition of the reduced model (MLR) into scenario group subproblems (**L4-MLR$^{Gs}$**) rather than individual scenarios in the previous cases. Therefore, we also refer it as a partial decomposition approach.

**(L4-MLR$^{Gs}$)**

$$\min \quad \sum_{s \in S_g} p^s \sum_{t \in T} c_t x_t^s + \sum_{t \in T_1} x_t^s \Big( \sum_{\substack{(s,s') \in P_3, s<s' \\ s.t.(s \in S_g) \wedge (s' \notin S_g)}} \lambda_t^{s,s'} - \sum_{\substack{(s',s) \in P_3, s>s' \\ s.t.(s \in S_g) \wedge (s' \notin S_g)}} \lambda_t^{s',s} \Big) \tag{6.1k}$$

$$s.t. \quad \sum_{\tau \le t} A_\tau^s x_\tau^s \le a_t^s \qquad \forall t, s \in S_g \tag{6.2k}$$

$$x_t^s = x_t^{s'} \quad \forall t \in T_I, \forall (s,s') \in P_3,\ s,s' \in S_g \tag{6.3k}$$

$$B_t^s x_t^s + C_t^s z_t^{s,s'} \le d_t^s \qquad \forall t \in T_C, \forall (s,s') \in P_3, s,s' \in S_g \tag{6.4k}$$

$$-M(1 - z_t^{s,s'}) \quad \le x_t^s - x_t^{s'} \quad \forall t \in T_C, \forall (s,s') \in P_3, s,s' \in S_g \tag{6.5m}$$

$$M(1 - z_t^{s,s'}) \quad \ge x_t^s - x_t^{s'} \quad \forall t \in T_C, \forall (s,s') \in P_3, s,s' \in S_g \tag{6.5n}$$

$$x_{jt}^{s} \in \{0,1\} \qquad \forall t, \forall s \in S_g, \forall j \in J' \qquad (6.6k)$$

$$x_{jt}^{s} \in R \qquad \forall t, \forall s \in S_g, \forall j \in J \setminus J' \qquad (6.7k)$$

The structure of model (L4-MLR$^G$) can be seen in Figure 6.13, where each scenario group subproblem that contains its corresponding initial and conditional NACs can be solved independently, and where only a small fraction of the total initial and conditional NACs are dualized and removed, respectively. Since, the resulting subproblems capture the more relevant information, i.e. the one corresponding to the later time periods, the dual bound should be tighter.

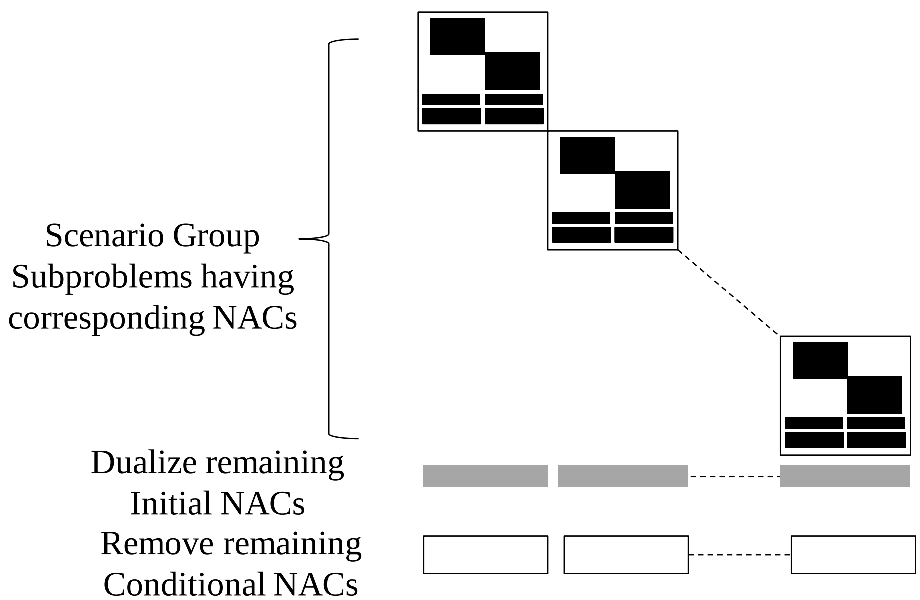


Figure 6.13: Scenario decomposition approach in the proposed Lagrangean Decomposition

We can then state the following proposition:

**Proposition 6.1:** ***The dual bound obtained from the proposed Lagrangean problem (L4-MLR$^G$) at root node is at-least as tight as the dual bound obtained from the standard Lagrangean decomposition approach (L1-MLR) i.e. the model (L1-MLR) is a relaxation of the model (L4-MLR$^G$).***

*Proof:* To prove this proposition it is sufficient to establish that,

(a) The feasible region of the proposed Lagrangean problem (L4-MLR$^G$) is contained within the feasible region of the model L1-MLR.

(b) The objective function value of the proposed Lagrangean problem (L4-MLR$^G$) over its feasible solutions $x_t^s$ is at-least as large (assuming minimization case) as the objective function value of the model L1-MLR.

For (a), since scenario constraints (6.2) in L1-MLR are equivalent to constraints (6.2i) in L4-MLR$^G$. Therefore, the only difference between both of these models is that L4-MLR$^G$ has the additional constraints (6.3i), (6.4i), (6.5i) and (6.5j) in the model. Hence, the feasible region of the model L4-MLR$^G$ is contained within the feasible region of the standard Lagrangean problem L1-MLR which has more feasible solutions.

For (b), we first rewrite the model L1-MLR as **L1-MLR'** where $\eta_t^{s,s'} \geq 0$ represent the Lagrangean multipliers corresponding to the dualized inequalities $(x_t^s - x_t^{s'} \leq 0)$ and multipliers $\mu_t^{s,s'} \geq 0$ correspond to the inequalities $(-x_t^s + x_t^{s'} \leq 0)$. We use the inequality format of the initial NACs (eq. (6.3a)) to dualize them in the objective function.

**(L1-MLR')**

$$\min \sum_{s \in S} p^s \sum_{t \in T} c_t x_t^s + \sum_{t \in T_1} \sum_{(s,s') \in P_3} \eta_t^{s,s'} (x_t^s - x_t^{s'}) + \sum_{t \in T_1} \sum_{(s,s') \in P_3} \mu_t^{s,s'} (-x_t^s + x_t^{s'}) \tag{6.1l}$$

s.t. (6.2), (6.6) and (6.7)

Similarly, model L4-MLR$^G$ can be rewritten as follows:

**(L4-MLR$^{G'}$)**

$$\min \sum_{S_g \in G} \left\{ \sum_{s \in S_g} p^s \sum_{t \in T} c_t x_t^s + \sum_{t \in T_1} \sum_{\substack{(s,s') \in P_3 \\ s.t.\,(s \in S_g) \wedge (s' \notin S_g)}} \eta_t^{s,s'} (x_t^s - x_t^{s'}) + \sum_{t \in T_1} \sum_{\substack{(s,s') \in P_3 \\ s.t.\,(s \in S_g) \wedge (s' \notin S_g)}} \mu_t^{s,s'} (-x_t^s + x_t^{s'}) \right\} \tag{6.1m}$$

s.t. (6.2i), (6.3i), (6.4i), (6.5i), (6.5j), (6.6i) and (6.7i)

On subtracting the objective functions (6.1l) and (6.1m), we have the following summation,

$$\sum_{S_g \in G} \left\{ \sum_{t \in T_1} \sum_{\substack{(s,s') \in P_3 \\ s.t.\,(s \in S_g) \wedge (s' \in S_g)}} \eta_t^{s,s'} (x_t^s - x_t^{s'}) + \sum_{t \in T_1} \sum_{\substack{(s,s') \in P_3 \\ s.t.\,(s \in S_g) \wedge (s' \in S_g)}} \mu_t^{s,s'} (-x_t^s + x_t^{s'}) \right\} \tag{6.1n}$$

To prove that the objective function value of the model L4-MLR$^G$ over its feasible solutions $x_t^s$ is at least as large as the objective function value of the model L1-MLR, it is sufficient to prove that,

$$\sum_{S_g \in G} \left\{ \sum_{t \in T_1} \sum_{\substack{(s,s') \in P_3 \\ s.t.\,(s \in S_g) \wedge (s' \in S_g)}} \eta_t^{s,s'} (x_t^s - x_t^{s'}) + \sum_{t \in T_1} \sum_{\substack{(s,s') \in P_3 \\ s.t.\,(s \in S_g) \wedge (s' \in S_g)}} \mu_t^{s,s'} (-x_t^s + x_t^{s'}) \right\} \le 0 \qquad (6.1o)$$

For any feasible solution $x_t^s$ to the model L4-MLR$^G$ and for any $\eta_t^{s,s'} \ge 0$ and $\mu_t^{s,s'} \ge 0 \;\; \forall (s,s') \in P_3, t \in T$, the penalty terms $\eta_t^{s,s'}(x_t^s - x_t^{s'})$ and $\mu_t^{s,s'}(-x_t^s + x_t^{s'})$ in the objective function are less than or equal to zero. Hence, their summation in inequality (6.1o) also holds true. In other words, we can also state that the model L1-MLR is a Lagrangean relaxation of the model L4-MLR$^G$ and therefore, it provides a valid lower bound on the objective function value of the model L4-MLR$^G$. □

The rest of the steps of the algorithm are similar to the standard Lagrangean decomposition (Figure 6.2) where scenario group subproblems L4-MLR$^{Gs}$ are solved during each iteration, and multipliers are updated using either subgradient method (Fisher, 1985) or an alternative scheme as in Mouret et al. (2011); Oliveira et al. (2013), and Tarhan et al. (2013). Moreover, the algorithm can be further extended within a duality based branch and bound search (as proposed in Goel and Grossmann, 2006; Tarhan et al., 2009; and Tarhan et al., 2011) if the gap between the lower and upper bound is still large. As will be shown in the results, the main advantage with the proposed approach is that the resulting dual bound is significantly strengthened at the root node itself since a large fraction of the NACs are included as explicit constraints in the subproblems. This will eventually reduce the number of iterations required to converge at each node and the total number of nodes in the branch and bound search.

### 6.5.3 Alternate Proposed Lagrangean Decomposition Algorithm

It should be noted that few conditional NACs (eqs. (6.5k) and (6.5l)) still need to be removed while formulating the scenario group subproblems (L4-MLR$^{Gs}$) in the above method. Therefore, the best lower bound at the root node cannot be better than the optimal solution of the model without these conditional NACs. To further close the gap at the root node, we also propose an alternate Lagrangean decomposition approach that may provide a stronger bound at the root node. However, it involves solving more subproblems, and it may be computationally more expensive than the proposed approach in the previous section. Therefore, it is only useful for a certain class of problems.

The main idea is that we select all the scenario groups instead of a subset of the scenario groups as we did in the previous section 6.5.1. However, since a scenario can appear in more than one of these scenario groups, we need to equate the decisions for this scenario in all of these scenario groups where it occurs. In other words, we create a copy of each scenario for every scenario group problem where it can appear and equating the decisions corresponding to all time periods for that scenario for each of these scenario groups. The resulting model (Figure 6.14(b)) will be equivalent to the reduced model (MLR) (Figure 6.14(a)) where {1’,2’,3’,4’} are the copy of the scenarios {1,2,3,4} and the connections between them are the added equality constraints.

Therefore, to decompose the resulting problem (Figure 6.14(b)) into 4 scenario group subproblems {(1,2),(1’,3’),(2’,4’), (3,4)}, we dualize the equality constraints correspond to each scenario and its copy variables, instead of dualizing or removing the NAC constraints. This yields a set of 4 scenario group subproblems (Figure 6.14(c)) i.e. {(1,2),(1’,3’),(2’,4’), (3,4)}. Since, none of the conditional and initial NAC constraints are removed from the subproblems, the bound is in general stronger. We can compare this decomposition with the proposed one in Figure 6.7 where we obtain 2 scenario group problems.

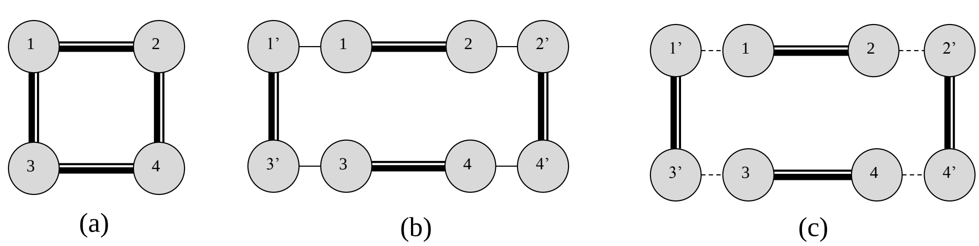


Figure 6.14: Alternate proposed Lagrangean decomposition approach for 4 scenario problem

Qualitatively, this decomposition can be considered as the decomposition of the reduced model (Figure 6.14(a)) at vertices as compared to the arcs in standard/proposed decomposition described earlier. Notice that although this alternate decomposition is computationally expensive since more subproblems are involved than in the previous method, it can however be used in a hybrid scheme with the proposed decomposition to improve the quality of lower bound. For instance in Figure 6.10, we can first select the 4 scenario groups based on the rules that are defined earlier, and then use this approach to further decompose each group into subgroups by creating a copy of the scenarios in each of these groups instead of the partitions used in Figure 6.11.

## 6.6 Numerical Results

### 6.6.1 Process network planning under uncertain yield

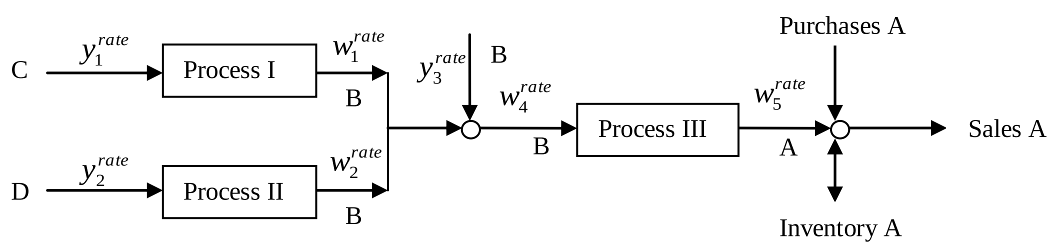


Figure 6.15: 3 Process Network Example

**Case (i): Planning of 3 process network over 10 years**

To illustrate the application of the various decomposition approaches for multistage stochastic programming with endogenous uncertainties, we consider the following problem from Goel and Grossmann (2006). Given is a process network (Figure 6.15) that is used to produce product A. Currently, the production of A takes place only in Process III with installed capacity of 3 tons/hour and yield of 0.70, that consumes an intermediate product B which is purchased. If needed, the final product A can also be purchased so as to maintain its inventory. The demand for the final product, which is known, must be satisfied for all time periods over the given time horizon. Two new technologies (Process I and Process II) are considered for producing the intermediate B from two different raw materials C and D. These new technologies exhibit uncertainty in the yields. The yield of Process I and Process II can take 2 discrete values each with equal probability of 0.5. These two realizations of yield for each of Process I and Process II give rise to a total of 4 scenarios (Table 6.1).

The problem consists of finding the expansion and operation decisions for this process network for a 10 year planning horizon so as to minimize the total expected cost of the project. The size of the resulting fullspace model (MLR) and each individual scenario can be seen in Table 6.2 where the optimal expected cost of the problem is $379,070. Notice that there is a significant increase in the total number of constraints for the fullspace MSSP model due to the non-anticipativity requirements.

Table 6.1: 3 Process Network Example (4 Scenarios)

| Scenario | s1 | s2 | s3 | s4 |
|---|---|---|---|---|
| Process I yield | 0.69 | 0.81 | 0.69 | 0.81 |
| Process II yield | 0.65 | 0.65 | 0.85 | 0.85 |
| Scenario Probability | 0.25 | 0.25 | 0.25 | 0.25 |

Table 6.2: Model statistics for the 3 Process Network Example

| Problem Type | Number of Constraints | Continuous Variables | Binary Variables |
|---|---|---|---|
| Reduced Model (MLR) | 1,869 | 845 | 120 |
| Individual Scenario | 192 | 202 | 30 |

After applying the various decomposition approaches, we obtain the results shown in Figure 6.16 and Table 6.3, where an optimality tolerance of 1% and maximum of 30 subgradient iterations (whichever comes first) are used as the termination criteria. It can be observed that the proposed approach (section 6.5.2) using SG2 scenario groups {(1,3),(2,4)} outperforms the other approaches since it yields the tightest lower bound ($378,710) within 2 iterations (see Table 6.3). The lower bound at the root node from the standard approach (section 6.4.1) after many iterations is worse than the initial bound with the proposed approach ($375,880 vs. $377,290). In addition, the best upper bound from the proposed approach is same as the optimal solution ($379,070) whereas the standard approach could only yield the feasible solution with expected cost of $380,880 even after 30 iterations (see Table 6.3). The decomposition approaches based on dualizing all the initial and conditional NACs do not yield good bounds (especially the direct approach (i) in section 6.4.2) compared to the proposed approach with SG2 partitions.

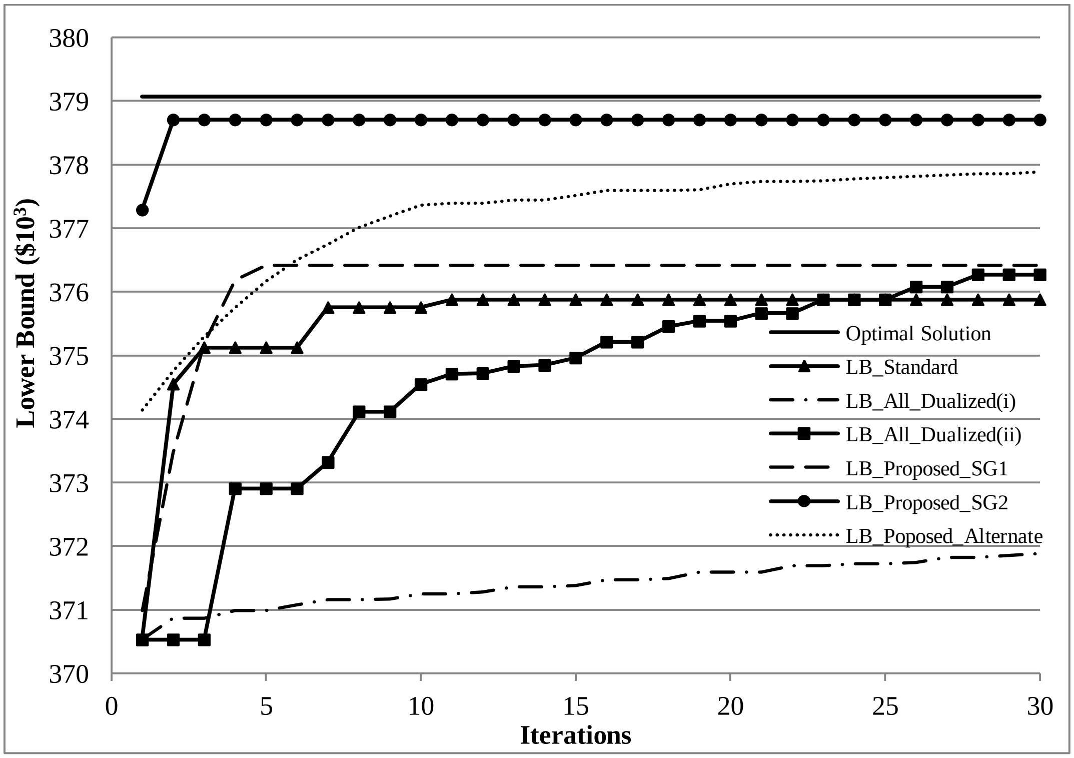


Figure 6.16: Comparison of the various decomposition schemes for 3 process network example

The alternate decomposition (section 6.5.3) using all the 4 scenario groups also performs reasonably well. Since, the total variations in the scenario costs for the scenario group set SG2 {(1,3),(2,4)} is large compared to the scenario group set SG1 {(1,2),(3,4)} ($69,990 vs. $44,590), it yields tighter bounds and faster convergence (see Table 6.4). Notice that the scenario groups in SG1 represent the sensitivity of the Process I yield with respect to the cost, whereas SG2 correspond to the sensitivity of the Process II yield that has a large variance (Table 6.3) and a larger impact on the scenario costs. The MILP models for all the process network examples are implemented in GAMS 23.6.3 and run on Intel Core i7, 4GB RAM machine using XPRESS 21.01 solver.

Table 6.3: Comparison of the various decomposition schemes for 3 Process Network Example

| | Standard | All Dualized (i) direct | All Dualized (ii) indirect | Proposed SG1 | Proposed SG2 | Proposed Alternate |
|---|---|---|---|---|---|---|
| UB ($\$10^3$) | 380.88 | 380.88 | 380.88 | 380.88 | 379.07 | 379.07 |
| LB ($\$10^3$) | 375.88 | 371.88 | 376.27 | 376.42 | 378.71 | 375.75 |
| Solution Time (s) | 8.89 | 5.24 | 9.51 | 5.86 | 0.94 | 2.12 |
| % Gap | 1.33% | 2.42% | 1.22% | 1.19% | <1% | <1% |
| # iterations | 30 | 30 | 30 | 30 | 2 | 4 |

Table 6.4: Variations in the objective function value with uncertain parameters(a) Individual Scenario Costs (b) Scenario groups cost variations

| | Cost ($\$10^3$) |
|---|---|
| s1 | 410.32 |
| s2 | 365.73 |
| s3 | 353.03 |
| s4 | 353.03 |

| | SG1 | SG2 |
|---|---|---|
| s1-s2 | 44.59 | - |
| s3-s4 | 0 | - |
| s1-s3 | - | 57.29 |
| s2-s4 | - | 12.70 |
| Total cost variations ($\$10^3$) | 44.59 | 69.99 |

**Case (ii): Planning of 5 process network over 10 years**

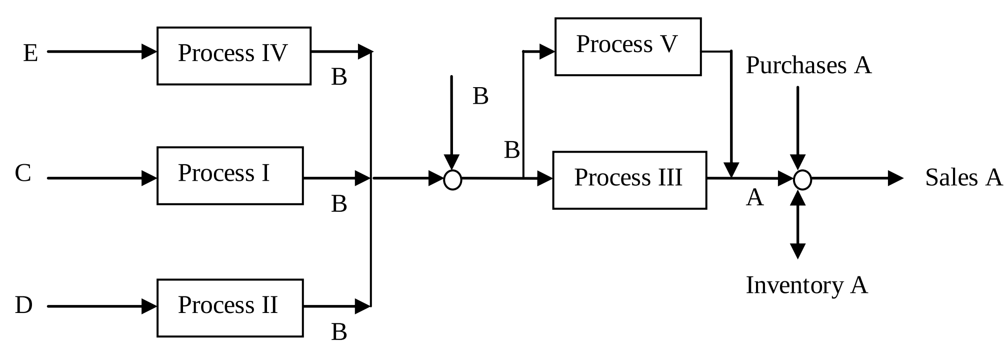


Figure 6.17: 5 Process Network Example

In this instance, we consider a 5 process network (Figure 6.17) having 3 uncertain parameters, i.e. yield of Process I, Process II, and Process V. Here we consider 2 new additional processes compared to the previous example in which

Process IV converts E into B with a yield of 0.75, and Process V that converts B into final product A. Each of the uncertain yields has 2 realizations and gives rise to a total of 8 scenarios with equal probabilities as shown in Table 6.5. The problem consists of finding the expansion and operation decisions for this process network over a 10 year planning horizon to minimize the total expected cost of the project (see chapter 4 for details).

Table 6.5: 5 Process Network Example (4 Scenarios)

| Scenario | s1 | s2 | s3 | s4 | s5 | s6 | s7 | s8 |
|---|---|---|---|---|---|---|---|---|
| Process I yield | 0.69 | 0.81 | 0.69 | 0.81 | 0.69 | 0.81 | 0.69 | 0.81 |
| Process II yield | 0.65 | 0.65 | 0.85 | 0.85 | 0.65 | 0.65 | 0.85 | 0.85 |
| Process V yield | 0.60 | 0.60 | 0.60 | 0.60 | 0.80 | 0.80 | 0.80 | 0.80 |
| Scenario Probability | 0.125 | 0.125 | 0.125 | 0.125 | 0.125 | 0.125 | 0.125 | 0.125 |

To use the proposed decomposition approach for this 8 scenario problem, we partition the scenarios into scenario groups where each one has either 2 or 4 scenarios as in Figure 6.12. These scenario groups are denoted as follows:

(a) SG1: {(1,2),(3,4), (5,6),(7,8)}; SG2: {(1,5),(2,6), (3,7),(4,8)}; SG3: {(1,3),(2,4), (5,7),(6,8)};

(b) SG4: {(1,2,3,4), (5,6,7,8)}; SG5: {(1,2,5,6), (3,4,7,8)}, and SG6: {(1,3,5,7), (2,4,6,8)}

After applying the proposed decomposition approach (section 6.5.2) to these 6 scenario group sets, we can see from Figure 6.18 that the quality of the lower bound improves from \$357,920 (SG1) to \$361,500 (SG6) as the total cost variations for the corresponding scenario group set increases from \$41,000 to \$224,810 as in the previous instance. Moreover, the bound obtained from the larger subproblems having 4 scenarios (SG4, SG5, SG6) is tighter as compared to the subproblems having 2 scenario each as in SG1, SG2 and SG3. This is due to the fact that larger subproblems need only few conditional NACs to be relaxed compared to the smaller subproblems. Table 6.6 and Figure 6.19 compare the progress of the lower bounds, number of iterations and solution time required to reach within 1% of optimality tolerance (or 30 iterations) for the standard and proposed approaches with different scenario partitions. We can observe that scenario group set SG6 outperforms other approaches since it provides the strongest lower bound ($361,500) in just 2 iterations within 8.9s. Moreover, there is a trade-off between the computational cost per iteration and the quality of the bound obtained. It is interesting to note that in most of the cases, even the initial bound using proposed scenario decompositions is much better than the final bound from the standard approach ($355,180) and the rate of convergence to the best possible dual bound is faster.

Table 6.6: Comparison of the standard vs. proposed approach for 5 process network example

| | Standard | Proposed SG1 | Proposed SG2 | Proposed SG3 | Proposed SG4 | Proposed SG5 | Proposed SG6 |
|---|---|---|---|---|---|---|---|
| UB ($\$10^3$) | 364.12 | 364.12 | 364.12 | 364.12 | 364.12 | 364.12 | 364.12 |
| LB ($\$10^3$) | 355.18 | 357.92 | 358.08 | 358.62 | 360.82 | 361.35 | 361.50 |
| Solution Time (s) | 16.32 | 24.59 | 15.38 | 20.40 | 7.63 | 12.44 | 8.9 |
| % Gap | 2.52% | 1.73% | 1.69% | 1.53% | <1% | <1% | <1% |
| # iterations | 30 | 30 | 30 | 30 | 2 | 5 | 2 |

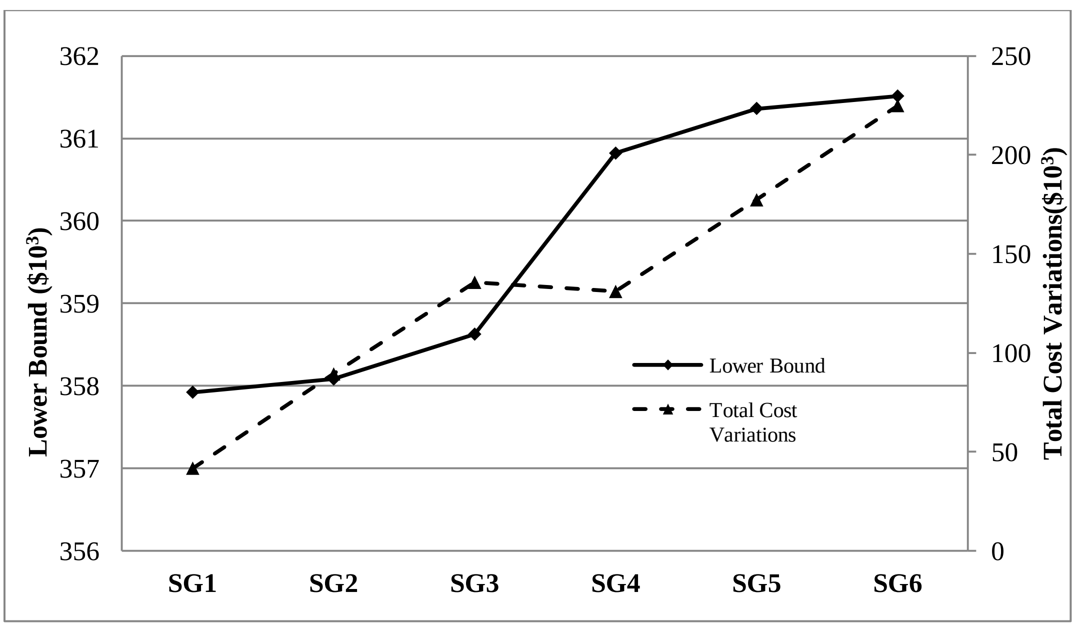


Figure 6.18: Variations in the scenario costs vs. bound obtained for different scenario partitions

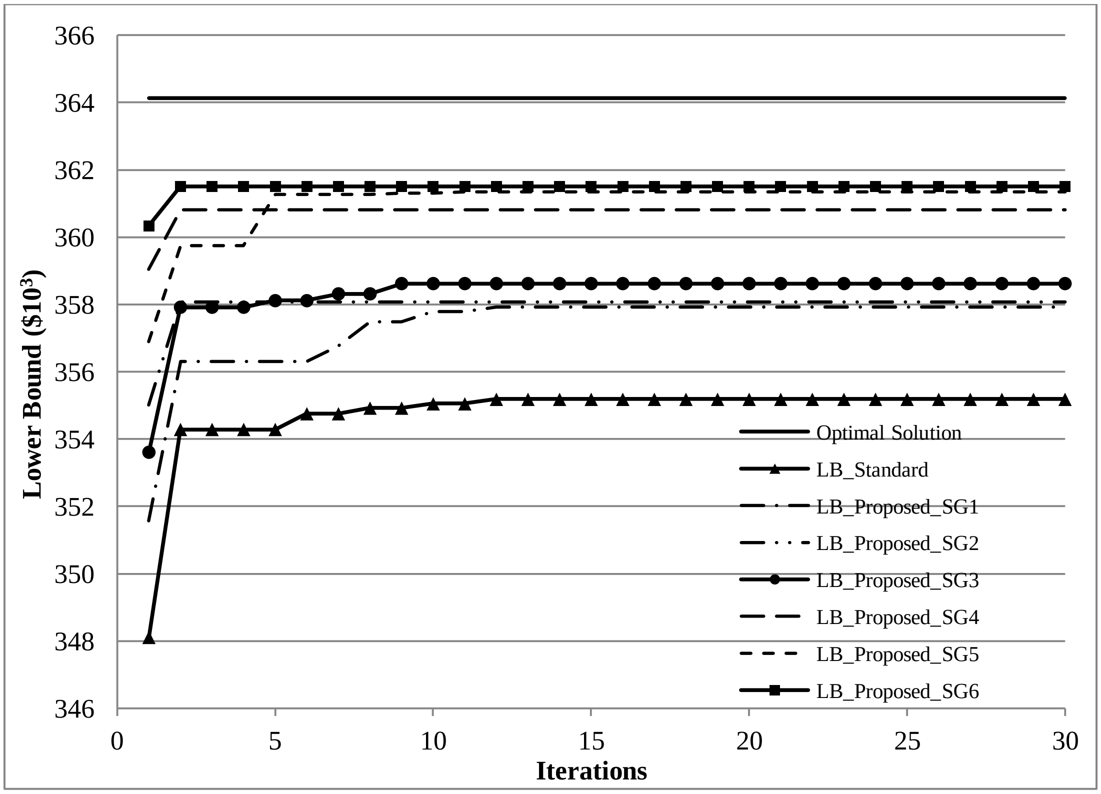


Figure 6.19: Comparison of the standard vs. proposed approach for 5 process network example

### 6.6.2 Oilfield development planning under uncertain field parameters

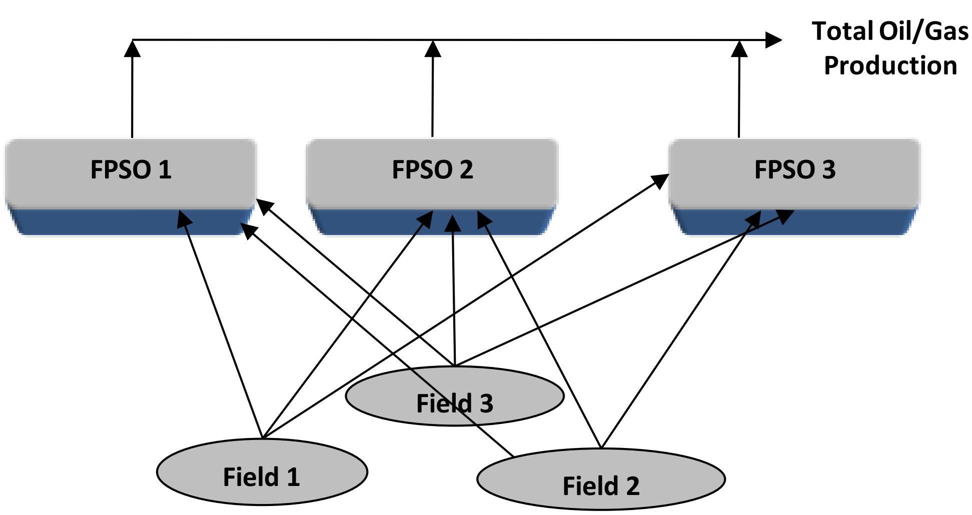


Figure 6.20: 3 oilfield planning example

**Case (i): Uncertainty in the field size only (4 scenarios)**

In this instance, we consider 3 oilfields, 3 potential FPSO's and 9 possible connections among field-FPSO (Figure 6.20). A total of 30 wells can be drilled in the fields and the planning horizon is 10 years. Field 3 has a recoverable oil volume (field size) of 500 MMbbls. However, there is uncertainty in the size of fields 1 and 2 where each one has two possible realizations (low, high) with equal probability. Therefore, there are a total of 4 scenarios each with a probability of 0.25 (see Table 6.7). The problem is to determine the investment (FPSO installations and expansions, field-FPSO connections and well drilling) and operating decisions (oil production rate) for this infrastructure with an objective to maximize the total expected NPV (ENPV) over the planning horizon.

We consider the multistage stochastic MILP model presented in chapter 5 for this oilfield development planning problem, which is an extension of the previous deterministic model presented in chapter 2. The model for all the oilfield planning instances are implemented in GAMS 23.6.3 and run on Intel Core i7, 4GB RAM machine using CPLEX 12.2 solver. The optimal ENPV for this problem is \$11.50 $x10^9$ when the reduced model (MLR) is solved in fullspace, and requires 1184s. Table 6.8 represents the model statistics for this instance.

Table 6.7: 3 Oilfield Example (4 Scenarios), case (i)

| Scenarios | s1 | s2 | s3 | s4 |
|---|---|---|---|---|
| Field 1 Size (MMbbls) | 57 | 403 | 57 | 403 |
| Field 2 Size (MMbbls) | 80 | 80 | 560 | 560 |
| Scenario Probability | 0.25 | 0.25 | 0.25 | 0.25 |

Table 6.8: Model statistics for the 3 Oilfield Example, case (i)

| Problem Type | Number of Constraints | Continuous Variables | Discrete Variables | SOS1 Variables |
|---|---|---|---|---|
| Reduced Model (MLR) | 16,473 | 9,717 | 876 | 240 |
| Individual Scenario | 3,580 | 2,390 | 179 | 60 |

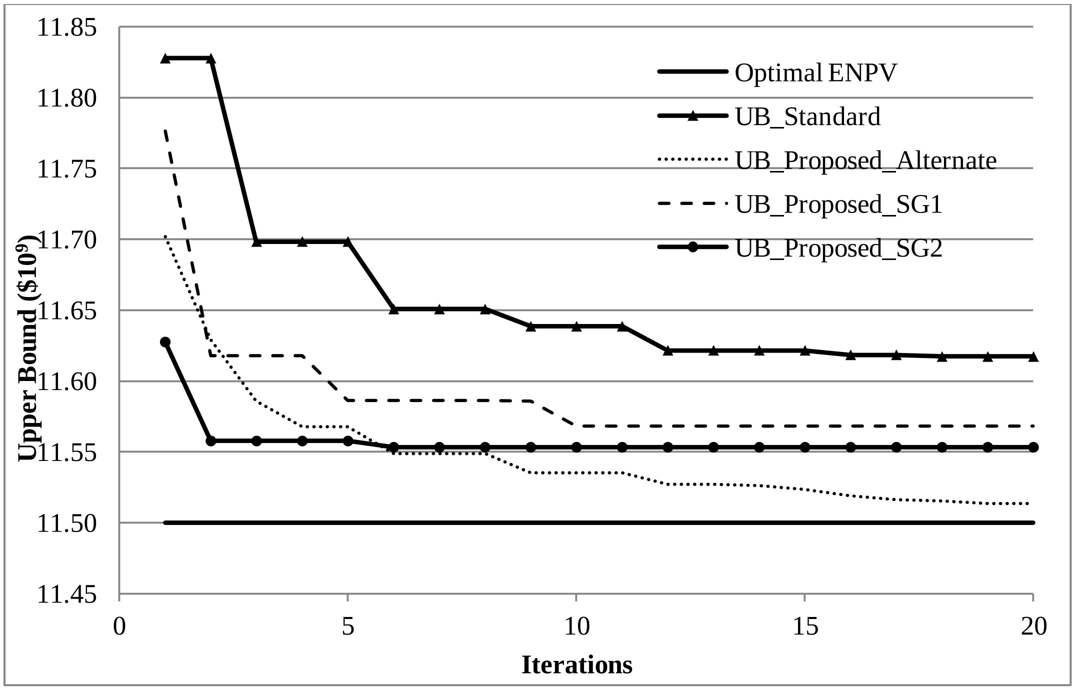


Figure 6.21: Comparison of the various decomposition schemes for oilfield example, case (i)

Figure 6.21 compares the performance of the upper bounds obtained at the root node using standard Lagrangean decomposition based on dualizing the initial NACs and removing the conditional NACs (section 6.4.1) with the decomposition approaches proposed in section 6.5. A termination criterion of either 1% gap or 20 iterations is used. The proposed algorithm based on scenario groups SG1: {(1,2),(3,4)} and SG2: {(1,3),(2,4)} yield stronger upper bounds, $11.59 x$10^9$ and $11.56 x$10^9$ respectively, than the standard Lagrangean decomposition (section 6.4.1) ($11.62 x$10^9$). Additionally, the total computational effort is less with the proposed approach since only 2 subproblems need to be solved at each iteration, and only few iterations are needed to satisfy a 1% of optimality tolerance (Table 6.9). SG2 performs better than SG1 as can be observed from the total variations in the scenario NPVs with respect to the change in the field sizes as calculated in Table 6.10 ($6.63 x$10^9$ vs. $4.77 x$10^9$). This result is similar to the process network example in the previous section. We can also observe that the alternate proposed approach that considers 4 scenario groups (Figure 6.14(c)) performs well but it is more expensive to solve (429s). It is important to see that the quality of upper bound from SG2 is similar in the first iteration with the quality of UB obtained from the scenario subproblems (section 6.4.1) after 20 iterations (see Figure 6.21). Moreover, for clarity we only plotted the progress of the upper bounds with iterations and the optimal NPV in Figure 6.21.

Table 6.9: Comparison of the various decomposition schemes for oilfield example, case(i)

| | Standard | Proposed SG1 | Proposed SG2 | Proposed Alternate |
|---|---|---|---|---|
| UB ($\$10^9$) | 11.62 | 11.59 | 11.56 | 11.58 |
| LB ($\$10^9$) | 11.50 | 11.50 | 11.50 | 11.50 |
| Solution Time (s) | 466 | 382 | 172 | 429 |
| % Gap | 1.02% | <1% | <1% | <1% |
| # iterations | 20 | 5 | 2 | 3 |

Table 6.10: Variations in the objective function value with uncertain parameters, case (i)

(a) Individual Scenario NPV

| | NPV ($\$10^9$) |
|---|---|
| s1 | 8.95 |
| s2 | 11.39 |
| s3 | 12.32 |
| s4 | 14.65 |

(b) Scenario groups NPV variations

| | SG1 | SG2 |
|---|---|---|
| s1-s2 | 2.44 | - |
| s3-s4 | 2.33 | - |
| s1-s3 | - | 3.37 |
| s2-s4 | - | 3.26 |
| Total NPV variations ($\$10^9$) | 4.77 | 6.63 |

**Case (ii): Uncertainty in the field size, oil deliverability, WOR and GOR (4 scenarios)**

In this case we consider uncertainty in the field size, oil deliverability, water-oil ratio (WOR) and gas-oil-ratio (GOR) for oilfields 1 and 2. Notice that oil deliverability, WOR and GOR are represented by the univariate polynomials in terms of the fractional oil recovery as shown in equations (6.11)-(6.13) respectively. The uncertainty in these parameters is characterized by the corresponding parameters $\alpha_o$, $\alpha_w$ and $\alpha_g$. We assume that the uncertain parameters for a field are correlated and uncertainty in these parameters is resolved at the same time. This allows reducing a large number of scenarios. The two possible combinations of these parameters for each field results in a total of 4 scenarios each with a probability of 0.25 as can be seen in Table 6.11. The data for the rest of the problem are as in case (i).

$$Q^d = \alpha_o \cdot g(fc) \tag{6.11}$$

$$wor = \alpha_w \cdot g(fc) \tag{6.12}$$

$$gor = \alpha_g \cdot g(fc) \tag{6.13}$$

Figure 6.22 and Table 6.12 compare the performance of the upper bounds obtained at the root node using standard Lagrangean decomposition (section 6.4.1) with the proposed decomposition approaches and the similar trends can be observed as in the previous instance. SG2 {(1,3), (2,4)} performs best compared to the other approaches due to the stronger initial bound ($12.07x10$^9$). Moreover, since the scenario group set SG2 has a larger total NPV variations ($8.70x10$^9$) than set SG1 {(1,2), (3,4)} ($5.72x10$^9$), it yields a stronger dual bound. Although, SG1 and the alternate approach are somewhat more expensive compared to the standard decomposition approach, they yield a stronger dual bound in a given amount of solution time. This will eventually reduce the total number of nodes in the branch and bound search tree.

Table 6.11: 3 Oilfield Example (4 Scenarios), case (ii)

| Scenarios | | s1 | s2 | s3 | s4 |
|---|---|---|---|---|---|
| Field 1 | Size (MMbbls) | 57 | 403 | 57 | 403 |
| | $\alpha_o$ | 0.75 | 1.25 | 0.75 | 1.25 |
| | $\alpha_w$ | 0.75 | 1.25 | 0.75 | 1.25 |
| | $\alpha_g$ | 0.75 | 1.25 | 0.75 | 1.25 |
| Field 2 | Size (MMbbls) | 80 | 80 | 560 | 560 |
| | $\alpha_o$ | 0.75 | 0.75 | 1.25 | 1.25 |
| | $\alpha_w$ | 0.75 | 0.75 | 1.25 | 1.25 |
| | $\alpha_g$ | 0.75 | 0.75 | 1.25 | 1.25 |
| Scenario Probability | | 0.25 | 0.25 | 0.25 | 0.25 |

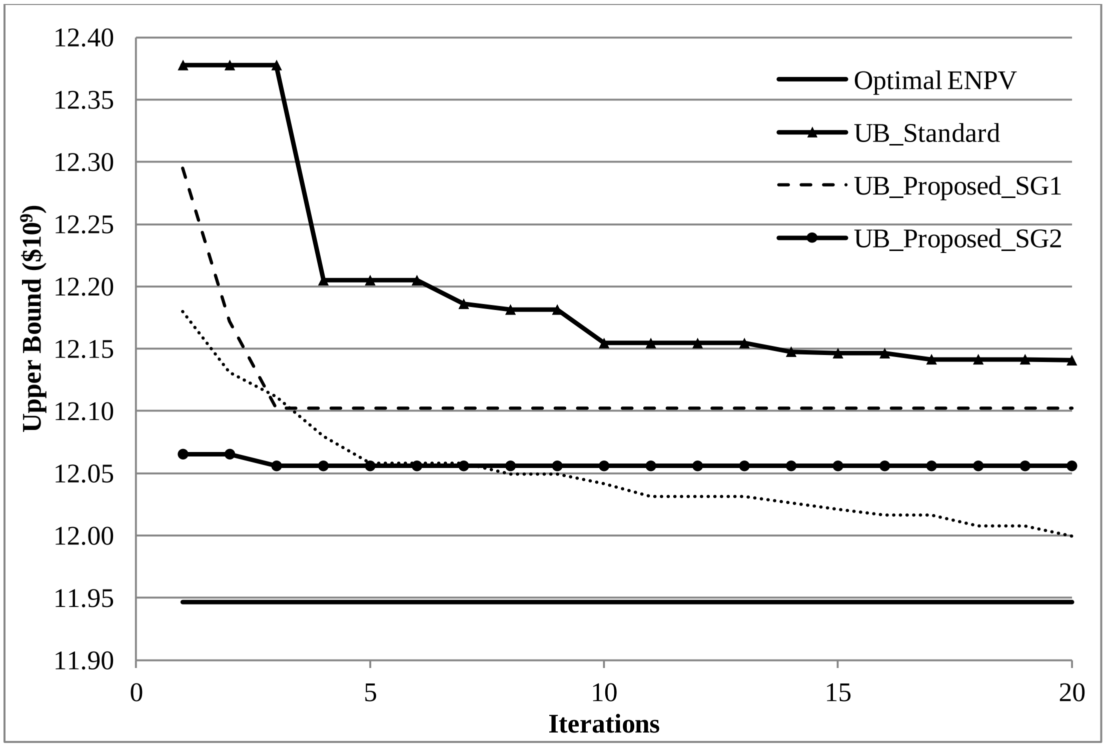


Figure 6.22: Comparison of the various decomposition schemes for oilfield example, case (ii)

Table 6.12: Comparison of the various decomposition schemes for oilfield example, case(ii)

| | Standard | Proposed SG1 | Proposed SG2 | Proposed Alternate |
|---|---|---|---|---|
| UB ($\$10^9$) | 12.14 | 12.10 | 12.07 | 12.06 |
| LB ($\$10^9$) | 11.94 | 11.94 | 11.94 | 11.94 |
| Solution Time (s) | 438 | 1780 | 84 | 1045 |
| % Gap | 1.66% | 1.28% | <1% | <1% |
| # iterations | 20 | 20 | 1 | 5 |

**Case (iii) and (iv): Extension of the cases (i) and (ii), respectively, for 9 scenarios**

In these instances we consider 3 realizations for each uncertain parameter (low, medium, high) compared to two realizations (low, high) in the previous cases (i) and (ii) of oilfield development problem. This results in the corresponding 9 scenario cases (iii) and (iv). Figures 6.23 and 6.24 compare the performance of the dual bounds at the root node from various decomposition schemes for these 3 oilfield and 9 scenario instances, whereas Table 6.13 summarizes the computational results. Since the alternate decomposition (section 6.5.3) is very expensive to solve for these cases, we only compare the proposed approach relying on the scenario groups SG1 {(1,2,3),(4,5,6),(7,8,9)} and SG2 {(1,4,7),(2,5,8),(3,6,9)} with the standard approach (section 6.4.1). We can observe that the initial bound with the proposed strategy (\$11.93 $x10^9$) is much better as compared to the final bound obtained from the standard Lagrangean decomposition at the root node (\$11.96 $x10^9$) for case (iii). It takes only 2 and 1 iterations in cases (iii) and (iv), respectively, for the proposed approach using set SG2 to reach within 1% of optimality tolerance. On the other hand, the standard and the proposed approach with set SG1 cannot reach within this gap even after 20 iterations or a given time limit of one hour.

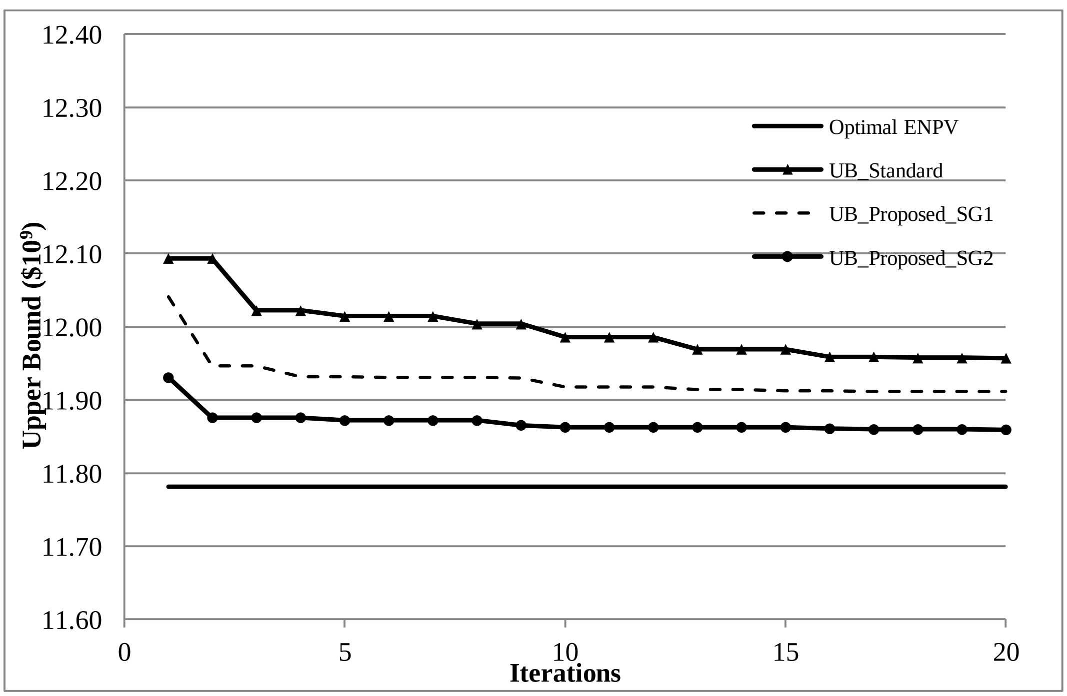


Figure 6.23: Comparison of the various decomposition schemes for oilfield example, case (iii)

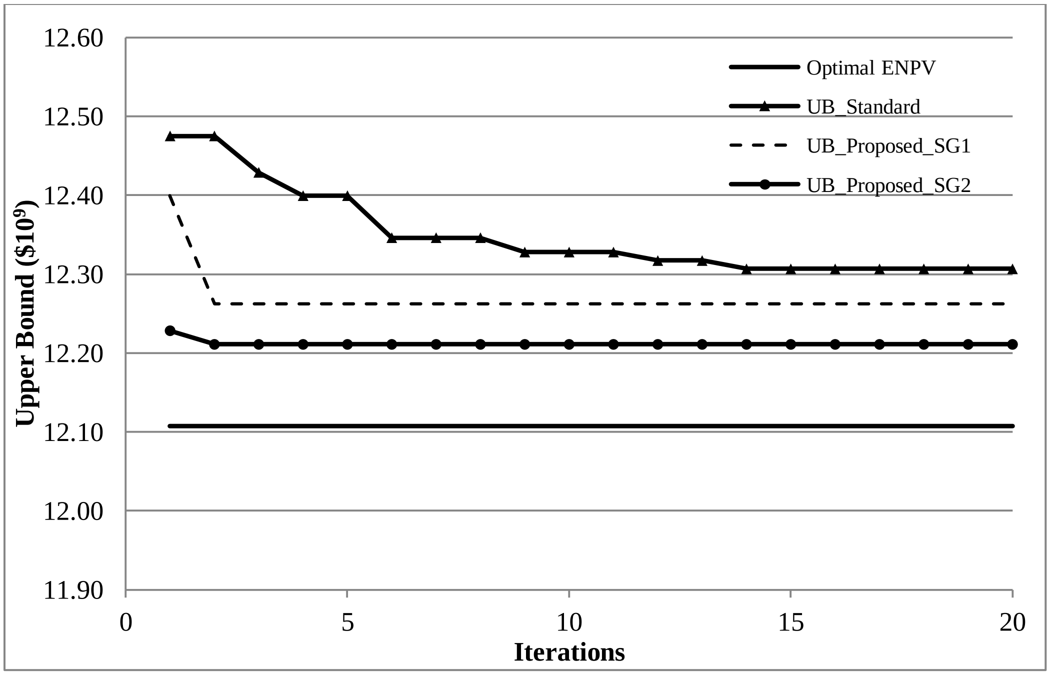


Figure 6.24: Comparison of the various decomposition schemes for oilfield example, case (iv)

Table 6.13: Comparison of the decomposition schemes for oilfield example, case (iii) and (iv)

| | Case (iii) | | | Case (iv) | | |
|---|---|---|---|---|---|---|
| | Standard | Proposed SG1 | Proposed SG2 | Standard | Proposed SG1 | Proposed SG2 |
| UB ($\$10^9$) | 11.96 | 11.92 | 11.88 | 12.31 | 12.26 | 12.23 |
| LB ($\$10^9$) | 11.78 | 11.78 | 11.78 | 12.11 | 12.11 | 12.11 |
| Solution Time (s) | 1327 | >3,600 | 764 | 1542 | >3,600 | 439 |
| % Gap | 1.47% | 1.15% | <1% | 1.62% | 1.27% | <1% |
| # iterations | 20 | 10 | 2 | 20 | 8 | 1 |

***Remarks:***

1. Based on the computational results, we can observe that the selection of a particular scenario group set is critical in the proposed approach such as set SG2 performs better than SG1 in all the instances.
2. The increase in the solution time per iteration with the proposed approach is problem specific. For instance, the increase in the solution time per

iteration for the process networks examples is not that significant as in the oilfield planning problem. Therefore, if the solution time per iteration for a given problem increases drastically using the proposed decomposition, then one may want to use the standard scenario based approach to explore more nodes quickly in the branch and bound search tree or use subproblems with smaller sizes in the proposed approach.

3. In general, for a given amount of the solution time the proposed approach yields better dual bound and feasible solution as can be seen from the numerical experiments. This is due to the fact that the increase in the solution time per iteration is offset by the significant reduction in the total number of iterations resulting in the lesser total solution time.
4. It should be noted that although the initial gap between lower and upper bounds for the examples presented is not very large for the given data set. However, based on Proposition 6.1 and computational experiments, we can conclude that the performance of the proposed approach should be similar for the large gap problems given that we select the scenario group sets as described.

## 6.7 Conclusions

In this chapter, we have proposed a new approach for solving multistage stochastic programs (MSSP) with endogenous uncertainties using Lagrangean decomposition. The proposed approach relies on dividing the fullspace model into scenario groups. Since the number of these scenario groups can be large, there are several alternatives to select a particular set of scenario groups. Therefore, we also presented few rules to identify and formulate a reasonable scenario group set that can be used for the proposed partial decomposition approach within an iterative scheme to update the multipliers. Specifically, the resulting subproblems involve a subset of the NACs as explicit constraints while dualizing and relaxing the rest of these constraints, which enhances the overall performance. An alternate decomposition scheme that may even yield a tighter bound, but usually becomes more expensive for the large cases, is also proposed.

The results on the process network and oilfield planning problems show that the dual bound obtained at the root node from the proposed approaches are stronger than the standard one used in chapters 4 and 5 since the impact of the later time periods is also considered in the subproblems. Moreover, there is a significant reduction in the number of iterations required to converge within a specified tolerance. In most of the cases, even the initial bound with the proposed approach is stronger than the corresponding final bound in the standard approach. Given the tighter bound at the root node, the total number of potential nodes that will be required in the branch and bound search should be smaller and branching rules will be easier to identify. However, the solution time required per iteration in the proposed approach is usually larger as compared to the standard approach, but the difference is problem specific. Therefore, the comparison between the qualities of the bounds obtained within a given amount of solution time should also be considered while selecting a particular decomposition approach for the problems in this class.

# Chapter 7

# Improving dual bound for stochastic MILP models using sensitivity analysis

## 7.1 Introduction

In this chapter, based on the previous work by Tarhan (2009), we introduce a method to improve the dual bound during the solution of a general two-stage stochastic mixed-integer linear programming model using dual decomposition (Carøe and Schultz, 1999) and integer programming sensitivity analysis (Dawande and Hooker, 2000). In particular, the method extracts the relevant sensitivity information from the branch and bound tree of every scenario subproblem, and uses that information to update the Lagrange multipliers and improve the dual bound.

The outline of the chapter is as follows: In section 7.2, we introduce the two-stage stochastic programming model under consideration and the standard Lagrangean decomposition procedure to solve the model in the subsequent section. To overcome the limitations of the standard approach, integer or mixed-integer programming sensitivity analysis methods that will be used are introduced in section 7.4. Sections 7.5 and 7.6 outline the procedure to combine the sensitivity analysis with Lagrangean decomposition to improve the dual bounds of stochastic integer or mixed-integer programming. Section 7.7 illustrates the proposed method with numerical examples and compares it with the conventional subgradient method.

## 7.2 Two-stage Stochastic programming

The main idea behind two-stage stochastic programming (see Figure 7.1) is that we take some decisions (stage 1) here and now based on the possibility of future outcomes of the uncertain parameters. While the rest of the decisions are stage -2 (recourse actions) decisions that are taken after uncertainty in those parameters is revealed (e.g. low, medium or high scenarios). The objective is to minimize the total cost of the first stage decisions and expected cost of the second stage decisions.

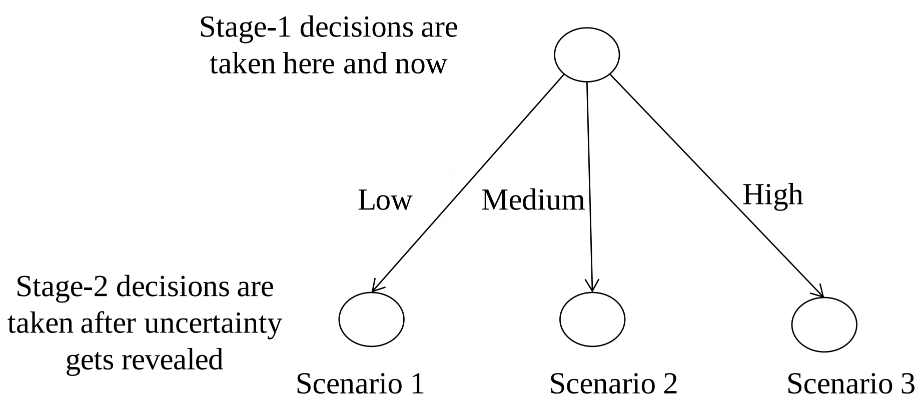


Figure 7.1: Scenario tree for a two-stage stochastic programming

A typical two-stage stochastic mixed-integer linear (MILP) model **(P-MILP)** involves discrete and continuous decisions in the first and/or second stages where all the constraints and objective function are in linear or mixed-integer linear form. Objective function (7.1) is the minimization of the expected cost over all the scenarios s where $p^s$ is the probability of scenario s. First stage decisions $x^s$ are taken here and now, while second stage decisions $y^s$ are taken after the uncertainty is revealed. Constraints (7.2) and (7.3) correspond to each scenario separately. To ensure that the first stage decisions are same for all the scenarios, non-anticipativity (NA) constraints (7.4) are introduced in the model, which makes the problem harder to solve since it couples all the scenarios. Constraints (7.5)-(7.8) define the domain of the first and second stage variables. Reader should refer to the nomenclature section at the end of this chapter.

$$\textbf{(P-MILP)} \qquad \min \quad z = \sum_{s \in S} p^s (cx^s + d^s y^s) \tag{7.1}$$

$$s.t. \quad Ax^s \geq a \quad \forall s \in S \tag{7.2}$$

$$B^s y^s + Tx^s \geq b^s \quad \forall s \in S \tag{7.3}$$

$$x^s = x^{s'} \quad \forall s, s' \in S, s < s' \tag{7.4}$$

$$x_j^s \in Z^+ \quad \forall s \in S, j \in J' \tag{7.5}$$

$$x_j^s \in R \quad \forall s \in S, j \in J \setminus J' \tag{7.6}$$

$$y_k^s \in Z^+ \quad \forall s \in S, k \in K' \tag{7.7}$$

$$y_k^s \in R \quad \forall s \in S, k \in K \setminus K' \tag{7.8}$$

In general industrial planning, scheduling, supply-chain etc. problems under uncertainty are formulated as a two-stage stochastic MILP shown above. These problems become difficult to solve directly in practice since the problem size increases (constraints and variables) with the number of scenarios, whereas the solution time increasers exponentially. Therefore, special solution techniques are used to solve the problems in this class.

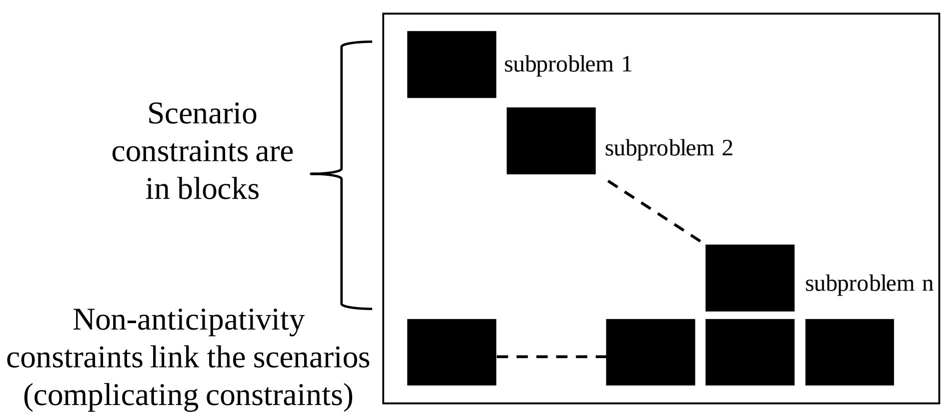


Figure 7.2: Decomposable MILP model structure

Lagrangean decomposition is a widely used technique to solve the problems that have similar decomposable structure as two-stage stochastic MILPs (see Figure 7.2). It exploits the fact that there are certain set of constraints that make the problem harder to solve since it links the different small subproblems. If these constraints are removed the resulting subproblems can be solved independently in an efficient manner. In the case of two-stage stochastic MILPs, non-anticipativity constraints (7.4) are the difficult constraint and each subproblem corresponds to the scenario problem. Therefore, model (P-MILP) has the decomposable structure that is required for the Lagrangean decomposition. In the next section we briefly outline the conventional Lagrangean decomposition procedure.

## 7.3 Lagrangean Decomposition

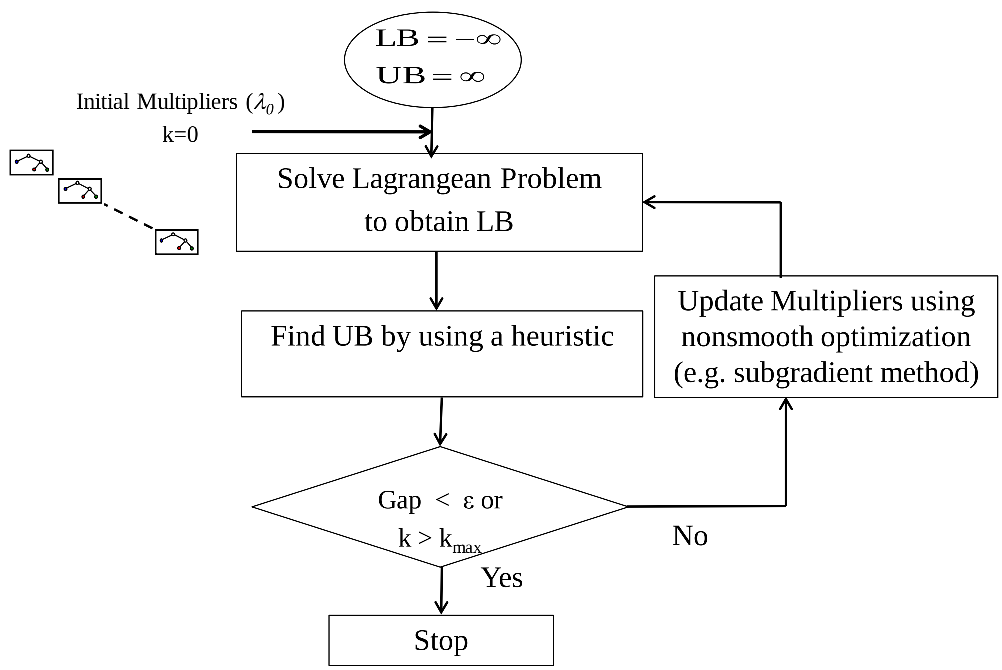


Figure 7.3: Lagrangean Decomposition Algorithm (standard)

The standard Lagrangean decomposition approach involves three steps (see Figure 7.3):

(a) Dualize complicating constraints in the objective function using Lagrangean multipliers $(\lambda)$ to decompose the problem into subproblems

(b) Solve each subproblem independently to obtain the lower bound (LB) on the original problem and use a heuristic procedure to generate the feasible solution i.e. an upper bound (UB)

(c) Based on the subproblem solutions and UB update the Lagrangean multipliers $(\lambda)$ using a non-smooth optimization (e.g. subgradient method) for the next iteration

The procedure is repeated until the gap between upper and lower bound is within a specified tolerance or a maximum iteration limit is reached. Due to the presence of discrete variables, a duality gap may exist. Notice that if we dualize the non-anticipativity constraints (7.4) in the objective function (7.1), problem (P-MILP) decomposes into scenario subproblems **(SP-MILP)** and we can solve it using Lagrangean decomposition.

**(SP-MILP)**

$$\min \quad z = \sum_{s \in S} [(p^s c + \sum_{s<s'} \lambda^{s,s'} - \sum_{s'<s} \lambda^{s',s}) x^s + \quad p^s d^s y^s)] \tag{7.9}$$

$$\text{s.t.} \qquad (7.2), (7.3), (7.5)\text{-}(7.8).$$

The main drawback of the above nonsmooth optimization approach used within Lagrangean decomposition algorithm for MILPs (e.g. 2-stage stochastic) is that only the optimal solution of each subproblem is considered while updating the multipliers in each iteration. All the relevant information generated during branch and bound algorithm while solving each subproblem is discarded. This information could be useful to improve the lower bound efficiently. Therefore, the total number of iterations required to reach convergence within the tolerance limit is usually very large using the standard nonsmooth optimization approach such as subgradient method (Fisher, 1985). In addition, it needs a heuristic procedure to update the step size and an upper bound during each iteration. Overall, it may result in slow convergence of the Lagrangean decomposition algorithm. There has been some work done in this direction e.g. Bundle methods (Lemaréchal, 1974), Volume algorithm (Barahona and Anbil, 2000), etc. However, the improvement in the number of iterations is not very significant using these approaches. Our work is motivated by using more information from each subproblem solution to improve the performance of the Lagrangean decomposition algorithm. The main goals of this work can be summarized as follow:

1. Extract the useful information from the branch and bound tree of each subproblem during Lagrangean decomposition and use it to improve the lower bound efficiently
2. Propose a new Lagrangean decomposition algorithm for MILP models with decomposable structure (e.g. 2-stage stochastic) and benchmark the results against the subgradient method

In the next section, we show that how the integer programming (IP) sensitivity analysis can be used to extract useful information from the branch and bound tree of each subproblem, and how it can further be used in the context of Lagrangean decomposition algorithm to update the multipliers in each iteration. Although we introduce the idea as a possible improvement over current stochastic programming solution methods, the method is fairly general and can be applied to a majority of the problems where Lagrangean decomposition is applicable.

## 7.4 Integer Programming (IP) Sensitivity Analysis

IP sensitivity Analysis (Primal Analysis and Dual Analysis) allow us to find valid tight bounds for the objective function value when the objective function coefficients are perturbed, using the information coming from the branch and bound solution tree.

To understand this, let us consider that ( $P$ ) is the original MILP model whereas ( $\hat{P}$ ) is the perturbed problem after changing the objective function coefficients from ( $c$ ) to ( $c+\Delta c$ ). Given that ( $P$ ) is an MILP, it is solved with a branch and bound (or cut) method. The IP sensitivity analysis can be used to calculate the range of the objective function value of the perturbed problem ( $\hat{P}$ ) without resolving this model. In particular, IP sensitivity analysis involves two parts: Primal analysis and Dual analysis, which provide the upper and lower bounds, respectively, on the perturbed problem ( $\hat{P}$ ).

Original Problem ( $P$ ):

$$\min \quad z = cx \tag{7.10}$$

$$s.t. \quad Ax \geq a \tag{7.11}$$

$$x_j \in Z^+ \quad \forall j \in J' \tag{7.12}$$

$$x_j \in R \quad \forall j \in J \setminus J' \tag{7.13}$$

$$L_j \le x_j \le U_j \quad \forall j \in J \tag{7.14}$$

Perturbed Problem ( $\hat{P}$ ):

$$\min \quad \hat{z} = (c + \Delta c)x \tag{7.15}$$

s.t. (7.11) - (7.14)

Bounds on the perturbed problem using IP sensitivity analysis:

$$LB \le \hat{z} \le UB \tag{7.16}$$

Dual Analysis    Primal Analysis

### 7.4.1 Primal Analysis

When the IP or MIP problem is solved using the branch and bound method, each leaf node belongs to one of the following three sets of nodes (Figure 7.4):

$N_1$: Set of nodes pruned by optimality (feasible integer solutions. e.g. node 3)

$N_2$: Set of nodes pruned by bound (non-integer feasible solutions. e.g. node 1)

$N_3$: Set of nodes pruned by infeasibility (leaf nodes pruned by infeasibility. e.g. node 4)

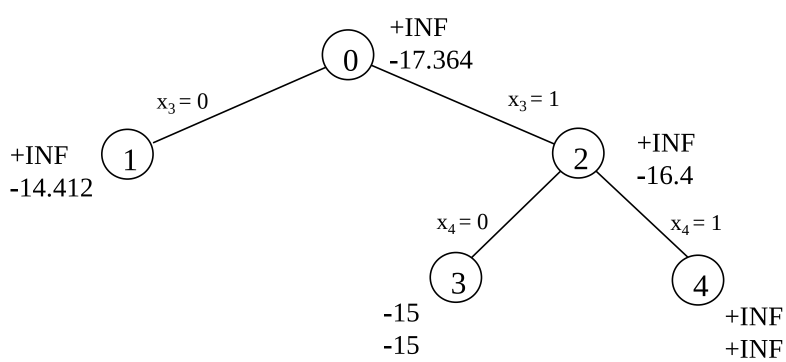


Figure 7.4: A typical branch and bound solution tree for MILP

Primal Analysis says that the feasible solutions at any node in $N_1$ stays feasible (but not necessarily optimal) when the objective function coefficients change to ( $c + \Delta c$ ). The best feasible solution is the minimum of the available solutions. Therefore, the tightest upper bound on the objective function value of the perturbed problem ( $\hat{P}$ ) can be obtained by solving the following optimization problem **(PA-LP)** that uses the information from the feasible nodes ($N_1$) of the branch and bound solution tree of the original problem ( $P$ ).

**(PA-LP)**

$$\max \quad UB \tag{7.17}$$

$$s.t. \quad UB \le z_n + \sum_{j \in J} v_j^n \Delta c_j \quad \forall n \in N_1 \tag{7.18}$$

In particular, for the given optimal values of the variables $x_j$ at node $n$ (i.e. $v_j^n$ ) and perturbations $\Delta c_j$ the problem can be solved for the tightest upper bound ($UB$) on the perturbed problem. However, it should be noted that during the proposed method $\Delta c_j$ will be treated as a variable instead of a parameter to obtain the desired perturbations.

### 7.4.2 Dual Analysis

Dual analysis involves a set of linear constraints **(DA-LP)** that give the maximum amount of decrease in the objective function value ( $\Delta z \ge 0$ ) when the objective function coefficients are perturbed from $c$ to $c + \Delta c$, see Dawande and Hooker (1998) for details. In particular, the analysis states that the lower bound on the objective function value of the perturbed problem ( $\hat{P}$ ), i.e. $\hat{z} \ge z - \Delta z = LB$, remains valid if we can find free variables $r_n$ and $s_j^n$ that satisfy the constraints (7.19)-(7.24).

**(DA-LP)**

$$\sum_{j \in J} \Delta c_j \underline{v}_j^n - s_j^n (\overline{v}_j^n - \underline{v}_j^n) \ge -r_n \quad \forall n \in N_1 \cup N_2 \tag{7.19}$$

$$r_n = -\sum_{j \in J} q_j^n \overline{v}_j^n + \overline{\lambda}^n a - z_n + \Delta z \quad \forall n \in N_1 \tag{7.20}$$

$$r_n = -\sum_{j \in J} q_j^n \overline{v}_j^n + \overline{\lambda}^n a - \overline{z}_n + \Delta z \quad \forall n \in N_2 \tag{7.21}$$

$$s_j^n \ge -\Delta c_j \quad \forall j \in J, \forall n \in N_1 \cup N_2 \tag{7.22}$$

$$s_j^n \ge -q_j^n \quad \forall j \in J, \forall n \in N_1 \cup N_2 \tag{7.23}$$

$$\text{where} \quad q_j^n \quad = \overline{\lambda}^n A - c \tag{7.24}$$

Notice that the parameters $\underline{v}_j^n$ (lower bound on variables), $\overline{v}_j^n$ (upper bound on variables) $\overline{\lambda}^n$ (shadow price of the constraints), $z_n$ (objective value) and $\overline{z}_n$ (incumbent solution) at node $n$ are obtained from the branch and bound solution tree of the original problem ( $P$ ). In addition to calculating the possible decrease in the objective function value ( $\Delta z \geq 0$ ) for a given change in the objective function coefficients ( $\Delta c$ ), the analysis also allows us to find the possible perturbations $\Delta c$ that are allowed for a given value of $\Delta z$ .

## 7.5 Application of IP Sensitivity Analysis for Multiplier Updating in Two-stage Stochastic Programs

In this section, we explain how we combine the above integer programming sensitivity analysis to extract the information from the branch and bound solution tree of each scenario subproblem, and then update the multipliers during Lagrangean decomposition for a two-stage stochastic MILP program. Notice that here we consider two-stage stochastic MILPs having decomposable structure to illustrate the proposed approach, but the method is general and can be applied to any MILP model involving similar structure such as multistage stochastic, large scale MILPs.

First, we can observe that in each iteration of the Lagrangean decomposition algorithm (Figure 7.3) we update the multiplier values that only appear in the objective function coefficients and resolve the resulting subproblems. Therefore, eventually only the objective functions coefficients are perturbed during each iteration (e.g. eq. (7.9)). This perturbation in the objective function coefficients has direct correspondence to the perturbation that is explained in the IP sensitivity analysis section above. For instance eq. (7.9) and (7.15) yield eq. (7.25).

$$\Delta c^s = \sum_{s<s'} \lambda^{s,s'} - \sum_{s'<s} \lambda^{s',s} \tag{7.25}$$

In addition, we also know that the integer programming sensitivity analysis provides LB and UB on the perturbed problem objective value without resolving it, by using the information from branch and bound tree of the original problem.

Based on these observations we extract the information required for sensitivity analysis from the branch and bound tree of each subproblem during Lagrangean decomposition. This additional information, rather than just the optimal solution, can be used to construct a linear program that allow us to search for those perturbations in the objective function coefficients (i.e. $\Delta c^s$ ) for the next iteration that can potentially give us better directions and step size. The resulting perturbations from such a linear program can therefore improve the lower bound in an efficient manner than a simple nonsmooth optimization method.

**(SA-LP)** $\max \quad w_1 UB \quad + \quad w_2 LB$ (7.26)

$$s.t. \quad UB = \sum_s UB_s \tag{7.27}$$

$$UB_s \le \hat{z}_n^{s,k} + \sum_{j \in J} v_j^{n,s,k} \Delta c_j^s \quad \forall s \in S, \forall n \in N_1^{s,k}, k \in \{1,2,3..k\} \tag{7.28}$$

$$LB = \sum_s (z^s - \Delta z^s) \tag{7.29}$$

$$\sum_{j \in J} \Delta c_j^s \underline{v}_j^{n,s} - s_j^{n,s} (\overline{v}_j^{n,s} - \underline{v}_j^{n,s}) \ge -r_n^s \quad \forall s \in S, \forall n \in N_1^s \cup N_2^s \tag{7.30}$$

$$r_n^s = -\sum_{j \in J} q_j^{n,s} \overline{v}_j^{n,s} + \overline{\lambda}^{n,s} a - z_n^s + \Delta z^s \quad \forall s \in S, \forall n \in N_1^s \tag{7.31}$$

$$r_n^s = -\sum_{j \in J} q_j^{n,s} \overline{v}_j^{n,s} + \overline{\lambda}^{n,s} a - \overline{z}_n^s + \Delta z^s \quad \forall s \in S, \forall n \in N_2^s \tag{7.32}$$

$$s_j^{n,s} \ge -\Delta c_j^s \quad \forall s \in S, \forall j \in J, \forall n \in N_1^s \cup N_2^s \tag{7.33}$$

$$s_j^{n,s} \ge -q_j^{n,s} \quad \forall s \in S, \forall j \in J, \forall n \in N_1^s \cup N_2^s \tag{7.34}$$

$$\text{where} \quad q_j^{n,s} = \overline{\lambda}^{n,s} A - c \tag{7.35}$$

$$\left| \Delta c_j^s \right| \le \gamma \max_{j \in \bar{J}} \left| c_j^s \right| \quad \forall j \in \bar{J}, \forall s \in S \tag{7.36}$$

Therefore, the main idea now is to formulate such a multiplier updating linear program **(SA-LP)** that maximizes a weighted sum of upper and lower bounds generated by primal and dual analysis (7.26), while taking into account the branch and bound tree information of the subproblem solutions from the previous iteration. The reason for maximizing the sum of tightest possible upper bound for each scenario is to move in the direction that overall improves the lower bound on the original problem based on the feasible nodes that have been explored so far. The idea to maximize the sum of lower bounds is to reduce the possibility of decrease ($\Delta z \geq 0$) in the current lower bound on the original problem. This corresponds to minimizing the risk of finding a worse solution when the model is re-optimized after the objective function coefficients are changed to the values proposed by the method.

The proposed linear program (SA-LP) involves linear constraints (7.27)-(7.28) and (7.29)-(7.35) that correspond to the primal and dual analysis, respectively. The additional restriction (7.36) on the search space for the perturbations is included to keep the LP solution bounded considering the fact that all the feasible solutions for each subproblem are usually not explored in branch and bound method and therefore the search space may be too relaxed. In particular, we bound the $\left|\Delta c_j^s\right|$ value to be less than or equal to a fraction ($\gamma$) of the maximum of the absolute value of objective function coefficients $\left|c_j^s\right|$ corresponding to the duplicated variables to keep the search space neither very restrictive nor relaxed.

Notice that the accumulation of the feasible nodes ($N_1$) generated during the previous iterations ($k$=1,2,….*k-1*) in the form of additional cuts (i.e. constraints (7.28)) ensures that the search space for the new perturbations is restricted to only to what has not been explored so far. It may potentially reduce the oscillations in the lower bounds in successive iterations and reduce the number of iterations required, while ensuring convergence. Notice that both $\Delta c^s$ and $\Delta z^s$ are variables in the model that allow us to obtain the optimal multipliers values considering the trade-offs associated with the potential improvement in the lower bound on the original problem while minimizing the risk of deteriorations in the current lower bound for these perturbations. The subjective parameters values ($w_1, w_2, \gamma$) are explained in the results section.

## 7.6 Proposed Lagrangean Decomposition Algorithm

In comparison to the standard nonsmooth optimization method for multiplier updating, the proposed Lagrangean decomposition algorithm for two-stage stochastic programming involves solution of the linear program (SA-LP) during each iteration as can be seen from Figure 7.5. Particularly, the proposed algorithm allows us to extract the information from the branch and bound solution tree of each subproblem using IP sensitivity analysis, and uses that information constructively in the LP problem so that a better estimate of the Lagrangean multipliers can be obtained as compared to a simple nonsmooth optimization method.

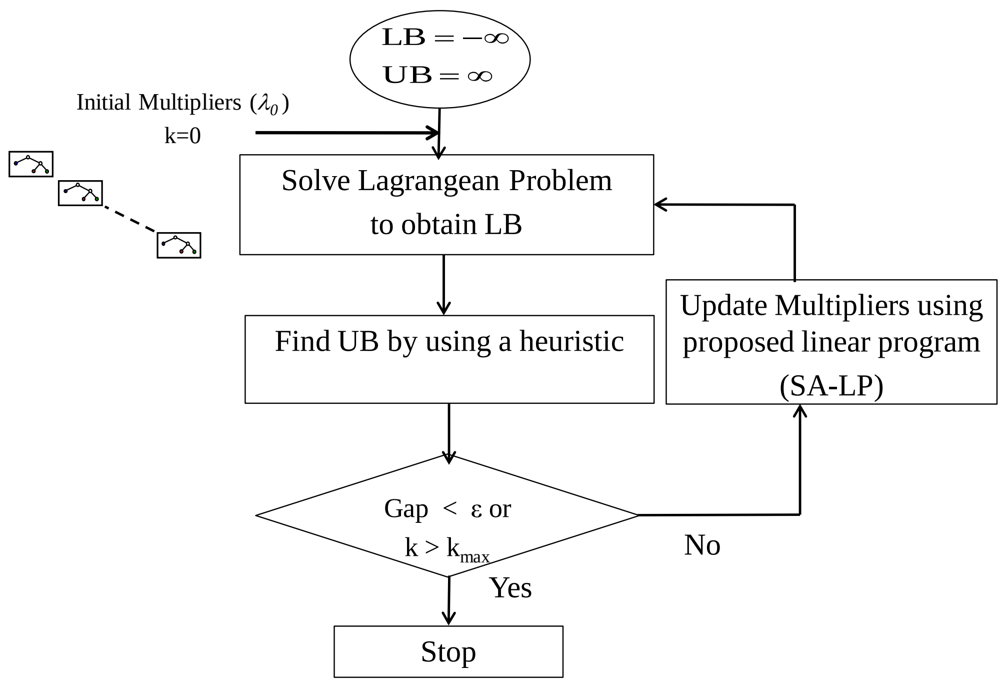


Figure 7.5: Lagrangean Decomposition Algorithm (proposed)

Therefore, the algorithm has the potential to reduce the number of iterations and the corresponding solution time, especially when each subproblem solution (MILPs) is expensive. Moreover, it can also be applied to other decomposable

MILPs. In the next section, we investigate the performance of the proposed algorithm as compared to the subgradient method for two examples of two-stage stochastic MILP models. Notice that we are not focusing on feasible solution (UB) generation during this work since the idea is to improve the lower bound efficiently. The upper bound can be calculated by using an efficient heuristic procedure. In addition, comparison of the algorithm performance is in terms of number of iterations since a basic branch and bound implementation is used for subproblem solutions.

## 7.7 Numerical Results

### 7.7.1 Example 1

We consider a two-stage stochastic integer program (7.37)-(7.42) from Carøe and Schultz (1999) with uncertainty in the right-hand side of the constraints, i.e. parameters $(\xi_1, \xi_2)$. Two instances of the problem involving 3 and 50 scenarios are generated based on the values of the uncertain parameters. The sizes of the deterministic equivalent models are presented in Table 7.1. In the 3 scenario instance, it is assumed that the uncertainty is represented by the three scenarios $(\xi_1, \xi_2) = \{(5,8), (10,7), (15,12)\}$ with each one being equally likely. The optimal solution of the problem with 3 scenarios is -64.33. For the larger instance having 50 scenarios, parameters have been sampled randomly and each scenario is assumed to have equal probability.

$$\min \quad -1.5x_1 - 4x_2 + \sum_{s \in S} p^s Q^s(x_1, x_2) \tag{7.37}$$

$$s.t. \qquad (x_1, x_2) \in [0,5] \cap Z^+ \tag{7.38}$$

$$Q^s(x_1, x_2) = \min -16y_1^s - 19y_2^s - 23y_3^s - 28y_4^s \tag{7.39}$$

$$s.t. \qquad 2y_1^s + 3y_2^s + 4y_3^s + 5y_4^s \le \xi_1^s - x_1 \tag{7.40}$$

$$6y_1^s + 1y_2^s + 3y_3^s + 2y_4^s \le \xi_2^s - x_2 \tag{7.41}$$

$$y_1^s, y_2^s, y_3^s, y_4^s \in \{0,1\} \tag{7.42}$$

Table 7.1: Model statistics (deterministic equivalent) for Example 1 instances

| Scenarios | Discrete Variables | Continuous Variables | Constraints | First Stage Variables | Second Stage Variables |
|---|---|---|---|---|---|
| 3 | 18 | 0 | 12 | 6 | 12 |
| 50 | 300 | 0 | 2,550 | 100 | 200 |

In the proposed method, the sensitivity problem (SA-LP) is used to update the multipliers during each iteration of the Lagrangean decomposition. In particular, after solving each scenario independently all the necessary data ( $N_1^s, N_{2,}^s z^s, z_n^s, \bar{z}_n^s, v_{j,n}^{n,s}, \underline{v}_j^{n,s}, \bar{v}_j^{n,s}, \bar{\lambda}^{n,s}, q^{n,s}$ ) for the sensitivity problem are extracted and used in the model (SA-LP) to optimize. The result of the sensitivity problem (SA-LP) proposes the multipliers ( $\lambda^{s,s'}$ ) and the resulting objective function coefficients ( $\Delta c_j^s$ ) that improve the dual bound. After some experience with the method on a number of instances, we have set using the weights in the objective function as $w_1 = 10 w_2$ and the value of parameter $\gamma = p^s$ in eq. (7.36) throughout all the examples.

On the other hand, during the subgradient iterations, a step length is calculated using the solutions of scenario subproblems and prediction of the optimal objective function value. Since we try to make the comparison between methods as fair as possible, we have employed the optimal solution of the example as predicted solution during the calculation of the stepsize in the subgradient optimization. This gives subgradient method an advantage, but if the proposed method performs better even under these conditions, then it will be a clear evidence for potentially better performance in actual situations.

Both the methods are implemented in AIMMS 3.11 and problems are solved using CPLEX 12.2 solver for all the instances. The initial multipliers are assumed to be zero for both the approaches. The first subgradient iteration corresponds to solving each scenario subproblem individually, which is also required for generating the data for the model SA-LP. The methods have been compared over iterations instead of solution time. The main reason is that during the time of implementation, it was not possible to collect some of the necessary information for SA-LP using a commercial solver via callbacks. In order to extract the necessary information, such as $\overline{\lambda}^{n,s}$ values, a simple branch and bound procedure has been implemented. Since, it would not be fair to compare our branch and bound implementation with a commercial one, we decided performing a comparison over iterations. The time difference between the two approaches occurs since the subgradient method uses a simple arithmetic operation to update multipliers whereas in SA-LP a relatively more time consuming LP is optimized. However, for all the instances solved the additional time needed for solving such LP is just a few seconds. The proposed method improves the bound to −65.983 in 3 iterations for this 3 scenario instance (Table 7.2(b)) whereas the subgradient method reaches to the same bound in 70 iterations (Table 7.2(a)). Therefore, extracting useful sensitivity data from the branch and bound procedure at each iteration, and utilizing them within the SA-LP model, cuts down the number of iterations needed to achieve same bound.

Table 7.2: Results for example 1 with 3 scenarios

(a) Subgradient Method

| Iteration Number | Lower Bound |
|---|---|
| 1 | -69.5 |
| 14 | -68.536 |
| 22 | -67.345 |
| 28 | -67.037 |
| 32 | -66.344 |
| 47 | -66.00 |
| 70 | -65.983 |

(b) Proposed Method

| Iteration Number | Lower Bound |
|---|---|
| 1 | -69.5 |
| 2 | -66.9 |
| 3 | -65.983 |

The same problem was scaled up for 50 scenarios. The optimal solution of the problem is −65.30. As shown in Figure 7.6, the proposed method improved the bound to −66.775 in 6 iterations, while the subgradient method provides a dual bound of −66.761 in 75 iterations. Therefore, the method outperforms the subgradient method in terms of the number of iterations.

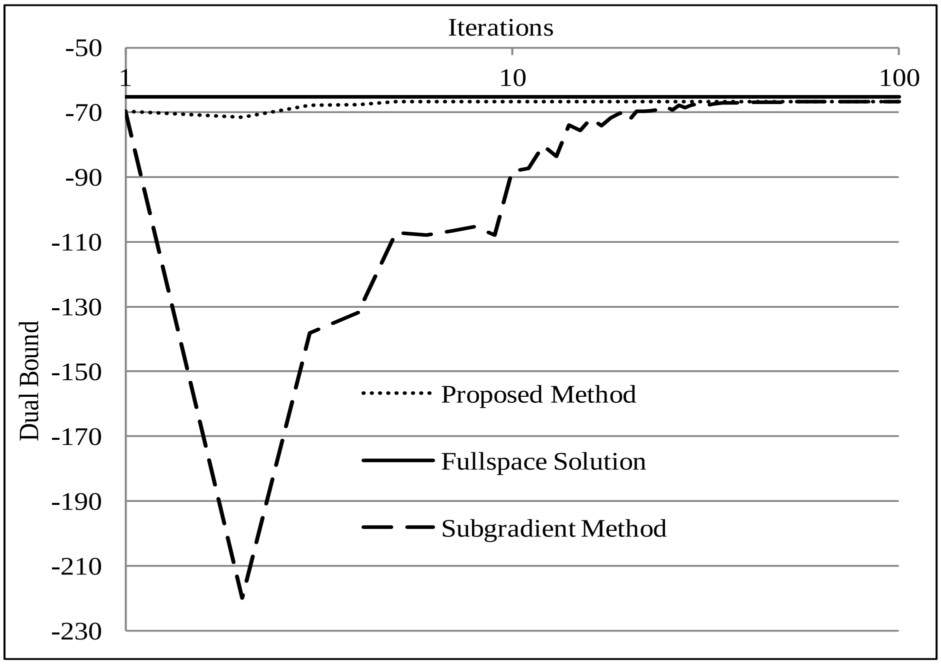


Figure 7.6: Results for example 1 with 50 scenarios (Proposed vs. Subgradient method)

### 7.7.2 Example 2 (Dynamic Capacity Allocation Problem (DCAP))

We investigate the performance of the proposed algorithm on Dynamic Capacity Allocation Problem (DCAP) which is formulated as a two-stage stochastic MILP. Data and problem details are adapted from Ahmed and Garcia (2003). This problem has mixed-integer first-stage variables, pure binary second-stage variables, and discrete distributions of the uncertain parameters. Uncertainty is in the coefficient matrix of the constraints. Table 7.3 represents the sizes of the deterministic equivalents for 2 problem instances (10 and 200 scenarios). Notice that the fullspace problem is modeled in the extensive form considering NA constraints (7.4).

Both instances (10 and 200 scenarios) are initially solved as fullspace problems that yield the solutions 1571.682 and 1756.592, respectively. Given the decomposable structure of this two-stage stochastic MILP problem, it is also solved using the subgradient method as well as the proposed method. The results in Figures 7.7 (a)-(b) show that the convergence of the subgradient method is relatively slow and it takes more than 200 iterations to converge to the best possible lower bound for both the instances.

Table 7.3: Model statistics (deterministic equivalent) for Example 2 (DCAP) instances

| Scenarios | Discrete Variables | Continuous Variables | Constraints | First Stage Variables | Second Stage Variables |
|---|---|---|---|---|---|
| 10 | 330 | 60 | 840 | 120 | 270 |
| 200 | 6,600 | 1,200 | 2,44,800 | 2,400 | 5,400 |

In contrast, the proposed method converges in less than 10 iterations to yield the solution of similar quality as the subgradient method for both the instances. This more than an order of magnitude reduction in the number of iterations, is due to the fact that during the subgradient method only the optimal solution of the scenario subproblems is used to update the multipliers, whereas the proposed method solves a linear program formulated using the information from the branch and bound tree of each subproblem solution and search in the space of multipliers. Notice that we use a higher weight on primal analysis as compared to the dual analysis ( $w_1 = 10$ and $w_2 = 1$ ) and restrict the search space for perturbation based on the probability of the scenario (i.e. $\gamma = p^s$ ) during the proposed method as in the previous example.

**Remarks:**

The solution time of the proposed linear program is negligible as compared to the solution time of MILP subproblem. Therefore, the reduction in the number of iterations using the proposed method dominates the additional cost of solving the LP problem at each iteration. Moreover, for the models where each subgradient iteration is expensive to perform due to many MILP subproblems to be solved at each iteration, the proposed method can potentially decrease the total solution time significantly since it reduces the number of iterations.

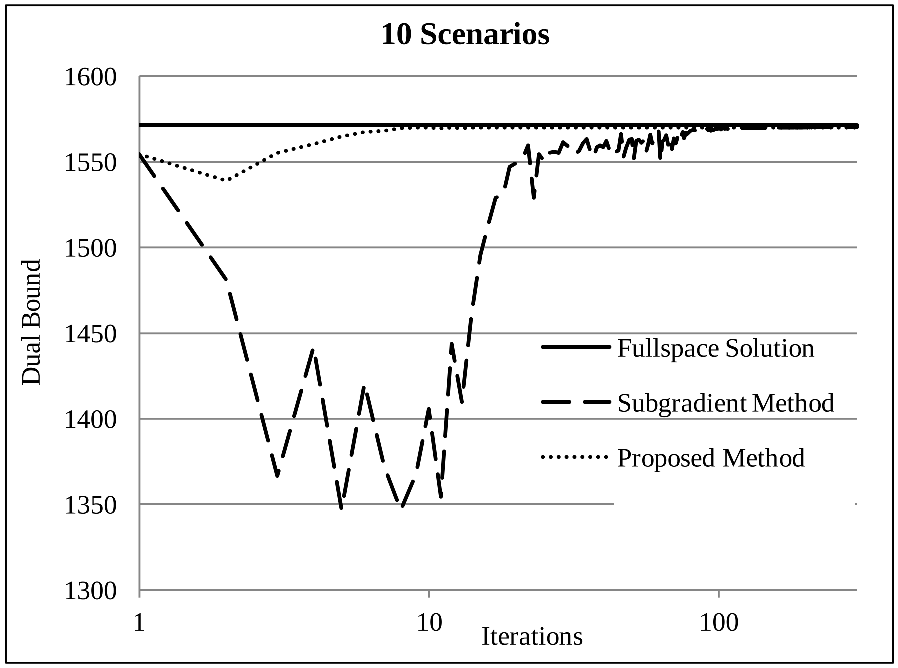


(a) 10 Scenario instance

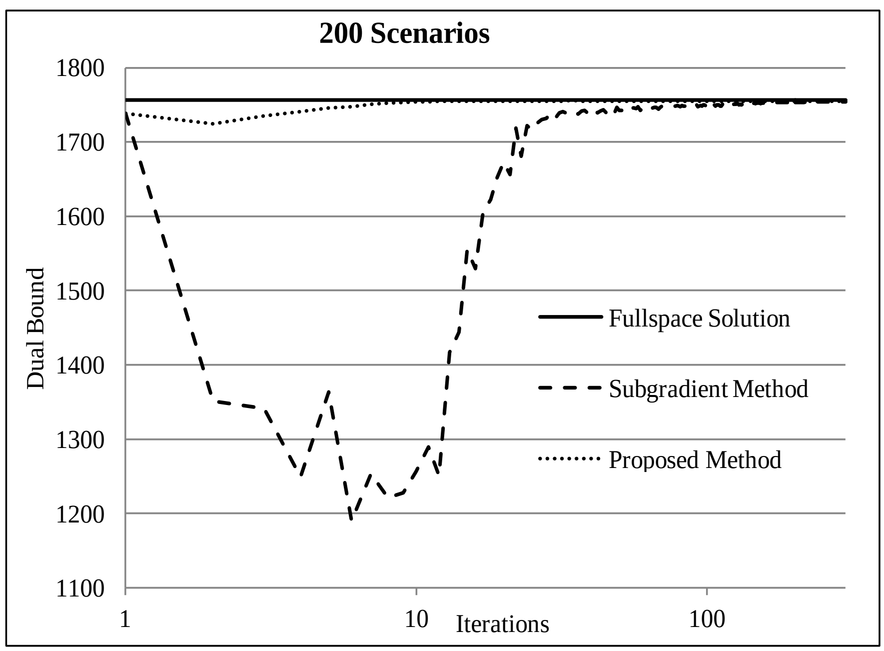


(b) 200 Scenario instance

Figure 7.7: Results for example 2 (Proposed vs. Subgradient method)

However, similar to other nonsmooth optimization methods, the proposed method has some arbitrary components such as the weights assigned to primal ( $w_1$ ) and dual ( $w_2$ ) bound in the objective function of SA-LP. The value of these weights depends on the user's experience with the proposed method. As explained during the numerical examples, these weights were fixed as $w_1 = 10w_2$. Our experience shows that the method performs well for various instances with weights fixed at those values. We believe although such values are a good starting point, more insight will be gained as the method is applied to other problems.

Moreover, there is a direct relation between the relative weight assigned to the dual bound and the fraction of all feasible solutions explored in search tree. If most of the feasible solutions are explored during the search process, then the weight on dual bound can be much lower than weight on primal. In such a case, for any value of ( $\Delta c_j^s$ ) the optimal solution is most likely be one of the feasible solutions already explored in the search tree. Since in practice we do not enumerate all possible solutions during the branch and bound search, we need a nonnegative value for the dual weight and some bounds on ( $\Delta c_j^s$ ).

## 7.8 Conclusions

In this chapter, we have proposed a method for improving the dual bound of decomposable MILP models using IP sensitivity analysis. In particular, a new linear program is proposed based on the ideas of primal and dual analysis that uses the information from branch and bound tree of each subproblem solution during Lagrangean decomposition, and yields improved multipliers that results in faster convergence of the algorithm. Based on the computational experiments on two-stage stochastic MILPs, the method outperforms standard subgradient method in terms of number of iterations (more than an order of magnitude reduction). Given that a large number of subproblems (MILPs) are solved during each iteration of the Lagrangean decomposition algorithm, the reduction in the number of iterations can result in significant potential computational savings where optimizing each of these subproblem takes a long time. Moreover, the algorithm can be applied to more general classes of MILPs such as multistage stochastic models, and MILPs with decomposable structure.

## Nomenclature

$A$ : matrix of constraint coefficients.

$a$ : vector of right-hand-side coefficients.

$c$ : vector of objective function coefficients.

$\Delta c_j$ : change in the objective function coefficient corresponding to variable $x_j$

$J$ : set of variables.

$j$ : element of set $J$ .

$S$ : set of scenarios.

$s, s'$ : element of the set $S$ .

$LB$ : lower bound for the optimal solution of problem ( $\hat{P}$ ).

$N_1$ : set of leaf nodes pruned by optimality in branch and bound tree.

$N_2$ : set of leaf nodes pruned by bound in branch and bound tree.

$N_3$ : set of leaf nodes pruned by infeasibility in branch and bound tree.

$n$ : element of sets $N_1 \cup N_2 \cup N_3$ .

$r_n$ : free variable.

$s_j^n$ : free variable.

$UB$ : upper bound for the optimal solution of problem ( $\hat{P}$ ).

$v_j^n$ : optimal value of variable $x_j$ at node $n$ .

$\bar{v}_j^n$ : upper bound for variable $x_j$ at node $n$ .

$\underline{v}_j^n$ : lower bound for variable $x_j$ at node $n$ .

$x_j$ : continuous or discrete variable.

$x$ : vector of variable $x_j$ .

$z_n$ : objective function value of node n in branch and bound tree.

$\bar{z}_n$ : incumbent solution used for pruning node $n$ .

$z$ : optimal objective function value of the original model ( $P$ ).

$\hat{z}$ : optimal objective function value of the perturbed model ( $\hat{P}$ ).

$\Delta z$ : maximum allowable change in the objective function value. ( $\Delta z \geq 0$)

$\bar{\lambda}^n$ : vector of Lagrange multipliers found at node n during branch and bound algorithm.

$\gamma$ : parameter used for setting a bound on the change in the objective function coefficients.

# Chapter 8

# Conclusions

In this thesis, we have developed new mixed-integer optimization models and solution strategies for optimal development planning of offshore oil and gas field infrastructure. Particularly, we considered a multi-field site with realistic information in the planning such as fiscal rules of the agreements with the host government and endogenous uncertainties in the field parameters. In chapters 2 and 3, we have proposed the deterministic models for the problem with/without fiscal considerations. In chapter 4, we have presented a general multistage stochastic programming framework and solution approaches for the endogenous uncertainty problems, where timing of uncertainty realization is decision-dependent. The deterministic oilfield planning models are then extended in chapter 5 to include uncertainty in the field parameters relying on the ideas from chapter 4. To improve the quality of the bounds during Lagrangean decomposition in chapters 4 and 5, a new decomposition scheme is proposed in chapter 6. Finally, in chapter 7 we introduced a new method for improving the dual bound generated during the solution of a general two-stage stochastic mixed-integer linear program.

## 8.1 An efficient multiperiod MINLP model for optimal planning of offshore oil and gas field infrastructure

In chapter 2 we presented a novel deterministic mixed-integer nonlinear programming (MINLP) model for offshore oil and gas infrastructure planning. As compared to the previous work, the proposed realistic model considers multiple fields, three components (oil, water and gas) explicitly in the formulation, facility expansions decisions in the future, drilling rig limitations and nonlinear reservoir profiles with an objective to maximize the net present value for the enterprise. The decisions involve installation and expansion schedule of FPSO facilities and respective oil, liquid and gas capacities, connection between the fields and FPSO's, well drilling schedule, and production rates of oil, water and gas in a multiperiod setting to consider a long-term planning horizon incorporating several economic trade-offs.

The major nonlinearities in the model are univariate polynomials and bilinear terms (both involving continuous and discrete variables). In order to solve the problem reliably, especially for the instances when more complex features are incorporated into the model such as fiscal rules or uncertainties in the following chapters, we first proposed to reformulate the MINLP formulation (Model 1) using two new properties (see Appendix A). Using integration, the properties allow representing the reservoir profiles in terms of the cumulative water and cumulative gas produced as univariate polynomials rather than water-oil ratio and gas-oil ratio and corresponding bilinear terms. Therefore, the new MINLP (Model 2) has nonlinearities only in term of the univariate polynomials and bilinear terms involving discrete variables. The reformulation allows converting the MINLP model to an MILP approximation (Model 3). In particular, the Model 2 has been reformulated into an MILP using piecewise linearization and exact linearization techniques with which the problem can now be solved to global optimality in a more consistent manner. The proposed MINLP and MILP formulations are further improved by using a binary reduction scheme based on the assumption that the connection costs are relatively small compared to the other costs.

In terms of the numerical experiments on the proposed models, we considered 3 realistic oilfield development instances involving up to 10 fields, 3 FPSO's and 20 years planning horizon. The models were implemented in GAMS 23.6.3 and run on Intel Core i7 machine. In the first instance, we considered 3 oil fields, 3 FPSOs, a total of 25 wells and the planning horizon of 10 years. Based on the computational results, we observed that DICOPT performs best among other MINLP solvers (e.g. SBB) in terms of computational time for Models 1 and

2. The number of OA iterations required was approximately 3-4 in both cases, and solving Model 2 was slightly easier than solving Model 1 directly with this solver. However, the solutions obtained were not guaranteed to be the global solution. The global solver BARON 9.0.6 took more than 36,000s to be within ~10% of optimality gap even for this small instance. The binary reduction scheme allowed one third reduction in the number of binary variables for both models and a significant decrease in the solution time. In contrast, the MILP Model 3 and its binary reduction Model 3R that are formulated from Model 2 and Model 2R, respectively, solved with CPLEX 12.2 and results showed the significant reduction in the solution time after binary reduction (6.55s vs. 37.03s), while both the models gave the same optimal NPV i.e. $7030.90M. Notice that the approximate MILP models are solved to global optimality in few seconds, while global solution of the original MINLP formulations is much more expensive to obtain. The MILP solution was further used to improve the quality of local solutions obtained from the MINLP formulations. Similar trends were observed for the other two larger instances.

Therefore, it can be concluded that while the proposed MINLP models may sometimes lead to near optimal solutions, the MILP approximation is an effective way to consistently obtain these solutions. These MILP solutions also provide a way to assess the quality of suboptimal solutions from the MINLPs, or finding optimal or near optimal solutions by using the discrete decisions from this model. None of the MINLP solvers could find better solutions than the ones obtained using the MILP solution within a certain amount of time. Moreover, the solutions from the convex MINLP solvers can be sub-optimal when we extend it to more complex cases (chapter 3), and they cannot provide any guarantees of the valid upper bound in the Lagrangean decomposition unless each subproblem is solved to global optimality (chapter 5). Therefore, we used the MILP model for including complex fiscal rules and/or uncertainties in the subsequent chapters.

The results of the chapter led to many challenges that need to be addressed. The global solution of the proposed MINLP models is expensive using a state-of-the-art solver directly. Therefore, the models can be used as a basis to develop global optimization based approaches even though the MINLP solvers that rely on convexity assumption can yield good solutions in an ad-hoc manner. The MILP approximate model can be solved to global optimality using more reliable commercial MILP solvers. However, the solution time for the realistic instances is still large, especially if we consider many point estimates for the polynomials. Therefore, a more reliable approximation scheme or a decomposition approach such as a bi-level decomposition algorithm can be investigated to reduce the total computational effort while maintaining the solution quality.

## 8.2 Modeling and computational strategies for optimal development planning of offshore oilfields under complex fiscal rules

In chapter 3, we extended the deterministic models presented in chapter 2 for offshore oil and gas field infrastructure planning to incorporate complex fiscal rules of the agreements with the host government. In particular, we considered progressive production sharing agreements with ringfencing provisions in the proposed general model so that it can be used as a basis to represent a variety of contracts used in the industry. The fiscal model considers the trade-offs between optimal investment and operating decisions and resulting NPV for the oil company after paying government share, and yields improved decisions compared to a simple NPV based optimization used in chapter 2. However, the major challenge with this extension is that the computational expense increases significantly mainly due to the progressive nature of the profit share, and the ringfencing provisions. In particular, additional binary variables need to be introduced to represent the tiers that define the progressive terms, and the relaxation of the model is generally weak due to the absence of the good bounds on the variables. Therefore, we have also proposed a tighter formulation (Model 3RF-L) by introducing additional logic constraints and valid inequalities in the model that improve the relaxation and reduce the branch and bound search tree. Heuristic approaches that relax and approximate the sliding scale terms, Model

3RI and Model 3RI-A, respectively, in the form of simple linear inequalities are also proposed to obtain the reasonable solutions for the large instances.

To illustrate the impact of the fiscal terms and the proposed approaches, we considered three instances of the realistic oilfield planning problem involving progressive production sharing agreements. The models were implemented in GAMS 23.6.3 and run on Intel Core i7, 4GB RAM machine using CPLEX 12.2. Instance 1 did not involve ringfencing provisions, while instances 2 and 3 were solved with and without ringfencing provisions to illustrate the additional computational cost associated to these provisions. The first instance considered 3 fields, 3 FPSOs, a total of 25 wells that can be drilled, and 15 years planning horizon. The sequential approach that first maximizes NPV, i.e. Model 3, and then calculates the contractor share based on these decisions and fiscal rules yields a total NPV of $1362.67M, which is significantly lower than the optimal solution ($1497.69M) of the model with fiscal considerations (Model 3F). In addition, investment and operating decisions were also very different, i.e. mostly front ended in the case of sequential approach. This is due to the optimistic nature of the sequential approach that tries to generate as much revenue as possible at the beginning of the planning horizon, neglecting the trade-offs that are associated to the fiscal part. Therefore, it may lead to the decisions that can incur large losses in the long term after considering the impact of the fiscal calculations since higher tiers (higher tax rates) become active in the earlier years during the planning horizon. Model 3RF which is obtained after binary reduction from Model 3F yields the same solution in an order of magnitude less time (337s vs. 3,359s). In contrast, solving the corresponding MINLP formulation Model 2F with BARON 9.0.6 could only provide a solution having NPV of $1198.44M with a 60% gap in more than 10 hours. Moreover, we observed that solving Model 2F directly with DICOPT requires a good initialization due to the additional binary variables and constraints that are added in this fiscal model compared to Model 2. Therefore, the optimal solution from the corresponding MILP formulations (Model 3F and Model 3RF) provides optimal or near optimal solutions of the original Model 2F. We fixed the design decisions in Model 2F from the optimal solution of Model

3RF, and solved the resulting NLP problem that yields an NPV of $1496.26 M, which shows that the accuracy of the MILP solution is within 0.1% of the MINLP formulation. Therefore, the proposed MILP formulations performed very efficiently and provided near optimal solutions.

Similarly, significant savings and different decisions were obtained with fiscal considerations during planning for instance 2 having 5 fields and 20 years of time horizon. The tighter formulation Model 3RF-L is solved in one fourth of the time than Model 3RF. The relaxed Model 3RI was solved more than 20 times faster than the original Model 3RF, while the approximate Model 3RI-A took only 82s as compared to Model 3RF (1164s), and yielded the optimal solution after we fixed the decisions from this model in the original one. Both the relaxed and approximate models were even ~3 times faster than the model without any fiscal terms (Model 3R) that took 190s. We also considered two ringfences for instance 2 where progressive PSA terms were defined for each of these ringfences separately. We observed that including ringfencing provisions made Model 3RF expensive to solve (>10 hrs) compared to the one without any ringfences that required only 1,164s. This is due to the additional binary variables that were required in the model for each of the two ringfences, their trade-offs and FPSO cost disaggregations. In contrast, since Models 3RI and 3RI-A did not require binary variables for the sliding scale in disjunction (3.30), they solved much faster than Model 3RF (>300 times faster) and Model 3RF-L (~30 times faster). Preliminary results on a bi-level decomposition approach were also presented for this instance that provided the rigorous bounds on the objective function value for the fiscal model involving ringfencing provisions. The largest instance we solved involves 10 oil fields, 3 FPSOs, a total of 84 wells, 20 years planning horizon, and 3 ringfences.

The main conclusion that can be drawn from this chapter is that the explicit consideration of the fiscal rules is important for the oilfield infrastructure planning instead trying to solve a simple NPV based model to global optimality, since it may yield a completely different solution and significant improvement in the net present value.  This is due to the fact that the royalties and/or government profit oil share that result from a particular contract can represent a significant amount of the gross revenues (~50% or more). Therefore, it is critical to consider these contracts explicitly during the oilfield planning phase to assess the actual economic potential of such a project. Moreover, the mathematical programming model presented in this chapter is the first one in the literature that considers progressive fiscal terms with ringfencing provisions and can serve as a basis to further develop more efficient solution approaches.

## 8.3 Solution strategies for multistage stochastic programming with endogenous uncertainties in the planning of process networks

In chapter 4, we presented a general multistage stochastic mixed-integer linear programming model for multiperiod planning problems where optimization decisions determine the times when the uncertainties in some of the parameters will be resolved, i.e. decision-dependent uncertainty (Jonsbraten et al., 1998; Goel and Grossmann, 2006; and Tarhan and Grossmann, 2008). The model involves initial and conditional non-anticipativity constraints in terms of the equalities and disjunctions, respectively, to enforce the same decisions among the scenarios in time period t if they are in the same state. Since, the number of NACs increases exponentially with the number of uncertain parameters and/or their realizations, realistic problem instances becomes intractable to solve. To reduce the required NACs in the model, we have identified a new Property 3 that together with two properties previously presented by Goel and Grossmann (2006), significantly reduces the problem size and the solution time. In particular, the property exploits the transitivity relation among the scenarios and can be considered as an extension to the previous properties to those cases where each uncertain parameter has more than two realizations.

The resulting reduced model still may be too large to solve directly. Therefore, we have proposed a *k*-stage constraint strategy that yields the global optimum in particular cases, and is useful for problems where endogenous uncertainty is revealed during the first few time periods of the planning horizon.

To solve more general problems of large size, we also proposed a NAC relaxation strategy based on relaxing the NA constraints and adding them if they are violated. It has been observed that very few inequality NA constraints (~6-7% of the total inequality NA constraints in the reduced model) are added as cuts in the complete solution procedure that involves two phases. As compared to the branch-and-cut solution method by Colvin and Maravelias (2010), the proposed NAC relaxation strategy is much easier to implement using the available commercial solvers directly, although there might be some trade-offs between these solution strategies in terms of the solution times. Finally, we described a Lagrangean decomposition algorithm that relaxes the conditional NACs and dualize the initial NACs to decompose the model into individual scenarios, and predicts rigorous lower bounds for the optimal solution. Notice that in contrast to the method presented by Goel and Grossmann (2006), no branch and bound method is performed here with which the dual gap may not be closed for the problem. Therefore, if the gap between lower and upper bounds is large then in principle we would have to also incorporate a branch and bound procedure to reduce this gap. In our experience, however, we have observed that for problems in this class a good feasible solution is often found at the root node itself.

The proposed solution strategies have been applied to two process network problems having uncertainty in the process yields that can only be revealed once an investment is made in the process. The first problem that involves 3 processes is taken from Goel and Grossmann (2006) but with more realizations for the uncertain parameters, i.e. a total of 25 scenarios. The second larger example has 5 processes and there are 4 uncertain parameters with 81 scenarios. This problem could not be solved in the fullspace for the original model and even after using Property 1. The solution time with only considering Properties 1-2 (Goel and Grossmann, 2006) is 1.5 times more than the solution time from using Properties 1-3 proposed in the chapter since the model has fewer NACs. The *k*-stage constraint model and the NAC relaxation strategy take significantly less time (~70% less) than the reduced model. The Lagrangean decomposition strategy is most efficient in terms of the solution time but terminates with a gap of ~3.5%.

However, it is only up to moderate size problems that the *k*-stage constraint strategy and the NAC relaxation strategy may perform better than Lagrangean decomposition strategy because of the tight lower bounds and corresponding better solutions obtained in these cases. However, for realistic instances Lagrangean decomposition has the advantage that it allows solving each scenario independently. The two-stage stochastic model corresponding to this example gives about 5% higher total expected cost ($387,421 vs. $368,650) due to the absence of appropriate recourse for the investment decisions in the model. The total expected cost is about 3-6 % higher for the expected value problem (EVP) in comparison to the multistage stochastic programming model for all the cases considered. Notice that the proposed solution strategies are fairly general and can be applied to a wide range of problems having endogenous uncertainty in some of the parameters such as oilfield development planning.

## 8.4 Multistage stochastic programming approach for offshore oilfield infrastructure planning under production sharing agreements and endogenous uncertainties

In chapter 5, we presented a multistage stochastic programming model for offshore oil and gas field development planning that maximizes the expected NPV for the given planning horizon. The model is an extension of the deterministic models presented in chapters 2 and 3 considering decision-dependent uncertainty in the field parameters, which resolves as a function of investment and operating decisions as ones in chapter 4. As compared to the conventional models in the literature where either fiscal rules or uncertainty in the field parameters are considered, the proposed model is the first one that includes both of these complexities simultaneously in an efficient manner. In particular, a tighter formulation for the production sharing agreements based on chapter 3, and correlation among the endogenous uncertain parameters (field size, oil deliverability, water-oil ratio and gas-oil ratio) are considered that reduce the total number of scenarios in the resulting multistage stochastic formulation. To solve large instances of the problem, the Lagrangean decomposition approach proposed in chapter 4 was implemented with parallel solution of the scenario subproblems with up to 8 processors. Notice that in practice the model needs to be solved not just once for the entire planning horizon, but multiple times in a rolling horizon manner with updated information.

The model was implemented in GAMS 23.6.3 and ran on Intel Core i7, 4GB RAM machine using CPLEX 12.2 solver. Computational results on a variety of oilfield development planning examples with/without fiscal considerations have been presented to illustrate the efficiency of the model and the proposed solution approach. In particular, the first example considered 3 oilfields, 3 potential FPSO's and 9 possible connections among field-FPSO. A total of 30 wells could be drilled in the fields and the planning horizon was 10 years. However, there was uncertainty in the sizes of 2 fields that resulted in a total of 4 scenarios each with a probability of 0.25. The optimal scenario-tree from the proposed model was decision-dependent, which was not known a-priori. In particular, more wells were drilled in the favorable scenarios compared to the unfavorable ones. We also observed that the problem solved to ~1% optimality tolerance within only 466s using Lagrangean decomposition compared to the fullspace model that takes 1184s. However, the solution of the expected value problem, considering mean value of the field sizes, is $\$11.28 \times 10^9$ with which the value of stochastic solution for this case is $\$220 \times 10^6$ or ~2%. We also considered the extension of 3 oilfield instance to the case where we included the progressive production sharing agreements with 15 years of planning horizon. The resulting fullspace model became very difficult to solve with CPLEX 12.2 since the best solution obtained after 10 hours is $\$2.97 \times 10^9$ with more than 21% of optimality gap. On the other hand, Lagrangean decomposition could solve this problem in approximately 2 hrs for sequential implementation of the scenario subproblem solutions and in about 1 hr for a parallel implementation involving 8 processors, and yielded a higher ENPV $\$3.04 \times 10^9$ within 0.7% optimality tolerance.

Therefore, the importance of the decomposition algorithm, especially the one with parallel solution of the scenario subproblems, increases as more complexities are added to the deterministic problem such as fiscal contracts. Similar trends were also obtained for the large instance involving 5 fields and 20 years of planning horizon. In particular, only the parallel implementation could solve the problem within a limit of 10hrs of solution time. Notice that the MILP model allows using robust and advanced commercial solvers to solve the problem globally, and also to use the Lagrangean decomposition with valid bounds which may have been difficult if one considers the original MINLP formulation. However, based on the computational results, it is still challenging to solve the large instances involving many scenarios or fiscal contracts with progressive terms and ringfencing provisions.

## 8.5 A new decomposition algorithm for multistage stochastic programs with endogenous uncertainties

The Lagrangean decomposition approach presented in chapters 4 and 5 may perform reasonably well for a certain class of problems with a given set of data. However, due to the limitations of the quality of the dual bound obtained at root node with this approach, since conditional NACs are relaxed, we have proposed a novel decomposition approach in chapter 6 for solving a general multistage stochastic mixed-integer linear programming model with endogenous uncertainties. In particular, we considered type 2 endogenous uncertainty problems where decisions are used to gain more information, and resolve uncertainty either immediately or in a gradual manner. Therefore, the resulting scenario tree is decision-dependent and requires modeling a superstructure of all possible scenario trees that can occur based on the timing of the decisions as can be seen in chapters 4 and 5. In contrast to the standard approaches that either relax or dualize all conditional NACs that appear as big-M constraints in the model, the proposed approach relies on dividing the fullspace model into scenario groups. Due to the several possible alternatives to formulate the scenario groups, we presented few rules to identify and formulate a reasonable scenario group set that can be used for the proposed partial decomposition approach within an iterative scheme to update the multipliers. In particular, the resulting subproblems involve a subset of the NACs as explicit constraints, while dualizing and relaxing the rest of these constraints, which enhances the overall performance. An alternate decomposition scheme that may even yield a tighter bound, but usually becomes more expensive for the large cases, has also been proposed.

The computational results have been presented on two process network examples (chapter 4) and four instances of an oilfield planning problem (chapter 5). The process networks examples involve 3 and 5 processes with 4 and 8 scenarios, respectively. The results show that the dual bound obtained at the root node from the proposed approach are significantly stronger than the standard one used in chapter 4 since the impact of the later time periods is also considered in the subproblem formulations. Moreover, there is a significant reduction in the number of iterations required to converge within a specified tolerance. In both the cases, even the initial bound with the proposed approach is stronger than the corresponding final bound in the standard approach. We also observed that the selection of a particular scenario group set is critical in the proposed approach such as set SG2 performs better than SG1 in both instances since it involves large variations in the corresponding scenario costs. The results on the oilfield problem having 3 oilfield and scenarios ranging from 4 to 9 in cases (i)-(iv), also showed similar trends.

Since, we obtained a tighter bound at the root node with the proposed approach, the total number of potential nodes that will be required in the branch and bound search should be smaller and branching rules should be easier to identify. However, the solution time required per iteration in the proposed approach is usually larger as compared to the standard approach, but the difference is problem specific. For instance, the increase in the solution time per iteration for the process networks examples is not that significant as in the oilfield planning problem. Therefore, if the solution time per iteration for a given problem increases drastically using the proposed decomposition, then one may want to use the standard scenario based approach to explore more nodes quickly in the branch and bound search tree or use subproblems with smaller sizes in the proposed approach. In general, for a given amount of the solution time the proposed approach yields better dual bound and feasible solution as can be seen from the numerical experiments in the chapter. This is due to the fact that the increase in the solution time per iteration is offset by the significant reduction in the total number of iterations resulting in lower total solution time. Overall, the comparison between the qualities of the bounds obtained within a given amount of solution time should also be considered while selecting a particular decomposition approach for the problems in this class.

## 8.6 Improving dual bound for stochastic MILP models using sensitivity analysis

In chapter 7, based on the previous work by Tarhan (2009), we have introduced a method to improve the dual bound during the solution of a general two-stage stochastic mixed-integer linear programming model that appears in several planning, scheduling and supply-chain problems. Combining the idea of dual decomposition (Carøe and Schultz, 1999) and integer programming sensitivity analysis (Dawande and Hooker, 2000), the method extracts the relevant sensitivity information from the branch and bound tree of every scenario subproblem, and uses that information to update the Lagrange multipliers and improve the dual bound. In particular, a new linear program has been proposed that involves constraints from the primal and dual sensitivity analysis using the information from branch and bound tree of each subproblem solution during Lagrangean decomposition. The objective function is to maximize the weighted sum of the upper and lower bounds from these analysis, and the model yields improved multipliers which result in the faster convergence of the algorithm.

Several instances of the two-stage stochastic MILPs have been considered for the computational experiments, and to compare the method with the standard subgradient approach. The method was implemented in AIMMS 3.11 and problems were solved using the CPLEX 12.2 solver. The first example was adapted from Carøe and Schultz (1999) involving 3 and 50 scenarios, while the second one was from Ahmed and Garcia (2003) and involved 10 and 200 scenarios. The results for both the examples showed that the subgradient method takes approximately an order of magnitude more iterations to converge to the best possible lower bound compared to the proposed method that converges in less than 10 iterations in most of the instances. This is due to the fact that during the subgradient method only the optimal solution of the scenario subproblems is used to update the multipliers, where the proposed method solves a linear program formulated using the information from the branch and bound tree of each subproblem solution and search in the space of multipliers.

Notice that for the models where each subgradient iteration is expensive to perform due to many MILP subproblems to be solved in each iteration, the proposed method can potentially decrease the total solution time very significantly by reducing the number of iterations, since the solution time for the proposed LP is negligible. However, the method should not be considered a substitute for the non-smooth optimization methods, but a viable alternative for the cases in which optimizing each scenario subproblem takes a long time, thus preventing the use of non-smooth optimization methods for large number of iterations. In addition, there are still many implementation challenges to overcome such as efficient data gathering and storage for large scale systems, integrating the commercial solvers for the subproblem solutions, application to a variety of problems, etc.

## 8.7 Contributions of the thesis

The main contributions of the thesis can be summarized as follows.

1. A new realistic and general MINLP model is proposed in chapter 2 for offshore oil and gas field infrastructure planning considering multiple fields, three components (oil, water and gas) explicitly in the formulation, facility expansions decisions, drilling rig limitations and nonlinear reservoir profiles.
2. Two theoretical properties are proposed in chapter 2 for the above model to reformulate the water-oil ratio and gas-oil ratio profiles in terms of cumulative water produced and cumulative gas produced, respectively. It allows removing the bilinear terms from the model and further converting the resulting non-convex MINLP into an MILP using piecewise linear

approximations and exact linearization techniques with which the problem can be solved to global optimality. Realistic instances involving 10 fields, 3 FPSO's and 20 years planning horizon have been solved in reasonable times.

3. A new model for multi-field site problems is proposed in chapter 3 that accounts for the fiscal calculations in the objective functions and constraints explicitly. A variety of the fiscal contracts have also been derived from the proposed general model. It is shown that the model yields an optimal NPV significantly higher than the case where fiscal considerations are not accounted for.
4. Logic constraints and valid inequalities are derived to be included in the above fiscal model to tighten the relaxation and improve the solution time. In addition, to solve large-scale instances with orders of magnitude less CPU times compared to a state-of-art commercial solver, heuristic approaches are also proposed that relax and approximate the sliding scale fiscal rules using inequalities avoiding the disjunctions.
5. Efficient solution strategies are proposed in chapter 4 for general multistage stochastic mixed-integer linear programming problems with endogenous uncertainties, where timings of uncertainty realizations depend on the optimization decisions. In particular, we have identified a new Property 3 to reduce the model size; a *k*-stage constraint strategy that is useful for problems where endogenous uncertainty is revealed during the first few time periods; a NAC relaxation strategy based on the fact that only few inequality NA constraints are active at the optimal solution; and a Lagrangean decomposition algorithm that can predict the rigorous lower bounds for the solution obtained.
6. A multistage stochastic programming model for offshore oil and gas field infrastructure planning is presented in chapter 5 that considers nonlinear reservoir profiles, progressive production sharing agreements, and endogenous uncertainty in the field parameters. Correlations among the endogenous uncertain parameters for a field such as field size, oil

deliverability, water-oil ratio and gas-oil ratio are also considered that reduce the model size significantly. In order to solve large instances of this model, a Lagrangean decomposition algorithm with parallel solution of the scenario subproblems in the GAMS grid computing environment is implemented, which outperforms the sequential approach and the direct solution using a commercial solver.

7. A novel partial decomposition approach for solving multistage stochastic programs with endogenous uncertainties is proposed in chapter 6 that relies on dividing the fullspace model into certain scenario groups. The method yields a tighter dual bound at root node and requires fewer iteration to converge within a specified tolerance compared to the standard approach. An alternate decomposition scheme that may even yield a better bound, but usually becomes more expensive for the large cases, is also proposed.
8. A new method for improving the dual bound of decomposable MILP models using integer programming sensitivity analysis has been investigated. In particular, a new linear program is proposed that uses the information from branch and bound tree of each subproblem solution during Lagrangean decomposition, and yields improved multipliers which result in faster convergence of the algorithm. Based on the computational results on two-stage stochastic MILPs, the method outperforms standard subgradient method in terms of number of iterations (more than an order of magnitude reduction), which can result in potential significant computational savings.

## 8.8 Recommendations for future work

1. The oilfield development planning model presented in chapter 2 assumes that there is no water or gas re-injection i.e. natural depletion of the reserves. It may be useful to extend the model to include this flexibility so that more realistic investment and operating decisions can be made. In addition, the model is formulated considering approximate reservoir

profiles in terms of the polynomials (for MINLPs) and piecewise linear functions (for MILPs). Integrating reservoir simulators such as ECLIPSE (Schlumberger, 2008) with the optimization model more tightly using a specific response surface methodology (Myers and Montgomery, 2002) to approximate the output of the simulator should yield decisions with a higher quality. An improved piecewise linear approximation scheme for polynomials such as based on logarithmic number of binary variables can also be investigated (Vielma et al., 2010).

2. In chapter 3, we have primarily focused on modeling and solving the oilfield problem assuming that the fiscal parameters are known. It may be more interesting for an oil company to analyze the sensitivity of the objective function value for different values of fiscal parameters such as a range of cost oil recovery limits, tier thresholds and profit oil fractions (Tordo, 2007) so that better contract terms can be negotiated. The impact of the crude oil price and discounting factors on optimization decisions should also be analyzed. However, few sliding scale parameters, e.g. rate of return may introduce nonlinearities in the model and require expensive global optimization approaches to solve the problem. Therefore, further investigation is required to develop efficient models and solution strategies to overcome the computational expense for the fiscal models relying on these parameters.
3. The proposed multistage stochastic models and algorithms in chapters 4, 5 and 6 only consider endogenous uncertain parameters. Therefore, it would be interesting to extend the methods to incorporate exogenous uncertain parameters such as oil price to be applicable to more general class of problems. Moreover, the objective functions in the proposed stochastic models are based on an expectation criterion neglecting the risk due to the potential additional computational effort. Therefore, there is an opportunity to incorporate various risk management strategies, e.g. variance reduction, downside risk, probabilistic financial risk, etc. (You et

al., 2009) in the proposed model especially that allow decomposing the fullspace model, and analyze their impact on the solution.

4. The total number of scenarios for multistage stochastic oilfield planning model in chapter 5 increases exponentially with the number of fields. Therefore, it may be interesting to investigate the correlations among the parameters for a single field and among the fields to reduce the number of scenarios in the model while maintaining the quality of the solution. Scenario reduction techniques (Heitsch and Römisch, 2003) and Monte Carlo sampling procedures (Shapiro, 2003) that are tailored for the endogenous uncertainty problems also need to be developed so that realistic problem instances can be solved.
5. During the proposed Lagrangean decomposition algorithm (chapters 4, 5 and 6), the subproblems at any iteration differs from the subproblems at the previous iteration only in terms of the coefficients in the objective function. Therefore, the branch and bound trees generated during the subproblem solutions can be used to provide a warm start for solving the subproblems in the next iteration that can significantly reduce the total solution time (Ralphs and Guzelsoy, 2006). In addition, as compared to the subgradient method to update the Lagrangean multipliers, alternative schemes as in Mouret et al. (2011), Oliveira et al. (2013), etc. should also be investigated to improve the efficiency of the proposed algorithm. We consider the GAMS grid computing facility for solving scenario problems independently on a CPU with multiple processors (chapter 5), there is an opportunity to take advantage of the more advanced parallel and grid computing facilities to solve the realistic problems instances (Linderoth and Wright, 2003).
6. In chapter 3, we have included the preliminary results on a bi-level decomposition approach for solving fiscal model that involves ringfencing provisions. The method can further be tested on a variety of examples. In addition, there is a potential to incorporate this approach with the Lagrangean decomposition algorithm in chapter 5 to develop a hybrid

scheme as in Terrazas-Moreno and Grossmann (2011) for solving multistage stochastic oilfield planning models with fiscal contracts involving ringfences.

7. Given the impact of the fiscal contracts on the optimization decisions and the profit as seen in chapter 3, it would be interesting to incorporate the relevant financial elements in the planning models for a variety of applications, rather using a simple objective function such as NPV or cost. For instance, modeling of purchase and sales contracts in supply chain optimization (Park et al., 2006, and Lanez et al., 2009), capacity expansions planning using internal rate of return or return on investments rather NPV (Bagajewicz, 2008), etc. In addition, the proposed multistage stochastic model and algorithms for endogenous uncertainty problems can be applied to several other interesting applications such as project portfolio optimization problem (Solak, 2007), open pit mine production scheduling problem (Boland et al., 2008), new drug development (Colvin and Maravelias, 2008), or it can be used as a basis to introduce new applications in this area.
8. Although the multistage stochastic model for endogenous uncertainties provides decisions with higher quality, the exponential increase in the model size with uncertain parameters and their realizations is still an issue. Alternate approaches to incorporate this uncertainty more efficiently and their impact on the solution need to be investigated. For example, there have been some real options approaches for oilfield development projects (Lund, 2000; and Dias, 2002) that can be compared with stochastic programming methods. In addition, Vayanos et al. (2011) recently considered an approximation scheme for multistage problems with decision-dependent information discovery based on robust optimization techniques. The authors presented a mixed-binary linear program by restricting the spaces of measurable binary and real-valued decision rules to those that are representable as piecewise constant and linear functions of the uncertain parameters, respectively. A further investigation can

provide a better insight about the advantages and limitations of this approach for the large instances of oilfield development projects.

9. The sensitivity based multiplier updating method of chapter 7 can be applied to more general class of MILPs (e.g. multistage stochastic models, MILPs with decomposable structure) to investigate its performance and scaling. Since, a basic branch and bound implementation is used for the computational study during this thesis, the integration of the procedure with branch-and-cut solvers may be the next step to improve the implementation efficiency of the method. After this integration, it will allow the solution of larger instances taking advantage of the commercial/open source MIP solvers. Finally, the decomposable structure of the problems in this class can further be exploited by potential parallelization of the subproblem solutions in HPC environment during each iteration.

# Appendices

## Appendix A

## Derivation of the Reservoir Profiles for Model 2 from Model 1 in Chapter 2

Model 1 involves nonlinearities in the form of three polynomials for oil deliverability, water-oil ratio (WOR) and gas-oil ratio (GOR), (A.1)-(A.3), and two bilinear equations for water and gas flow rates, (A.4)-(A.5), respectively.

$$Q_f^d = a_{1,f}(fc_f)^3 + b_{1,f}(fc_f)^2 + c_{1,f}\,fc_f + d_{1,f} \qquad \forall f \qquad \text{(A.1)}$$

$$wor_f = a_{2,f}(fc_f)^3 + b_{2,f}(fc_f)^2 + c_{2,f}\,fc_f + d_{2,f} \qquad \forall f \qquad \text{(A.2)}$$

$$gor_f = a_{3,f}(fc_f)^3 + b_{3,f}(fc_f)^2 + c_{3,f}\,fc_f + d_{3,f} \qquad \forall f \qquad \text{(A.3)}$$

$$w_f = wor_f\,x_f \qquad \forall f \qquad \text{(A.4)}$$

$$g_f = gor_f\,x_f \qquad \forall f \qquad \text{(A.5)}$$

To derive the reservoir profile for Model 2 from the above equations of Model 1 we consider the following two properties:

1. **The area under the curve GOR vs. cumulative oil produced for a field yields the cumulative amount of gas produced.**
2. **The area under the curve WOR vs. cumulative oil produced for a field yields the cumulative amount of water produced.**

**<u>Explanation of Property 1</u>**

From equation (A.3) we have GOR for a field as a cubic function in terms of fractional oil recovery, i.e. (A.6), or alternatively in terms of the cumulative oil produced $xc_f$ and recoverable oil volume $REC_f$ as in eq. (A.7) that corresponds to Model 1.

$$gor_f = a_{3,f}\, fc_f^3 + b_{3,f}\, fc_f^2 + c_{3,f}\, fc_f + d_{3,f} \tag{A.6}$$

$$gor_f = a_{3,f}\left(\frac{xc_f}{REC_f}\right)^3 + b_{3,f}\left(\frac{xc_f}{REC_f}\right)^2 + c_{3,f}\left(\frac{xc_f}{REC_f}\right) + d_{3,f} \tag{A.7}$$

A differential change in the cumulative oil produced multiplied by the GOR yields the corresponding fractional change in the cumulative amount of gas produced, $gc_f$, as seen in Figure A.1 and corresponding equation (A.8).

$$d(gc_f) = gor_f . d(xc_f) \tag{A.8}$$

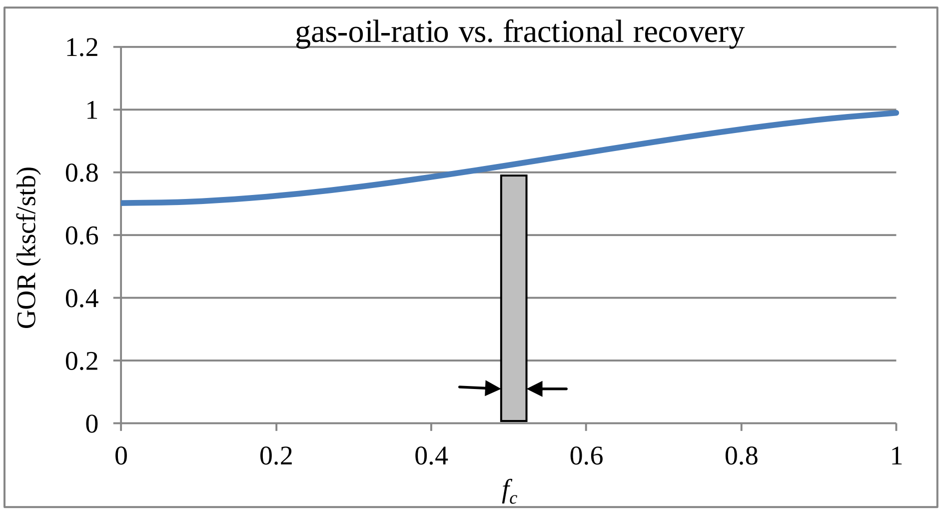


Figure A.1: GOR profile for field (F1) and FPSO (FPSO 1) connection

We should note that Figure A.1 corresponds to GOR vs. $f_c$ but it is easy to convert it to GOR vs. $xc_f$ given that the reservoir size ($REC_f$) is known. Integrating in (A.8) both sides from zero, i.e. area under the curve between GOR and $xc_f$, that yields eq. (A.9) and hence we can obtain equations (A.10)-(A.14).

$$\int_0^{gc_f} d(gc_f) = \int_0^{xc_f} gor_f . d(xc_f) \tag{A.9}$$

$$\int_0^{gc_f} d(gc_f) = \int_0^{xc_f} \left\{ a_{3,f}\left(\frac{xc_f}{REC_f}\right)^3 + b_{3,f}\left(\frac{xc_f}{REC_f}\right)^2 + c_{3,f}\left(\frac{xc_f}{REC_f}\right) + d_{3,f} \right\} . d(xc_f) \tag{A.10}$$

$$gc_f = \frac{a_{3,f}}{4}(\frac{xc_f^4}{REC_f^3}) + \frac{b_{3,f}}{3}(\frac{xc_f^3}{REC_f^2}) + \frac{c_{3,f}}{2}(\frac{xc_f^2}{REC_f}) + d_{3,f}(xc_f) \quad \text{(A.11)}$$

$$gc_f = \frac{a_{3,f}.REC_f}{4}(\frac{xc_f}{REC_f})^4 + \frac{b_{3,f}.REC_f}{3}(\frac{xc_f}{REC_f})^3 + \frac{c_{3,f}.REC_f}{2}(\frac{xc_f}{REC_f})^2 + d_{3,f}.REC_f(\frac{xc_f}{REC_f})$$

(A.12)

$$gc_f = \frac{a_{3,f}.REC_f}{4}(fc_f)^4 + \frac{b_{3,f}.REC_f}{3}(fc_f)^3 + \frac{c_{3,f}.REC_f}{2}(fc_f)^2 + d_{3,f}.REC_f(fc_f) \quad \text{(A.13)}$$

$$gc_f = a'_{3,f}(fc_f)^4 + b'_{3,f}(fc_f)^3 + c'_{3,f}(fc_f)^2 + d'_{3,f}(fc_f) \quad \text{(A.14)}$$

Eq. (A.14) is the desired expression for the cumulative gas produced as a function of fractional oil recovery (or cumulative oil produced), i.e. area under the curve GOR vs. fractional oil recovery (or cumulative oil produced) that is used in Model 2. We can see that the order of the polynomial for $gc_f$ expression (4$^{th}$ order) is one more than the order of the polynomial corresponding to the GOR expression in (A.6). Also, there is a direct correspondence between the coefficients of the both of these polynomials. The $gc_f$ vs. $f_c$ curve (4$^{th}$ order polynomial) corresponding to the Figure A.1 (GOR vs. $f_c$) that represents expression (A.14) is shown in Figure A.2.

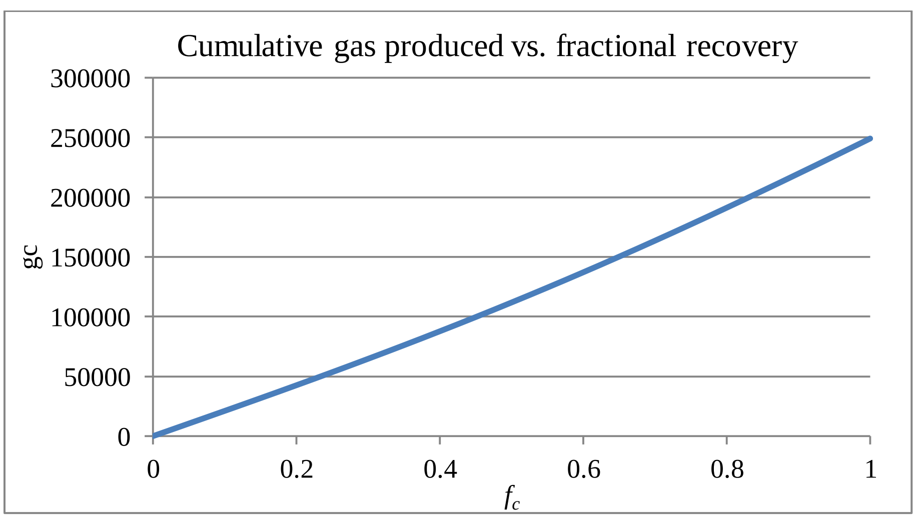


Figure A.2: gc profile for field (F1) and FPSO (FPSO 1) connection

Similarly, we can derive the following expression (A.15) for cumulative water produced $wc_f$ as a function of fractional oil recovery (or cumulative oil produced) using corresponding WOR expression (A.2), i.e. Property 2.

$$wc_f = a'_{2,f}(fc_f)^4 + b'_{2,f}(fc_f)^3 + c'_{2,f}(fc_f)^2 + d'_{2,f}(fc_f) \qquad \text{(A.15)}$$

Notice that using the same procedure we can derive the expressions (polynomial or any other functions) from the existing model of GOR and WOR to $gc_f$ and $wc_f$ in terms of fractional oil recovery (or cumulative oil produced), respectively, and vice-versa.

## Appendix B

# Comparison of the models based on (GOR, WOR) and (gc, wc) functions, i.e. Model 1 and 2, in Chapter 2

1. Model 1 (GOR and WOR as a function of cumulative oil produced) requires the bilinear equations (B.1) and (B.2) for gas and water flow rates while Model 2 does not need these equations as these flowrates can be expressed as equations (B.3) and (B.4) given that the polynomials for cumulative gas produced ( $gc_f$ ) and cumulative water produced ( $wc_f$ ) are available. Hence, Model 2 involving only univariate separable polynomials should computationally perform better.

$$g_{f,t} = gor_{f,t} x_{f,t} \qquad \forall f,t \qquad \text{(B.1)}$$

$$w_{f,t} = wor_{f,t} x_{f,t} \qquad \forall f,t \qquad \text{(B.2)}$$

$$g_{f,t} = (gc_{f,t} - gc_{f,t-1}) / \delta_t \qquad \forall f,t \qquad \text{(B.3)}$$

$$w_{f,t} = (wc_{f,t} - wc_{f,t-1}) / \delta_t \qquad \forall f,t \qquad \text{(B.4)}$$

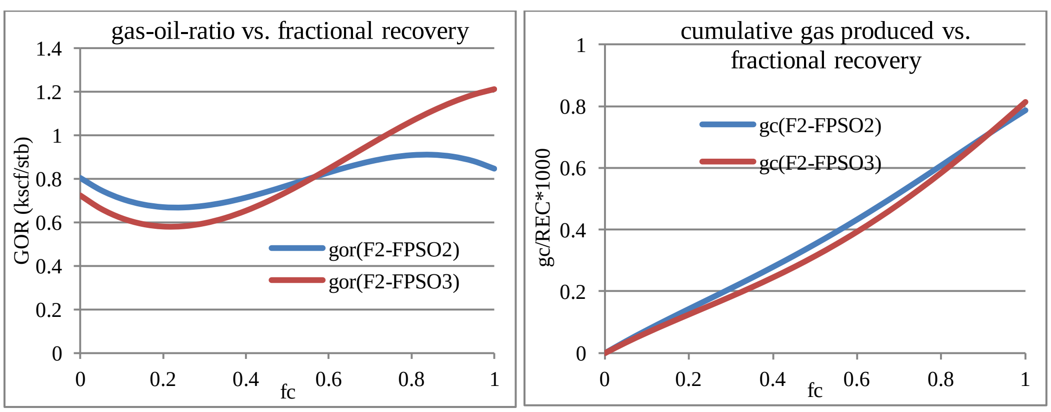


Figure B.1: GOR and gc profiles for 1 field and 2 FPSO connections

2. The WOR and GOR functions in (A.2) and (A.3) introduce a large number of non-convexities in Model 1 as compared to the $wc_f$ and $gc_f$ functions in (A.15) and (A.14), respectively, that are univariate monotonically increasing functions. Hence, these functions will be better to approximate using

piecewise linearization techniques. As an example the GOR and corresponding $gc_f$ functions for a field are shown in Figure B.1.

3. In Model 1 we assume that the WOR and GOR equations (B.5) and (B.6) used in time period t are calculated in terms of the fractional oil recovery by the end of previous time period t-1, i.e. point estimates are used. Therefore, WOR and GOR essentially perform as constants in current time period t, and the oil flowrate does not account for the variability in WOR and GOR values during that time period.

$$wor_{f,t} = a_{2,f}(fc_{f,t-1})^3 + b_{2,f}(fc_{f,t-1})^2 + c_{2,f}\, fc_{f,t-1} + d_{2,f} \qquad \forall f,t \qquad \text{(B.5)}$$

$$gor_{f,t} = a_{3,f}(fc_{f,t-1})^3 + b_{3,f}(fc_{f,t-1})^2 + c_{3,f}\, fc_{f,t-1} + d_{3,f} \qquad \forall f,t \qquad \text{(B.6)}$$

$$w_{f,t} = wor_{f,t}\, x_{f,t} \qquad \forall f,t \qquad \text{(B.7)}$$

$$g_{f,t} = gor_{f,t}\, x_{f,t} \qquad \forall f,t \qquad \text{(B.8)}$$

However, equations (B.9) and (B.10) for $wc_f$ and $gc_f$ explicitly predicts the cumulative amount of water and gas produced, respectively, by the end of period t as a function of cumulative oil produced by the end of period t, and hence also accounts for the variability of the WOR and GOR values during current period t. In other words these profiles consider the average values of WOR and GOR over the time period t. Therefore, Model 2 is also better in terms of representing the physical reservoir characteristics.

$$wc_{f,t} = a'_{2,f}(fc_{f,t})^4 + b'_{2,f}(fc_{f,t})^3 + c'_{2,f}(fc_{f,t})^2 + d'_{2,f}\, fc_{f,t} \qquad \forall f,t \qquad \text{(B.9)}$$

$$gc_{f,t} = a'_{3,f}(fc_{f,t})^4 + b'_{3,f}(fc_{f,t})^3 + c'_{3,f}(fc_{f,t})^2 + d'_{3,f}\, fc_{f,t} \qquad \forall f,t \qquad \text{(B.10)}$$

Notice that equations (B.5) and (B.6) for Model 1 could also be represented as a function of fractional oil recovery by the end of time period t instead of time period t-1, however, the model will still consider the WOR and GOR values based on the point estimate instead average values over the time period t as used in Model 2.

# Appendix C

## Nomenclature for the Fiscal Model in Chapter 3

**Indices**

| | |
|---|---|
| *t, τ* | time periods, $t, \tau \in T$ |
| *f* | field |
| *fpso* | FPSO facility |
| *rf* | ringfence |
| *i* | tier |

**Integer Variables**

| | |
|---|---|
| $I_{f,t}^{well}$ | Number of wells drilled in field *f* at the beginning of time period t |

**Binary Variables**

| | |
|---|---|
| $b_{fpso,t}^{FPSO}$ | whether or not FPSO facility *fpso* is installed at the beginning of time period *t* |
| $b_{f,fpso,t}$ | whether or not a connection between field *f* and FPSO facility *fpso* is installed at the beginning of time period *t* |
| $b_{f,fpso}^{on}$ | whether or not a connection between field *f* and FPSO facility *fpso* is installed |
| $Z_{rf,i,t}$ | whether or not tier *i* is active in time *t* for ringfence *rf* |
| $b_{rf,t}^{co}$ | whether or not cost ceiling is active in time period *t* for ringfence *rf* |

**Continuous Variables**

| | |
|---|---|
| $NPV$ | net present value |
| $TotalConSh_t^{tot}$ | total contractor share in time period *t* |
| $CAP_t^{tot}$ | total capital costs in time period *t* |

| | |
|---|---|
| $OPER_t^{tot}$ | total operating costs in time period $t$ |
| $TotalConSh_{rf,t}$ | contractor share in time period $t$ for ringfence $rf$ |
| $COST_{rf,t}$ | total capital and operating costs in time period $t$ for ringfence $rf$ |
| $CAP_{rf,t}$ | capital costs in time period $t$ for ringfence $rf$ |
| $CAP1_{rf,t}$ | field specific capital costs in time period $t$ for ringfence $rf$ |
| $CAP2_{rf,t}$ | FPSO specific capital costs in time period $t$ for ringfence $rf$ |
| $OPER_{rf,t}$ | operating costs in time period $t$ for ringfence $rf$ |
| $FPSOC_{fpso,t}$ | total cost of FPSO facility $fpso$ in time period $t$ |
| $DFPSOC_{rf,fpso,t}$ | disaggregated cost of FPSO facility $fpso$ in time period $t$ for ringfence $rf$ |
| $DFPSOC_{f,fpso,t}^{field}$ | disaggregated cost of FPSO facility $fpso$ in time period $t$ for field $f$ |
| $REV_{rf,t}$ | total revenues in time period $t$ for ringfence $rf$ |
| $ZD_{f',f,fpso,t}^{field}$ | auxiliary variable for $b_{f',fpso}^{on} \cdot DFPSOC_{f,fpso,t}^{field}$ |
| $ZD1_{f',f,fpso,t}^{field}$ | auxiliary variable for $b_{f',fpso}^{on} \cdot DFPSOC_{f,fpso,t}^{field}$ |
| $ZD_{f,fpso,t}$ | auxiliary variable for $b_{f,fpso}^{on} \cdot FPSOC_{fpso,t}$ |
| $ZD1_{f,fpso,t}$ | auxiliary variable for $b_{f,fpso}^{on} \cdot FPSOC_{fpso,t}$ |
| $x_{rf,t}^{tot}$ | total oil production rate from ringfence $rf$ in time period $t$ |
| $w_{rf,t}^{tot}$ | total water production rate from ringfence $rf$ in time $t$ |
| $g_{rf,t}^{tot}$ | total gas production rate from ringfence $rf$ in time period $t$ |
| $xc_{rf,t}$ | cumulative oil produced from ringfence $rf$ by the end of time period $t$ |
| $x_{f,t}$ | oil production rate from field $f$ in time period $t$ |

| | |
|---|---|
| $w_{f,t}$ | water production rate from field *f* in time period *t* |
| $g_{f,t}$ | gas production rate from field *f* in time period *t* |
| $xc_{f,t}^{field}$ | cumulative oil produced from field *f* by the end of time period *t* |
| $wor_{f,fpso,t}$ | water-to-oil ratio for field-FPSO connection in time *t* |
| $gor_{f,fpso,t}$ | gas-to-oil ratio for field-FPSO connection in time period *t* |
| $wc_{f,fpso,t}$ | cumulative water produced from field *f* to FPSO facility *fpso* by the end of time period *t* |
| $gc_{f,fpso,t}$ | cumulative gas produced from field *f* to FPSO facility *fpso* by the end of time period *t* |
| $fc_{f,t}$ | fraction of oil recovered from field *f* by the end of time period *t* |
| $Q_{f,fpso,t}^{d,well}$ | field deliverability (maximum oil flow rate) per well for field *f* and FPSO facility *fpso* combination in time period *t* |
| $QI_{fpso,t}^{liq}$ | liquid installation capacity of FPSO facility *fpso* at the beginning of time period *t* |
| $QI_{fpso,t}^{gas}$ | gas installation capacity of FPSO facility *fpso* at the beginning of time period *t* |
| $QE_{fpso,t}^{liq}$ | liquid expansion capacity of FPSO facility *fpso* at the beginning of time period *t* |
| $QE_{fpso,t}^{gas}$ | gas expansion capacity of FPSO facility *fpso* at the beginning of time *t* |
| $CO_{rf,t}$ | cost oil in time period *t* for ringfence *rf* |
| $PO_{rf,t}$ | profit oil in time period *t* for ringfence *rf* |
| $CR_{rf,t}$ | cost recovery in time period *t* for ringfence *rf* |

| | |
|---|---|
| $CRF_{rf,t}$ | cost recovery carried forward in time $t$ for ringfence $rf$ |
| $Tax_{rf,t}$ | income tax in time period $t$ for ringfence $rf$ |
| $ConSh_{rf,t}^{beforetax}$ | contractor before tax share in profit oil in time period $t$ for ringfence $rf$ |
| $ConSh_{rf,t}^{aftertax}$ | contractor after tax share in profit oil in time period $t$ for ringfence $rf$ |
| $DPO_{rf,i,t}$ | disaggregated profit oil for tier $i$ in time period $t$ for ringfence $rf$ |
| $DConSh_{rf,i,t}^{beforetax}$ | disaggregated contractor before tax share in profit oil for tier $i$ in time period $t$ for ringfence $rf$ |
| $Dxc_{rf,i,t}$ | disaggregated cumulative oil produced from ringfence $rf$ by the end of time period $t$ for tier $i$ |
| $Royalty_{rf,t}$ | amount of royalty in time period $t$ for ringfence $rf$ |
| $SV_{rf,t}$ | sliding scale variable in time period $t$ for ringfence $rf$ |

**Parameters**

| | |
|---|---|
| $FC_{fpso,t}^{FPSO}$ | fixed capital cost for installing FPSO facility *fpso* at the beginning of time period t |
| $FC_{f,fpso,t}$ | fixed cost for installing the connection between field *f* and FPSO facility *fpso* at the beginning of time period t |
| $FC_{f,t}^{well}$ | fixed cost for drilling a well in field *f* at the beginning of time period t |
| $VC_{fpso,t}^{liq}$ | variable capital cost for installing or expanding the liquid (oil and water) capacity of FPSO facility *fpso* at the beginning of time period t |

| | |
|---|---|
| $VC^{gas}_{fpso,t}$ | variable capital cost for installing or expanding the gas capacity of FPSO facility *fpso* at the beginning of time period t |
| $OC^{liq}_{rf,t}$ | operating cost for per unit of liquid (oil and water) produced in time period t for ringfence *rf* |
| $OC^{gas}_{rf,t}$ | operating cost for per unit of gas produced in time period t for ringfence *rf* |
| $REC_f$ | total amount of recoverable oil from field *f* |
| $f^{tax}_{rf,t}$ | income tax rate in time period *t* for ringfence *rf* |
| $f^{CR}_{rf,t}$ | cost recovery ceiling fraction in time *t* for ringfence *rf* |
| $f^{PO}_{rf,i}$ | profit oil fraction of the contractor in tier *i* for ringfence *rf* |
| $f^{royal}_{rf,t}$ | royalty rate in time period *t* for ringfence *rf* |
| $f^{eff,taxrate}_{rf,t}$ | effective tax rate in time period *t* for ringfence *rf* |
| $f^{profit\,tax}_{rf,t}$ | profit tax rate in time period *t* for ringfence *rf* |
| $L^{oil}_{rf,i}$ | lower threshold for profit oil split in tier *i* for ringfence *rf* |
| $U^{oil}_{rf,i}$ | upper threshold for profit oil split in tier *i* for ringfence *rf* |
| $l_1$ | lead time for initial installation of a FPSO facility |
| $l_2$ | lead time for expansion of an earlier installed FPSO facility |
| $\alpha_t$ | price of oil in time period *t* |
| $dis_t$ | discounting factor for time period *t* |
| $\delta_t$ | number of days in time period *t* |
| $M, U$ | big-M parameters |
| $a_{()}, b_{()}, c_{()}, d_{()}$ | coefficients for polynomials used for reservoir models |

## Appendix D

# Proof of the Propositions in Chapter 3

**Proposition 3.1:** If the sliding scale variable for profit oil share of the contractor is cumulative oil produced, the following inequalities are satisfied at the optimal solution of Model 3RF:

$$\sum_{\tau \le t} (Contsh_{rf,\tau}^{beforetax} / \alpha_\tau) \le \sum_{i'=1}^{i' \le i} (f_{rf,i'}^{PO} - f_{rf,i'-1}^{PO}) \cdot (xc_{rf,t} - L_{rf,i'}) - f_{rf,i^{end}}^{PO} \cdot \sum_{\tau \le t} (CO_{rf,\tau} / \alpha_\tau)$$

$$\forall rf, i, t \qquad \text{(D.1)}$$

*Proof.* The proof follows from bounding the cumulative contractor's share in each time period for every ringfence. We know that the revenue generated from a ringfence rf in time period t, equation (D.2), is the total oil produced from this ringfence in that time period times the price of oil $(\alpha_t)$. From Figure 3.2, we can observe that the total profit oil for a ringfence in time period t is the difference between revenue and cost oil for that ringfence, where we consider no royalty provisions that yields equation (D.3).

$$REV_{rf,t} = \alpha_t x_{rf,t}^{tot} \qquad \forall rf, t \qquad \text{(D.2)}$$

$$PO_{rf,t} = REV_{rf,t} - CO_{rf,t} \qquad \forall rf, t \qquad \text{(D.3)}$$

If tier *i(t)* is active in time period t for ringfence rf, then the contractor share in the profit oil for that ringfence can be calculated in eq. (D.4) as the corresponding profit oil times the tier fraction which is active in the current period t, $f_{rf,i(t)}^{PO}$. Equation (D.4) can be re-written as eq. (D.5) using eq. (D.3), and dividing the both sides of the resulting equation by price of oil to represent the contractor's share in terms of oil volume instead of price.

$ContSh_{rf,t}^{beforetax} = f_{rf,i(t)}^{PO} \cdot PO_{rf,t}$ , where tier *i(t)* is active for rf in time period *t*

$$\forall rf, t \qquad \text{(D.4)}$$

$ContSh_{rf,t}^{beforetax} / \alpha_t = f_{rf,i(t)}^{PO} \cdot (REV_{rf,t}^{tot} - CO_{rf,t}) / \alpha_t$ , where tier *i(t)* is active for rf in time t $\qquad \forall rf, t \qquad$ (D.5)

The cumulative contractor's share by the end of time period t can be obtained in equation (D.6) by summing (D.5) from period 1 to current period t, which can further be re-written as equation (D.7) using revenue definition form equation (D.2).

$$\sum_{\tau=1}^{t} ContSh_{rf,\tau}^{beforetax} / \alpha_\tau = \sum_{\tau=1}^{t} f_{rf,i(\tau)}^{PO} \cdot (REV_{rf,\tau}^{tot} - CO_{rf,\tau}) / \alpha_\tau \qquad \forall rf,t \qquad \text{(D.6)}$$

$$\sum_{\tau=1}^{t} ContSh_{rf,\tau}^{beforetax} / \alpha_\tau = \sum_{\tau=1}^{t} f_{rf,i(\tau)}^{PO} \cdot x_{rf,\tau}^{tot} - \sum_{\tau=1}^{t} f_{rf,i(\tau)}^{PO} \cdot CO_{rf,\tau} / \alpha_\tau \qquad \forall rf,t \qquad \text{(D.7)}$$

The first term in RHS of equation (D.7) can be written as in equation (D.8) for an active tier *i(t)* for ringfence rf in time period t, where, $t_1$, $t_2$ and so on are the time periods until previous tiers 1, 2, 3, etc. were active, respectively, for the corresponding ringfence. Equation (D.9) represents (D.8) in terms of cumulative oil produced in each tier until tier i(t).

$$\sum_{\tau=1}^{t} f_{rf,i(\tau)}^{PO} \cdot x_{rf,\tau}^{tot} = f_{rf,1}^{PO} \sum_{\tau=1}^{t_1} x_{rf,\tau}^{tot} + f_{rf,2}^{PO} \sum_{\tau=t_1+1}^{t_2} x_{rf,\tau}^{tot} + \ldots + f_{rf,i-1}^{PO} \sum_{\tau=t_{i-2}+1}^{t_{i-1}} x_{rf,\tau}^{tot} + f_{rf,i(t)}^{PO} \sum_{\tau=t_{i-1}+1}^{t} x_{rf,\tau}^{tot}$$

$$\forall rf,t \qquad \text{(D.8)}$$

$$\sum_{\tau=1}^{t} f_{rf,i(\tau)}^{PO} \cdot x_{rf,\tau}^{tot} = f_{rf,1}^{PO} xc_{rf,t_1} + f_{rf,2}^{PO} xc_{rf,t_2-t_1} + \ldots + f_{rf,i-1}^{PO} xc_{rf,t_{i-1}-t_{i-2}} + f_{rf,i(t)}^{PO} xc_{rf,t-t_{i-1}}$$

$$\forall rf,t \qquad \text{(D.9)}$$

The maximum amount of cumulative oil produced during each tier that lies before tier i(t) as in (D.10), will be the difference between the lower thresholds of the corresponding consecutive tiers as represented in inequality (D.11) and can be seen in Figure 3.5.

$$f_{rf,1}^{PO} > f_{rf,2}^{PO} > \ldots\ldots > f_{rf,i-1}^{PO} > f_{rf,i(t)}^{PO} \geq 0 \qquad \text{(D.10)}$$

$$\sum_{\tau=1}^{t} f_{rf,i(\tau)}^{PO} \cdot x_{rf,\tau}^{tot} \leq f_{rf,1}^{PO}(L_{rf,2} - L_{rf,1}) + f_{rf,2}^{PO}(L_{rf,3} - L_{rf,2}) + \ldots + f_{rf,i-1}^{PO}(L_{rf,i} - L_{rf,i-1}) + f_{rf,i(t)}^{PO}(xc_{rf,t}^{tot} - L_{rf,i})$$

$$\forall rf,t \qquad \text{(D.11)}$$

Inequality (D.11) can further be rewritten as (D.12), which by reformulating the last term as in (D.13) and rearranging the corresponding terms for each tier gives inequality (D.14).

$$\sum_{\tau=1}^{t} f_{rf,i(\tau)}^{PO} \cdot x_{rf,\tau}^{tot} \leq -L_{rf,1} f_{rf,1}^{PO} - L_{rf,2}(f_{rf,2}^{PO} - f_{rf,1}^{PO}) - \ldots - L_{rf,i}(f_{rf,i}^{PO} - f_{rf,i-1}^{PO}) + f_{rf,i(t)}^{PO} xc_{rf,t}^{tot}$$

$$\forall rf, t \qquad \text{(D.12)}$$

$$\sum_{\tau=1}^{t} f_{rf,i(\tau)}^{PO} \cdot x_{rf,\tau}^{tot} \leq -L_{rf,1} f_{rf,1}^{PO} - L_{rf,2}(f_{rf,2}^{PO} - f_{rf,1}^{PO}) - \ldots - L_{rf,i}(f_{rf,i}^{PO} - f_{rf,i-1}^{PO})$$
$$+ xc_{rf,t}^{tot} \left\{ (f_{rf,i(t)}^{PO} - f_{rf,i-1}^{PO}) + (f_{rf,i-1}^{PO} - f_{rf,i-2}^{PO}) + \ldots (f_{rf,2}^{PO} - f_{rf,1}^{PO}) + f_{rf,1}^{PO} \right\}$$

$$\forall rf, t \qquad \text{(D.13)}$$

$$\sum_{\tau=1}^{t} f_{rf,i(t)}^{PO} \cdot x_{rf,\tau}^{tot} \leq \sum_{i'=1}^{i' \leq i(t)} (f_{rf,i'}^{PO} - f_{rf,i'-1}^{PO}) \cdot (xc_{rf,t} - L_{rf,i'}) = RHS(i(t))$$

$$\forall rf, t \qquad \text{(D.14)}$$

As it is unknown a priori which tier i gets active at what time, we need to write constraint (D.14) for each tier i in each time t. For those tiers that are not active in current period t, i.e. $i \neq i(t)$, (D.14) must be relaxed to be a valid inequality. Therefore, for $i^b < i(t)$, RHS of inequality (D.14) becomes:

$$RHS(i^b) = \sum_{i'=1}^{i' \leq i^b} (f_{rf,i'}^{PO} - f_{rf,i'-1}^{PO}) \cdot (xc_{rf,t} - L_{rf,i'}) \qquad \forall i^b < i(t), rf, t \qquad \text{(D.15)}$$

Furthermore, on subtracting RHS of eq. (D.14) and (D.15), it gives (D.16), and therefore, we obtain (D.17):

$$RHS(i(t)) - RHS(i^b) = \sum_{i'=1}^{i' \leq i(t)} (f_{rf,i'}^{PO} - f_{rf,i'-1}^{PO}) \cdot (xc_{rf,t} - L_{rf,i'}) - \sum_{i'=1}^{i' \leq i^b} (f_{rf,i'}^{PO} - f_{rf,i'-1}^{PO}) \cdot (xc_{rf,t} - L_{rf,i'})$$

$$\forall i^b < i(t), rf, t \qquad \text{(D.16)}$$

$$RHS(i(t)) - RHS(i^b) = \sum_{i'=i^b+1}^{i' \leq i(t)} (f_{rf,i'}^{PO} - f_{rf,i'-1}^{PO}) \cdot (xc_{rf,t} - L_{rf,i'})$$

$$\forall i^b < i(t), rf, t \qquad \text{(D.17)}$$

$$as \quad (f_{rf,i'}^{PO} - f_{rf,i'-1}^{PO} \leq 0) \wedge (xc_{rf,t} - L_{rf,i'} \geq 0) \qquad \forall i' \leq i(t), rf$$

Therefore, (D.17) yields (D.18) and hence we get (D.19) which say that the first term in equation (D.7) will be relaxed for all $i^b < i(t)$ compared to an active tier i(t).

$$RHS(i(t)) - RHS(i^b) \leq 0 \qquad \forall i^b < i(t), rf, t \qquad \text{(D.18)}$$

$$RHS(i(t)) \leq RHS(i^b) \qquad \forall i^b < i(t), rf, t \qquad \text{(D.19)}$$

For those tiers that lies after active tier i(t), i.e. $i^a > i(t)$, then RHS of inequality (D.14) becomes:

$$RHS(i^a) = \sum_{i'=1}^{i' \leq i^a} (f^{PO}_{rf,i'} - f^{PO}_{rf,i'-1}) \cdot (xc_{rf,t} - L_{rf,i'}) \qquad \forall i^a > i(t), rf, t \qquad \text{(D.20)}$$

On subtracting RHS of eq. (D.14) and (D.20), it gives (D.21), which reduces to (D.22):

$$RHS(i(t)) - RHS(i^a) = \sum_{i'=1}^{i' \leq i(t)} (f^{PO}_{rf,i'} - f^{PO}_{rf,i'-1}) \cdot (xc_{rf,t} - L_{rf,i'}) - \sum_{i'=1}^{i' \leq i^a} (f^{PO}_{rf,i'} - f^{PO}_{rf,i'-1}) \cdot (xc_{rf,t} - L_{rf,i'})$$
$$\forall i^a > i(t), rf, t \qquad \text{(D.21)}$$

$$RHS(i(t)) - RHS(i^a) = -\sum_{i'=i(t)+1}^{i' \leq i^a} (f^{PO}_{rf,i'} - f^{PO}_{rf,i'-1}) \cdot (xc_{rf,t} - L_{rf,i'}) \quad \forall i^a > i(t), rf, t \quad \text{(D.22)}$$

$$as \quad (f^{PO}_{rf,i'} - f^{PO}_{rf,i'-1} \leq 0) \wedge (xc_{rf,t} - L_{rf,i'} \leq 0) \qquad \forall i' \geq i(t), rf$$

Therefore, (D.22) yields (D.23) and hence we get (D.24) which say that the first term in equation (D.7) will be relaxed for $i^a > i(t)$ as compared to i(t).

$$RHS(i(t)) - RHS(i^a) \leq 0 \qquad \forall i^a > i(t), rf, t \qquad \text{(D.23)}$$

$$RHS(i(t)) \leq RHS(i^a) \qquad \forall i^a > i(t), rf, t \qquad \text{(D.24)}$$

Therefore, for any tier i which may be an active tier in time t, the first term in eq. (D.7) can be represented as inequality (D.14).

Equation (D.25) represents the second term of RHS for equation (D.7) in disaggregated form for each tier as explained above for total oil produced, i.e. equation (D.8). However, here we do not have any predefined threshold for the cost oil in each tier in contrast to the cumulative oil produced, we need to represent this term in the relaxed form to be valid for all tiers. Given that profit oil fraction decreases as we move to higher tier, eq. (D.10) and $CO_{rf,t} \geq 0, \alpha_t > 0$, we can replace the profit oil fractions for the previous tiers $i^b < i(t)$ with the profit oil fraction of the current tier i(t) that ensures a lower bound on the LHS of equation (D.25). Using this relaxation idea we obtain equation (D.26) which on further aggregation yields equation (D.27) and (D.28).

$$\sum_{\tau=1}^{t} f_{rf,i(t)}^{PO} \cdot CO_{rf,\tau} / \alpha_\tau = f_{rf,1}^{PO} \sum_{\tau=1}^{t_1} CO_{rf,\tau} / \alpha_\tau + f_{rf,2}^{PO} \sum_{\tau=t_1}^{t_2} CO_{rf,\tau} / \alpha_\tau + \ldots$$
$$+ f_{rf,i-1}^{PO} \sum_{\tau=t_{i-2}}^{t_{i-1}} CO_{rf,\tau} / \alpha_\tau + f_{rf,i}^{PO} \sum_{\tau=t_{i-1}}^{t} CO_{rf,\tau} / \alpha_\tau \qquad \forall rf, t \qquad \text{(D.25)}$$

$$\sum_{\tau=1}^{t} f_{rf,i(t)}^{PO} \cdot CO_{rf,\tau} / \alpha_\tau \geq f_{rf,i(t)}^{PO} \sum_{\tau=1}^{t_1} CO_{rf,\tau} / \alpha_\tau + f_{rf,i(t)}^{PO} \sum_{\tau=t_1}^{t_2} CO_{rf,\tau} / \alpha_\tau + \ldots$$
$$+ f_{rf,i(t)}^{PO} \sum_{\tau=t_{i-2}}^{t_{i-1}} CO_{rf,\tau} / \alpha_\tau + f_{rf,i(t)}^{PO} \sum_{\tau=t_{i-1}}^{t} CO_{rf,\tau} / \alpha_\tau \qquad \forall rf, t \qquad \text{(D.26)}$$

$$\sum_{\tau=1}^{t} f_{rf,i(t)}^{PO} \cdot CO_{rf,\tau} / \alpha_\tau \geq f_{rf,i(t)}^{PO} \sum_{\tau=1}^{t} CO_{rf,\tau} / \alpha_\tau \qquad \forall rf, t \qquad \text{(D.27)}$$

$$-\sum_{\tau=1}^{t} f_{rf,i(t)}^{PO} \cdot CO_{rf,\tau} / \alpha_\tau \leq -f_{rf,i(t)}^{PO} \sum_{\tau=1}^{t} CO_{rf,\tau} / \alpha_\tau \qquad \forall rf, t \qquad \text{(D.28)}$$

Similarly, for other tiers $i \neq i(t)$, we have:

$$-\sum_{\tau=1}^{t} f_{rf,i}^{PO} \cdot CO_{rf,\tau} / \alpha_\tau \leq -f_{rf,i}^{PO} \sum_{\tau=1}^{t} CO_{rf,\tau} / \alpha_\tau \qquad \forall rf, t, i \neq i(t) \qquad \text{(D.29)}$$

However,

$$f_{rf,1}^{PO} \sum_{\tau=1}^{t} CO_{rf,\tau} / \alpha_\tau \geq f_{rf,2}^{PO} \sum_{\tau=1}^{t} CO_{rf,\tau} / \alpha_\tau \geq \ldots\ldots f_{rf,i(t)}^{PO} \sum_{\tau=1}^{t} CO_{rf,\tau} / \alpha_\tau \geq \ldots\ldots \geq f_{rf,i^{end}}^{PO} \sum_{\tau=1}^{t} CO_{rf,\tau} / \alpha_\tau$$

Therefore, for equation (D.27) guaranteed to be valid for any tier $i$, we can use the last tier $i^{end}$ fraction instead which has minimum value, that yields equation (D.30):

$$\sum_{\tau=1}^{t} f_{rf,i}^{PO} \cdot CO_{rf,\tau} / \alpha_\tau \geq f_{rf,i^{end}}^{PO} \sum_{\tau=1}^{t} CO_{rf,\tau} / \alpha_\tau \qquad \forall rf, t, i \qquad \text{(D.30)}$$

Substituting (D.14) and (D.30) back in equation (D.7) for any active tier $i$ in time $t$, we can obtain (D.31) which is same as the desired expression (D.1).

$$\sum_{\tau \leq t} (Contsh_{rf,\tau}^{beforetax} / \alpha_\tau) \leq \sum_{i'=1}^{i' \leq i} (f_{rf,i'}^{PO} - f_{rf,i'-1}^{PO}) \cdot (xc_{rf,t} - L_{rf,i'}) - f_{rf,i^{end}}^{PO} \cdot \sum_{\tau \leq t} (CO_{rf,\tau} / \alpha_\tau)$$
$$\forall rf, i, t \qquad \text{(D.31)}$$

**Proposition 3.2:** If the sliding scale variable for profit oil share of the contractor is daily oil production, the following inequalities are satisfied at the optimal solution of Model 3RF:

$$Contsh_{rf,\tau}^{beforetax}/(\delta_t\alpha_\tau) \le \sum_{i'=1}^{i'\le i}(f_{rf,i'}^{PO} - f_{rf,i'-1}^{PO})\cdot(x_{rf,t}^{tot} - L_{rf,i'}) - f_{rf,i^{end}}^{PO} \cdot CO_{rf,\tau}/(\delta_t\alpha_\tau) \qquad \forall rf,i,t \qquad \text{(D.32)}$$

*Proof.* The proof follows similarly as for Proposition 3.1. However, in this case as the daily oil produced is the sliding scale variable, we do not apply the summation over time as we did for equation (D.5). In addition, it is also assumed that the incremental tax is applicable only on the amount of oil production rate that is above the given tier threshold of the previous tier which is usually the case in practice. However, this type of tier structure is more popular for sliding scale royalties than profit oil described here.

## Appendix E

# Sliding scale fiscal terms without binary variables in Chapter 3

**Proposition 3.3:** Any sliding scale (either appearing in PSA, Concessionary system, etc.) where the sliding scale variable (e.g. cumulative oil, daily oil produced) and portion of oil that needs to split between oil company and government can be represented in terms of a fraction of the current revenues (production) or cumulative revenue (cumulative production), and the sliding scale is incremental, then we can represent the sliding scale fiscal terms without binary variables.

For example, in the following cases, we do not need any binary variable for representing the sliding scale fiscal terms:

(a) A concessionary/PSA system where the sliding scale is defined only for royalties based on the production. Eq. (E.3(a))

(b) A concessionary/PSA system where the sliding scale is defined only for profit oil where royalty is a given fraction of the revenue and there is no cost oil. Eq. (E.3(b))

(c) A concessionary/PSA system where the sliding scale is defined only for profit oil where royalty and cost oil are a given fraction of the revenues. Eq. (E.3(c))

$$\bigvee_i \begin{bmatrix} Z_{rf,i,t} \\ ConSh_{rf,t} = f^{eff}_{rf,i} \cdot REV^{tot}_{rf,t} \\ L_{rf,i} \le SV_{rf,t} \le U_{rf,i} \end{bmatrix} \qquad \forall rf,t \qquad \text{(E.1)}$$

$$SV_{rf,t} = xc_{rf,t} \ or \ x_{rf,t} \qquad \forall rf,t \qquad \text{(E.2)}$$

$$f^{eff}_{rf,i} = \begin{cases} (1 - f^{royal}_{rf,i}) & (a) \\ (1 - f^{royal}_{rf}) \cdot f^{PO}_{rf,i} & (b) \\ (1 - f^{royal}_{rf} - f^{CO}_{rf}).\, f^{PO}_{rf,i} & (c) \end{cases} \qquad \forall rf,i \qquad \text{(E.3)}$$

*Proof.* The proof follows directly as in Proposition 3.1 where we use $f_{rf,i}^{eff}$ in place of $f_{rf,i}$. However, here we consider those cases (a)-(c) where the contractor's share can be represented directly as a fraction of revenue generated, the term that corresponds to the cost oil in RHS of equation (D.5) will not appear as $f_{rf,i}^{eff}$ has accounted for the cost oil and/or royalty if these are present. Therefore, we have (E.4) instead, that reduces to the simpler version of equation (D.1), i.e. (E.5) in the case of cumulative oil produced as the sliding scale variable. Whereas, if the sliding scale variable is daily oil produced then corresponding eq. (D.32) reduced to (E.6) instead of eq. (E.5)

$ContSh_{rf,t}^{beforetax} / \alpha_t = f_{rf,i(t)}^{eff} \cdot REV_{rf,t}^{tot} / \alpha_t$, where tier *i(t)* is active for rf in time t

$$\forall rf,t \qquad \text{(E.4)}$$

$$\sum_{\tau \le t} (Contsh_{rf,\tau}^{beforetax} / \alpha_\tau) \le \sum_{i'=1}^{i' \le i} (f_{rf,i'}^{eff} - f_{rf,i'-1}^{eff}) \cdot (xc_{rf,t} - L_{rf,i'}) \qquad \forall rf,t \qquad \text{(E.5)}$$

$$Contsh_{rf,\tau}^{beforetax} / (\delta_t \alpha_\tau) \le \sum_{i'=1}^{i' \le i} (f_{rf,i'}^{eff} - f_{rf,i'-1}^{eff}) \cdot (x_{rf,t}^{tot} - L_{rf,i'}) \qquad \forall rf,i,t \qquad \text{(E.6)}$$

In general, at-least one of the equation that corresponds to the active tier in (E.5) or (E.6) will be active in the optimal solution as contractor's share appears in the objective function. Therefore, the solution that it yields is usually the optimal for these cases, else it can serve as the valid inequality to generate the tight upper bound. This represents the sliding scale fiscal terms without binary variables.

# Appendix F

# Proposition used for the Approximate Model in Chapter 3

**Proposition 3.4:** If the sliding scale variable for profit oil share of the contractor is cumulative oil produced, the following inequalities will provide a good approximation of the optimal solution of Model 3RF:

$$\sum_{\tau \le t}(Contsh_{rf,\tau}^{beforetax}/\alpha_\tau) \le \sum_{i'=1}^{i' \le i}(f_{rf,i'}^{PO} - f_{rf,i'-1}^{PO})\cdot(xc_{rf,t} - L_{rf,i'}) - f_{rf,1}^{PO} \cdot \sum_{\tau \le t}(CO_{rf,\tau}/\alpha_\tau) \qquad \forall rf,i,t \qquad \text{(F.1)}$$

*Proof.* Notice that in equation (D.7), we use a relaxation of the second term in RHS as we do not know a priori when a tier i(t) becomes active and there is no limits that are available for cost oil for each tier which were available for cumulative oil produced. Ideally, it should be $f_{rf,1}^{PO}$ for the years until first tier is active and then $f_{rf,2}^{PO}$ for the duration of second tier and so on, to represent the second term accurately. Therefore, to obtain a better approximation of the second term, we can use the practical aspects of the problem. We know that most of the investments, cost oil recoveries take place in the initial years when low tier (1 or 2) are active, so it is better to use that fraction which approximate at-least the initial tiers as close the exact one as possible when costs are high. In the later years, cost oil values are small, so the approximation for the later years will not have significant impact on the solution quality. Therefore, fraction $f_{rf,1}^{PO}$ is the best choice to use as an approximation in equation (D.30) for the second term in equation (D.7).

$$\sum_{\tau=1}^{t} f_{rf,i}^{PO}\cdot CO_{rf,\tau}/\alpha_\tau \approx f_{rf,1}^{PO}\sum_{\tau=1}^{t} CO_{rf,\tau}/\alpha_\tau \qquad \forall rf,i,t \qquad \text{(F.2)}$$

On substituting (F.2) in equation (D.7) for any active tier i in current period t and using (D.1), we can obtain equation (F.1).

# Appendix G

## Bi-level decomposition approach for the Fiscal Model in Chapter 3

The fiscal Model 3RF involving ringfencing provisions becomes expensive to solve directly using commercial MILP solvers such as CPLEX as can be seen in the results section 3.6.2. Even the tighter formulation Model 3RF-L obtained after adding logic constraints and valid inequalities takes significant amount of time to close the gap if ringfencing provisions are present in the problem. This is due to the additional binary variables and constraints required to incorporate these provisions in the model and resulting in weak LP relaxations. Therefore, we propose a bi-level decomposition strategy to solve the fiscal model having ringfencing provisions in a more efficient manner that can be used for either of the proposed MILP formulations. However, we consider here Model 3RF-L as a basis to present the algorithm.

The proposed bi-level decomposition strategy involves two levels (see Figure G.1):

**(a) Upper Level:** At the upper level, an aggregate fiscal model (MILP) is solved that is formulated from the detailed fiscal Model 3RF-L by neglecting the ringfencing provisions. This is equivalent to a specific case of the model with only 1 ringfence that involves all the fields in it. Therefore, constraints (3.1)-(3.50) are written without index for ringfence *rf* in the aggregate model. Moreover, costs and revenues over various ringfences need not be disaggregated. Therefore, constraints (3.6)-(3.24) reduce to the simple total capital cost equation (3.52) as explained in section 3.4. The tier thresholds over various ringfences are also aggregated in disjunctions (3.30). The resulting aggregate fiscal model represents a relaxation of the original problem since it allows revenue and cost sharing among the ringfences, and yields an upper bound on the objective function value.

**(b) Lower Level:** At the lower level, the detailed fiscal model (Model 3RF-L) involving ringfencing provisions is solved as an MILP for the selected FPSO installations and field-FPSO connection decisions from the upper level problem. The model yields a feasible solution to the original problem in the restricted space and a lower bound on its objective function value. In particular, the remaining investment decisions such as well drilling, FPSO expansions and their capacities, and operating decisions, e.g. oil production rates are obtained at this level.

If the gap between the upper and lower bounds coming from the aggregate and detailed fiscal models, respectively, is less than the pre-specified tolerance, the procedure stops. Otherwise, an integer cut is added to the upper level problem in the next iteration that eliminates the selection of the same investment decisions that have already been explored in the previous iterations.

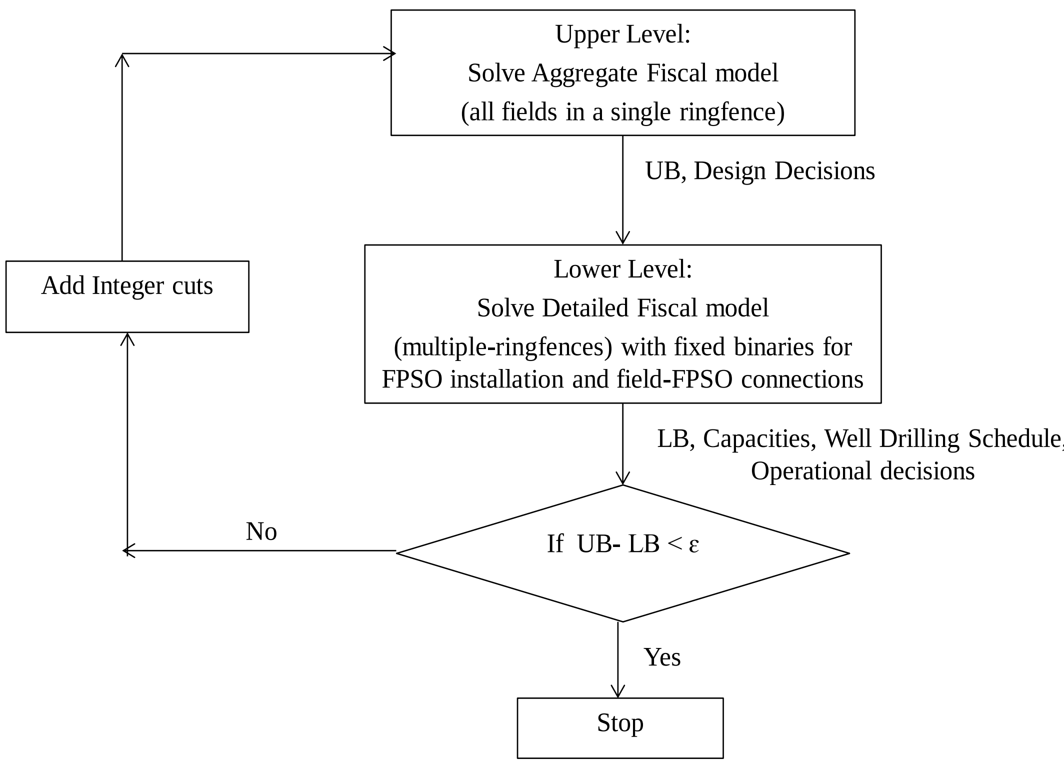


Figure G.1: Bi-level Decomposition Approach for the Fiscal model with Ringfencing provisions

Notice that the efficiency of the proposed bi-level decomposition approach depends on the efficiency of solving the upper and lower level problems. If the original problem size is large, even these individual models can become expensive to solve and/or may require several iterations to close the gap. However, the approach can still be used to generate “good” feasible solutions to these ringfencing problems. Moreover, it can be considered as a basis to solve the medium-size instances in reasonable time and can further be extended to improve the computational efficiency. Preliminary results on an oilfield instance are presented in section 3.6.2 based on this approach.

# Bibliography


Ahmed, S., 2000. Strategic planning under uncertainty: Stochastic integer programming approaches. Ph.D. thesis, University of Illinois at Urbana-Champaign.

Ahmed, S., Garcia, R., 2003. Dynamic capacity acquisition and assignment under uncertainty. Ann. of Oper. Res. 124, 267–283(17).

Ahmed, S., Tawarmalani, M., Sahinidis, N., 2004. A finite branch-and-bound algorithm for two-stage stochastic integer programs. Mathematical Programming, 100(2), 355–377.

Aronofsky J. S., Williams A. C., 1962. The use of linear programming and mathematical models in underground oil production. Manage. Sci., 8, 394–407.

Aseeri, A., Gorman, P., Bagajewicz, M. J., 2004. Financial risk management in offshore oil infrastructure planning and scheduling. Ind. Eng. Chem. Res., 43, 3063–3072.

Babusiaux, D., Favennec, J. P., Bauquis, P. R., Bret-Rouzaut, N., Guirauden, D., 2007. Oil and Gas Exploration and Production: Reserves, costs, contracts; Technip edition.

Bagajewicz, M. J., 2008. On the use of net present value in investment capacity planning models. Ind. Eng. Chem. Res., 47, 9413–9416.

Bailey, W. J., Couet, B., Wilkinson, D., 2005. Field Optimization Tool for Maximizing Asset Value. SPE Reservoir EVal. Eng., 8 (1), 7–21.

Barahona, F., Anbil, R., 2000. The volume algorithm: Producing primal solutions with a subgradient method. Math. Programming 87(3), 385–399.

Barnes, R., Linke, P., Kokossis, A., 2002. Optimization of oil-field development production capacity. European symposium on computer aided process engineering, Vol. 12 (p. 631).

Barnes, R.J., Kokossis, A., Shang, Z., 2007. An integrated mathematical programming approach for the design and optimisation of offshore fields. Computers and Chemical Engineering, 31, Issues 5-6, 612-629.

Begg, S. H., Bratvold, R., Campbell, J. C., 2001. Improving Investment Decisions Using A Stochastic Integrated Asset Model Presented at the SPE Annual Technical Conference and Exhibition, New Orleans, LA, Sep 30-Oct 3, Paper SPE 71414.

Behrenbruch, P., 1993. Offshore oilfield development planning. J. Pet. Technol., 45 (8), 735–743.

Birge, J. R., Louveaux, F., 1997. Introduction to stochastic programming. New York, NY: Springer.

Blake, A. J., Roberts, M. C., 2006. Comparing petroleum fiscal regimes under oil price uncertainty. Resources Policy, 31(2), 95–105.

Bohannon J., 1970. A linear programming model for optimum development of multi-reservoir pipeline systems. J. Petrol Tech., 22, 1429–1436.

Boland, N., Dumitrescu, I., Froyland, G., 2008. A multistage stochastic programming approach to open pit mine production scheduling with uncertain geology. http://www.optimizationonline.org/DBHTML/2008/10/2123.html.

BP Statistical Review of World Energy, 2011.

Carøe, C.C., Schultz, R., 1999: Dual decomposition in stochastic integer programming. Oper. Res. Lett. 24, 37–45.

Carvalho, M., Pinto, J. M., 2006a. A bilevel decomposition technique for the optimal planning of offshore platforms. Brazilian J. Chem. Eng., 23, 67–82.

Carvalho, M., Pinto, J. M., 2006b. An MILP model and solution technique for the planning of infrastructure in offshore oilfields. J. Pet. Sci. Eng., 51, 97–110.

Clay, R. L., Grossmann, I. E., 1997. A disaggregation algorithm for the optimization of stochastic planning models. Computers and Chemical Engineering 21 (7),751-774.

Colvin, M., Maravelias, C. T., 2008. A stochastic programming approach for clinical trial planning in new drug development. Computers and Chemical Engineering 32, 2626–2642.

Colvin, M., Maravelias, C.T., 2010. Modeling methods and a branch and cut algorithm for Pharmaceutical Clinical Trial Planning using Stochastic Programming, European Journal of Operational Research, 203, 205–215.

Conejo, A., Castillo, E., Minguez, R., Garcia-Bertrand, R., 2006. Decomposition Techniques in Mathematical Programming. New York: Springer.

Cullick, A. S., Heath D., Narayanan K., April J., Kelly J., 2003. Optimizing Multiple-Field Scheduling and Production Strategy with Reduced Risk. Presented at the SPE Annual Technical Conference and Exhibition, Denver, CO, Oct 5-8, Paper SPE 84239.

Cullick, A. S., Cude, R., and Tarman, M., 2007. Optimizing Field Development Concepts for Complex Offshore Production Systems, Paper SPE 108562-MS presented at Offshore Europe, Aberdeen, Scotland, U.K., 4-7 September.

Dawande, M. W., Hooker, J. N., 2000. Inference-based sensitivity analysis for mixed integer/linear programming. Operations Research 48 (4), 623–634.

Dias, M., 2002. Investment in information in petroleum, real options and revelation. In: Proceedings of the 6th Annual International Conference on Real Options. Real Options Group at Cyprus, Cyprus.

Elgsæter, S. M., Slupphaug O., Johansen T. A., 2010. A structured approach to optimizing offshore oil and gas production with uncertain models. Comput. Chem. Eng., 34(2), 163-176.

Ettehad, A., Jablonowski, C. J., Lake, L. W., 2011. Stochastic Optimization and Uncertainty Analysis for E&P Projects: A Case in Offshore Gas Field Development, Offshore Technology Conference.

Fisher, M. L., 1985. An Applications Oriented Guide to Lagrangian Relaxation. Interfaces 15, 10-21.

Frair, L. C., 1973. Economic Optimization of Offshore Oilfield Development. PhD Dissertation, University of Oklahoma, Tulsa, OK.

Glover, F., 1975. Improved Linear Integer Programming Formulations of Nonlinear Integer Problems. Manage. Sci., 22, 455.

Goel, V., Grossmann, I. E., 2004. A stochastic programming approach to planning of offshore gas field developments under uncertainty in reserves. Computers and Chemical Engineering 28 (8), 1409–1429.

Goel, V., Grossmann, I. E., 2006. A class of stochastic programs with decision dependent uncertainty. Mathematical Programming 108 (2-3, Ser. B), 355-394.

Goel, V., Grossmann, I. E., El-Bakry, A. S., Mulkay, E. L., 2006. A novel branch and bound algorithm for optimal development of gas fields under uncertainty in reserves. Computers and Chemical Engineering 30, 1076-1092.

Grossmann, I. E., 2002. Review of nonlinear mixed-integer and disjunctive programming techniques for process systems engineering. Optim. Eng., 3 (3), 227-252.

Grothey, A., McKinnon, K., 2000. Decomposing the optimization of a gas lifted oil well network. Tech Rept. MS 00-005, Department of Mathematics and Statistics, University of Edinburgh.

Guignard, M., 2003. Lagrangean relaxation. Top, 11(2), 151–200.

Gunnerud, V., Foss, B., 2010. Oil production optimization – A piecewise linear model, solved with two decomposition strategies. Computers and Chemical Engineering, 34, 1803–1812.

Gupta, V., Grossmann, I. E., 2011a. Solution Strategies for Multistage Stochastic Programming with Endogenous Uncertainties. Computers and Chemical Engineering 35, 2235–2247.

Gupta, V., Grossmann, I. E., 2011b. Offshore Oilfield Development Planning under Uncertainty and Fiscal Considerations. Optimization and Analytics in the Oil and Gas Industry, Part I; Springer Edition, submitted for publication.

Gupta, V., Grossmann, I. E., 2012a. An Efficient Multiperiod MINLP Model for Optimal planning of Offshore Oil and Gas Field Infrastructure. Industrial and Engineering Chemistry Research 51 (19), 6823–6840.

Gupta, V., Grossmann, I. E., 2012b. Modeling and Computational Strategies for Offshore Oilfield Development Planning under Complex Fiscal Rules. Industrial and Engineering Chemistry Research 51, 14438−14460.

Gupta, V., Grossmann, I. E., 2013a. Multistage Stochastic Programming Approach for Offshore Oilfield Infrastructure Planning under Production Sharing Agreements and Endogenous Uncertainties, manuscript in preparation.

Gupta, V., Grossmann, I. E., 2013b. A new Decomposition Algorithm for Multistage Stochastic Programs with Endogenous Uncertainties, submitted for publication.

Haugen, K. K., 1996. A stochastic dynamic programming model for scheduling of offshore petroleum fields with resource uncertainty. Eur. J. Oper. Res., 88 (1), 88–100.

Haugland, D., Hallefjord, A., Asheim, H., 1988. Models for petroleum field exploitation. Eur. J. Oper. Res., 37 (1), 58–72.

Heitsch, H., Römisch, W., 2003. Scenario reduction algorithms in stochastic programming, Computational Optimization and Applications, 24, 187–206.

Held, H., Woodruff, D. L., 2005. Heuristics for multi-stage interdiction of stochastic networks. Journal of Heuristics 11 (5-6), 483-500.

Ierapetritou, M. G., Pistikopoulos, E. N., 1994. Novel optimization approach of stochastic planning models. Industrial and Engineering Chemistry Research 33, 1930-1942.

Iyer, R. R., Grossmann, I. E., 1998. A bilevel decomposition algorithm for long-range planning of process networks. Industrial and Engineering Chemistry Research 37 (2), 474-481.

Iyer, R. R., Grossmann, I. E., Vasantharajan, S., Cullick, A. S., 1998. Optimal planning and scheduling offshore oilfield infrastructure investment and operations. Ind. Eng. Chem. Res., 37, 1380–1397.

Johnston, D., 1994. Petroleum Fiscal Systems and Production Sharing Contracts; PennWell Publishing Co.: Tulsa, Oklahoma.

Jonsbraten, T. W., 1998a. Oil-field optimization under price uncertainty. Journal of the Operational Research Society, 49, 811.

Jonsbraten, T. W., 1998b. Optimization models for petroleum field exploitation. PhD thesis, Norwegian School of Economics and Business Administration.

Jonsbraten, T. W., Wets, R. J. B., Woodruff, D. L., 1998. A class of stochastic programs with decision dependent random elements. Ann. Oper. Res., 82, 83–106.

Kaiser, M.J., Pulsipher, A.G., 2004. Fiscal System Analysis: Concessionary and Contractual Systems Used in Offshore Petroleum Arrangements. US Department of the Interior Mineral Management Services MMS 2004-016, 1-78.

Kosmidis, V., Perkins, J., Pistikopoulos, E., 2002. A mixed integer optimization strategy for integrated gas/oil production. In: European Symposium on Computer Aided Process Engineering. Vol. 12.

Kosmidis, V. D., Perkins, J. D., Pistikopoulos, E. N., 2005. A mixed integer optimization for the well scheduling problem on petroleum fields. Computers & Chemical Engineering Journal, 29, 1523–1541.

Laínez, J. M., Puigjaner, L., Reklaitis, G. V., 2009. Financial and financial engineering considerations in supply chain and product development pipeline management. Comput. Chem. Eng., 33, 1999–2011.

Lee A. S., Aronofsky J. S., 1958. A linear programming model for scheduling crude oil production. J. Petrol Tech., 10, 51–54.

Lemaréchal, C., 1974. An algorithm for minimizing convex functions. In: IFIP Congress. pp. 552–556.

Li, Z., Ierapetritou, M., 2012. Capacity expansion planning through augmented Lagrangian optimization and scenario decomposition. AIChE Journal, 58(3), 871–883.

Lin, X., Floudas, C. A., 2003. A Novel Continuous-Time Modeling and Optimization Framework for Well Platform Planning Problems. Optim. Eng., 4 (1-2), 65–95.

Linderoth, J., Wright, S., 2003. Decomposition algorithms for stochastic programming on a computational grid. Computational Optimization and Applications 24 (2-3), 207–250.

Lund, M. W., 2000. Valuing Flexibility in Offshore Petroleum Projects. Ann. Oper. Res., 99 (1-4), 325–349.

Meister, B., Clark, J. M. C., Shah, N., 1996. Optimisation of oilfield exploitation under uncertainty. Computers and Chemical Engineering 20, S1251–S1256, suppl. B.

Mouret, S., Grossmann, I. E., Pestiaux, P., 2011. A new Lagrangian decomposition approach applied to the integration of refinery planning and crude-oil scheduling. Computers and Chemical Engineering 35, 2750-2766

Oliveira, F., Gupta, V., Hamacher, S., Grossmann, I. E., 2013. A Lagrangean Decomposition Approach for Oil Supply Chain Investment Planning under

Uncertainty with Risk Considerations. Computers and Chemical Engineering 50, 184–195.

Ortiz-Gomez, A., Rico-Ramirez, V., Hernandez-Castro, S., 2002. Mixed-integer multiperiod model for the planning of oil-field production. Comput. Chem. Eng., 26(4–5), 703.

Park, M., Park, S., Mele, F.D., Grossmann, I.E., 2006. Modeling of purchase and sales contracts in supply chain optimization. Industrial and Engineering Chemistry Research, 45, 5013.

Pflug, G. Ch., 1990. Online optimization of simulated markovian processes. Mathematics of Operations Research Res. 15, No.3, 381-395.

Ralphs, T., Guzelsoy, M., 2006. Duality and warm starting in integer programming. In: Proceedings of the 2006 NSF Design, Service, and Manufacturing Grantees and Research Conference.

Raman, R., Grossmann, I. E., 1991. Relation between MILP Modeling and Logical Inference for Chemical Process Synthesis. Comput. Chem. Eng., 15 (2), 73-84.

Raman, R., Grossmann, I. E., 1994. Modeling and Computational Techniques for Logic-Based Integer Programming. Comput. Chem. Eng., 18, 563-578

Ruszczynski, A., 1997. Decomposition methods in stochastic programming. Math. Programming (Ser. B) 79, 333-353.

Sahinidis, N.V., 2004. Optimization under uncertainty: State-of-the-art and opportunities. Comput. Chem. Eng. 28 (6–7), 971–983.

Schlumberger, 2008. Eclipse 2008.1 reservoir engineering software. http://www.slb.com/content/services/software/reseng/index.asp.

Schultz, R., 2003. Stochastic programming with integer variables. Mathematical Programming 97 (1–2), 285–309.

Shapiro, A., 2003. Monte Carlo sampling methods. In: Ruszczynski, A., Shapiro, A. (Eds.) Stochastic Programming, Handbook in OR & MS, Vol. 10, North-Holland Publishing Company, Amsterdam.

Solak, S., 2007. Efficient solution procedures for multistage stochastic formulations of two problem classes. PhD thesis, Georgia Institute of Technology.

Stensland, G., Tjøstheim, D., 1991. Optimal decisions with reduction of uncertainty over time - an application to oil production. In: Lund, D., øksendal, B. (Eds.), Stochastic Models and Option Values. pp. 267-291.

Sullivan J., 1982. A computer model for planning the development of an offshore gas field. J. Petrol Tech., 34, 1555–1564.

Sunley, E. M., Baunsgaard T., Simard D., 2002. Revenue from the Oil and Gas Sector: Issues and Country Experience. IMF Conference Paper.

Tarhan, B., Grossmann, I. E., 2008. A multistage stochastic programming approach with strategies for uncertainty reduction in the synthesis of process networks with uncertain yields. Computers and Chemical Engineering 32, 766-788.

Tarhan, B., 2009. Stochastic programming approaches for decision-dependent uncertainty and gadual uncertainty resolution. Ph.D. thesis, Carnegie Mellon University, Pittsburgh.

Tarhan, B., Grossmann, I. E., Goel, V., 2009. Stochastic programming approach for the planning of offshore oil or gas field infrastructure under decision-dependent uncertainty. Industrial and Engineering Chemistry Research 48 (6), 3078-3097.

Tarhan, B., Grossmann, I. E., Goel, V., 2011. Computational strategies for non-convex multistage MINLP models with decision-dependent uncertainty and gradual uncertainty resolution. Annals of Operations Research, http://dx.doi.org/10.1007/s10479-011-0855-x.

Tarhan, B., Gupta V., Grossmann, I. E., 2013. Improving Dual Bound for Stochastic MILP Models using Sensitivity Analysis, to be submitted.

Terrazas-Moreno, S. and Grossmann, I.E., 2011. A multiscale decomposition method for the optimal planning and scheduling of multi-site continuous multiproduct plants, Chemical Engineering Science, 66, 4307-4318.

Tordo, S., 2007. Fiscal Systems of Hydrocarbons: Design Issues.Working Paper 123/07, World Bank, Washington, D.C.

Tsarbopoulou, C., 2000. Optimization of oil facilities and oil production. M.Sc. Dissertation, University College London, London, U.K..

Ulstein, N. L., Nygreen, B., Sagli, J. R., 2007. Tactical planning of offshore petroleum production. Eur. J. Oper. Res., 176, 550–564.

van den Heever, S. A., Grossmann, I. E., 2000. An iterative aggregation/disaggregation approach for the solution of a mixed integer nonlinear oilfield infrastructure planning model. Ind. Eng. Chem. Res., 39, 1955–1971.

van den Heever, S. A., Grossmann, I. E., Vasantharajan, S., Edwards, K., 2000. Integrating complex economic objectives with the design and planning of offshore oilfield infrastructures. Comput. Chem. Eng., 24, 1049–1055.

van den Heever, S. A., Grossmann, I. E., 2001. A Lagrangean Decomposition Heuristic for the Design and Planning of Offshore Hydrocarbon Field Infrastructures with Complex Economic Objectives. Ind. Eng. Chem. Res., 40, 2857–2875.

Vayanos, P., Kuhn, D., Rustem, B. 2011. Decision rules for information discovery in multistage stochastic programming. IEEE Conference on Decision and Control and European Control Conference, Orlando, USA.

Vielma, J., Ahmed, S., and Nemhauser, G., 2010. Mixed-Integer Models for Nonseparable Piecewise Linear Optimization: Unifying Framework and Extensions. Operations Research, 58,303-315.

Viswanath, K., Peeta, S., Salman, S. F., 2004. Investing in the links of a stochastic network to minimize expected shortest path length. Tech. rep., Purdue University.

World Bank, 2007. Contracts for Petroleum Development – Part 1-3. Petroleum Sector Briefing Note No. 7.

You F., Wassick J. M., Grossmann I. E., 2009. Risk management for global supply chain planning under uncertainty: models and algorithms. AIChE Journal, 55, 931-946.

Zabalza-Mezghani, I., Manceau, E., Feraille, M., Jourdan, A., 2004. Uncertainty management: From geological scenarios to production scheme optimization. J. Pet. Sci. Eng., 44, 11–25.